



**From tropical coral reefs to high latitude coral
communities: insights into population dynamics along
environmental gradients**

being a thesis submitted in fulfilment of the
requirements for the degree of
Doctor of Philosophy

in the University of Hull

by

Ho Yee Fiona Chong

March 2025

© 2025 Ho Yee Fiona Chong

Dedication

This thesis is dedicated to the loving memory of Dulcie van Egmond-Bailey.

“Somewhere between the 0s and 1s, that’s where I found my kingdom come,
my heart beats like a drum –”
Nemo, *The Code*

Acknowledgements

My deepest thanks to my PhD supervisors Maria Beger and Domino Joyce. To Maria, for an opportunity of a lifetime to work with you on this wonderful, fragile and fascinating system, and for your time that is simply invaluable. To Domino for facilitating my foray into genetics, your wisdom, and for picking me up when I'm down. You are both awesome women in science and such inspirations. Because of your support I have gone to places and met people I never dreamt was possible.

The warmest thank you to James Reimer and members of MISE lab at the University of the Ryukyus, Okinawa, who hosted our annual coral demographics fieldwork as well as my JSPS fellowship. You are the most insightful and helpful people working on coral reefs on the edge of the Pacific – my year in Okinawa was transformative and the people and place will always have a special place in my heart.

I am forever grateful to Brigitte Sommer for your generosity in spirit, and for kindling my passion for subtropical corals. The biggest thank you to Matt Spencer, for showing me how to approach big questions, and for being there through the hard times and the good.

There are so many fantastic people that I've crossed paths with and learnt from in the last five years, I cannot possibly list them all. But thank you in particular to Rob Salguero-Gómez, James Cant and my dive buddy Victoria Hsiao for the inspiration, intellectual stimulation and funny field memories. Thank you to everyone in the Marine Transitions Lab at Leeds, and my EEI friends at Hull for your feedback, advice and support.

Finally, thank you to my family, Professor Batman the cat and Stefano for your love, patience and confidence in me through this journey.

Publications

The work in Chapter Two has appeared in publication as follows:

- Chong, F., Sommer, B., Stant, G., Verano, N., Cant, J., Lachs, L., Johnson, M.L., Parsons, D.R., Pandolfi, J.M., Salguero-Gómez, R., Spencer, M. and Beger, M. (2023), High-latitude marginal reefs support fewer but bigger corals than their tropical counterparts. *Ecography*, 2023: e06835. <https://doi.org/10.1111/ecog.06835>

F. Chong conceived the study, conducted all statistical analyses and drafted the manuscript, under the supervision of M. Beger, B. Sommer, M. Spencer, R. Salguero-Gómez and M.L. Johnson. Data extraction was completed by G. Stant, N. Verano, L. Lachs and F. Chong. Fieldwork was conducted by M. Beger, B. Sommer, J. Cant and L. Lachs. Funding and resources from M. Beger, B. Sommer, J.M. Pandolfi and D.R. Parsons. All provided comments on the manuscript.

The work in Chapter Three has been prepared as a manuscript for publication as follows:

- Chong, F., Sommer, B., Beger, M. and Spencer, M. (in preparation). Model choice and sampling bias in fish and coral size spectra.

F. Chong conceived the study, conducted all statistical analyses and drafted the manuscript under the supervision of M. Spencer and M. Beger. Fieldwork was conducted by M. Beger and B. Sommer. All provided comments on the manuscript.

The work in Chapter Four has appeared in publication as follows:

- Chong, F., Soong, G. Y., Hakim, A. A., Burke, C., De Palmas, S., Gösser, F., Hsiao, W. V., Kise, H., Nishijima, M., Iguchi, A., Sommer, B., Joyce, D., Beger, M. and Reimer, J. D. (2024). Subtropical specialists dominate a coral range expansion front. *Coral Reefs*. (2024). <https://doi.org/10.1007/s00338-024-02601-w>

F. Chong conceived the study, conducted all statistical analyses and drafted the manuscript under the supervision of D. Joyce, M. Beger and J.D. Reimer. Fieldwork was conducted by F. Chong, C. Burke and S. De Palmas. Lab work was conducted by F. Chong with assistance from G.Y. Soong, A.A. Hakim, H. Kise and M. Nishijima. F. Gösser, W.V. Hsiao and B. Sommer contributed to the conception of the study and the interpretation of the results. A. Iguchi provided additional lab resources. All provided comments on the manuscript.

Abstract

Anthropogenic climate change affects coral communities globally, exposing them to increasingly frequent disturbances. Thermal stress events might differentially compromise the recovery capacity of coral taxa across biogeographic scales. While changes in total coral cover are used extensively to monitor the status of many tropical coral reefs, relatively little information is available on high latitude coral communities, yet understanding population structure is essential for the forecasting of population dynamics under climate change. This thesis links size-based demographic approaches and coral-symbiont genetics to further our understanding of ecological processes affecting coral communities in biogeographic transition zones.

The population size structure (or size spectra) of communities encompasses valuable information on the vital rates of populations. I explored how the population size structure of coral communities change along an approximately 900 km environmental gradient on the east coast of Australia, from the warmer and brighter southern Great Barrier Reef to the colder and more turbid rocky reefs of northern New South Wales. I found that there were fewer but bigger corals in the high latitude marginal reefs, implying that population persistence is reliant on fundamentally different demographic strategies along the gradient. Using compositional functional regression, I predicted the effect of increasingly marginal environments on entire coral size distributions. I further explored size spectra of fishes as well as corals along this environmental gradient, challenging the widespread assumption that the size-abundance relationship in ecological communities followed a (bounded) power law relationship. I also considered the common, but rarely-addressed issue of minus-sampling using photo-quadrats. I found that log-normal distributions might provide a better description to ecological size spectra, especially at the upper tails of the distribution. Finally, to understand the identity of coral taxa behind observed demographic differences along environmental gradients, I explored the genetic diversity of the *Pocillopora* species complex, and their Symbiodiniaceae endosymbiont community along a 1000 km environmental gradient in Japan. I found that high latitude corals are low in diversity and genetically distinct from their tropical congeners. This finding challenges the extent of tropicalisation in marine environments under climate change, with respect to sessile organisms such as corals.

Overall, this thesis sought to improve our understanding of demographic processes in coral communities across biogeographic transition zones. Using a combination of high-quality size abundance and genetic data, I highlight fundamental differences in tropical coral reefs and their high latitude counterparts. I use and present methods that incrementally improve our ability to describe and model ecological size spectra, which has wider conservation and management applications. As climate change continues to affect communities worldwide, quantitative demographic approaches such as those presented in this thesis will continue to shape our ability to capture and predict population viability and persistence.

Contents

Dedication.....	i
Acknowledgements.....	ii
Publications.....	iii
Abstract.....	iv
List of Figures	x
In Appendix A:	x
In Appendix B:	xi
In Appendix C:	xii
List of Tables.....	xiii
In Appendix A:	xiii
In Appendix B:	xiii
In Appendix C:	xiii
A note on style	xiv
Chapter 1 : General Introduction.....	1
1.1 Size-based demography in corals and reef fishes	3
1.2 Coral communities in biogeographic transition zones.....	5
1.3 Thesis aims and objectives.....	7
Chapter 2 : High-latitude marginal reefs support fewer but bigger corals than their tropical counterparts	9
2.1 Abstract	9
2.2 Introduction.....	10
2.3 Methods.....	13
2.3.1 Data collection	13
2.3.2 Coral taxonomic identity along the environmental gradient.....	15
2.3.3 Data analyses	15
2.3.4 Size-biased sampling.....	18
2.3.5 Model sensitivity to the 2016 bleaching event.....	19
2.4 Results.....	19

2.4.1 Summary statistics and linear regression	19
2.4.2 Compositional functional regression	20
2.5 Discussion	20
Chapter 3 : Model choice and sampling bias in fish and coral size spectra	30
3.1 Abstract	30
3.2 Introduction.....	30
3.3 Methods.....	33
3.3.1 Data collection	33
3.3.2 Fish data from Indonesia	34
3.3.3 Distributions, the theory on minus-sampling and parameter estimation	34
3.3.4 Data visualisation and model comparison.....	38
3.3.5 Model comparison using log-likelihoods	39
3.4 Results.....	40
3.4.1 Fish data from Indonesia	41
3.5 Discussion	42
Chapter 4 : Subtropical specialists dominate a coral range expansion front.....	51
4.1 Abstract	51
4.2 Introduction.....	53
4.3 Material and Methods	57
4.3.1 Specimen collection	57
4.3.2 Characterising the Kuroshio Current environmental gradient	57
4.3.3 DNA extraction, <i>Pocillopora</i> host sequencing & Symbiodiniaceae NGS.....	58
4.3.4 Haplotype network and Phylogenetic tree of <i>Pocillopora</i> ORF haplotypes	59
4.3.5 Testing the effect of the environmental gradient on coral and symbiont diversity	59
4.4 Results.....	61

4.4.1 Haplotype diversity and changes along the environmental gradient	61
4.4.2 Symbiont defining intragenomic variants (DIVs) & ITS2 type profile along the Kuroshio	62
4.5 Discussion	70
Chapter 5 : General Discussion	75
5.1 Ecological findings and implications	76
5.2 Methods progress and implications	77
5.3 Future research directions	78
5.4 Conclusions	80
References	82
Appendices	I
Appendix A: Supporting information for Chapter 2	I
S1: Supplemental tables and figures from the main analyses	I
S2: Coral taxonomic identity along the environmental gradient	VII
S3: Bayes Space	VIII
S4: Size-biased sampling	IX
S5: Further compositional functional regression results and model diagnostics	X
S6: Testing compositional functional regression model robustness	XI
S7: Model sensitivity to the 2016 bleaching event	XXII
References	XXXIII
Appendix B: Supporting information for Chapter 3	XXXIV
S1: Supplementary information	XXXIV
S2: Probability density function for the minus-sampled bounded power law 	XLIV
S3: Quantile-quantile plots of coral data for all sites	XLVI
S4: Quantile-quantile plots of fish data for all sites	LXVI
S5: Indonesian fish data from Carvalho <i>et al.</i> (2021)	LXXXVI
References	XC

Appendix C: Supporting information for Chapter 4XC

List of Figures

Figure 2.1.....	25
Figure 2.2.....	25
Figure 2.3.....	26
Figure 2.4.....	27
Figure 2.5.....	28
Figure 2.6.....	29
Figure 3.1.....	46
Figure 3.2.....	49
Figure 4.1.....	60
Figure 4.2.....	61
Figure 4.3.....	64
Figure 4.4.....	65
Figure 4.5.....	67
Figure 4.6.....	68
Figure 4.7.....	69

In Appendix A:

Figure A-1.....	XI
Figure A-2.....	XII
Figure A-3.....	XIII
Figure A-4.....	I
Figure A-5.....	II
Figure A-6.....	III
Figure A-7.....	IV
Figure A-8.....	V
Figure A-9.....	VI
Figure A-10.....	XII
Figure A-11.....	XIII
Figure A-12.....	XIV
Figure A-13.....	XV
Figure A-14.....	XVI
Figure A-15.....	XVII
Figure A-16.....	XVIII

Figure A-17.	XIX
Figure A-18.	XX
Figure A-19.	XXI
Figure A-20.	XXV
Figure A-21.	XXVI
Figure A-22.	XXVII
Figure A-23.	XXVIII
Figure A-24.	XXIX
Figure A-25.	XXX
Figure A-26.	XXXI
Figure A-27.	XXXII

In Appendix B:

Figure B-1.	XLI
Figure B-2.	XLII
Figure B-3.	XLIII
Figure B-4.	XLVI
Figure B-5.	XLVII
Figure B-6.	XLVIII
Figure B-7.	XLIX
Figure B-8.	L
Figure B-9.	LI
Figure B-10.	LII
Figure B-11.	LIII
Figure B-12.	LIV
Figure B-13.	LV
Figure B-14.	LVI
Figure B-15.	LVII
Figure B-16.	LVIII
Figure B-17.	LIX
Figure B-18.	LX
Figure B-19.	LXI
Figure B-20.	LXII
Figure B-21.	LXIII

Figure B-22.	LXIV
Figure B-23.	LXV
Figure B-24.	LXVI
Figure B-25.	LXVII
Figure B-26.	LXVIII
Figure B-27.	LXIX
Figure B-28.	LXX
Figure B-29.	LXXI
Figure B-30.	LXXII
Figure B-31.	LXXIII
Figure B-32.	LXXIV
Figure B-33.	LXXV
Figure B-34.	LXXVI
Figure B-35.	LXXVII
Figure B-36.	LXXVIII
Figure B-37.	LXXIX
Figure B-38.	LXXX
Figure B-39.	LXXXI
Figure B-40.	LXXXII
Figure B-41.	LXXXIII
Figure B-42.	LXXXIV
Figure B-43.	LXXXV
Figure B-44.	LXXXVI
Figure B-45.	LXXXVII
Figure B-46.	LXXXVIII
Figure B-47.	LXXXIX

In Appendix C:

Figure C-1.	XCIV
------------------	------

List of Tables

Table 3.1.....	46
Table 3.2.....	49

In Appendix A:

Table A-1.	I
Table A-2.	III
Table A-3.	VI
Table A-4.	VII
Table A-5.	VIII
Table A-6.	IX
Table A-7.	X
Table A-8.	XXIII

In Appendix B:

Table B-1.	XXXIV
Table B-2.	XXXVI
Table B-3.	XXXVIII
Table B-4.	XLIV
Table B-5.	XC

In Appendix C:

Table C-1.	XC
Table C-2.	XCII
Table C-3.	XCII
Table C-4.	XCIV
Table C-5.	XCV
Table C-6.	XCVII

A note on style

Chapters 2-4 of this thesis have been written in manuscript format intended for publication. I am the lead author on these data chapters, but I acknowledge the contributions of the co-authors by using 'we' and 'our' throughout these chapters. Chapters 1 and 5, the general introduction and discussion are my sole work, and the terms 'I' and 'my' are used throughout.

Chapter 1 : General Introduction

Climate change influences communities over large spatial scales, affecting the functioning of entire socio-ecological systems such as coral reefs (Williams *et al.*, 2019). Such global drivers affect large-scale, multi-species ecological patterns and processes (Brown, 1995; Beck *et al.*, 2012; Keith *et al.*, 2012), whose distribution transcends national boundaries (van Woesik *et al.*, 2022), necessitating the upscaling of ecological mechanisms underpinning small-scale, local processes to those relevant to regional and global contexts (McGill *et al.*, 2019). Analysing statistical relationships between abiotic (environmental) variables and biotic (organismal) responses has many modern theoretical and practical applications. For example, such work aids the identification of critical biodiversity trends, conservation priorities and species responses to environmental change (Beck *et al.*, 2012; Rapacciuolo, 2019). To understand and accurately predict population persistence under climate change, the demographic rates survival, growth and reproduction of populations (Easterling *et al.*, 2000; Merow *et al.*, 2014) must be considered across the entire geographic range of the species. In marine communities, demographic approaches call for size-based investigations to infer population size structure, which can better determine population viability than simply population size (Caswell, 2001). However, it remains unclear whether and how such demographic responses vary along environmental gradients, which limits the ability to differentiate between the correlation and causation of biodiversity patterns, and to identify the processes that drive them (Beck *et al.*, 2012; Dornelas *et al.*, 2023).

The magnitude and rapid rise of greenhouse gas emissions by human activities in the Anthropocene (Crutzen, 2006; Summerhayes *et al.*, 2024) has led to thermal conditions which surpass species physiological limits at the warm edge of their distribution (Pinsky *et al.*, 2019), exposing populations to dangerous temperatures that lead to decline (Pigot *et al.*, 2023). Although coral reefs have been characterised by disturbance regimes and environmental change through geological time (Connell, 1978; Nyström *et al.*, 2000), reef species are not exempt from the effects of anthropogenic change. One-third of known species are under heightened extinction risks (Carpenter *et al.*, 2008) and the status of entire lineages cannot be ascertained due to a lack of data (Dietzel *et al.*, 2021; Muir *et al.*, 2022). Earlier this year (2024), the fourth global bleaching event was

announced, which concurrently was also the fifth mass bleaching event for the Great Barrier Reef (AIMS, 2024b; Henley *et al.*, 2024; NOAA, 2024). Bleaching occurs when zooxanthellate corals lose their endosymbiotic algae due to suboptimal conditions, which is detrimental to corals as the endosymbionts provide a primary energy source (Ainsworth & Brown, 2021). The survival and recovery rates of this bleaching event is an area of active monitoring and research (AIMS, 2024a), but without urgent interventions, annual summer bleaching (“back-to-back bleaching”) is likely (Hoegh-Guldberg, 1999; Henley *et al.*, 2024), jeopardising the recovery process. Reefs also face a plethora of local, direct threats including but not limited to: pollution from land-based run-off (Dubinsky & Stambler, 1996), physical damage from human activities (Giglio *et al.*, 2020), overfishing (Zaneveld *et al.*, 2016) and predation by crown-of-thorns starfish in the Indo-Pacific (Deaker & Byrne, 2022). The combined impact of these threats is the long-term decline in coral cover, notably in the Caribbean (Gardner *et al.*, 2003; Cramer *et al.*, 2020) and in the Great Barrier Reef (De’ath *et al.*, 2012), with a shift towards macro/turf/crustose-coralline algae dominated reef states (Tebbett *et al.*, 2023). These conditions can put reef species that fail to adapt, acclimate and reproduce at risk of at the minimum, local extinctions (Capdevila *et al.*, 2020). It is important to understand the demographic features of reef populations affected by disturbances to tease out mechanisms driving reef recovery and persistence.

Reef species responses to anthropogenic stressors could vary due to divergent recovery dynamics based on taxa identity (Brown *et al.*, 2023). For example, reefs in the East Asian Seas maintain stable coral cover over decades (up to 40% of the total benthic cover) despite mass bleaching events (Chan *et al.*, 2023). This suggests that site-specific bio-physical differences might be driving these differential responses: for example, reefs with high habitat complexity and primary productivity (Rogers *et al.*, 2015) might be able to support higher biomass. Differences in existing management strategies (Cinner *et al.*, 2016) and disturbance regimes (Emslie *et al.*, 2024) could affect the resilience of reefs. Although these studies of benthic cover are insightful, only monitoring coral cover can mask patterns such as underlying shifts in taxonomic composition (Darling *et al.*, 2013; Edmunds *et al.*, 2014), and it would not provide enough resolution for change detection, especially when population sizes are small (Edmunds & Riegl,

2020). Monitoring beyond coral cover by measuring demographic parameters is needed to understand how populations in different locations respond to anthropogenic stressors (Edmunds & Riegl, 2020; van Woessik *et al.*, 2022). Identifying and protecting reefs that are demographically resilient to environmental stressors, e.g., through resistance to and/or recovery from disturbances (Capdevila *et al.*, 2020), and ensuring their connectivity to other reefs, could be central to spatial planning in coral reef conservation (Harrison *et al.*, 2012; Muenzel *et al.*, 2023).

1.1 Size-based demography in corals and reef fishes

Since survival, growth and reproduction rates follow allometric scaling in corals (e.g., Dornelas *et al.*, 2017) and in fishes (e.g., Hadj-Hammou *et al.*, 2024), the structure of a population contains important features regarding individual differences that are better predictors of population viability than estimates of population size (Easterling *et al.*, 2000). Population size structure (size spectra), i.e. the number of individuals at a given size, and how that changes is especially useful for understanding impacts of disturbances such as bleaching events (e.g., Lachs *et al.*, 2021) and pressures such as size-selective fishing (e.g., Charbonneau *et al.*, 2018) on populations. Besides being impacted by fishing, heightened sea water temperatures can affect metabolism and cause earlier maturation in fishes (Neuheimer & Grønkjær, 2012), which affects the population size structure by reducing the abundance of fish at the largest size classes (Tu *et al.*, 2018). Bak and Meesters (1999) hypothesised that increasingly degraded or marginal conditions would lead to a shift in coral size structure to one that has more larger corals, because recruitment would be reduced. This hypothesis was corroborated by e.g., Dietzel *et al.* (2020); Sommer *et al.* (2024), but e.g., Riegl *et al.* (2012); Pisapia *et al.* (2019) found that size spectra shifted to be dominated by smaller corals than pre-disturbance, mainly as a result of partial mortality and crown-of-thorns outbreaks. The loss of larger corals and their reproductive capacity would reduce the recovery potential of reefs (Hughes *et al.*, 2019); while the lack of small corals would suggest recruitment bottlenecks. Since most studies are limited in their biogeographic scope, these incongruences might not be surprising due to context specificity; they highlight a need for large-scale, gradient approaches that can simulate increasing abiotic stress for us to

understand how population size structure respond (Kreyling *et al.*, 2014; Dornelas *et al.*, 2023).

A power law relationship often describes the scaling of demographic rates, and other physiological rates, such as respiration and fish maximum ingestion (Andersen, 2019, table 2.2). Thus, body size is an important feature that defines predator-prey interactions and energy flows (Heather *et al.*, 2021), as well as population viability. Because of metabolism and resource use limits (White *et al.*, 2007), individual body size and abundance (size spectra) in communities have also been observed to follow a power law relationship, in which the abundance (N) and body size (M) follow $N \propto M^\lambda$, where the exponent λ should be roughly -2 (Andersen, 2019, equation 2.10). However, λ varies depending on the system investigated (e.g., Yoda *et al.*, 1963; Sheldon & Parsons, 1967; Muller-Landau *et al.*, 2006; Robinson *et al.*, 2017), demonstrating that exceptions are common. Despite this, the consistency of the exponent within the same system has inspired a long history of modelling abundance size distributions (size spectra) in forestry and in fisheries, where substantial deviations from the power law exponent hold information on the ecosystem and indicate effects of perturbations. For example, fishing that selectively removes larger individuals would steepen the size spectrum and give a more negative λ , it thus follows that fishing impacts and stock recovery after management, could also be assessed by monitoring changes in the λ (Jennings & Blanchard, 2004).

Whilst both coral and fish population ecologists describe population size structure, historically, log-normal distributions are favoured in describing coral community size distributions (Bak & Meesters, 1998), where single metrics such as mean size and skewness are compared between populations. There has been no work using power law distributions to describe coral population size structure, despite the apparent utility of the exponent λ . Testing which statistical distributions better describe community size spectra in both coral and fishes would be important for applications such as population structure reconstruction (Dietzel, 2020, chapter 4; Bernard *et al.*, 2024), as well as projecting population structure into the future to inform population viability (Cant *et al.*, 2020; Pisapia *et al.*, 2020). The ability to elegantly capture and retain information from the entire size distribution would be useful and have further applications beyond

demography, such as facilitating the calculation of population level calcification and photosynthesis rates (Carlot *et al.*, 2022), which are properties linked to the provision of ecosystem functions, such as carbon fixation.

1.2 Coral communities in biogeographic transition zones

While the effect of climate change is well-studied in tropical coral reef populations, relatively little is known about the ecology of marginal reef ecosystems and their responses to climate change. Marginal reefs include high latitude cold reefs that host coral communities (e.g., Abrego *et al.*, 2021; Toth *et al.*, 2021), turbid reef systems (e.g., Zweifler *et al.*, 2021; Santana *et al.*, 2023), and mesophotic reefs (e.g., Rocha *et al.*, 2018; Eyal *et al.*, 2021). Scleractinian corals surviving in marginal conditions, i.e. darker, colder and productive waters, prompted many questions on the demographic differences between marginal reef corals and their tropical counterparts, and whether they could act as refugia for tropical corals (e.g., Bongaerts *et al.*, 2010; Beger *et al.*, 2014; Soares, 2020) in the Anthropocene. How are tropical and marginal reef coral populations different to each other? What are the demographic strategies of corals that live in these varied conditions: out of survival, growth and reproduction, what processes do marginal and tropical corals expend more energy on to ensure population persistence (e.g., Cant *et al.*, 2022; Cant *et al.*, 2023)? What roles do the relationships between scleractinian coral host and symbiont communities play in the persistence of corals in marginal environments (e.g., Wicks *et al.*, 2010)? How will they fare under further abiotic disturbances? These questions continue to highlight gaps in our knowledge in the population dynamics of marginal coral populations, and large-scale demographic investigations in biogeographic transition zones are urgently needed.

Tropicalisation is an emerging process that affects coral reefs and marginal coral communities in biogeographic transition zones. Biogeographic transition zones are defined as “a geographic area of overlap, with a gradient of replacement and partial segregation between biotic components” (Ferro & Morrone, 2014). The tropical and subtropical (marginal) coral communities are connected by poleward flowing currents that transfers warm, oligotrophic waters to colder, more productive high latitude seas (Imawaki *et al.*, 2013). Physical drivers such as light availability and temperature, and biological factors such as larval connectivity and

competition determine the distribution of scleractinian coral communities at their poleward limits (Sommer *et al.*, 2018; Abrego *et al.*, 2021). Under climate change, some currents are projected to intensify by increasing their warm water transport poleward (Sen Gupta *et al.*, 2021), which could increase the connectivity of tropical reefs to high latitude marginal reefs. Coupled with intensifying marine heat waves and storms (Wernberg *et al.*, 2024), high latitude subtropical and temperate ecosystems might be “tropicalising”, which is when (sub)tropical taxa expand their ranges into latitudes that were previously unsuitable, while the ranges of temperate taxa recede (Zarzychny *et al.*, 2024). For example, temperate foundation species like kelp stands are increasingly replaced by increases in hard corals and turf algae (Vergés *et al.*, 2016; Kumagai *et al.*, 2018). These tropicalising reef states are reinforced by increases in the abundances of tropical grazing herbivores (Ling *et al.*, 2009; Zarzychny *et al.*, 2022). In Japan, the loss of seaweed beds and the resultant barren bottom is termed ‘isoyake’ (Yendo, 1903), which translates to ‘burnt rock’. This phenomenon has been known for over a century, but has become more widespread in the 20th and the 21st century. The reduction of associated temperate coastal fisheries, such as abalone, lobster and commercial seaweed have dramatic economic impacts, making seaweed bed restoration one of the priorities of the Japanese fishery agency (Fujita, 2010). Yet, coral-dominant, tropicalised high latitude reefs might bring new benefits and opportunities, such as new fisheries of tropical grazers such as rabbitfish (*Siganus* spp.), and increased underwater tourism for communities with higher diversity of corals and fishes, resembling tropical coral reefs (Vergés *et al.*, 2019). It is thus important to understand the processes controlling turnover in biogeographic transition zones, to monitor and predict the progress of coral population persistence going ahead.

Tropicalisation in biogeographic transition zones implies that coral loss in the tropics might be compensated by gains in the higher latitude marginal reef environments, with subsequent implications for ecosystem functioning (Vergés *et al.*, 2019). However, population viability of coral and fish communities in these transitional zones remain uncertain, especially when considering the establishment of any range shifting tropical taxa. While the demographic behaviour of corals grouped by genera or life-history appear different between the tropics and the high latitude reefs (Cant *et al.*, 2023), one fundamental

question remains: are the tropical coral taxa found at high latitudes: 1) tropical range expanders that are able to adapt and survive in novel conditions under climate change, or 2) high latitude sister species of the tropical taxa that managed to capitalise on the warmer conditions brought on by climate change? A contemporary baseline of genetic relatedness of coral and symbiont communities along biogeographic transition zones is necessary to understand evolution and adaptation as a result of tropicalisation and environmental change in the Anthropocene (Wogan & Wang, 2018).

1.3 Thesis aims and objectives

The overarching aim of this thesis is to advance our understanding of demographic processes in biogeographic transition zones at a community level, and to provide a demographic and genetic baseline for further monitoring under anthropogenic climate change. The first two data chapters aim to improve our understanding of population dynamics of communities along environmental gradients, by trialling improvements on methodologies currently used. I also provide assemblage level genetic data on *Pocillopora* and endosymbiont Symbiodiniaceae along an environmental gradient to further our understanding on how abiotic drivers structure genetic diversity.

Chapter 2 explores the population size structure of coral communities in twenty reefs in the east Australian biogeographic transition zone, following a 900 km tropical – marginal latitudinal gradient from the southern Great Barrier Reef to the kelp-dominated rocky reefs of New South Wales. By highlighting the differences in coral population structure, in which fewer but larger corals are found at the marginal reefs, I ask how coral populations respond or adapt to increasing environmental stress. This chapter also demonstrates the use of a new method, ‘compositional functional regression’, which models the entire size frequency distribution function based on predictor variables (e.g., environmental parameters) of interest, which is more insightful than modelling a choice summary statistic such as mean or median, which disregards the rest of the distribution.

Chapter 3 further explores population size structure in the east Australian reefs using the size spectrum (abundance-body size) theory and models commonly favoured in fisheries. Using fish and coral community data, this chapter compares the model performance of a bounded power law distribution versus a log-normal

distribution, both distributions are known for their ability to handle data spanning magnitudes. The chapter demonstrates that the conventionally used bounded power law might not be the best fit for ecological size-abundance data, despite the fact that for a given size interval, it offers a single parameter that appears to capture the size-abundance status of entire communities. This chapter also provides methods to deal with minus sampling biases of larger corals in the benthic photo quadrats, commonly used by coral ecologists.

Chapter 4 investigates the diversity, distribution and phylogenetic relationships of coral and symbionts in the *Pocillopora* species complex, along a tropical-marginal gradient from the southern islands of Japan to the south-eastern shores of mainland Japan, following the Kuroshio current. This chapter aims to qualify the extent of tropicalisation of subtropical / temperate environments by species with tropical lineages, and provide a contemporary baseline for the monitoring of potential tropicalisation in marginal high latitude reefs.

Chapter 2 : High-latitude marginal reefs support fewer but bigger corals than their tropical counterparts

2.1 Abstract

Anthropogenic impacts are typically detrimental to tropical coral reefs, but the effect of increasing environmental stress and variability on the size structure of coral communities remains poorly understood. This limits our ability to effectively conserve coral reef ecosystems because size specific dynamics are rarely incorporated. Our aim is to quantify variation in the size structure of coral populations across 20 sites along a tropical-to-subtropical environmental gradient on the east coast of Australia (~23°S to 30°S), to determine how size structure changes with a gradient of sea surface temperature, turbidity, productivity and light levels. We use two approaches: 1) linear regression with summary statistics (such as median size) as response variables, a method frequently favoured by ecologists; and 2) compositional functional regression, a novel method using entire size-frequency distributions as response variables. We then predict coral population size structure with increasing environmental stress and variability. Together, we find fewer but larger coral colonies in marginal reefs, where conditions are typically more variable and stressful, than in tropical reefs. Our model predicts that coral populations may become gradually dominated by larger colonies (> 148 cm²) with increasing environmental stress. Fewer but bigger corals suggest low survival of smaller corals, slow growth, and / or poor recruitment. This finding is concerning for the future of coral reefs, as it implies that current marginal populations, or future reefs in increasingly stressful environmental conditions may have low recovery potential. We highlight the importance of continuously monitoring changes to population structure over biogeographic scales.

2.2 Introduction

Population size has been a primary metric of population persistence and viability for decades (Shaffer, 1981; Dietzel *et al.*, 2021). However, the size structure of a population (*i.e.*, how many individuals of a given size range there are in the population) is as important, if not more so, for determining persistence and viability, especially in slow growing, sessile organisms (e.g., McClanahan *et al.*, 2008; Riegl *et al.*, 2012; Cousins *et al.*, 2014). The structure of a population details important features regarding individual heterogeneity that ultimately predict population outcomes better than simply population size (Hunter *et al.*, 2010; Radchuk *et al.*, 2013). Consequently, in recent decades, population structure has become the focus of demographic models (Easterling *et al.*, 2000; Caswell, 2001; Merow *et al.*, 2014).

External abiotic factors such as climate change (e.g., Radchuk *et al.*, 2013; Vetter *et al.*, 2020) can lead to shifts in population structure when the underlying vital rates (e.g., survival, change in size, reproduction) are affected differently. For example, Radchuk *et al.* (2013) showed that increases in temperature improve the fecundity of female bog fritillary butterflies (*Boloria eunomia*) and the survival of most life stages, except for the overwintering larvae. Yet the viability of the butterfly population is highly sensitive to the survival of overwintering larvae (Radchuk *et al.*, 2013), meaning that low larval survival, as a result of warming, would be detrimental to the viability of this population. However, warming is not constant, and is only one of many aspects of climate change (Dixon *et al.*, 2021), to which species and population responses are complex and poorly understood (Lawson *et al.*, 2015; Tavecchia *et al.*, 2016). Therefore, creating meaningful and realistic experimental manipulations to understand future anthropogenic impacts on population structure might be resource-intensive and not always practical (Kreyling *et al.*, 2014), and especially logistically challenging in the marine environment. An alternative approach to understand the directional effect of environmental change on populations is to sample from natural populations exposed to a gradient of environmental conditions (shift in mean conditions, increased variability and extremes), e.g., at the biogeographic scale (Beier *et al.*, 2012; Kreyling *et al.*, 2014; Elmendorf *et al.*, 2015). Gradient approaches have been shown to give larger estimated effects than experimental studies conducted in terrestrial grassland ecosystems, likely because they reflect long-term

responses, while experiments highlight short term plasticity (Wolkovich *et al.*, 2012; Elmendorf *et al.*, 2015). Since changes to population processes can take years before detection is possible (Evers *et al.*, 2021), it is a reasonable approach for predicting the long-term effects of environmental change on population viability.

Coral reefs are challenged by many anthropogenic perturbations, with climate change being the dominant threat (Pandolfi, 2015; Hoegh-Guldberg *et al.*, 2017; Hughes *et al.*, 2017a). Climate change will continue to increase thermal stress (Dixon *et al.*, 2022), flooding (Vitousek *et al.*, 2017) and storm intensity (Reguero *et al.*, 2019). These disturbances directly and indirectly influence coral mortality, changes in community composition (Hughes *et al.*, 2012; Ceccarelli *et al.*, 2020; Brunner *et al.*, 2021) and coral population size structure (e.g., Hughes *et al.*, 2018; Pisapia *et al.*, 2019; Dietzel *et al.*, 2020; Lachs *et al.*, 2021). Considering that the vital rates of survival, growth, and reproduction follow consistent allometric scaling in corals (Dornelas *et al.*, 2017; Madin *et al.*, 2020), changes to coral population size structure will have major consequences for their population dynamics and viability. Indeed, small corals tend to have a higher probability of whole-colony mortality, while larger corals have higher partial mortality (*i.e.*, shrinkage) and fission (Hughes & Connell, 1987; Hughes & Tanner, 2000; Madin *et al.*, 2020). Large corals also have higher reproduction, but lower relative growth rates (Connell, 1973; Dornelas *et al.*, 2017). Because of these allometric relationships, investigating differences in size structure across populations experiencing increased disturbance can help reveal the ecological mechanisms that underlie population viability, such as differences in survival, growth and reproduction rates. For example, over the length of the entire Great Barrier Reef, Dietzel *et al.* (2020) found decadal declines in the abundance of large coral colonies in the northern and central regions, but an increase in the southern region compared to historical baselines. The spatial variation in the decline of large corals might indicate the depletion of coral brood stocks in some regions (Hughes *et al.*, 2019) but not others, thereby affecting population viability differently.

Previous studies have examined changes in coral population size structure using summary statistics such as mean size, variance, skewness, and kurtosis (e.g., Bak & Meesters, 1998; Anderson & Pratchett, 2014). These metrics characterize

aspects of the shape of the size-frequency distribution. However, the summary statistics approach involves making arbitrary choices about which statistics to include, and does not use all the information in the distribution (Talská *et al.*, 2018). Also, the ecological interpretation of measures such as kurtosis is not straightforward. Adjeroud *et al.* (2007) observed negative kurtosis (a flattened distribution, with a wide peak around the mean) for a fast-growing species, and the opposite for a slow-growing species. Since then, coral reef ecologists have related this metric to population growth and turnover rates (e.g., Anderson & Pratchett, 2014; Kramer *et al.*, 2020), but the conditions under which the proposed relationship between kurtosis and growth rate holds are unclear. The assessment and comparison of entire coral size-frequency distributions as probability density functions can overcome these challenges. Recent advances in functional data analysis (Ramsay *et al.*, 2009; Talská *et al.*, 2018) remove the need to arbitrarily select a few summary statistics as response variables. Since the entire probability density function is treated as the response variable (Talská *et al.*, 2018), the method can accurately quantify which coral sizes are most affected by the explanatory variables. This approach is likely to better capture the effects of long-term environmental stress on coral size-frequency distributions than summary statistics, allowing for improved comparisons and understanding of their dynamics.

Here, we examine the changes of scleractinian coral population size structure over 900 km in eastern Australia. Using the tropical to subtropical gradient as a proxy for increasing environmental stress (Kreyling *et al.*, 2014), we aim to understand how coral population size structure responds to, or is locally adapted to increasingly marginal conditions. We use two methodologies: 1) linear regression with summary statistics as response variables, an approach classically favoured by coral reef ecologists, and 2) a novel compositional functional regression approach (Talská *et al.*, 2018) that has never been used in this context. We use both methods here to demonstrate their respective strengths and weaknesses. At higher latitudes, where conditions are harsh due to extremes in temperature, light levels and storm events, we expect fewer small coral colonies, because coral mortality rates are generally highest for the smallest corals (Connell, 1973), and sexual recruitment rates are low in these comparatively harsher conditions (Harriott & Banks, 1995; Abrego *et al.*, 2021;

Cant *et al.*, 2022). Potential differences in population size structure of corals along this environmental gradient might indicate the effect of stress on coral population dynamics, providing a lens to the future, where reefs might be affected by increased disturbances as a result of climate change.

2.3 Methods

2.3.1 Data collection

The eastern Australian biogeographic transition zone is a unique region in which to observe coral population dynamics. There, coral communities occur from tropical Queensland's Great Barrier Reef (GBR) to the temperate, sometimes kelp-dominated rocky reefs in New South Wales (~23°S to 30°S). With increasing latitude, sea surface temperature and incident light intensity decline, while storm intensity and frequency increase (Pepler & Coutts-Smith, 2013), making the reef habitat increasingly marginal for tropical hard corals (Harriott & Smith, 2000; Sommer *et al.*, 2018). Multiple oceanographic currents are present in the region, with the Eastern Australian Current (EAC) being the largest (Baird *et al.*, 2008). The EAC runs approximately 50 km offshore (Malcolm *et al.*, 2011), transporting warm, tropical waters from the Coral Sea poleward. The current may also be a source of fresh genetic material for the downstream reefs (Beger *et al.*, 2014; Sommer *et al.*, 2014). Though we note that a recent study suggested that coral larvae dispersed from the southern GBR have a low probability of being received at higher latitude reefs (Mizerek *et al.*, 2021), where endemic coral species are increasingly found (*e.g.*, Schmidt-Roach *et al.*, 2013; Baird *et al.*, 2017). Nonetheless, the eastern Australian biogeographic transition zone represents a natural laboratory that allows the examination of differences in coral population size structure with increasing marginality.

We sampled coral populations across 20 sites in the eastern Australian biogeographic transition zone using underwater photographic benthic transect surveys. 12 sites were sampled in September 2018, while the eight other sites were sampled in either 2010, 2011, 2012 or 2016 (Figure 2.1; Table A-1). At each site, three 30 m belt transects were haphazardly run at 8-10 m water depth. Downward-facing photographs were taken every metre, from approximately 70 cm above the benthos. Each included a 50 cm calibration stick held at the level of the substrate (as in Sommer *et al.*, 2011). Two cameras were used: a Canon S90 with a wide-angle lens at most sites, and a Sony RX100V with a Nauticam

WWL-1 wide angle lens at Julian Rock Nursery, Cook Island and Flinders Reef. Since the field of view of the two cameras varied, images from the Sony RX100V were batch processed and cropped in ImageJ (Schindelin *et al.*, 2012) to ensure comparability, such that each frame captured approximately 1 m² of seabed.

On each image, coral species were visually identified to the lowest taxonomic classification possible (usually genus) using Coral Finder 2021 (Kelley, 2021) and Corals of the World (Veron *et al.*, 2016). Coral morphological types were also included and standardised following the classification of Sommer *et al.* (2021). Where variable growth forms are observed for the genera *Montipora*, *Porites* and *Turbinaria*, they were placed into categories of 'branching,' 'encrusting,' 'laminar' and 'massive'. For *Acropora*, the categories were 'arborescent,' 'corymbose,' 'digitate,' 'hispidose' and 'tabular,' following Kelley (2021). For each coral colony, the following were recorded: 2D planar area, taxonomic identity, and whether the colony was partially out of frame. This procedure was conducted using the freely available 'SizeExtractR' (Lachs *et al.*, 2022) workflow in ImageJ (Schindelin *et al.*, 2012) and R (R Core Team, 2021). We traced each coral colony manually, added relevant alphanumeric annotations, and compiled the resulting size data into a single database. Transect images that did not visibly contain corals were skipped. In total, 16,598 coral colonies were examined across 1,426 images, capturing 41 coral taxonomic entities (species, genera, family, or groups with uniquely identifiable morphological characteristics; see S2: Coral taxonomic identity along the environmental gradient).

Light limitation, temperature minima, and fluctuations determine the distribution and abundance of corals in our study region (Sommer *et al.*, 2018). To characterise and compare long-term environmental trends among our study sites, we extracted 4 km monthly chl_a (chlorophyll *a* concentration – a proxy for productivity), kd₄₉₀ (diffuse attenuation coefficient at 490 nm – a proxy for turbidity), and PAR (photosynthetically available radiation) from January 2003 to April 2019 (NOAA, 2012a, 2012b, 2022); and 1 km monthly Sea Surface Temperature (SST) from June 2002 to May 2019 (NOAA, 2022). The minima, maxima, means, and standard deviations of each environmental variable were calculated for each site, resulting in a total of 16 variables. A principal component analysis (PCA) was used for dimension reduction of these environmental factors (Figure 2.2.2). The first axis (PC1) explains 63% of the observed variance and

reflects a gradient from warmer, brighter environments with low turbidity and productivity (negative PC1 scores) to darker, colder environments with high turbidity and productivity (positive PC1 scores). The second axis (PC2), explaining 17% of the variance, is driven by minimum productivity, turbidity, and variation in light availability. Negative PC2 scores reflect environments that have the lowest productivity and turbidity, yet unstable light regimes, while positive scores reflect sites whose lowest turbidity and productivity is the least extreme and have the most stable light regimes.

2.3.2 Coral taxonomic identity along the environmental gradient

For the purpose of quantifying population size structure, we did not differentiate between taxonomic groups and consider all corals from the same site a 'population' to overcome having small sample sizes in some marginal reefs. We acknowledge the limitations of this in the discussion. We used Canonical Correspondence Analysis (CCA) to examine differences in taxonomic composition along the environmental gradient (PC1 and PC2 scores), as environmental tolerances vary among species (Sommer *et al.*, 2014). We showed that some taxa were shared among sites but along the gradient there were likely different dominant taxa for each morpho-taxa group (Appendix A; Figure A-1; S2: Coral taxonomic identity along the environmental gradient).

2.3.3 Data analyses

Colony sizes were natural log-transformed to normalise their distribution for subsequent analyses and increase the resolution of the highly abundant smaller size classes (Bak & Meesters, 1998). Throughout, log refers to natural logarithm. Colonies marked partially out of frame were excluded as we lacked their true size. This filter resulted in 12,224 coral colonies from 1,321 images, corresponding to 41 coral taxonomic entities. We used two methods to characterise the coral population size structure and establish its relationship with environmental covariates. The first was the calculation of summary statistics (Bak & Meesters, 1998; Adjeroud *et al.*, 2007; Anderson & Pratchett, 2014) followed by linear regression with the scores of PC1 and PC2 and their interaction as explanatory variables. The model combinations were evaluated using Akaike's Information Criterion (AIC). For each site, the summary statistics calculated were: 1) average coral size (both mean and median), a surrogate for coral age and fecundity (Soong & Lang, 1992). We used the median in linear regressions as it is not

strongly influenced by extreme colony sizes, which are common in our study populations. 2) Coefficient of variation, which allows the comparison of size variation across different sites. 3) Skewness, which measures the asymmetry of size-frequency distributions, with left or right skew indicating the dominance of larger and smaller corals, respectively. 4) Kurtosis, which measures the relative peakedness of a distribution, and has been used to represent growth and recruitment rates (Bak & Meesters, 1998; Adjeroud *et al.*, 2007; Anderson & Pratchett, 2014).

We then used compositional functional regression (Talská *et al.*, 2018) to test the effect of environmental covariates (PC1 and PC2 scores) on the entire size-frequency distribution. The benefit of this approach is that it is possible to examine how the entire distribution changes, as opposed to a single summary statistic, which does not capture all relevant properties of the size distribution. Compositional functional regression is needed here because our response variable (coral size-frequency distribution) is a probability density function. Probability density functions must be non-negative everywhere and integrate to one (note that non-negativity is a property of the function, the probability density, rather than the value of the argument to the function, log coral size). Standard functional regression (where the response variable is a continuous function instead of a number (e.g., Yen *et al.*, 2015) is already familiar to some ecologists, but does not ensure that the predicted response is a valid probability density function. Compositional functional regressions overcome this problem by working in a real vector space (Bayes space) (Egozcue *et al.*, 2013), whose elements are continuous probability density functions (Egozcue *et al.*, 2006; van den Boogaart *et al.*, 2014) on which we can do “addition” and “scalar multiplication” operations, such that the result is always a probability density function (S3: Bayes Space for more details). Once these operations are defined, we can write down a linear regression model for probability density functions. Consider the standard linear regression $response = intercept + explanatory\ variable \times coefficient + error$, then the analogous compositional functional regression equation takes the form

response function = intercept function

\oplus (explanatory variable \odot coefficient function) \oplus error function,

where the error function has a mean of zero. In our particular case, the regression model is

$$y_i = \beta_0 \oplus (x_{1,i} \odot \beta_1) \oplus (x_{2,i} \odot \beta_2) \oplus \varepsilon_i, \quad (1)$$

where y_i is the *response*, a probability density function representing the log coral size-frequency distribution at the i th site, the *explanatory variables* $x_{1,i}$ and $x_{2,i}$ are the PC1 and PC2 scores at the i th site, the *intercept* β_0 is the size-frequency distribution when each explanatory variable has the value 0, *coefficients* β_1 and β_2 are probability density functions describing the effect of a unit increase in PC1 and PC2 respectively on the size-frequency distribution, and the *error* ε_i is a probability density function representing the residual or error at the i th site.

Estimating densities (continuous size-frequency distributions) to use as the response variable is a necessary step in compositional functional regression. We binned the individual log coral area observations from each site into a histogram, and smoothed the data to obtain a continuous approximation to the histogram, over the entire observed range across all sites (Talská *et al.*, 2018). The number of bins for each site was chosen using Sturges' rule (Sturges, 1926). Where there were empty bins, we replaced the zeros by $\left(\frac{2}{3}\right) \times \left(\frac{1}{n_i}\right)$, where n_i is the number of corals observed at that site (Martín-Fernández *et al.*, 2003; Machalová *et al.*, 2021, p. 1053). We followed typical practice in the field, but the theory on how density estimation affects subsequent results is not yet well developed (Petersen *et al.*, 2022, sections 3 and 5). We therefore checked the robustness of our compositional functional regression results to different bin numbers used in histogram smoothing, as well as to sites with only very few corals (S6: Testing compositional functional regression model robustness).

Then, the size-frequency distributions were centred log-ratio (clr) transformed to give standard addition and scalar multiplication operations, which allows for easier computation (van den Boogaart *et al.*, 2014). The clr transformed size-frequency distributions were smoothed using cubic compositional splines (ZB spline basis functions (Machalová *et al.*, 2021)) with four knots. The optimum smoothing parameter alpha was chosen by generalized cross validation for each site. The compositional regression model given in Equation 1 was fitted to the binned and smoothed size-frequency distributions (Machalová *et al.*, 2021).

Approximate 95% confidence bands were obtained using bootstrap approximations. We calculated pointwise and global R^2 which measure proportions of variation explained by the model in an analogous way to the usual coefficient of determination (Talská *et al.*, 2018).

To determine whether the estimated effects of PC1 and PC2 could be distinguished from zero (no effect), pointwise and global permutation F -tests were performed with the observed pointwise F -statistic, and its maximum over the whole interval, respectively (Ramsay *et al.*, 2009, p. 168). The F -tests were carried out by permuting rows of the ZB-spline coefficients and re-estimating the regression model 9,999 times. We compared observed pointwise and max F -statistics with the distributions of these statistics from permutations. The residual functions were plotted (and coloured by PC1 score) to check for systematic departures from the model. The coefficient functions β_0 , β_1 and β_2 on the clr scale were plotted to visualize the size-frequency distribution at the mean of PC1 and PC2 (β_0) and the effects of each. On the clr scale, positive values of the coefficient functions β_1 and β_2 suggest an increase in density at a given log area per unit increase in the explanatory variable, and *vice versa*. Because PC1 seemed to capture most of the environmental variability in our study region, we visualised its effect by plotting the predicted coral size-frequency distributions at the mean value (0) of PC2, for ten equally spaced values of PC1 from its minimum to its maximum.

2.3.4 Size-biased sampling

Size-frequency distributions estimated from photographs are subject to sampling bias. The larger a coral colony, the less likely it is to fit entirely in the sampling window. Thus, including only those colonies that fit in the sampling window (“minus sampling” (Baddeley, 1998, p. 40)) as we have in this study, biases the estimated size-frequency distribution towards smaller colonies. There are ways to avoid such sampling bias but these require information from outside the sampling window (Baddeley, 1998; sections 2.2-2.4, 2.6; Zvuloni *et al.*, 2008), which is unavailable in our data. In S4: Size-biased sampling, we show that this sampling bias does not affect estimates of the coefficient functions for the effects of explanatory variables (β_1 and β_2) in a compositional functional regression, although the bias does affect the estimated intercept function β_0 . These coefficient functions are only defined over the interval of sizes that could fit in the

sampling window, so we have no information about effects on the density of colonies larger than the window. Summary statistics and the effects of explanatory variables on the summary statistics will also be subject to sampling bias, but we currently do not have simple solutions to account for these biases.

2.3.5 Model sensitivity to the 2016 bleaching event

In 2016, severe coral bleaching was recorded in northern and central GBR (Hughes *et al.*, 2017b). Although bleaching was less severe in the southern GBR and at the high latitude Eastern Australian reefs (Hughes *et al.*, 2017b; Kim *et al.*, 2019), the anomalous thermal stress in the region could have had unobserved impacts on corals leading to potential changes in population size structure. For this reason, we examined the temporal effect of our data by adding a categorical explanatory variable of pre- or post- bleaching to both the linear regression and the compositional functional regression analyses (S7: Model sensitivity to the 2016 bleaching event).

2.4 Results

2.4.1 Summary statistics and linear regression

Sites had between 38 (Woolgoolga Reef) and 2,101 (Lady Musgrave Island) colonies (median 526, first quartile 148, third quartile 718). Statistical summaries of the coral size-frequency distributions are reported in Table A-2. Colder, darker reefs with higher turbidity and productivity (high PC1 scores) had fewer coral colonies ($F_{2,17} = 6.80$, $P = 0.007$, $R^2 = 0.379$; Figure 2.3a; Table A-3), but with larger median sizes ($F_{1,18} = 10.7$, $P = 0.004$, $R^2 = 0.338$; Figure 2.3c; Table A-4), and were more negatively (left) skewed ($F_{2,17} = 7.45$, $P = 0.005$, $R^2 = 0.404$; Figure 2.3-Figure 2.4; Table A-5). Reefs with more constant light levels and less extreme minima in turbidity and productivity (high PC2 scores) were associated with more coral colonies and a positive skew in the population size structure (Figure 2.3b and e; Table A-3 and Table A-5). Weak evidence showed that CV and kurtosis were lower at high PC1 scores, suggesting that colony size variation was lower ($F_{1,18} = 2.35$; $P = 0.143$; $R^2 = 0.066$), and that coral population size structure was flatter ($F_{1,18} = 2.54$; $P = 0.128$; $R^2 = 0.075$) at colder, darker reefs with higher turbidity and productivity compared to warmer, brighter and less turbid environments (Table A-6 and Table A-7; Figure A-2 and Figure A-3).

2.4.2 Compositional functional regression

Compositional functional regression showed that as PC1 increased, reflecting the transition from warmer, brighter environments to more productive and turbid environments, a higher proportion of corals were bigger: the mode of the predicted distribution of log coral area moved to the right, and the predicted distribution became broader and flatter (Figure 2.5, red to blue lines). At the lowest PC1 score, the predicted modal log coral area was approximately 3.5 log cm² (33.1 cm², Figure 2.5, red), while at the highest PC1 score, the predicted modal log coral area was approximately 5 log cm² (148 cm², Figure 2.5, blue). Thus, large changes in coral size-frequency distributions along the environmental gradient were plausible. We further showed that increases in PC1 may be associated with lower densities of small to moderate sized corals (~2-4 log cm²) (Figure 2.6, interval where the 95% confidence band did not cross zero). The global R² for our model was 0.18, so that the model explained relatively little of the variation in size-frequency distributions, although with higher amounts of variation explained at coral sizes 2-4 log cm² (Figure A-7). Similar peaks were observed for the pointwise *F* test statistics (Figure A-8). However, because the maximum pointwise *F* statistic (Figure A-8, dotted line) did not exceed the 0.95-quantile of the distribution of such maxima anywhere (Figure A-8, dashed line; functional *F*-test, observed maximum *F* = 0.83, *P* = 0.08 from 9,999 permutations), it was plausible that from the compositional functional regression alone, neither PC1 nor PC2 affected coral size-frequency distributions (see discussion). For the effect of the intercept and PC2, model fit and residual diagnostics, see S5: Further compositional functional regression results and model diagnostics.

2.5 Discussion

Understanding the drivers of change in population size structure is fundamental to robust predictions of population dynamics (Edmunds & Riegl, 2020; Edmunds, 2021). Here, examining population size structure of corals across 20 reefs along the tropical to subtropical transition zone in Eastern Australia, we found fewer but bigger corals in sites characterised by greater environmental stress and temporal variability compared to sites that have a more stable environmental regime. It is plausible that the high coral cover in Australian high-latitude coral communities (Harriott *et al.*, 1994; Sommer *et al.*, 2014) is created by few large coral colonies. This supports the idea that the lower growth rates and higher fission rates of

larger corals (Dornelas *et al.*, 2017) could be the main driver of coral persistence in marginal reefs (Cant *et al.*, 2022). We hypothesise that future reef persistence might be governed by low growth and recruitment, and be reliant on the survival and higher fecundity of larger corals (Bak & Meesters, 1999; Cant *et al.*, 2020; Dietzel *et al.*, 2020).

This is the first study to use compositional functional regression (Talská *et al.*, 2018) to examine population size structure changes along a large biogeographic gradient. The ability to model the entire probability density curve allows us to determine the effects of environmental drivers on corals of different sizes. Specifically, we show that with increasing environmental stress and variability, we risk losing small to medium sized corals at 7-55 cm². This cannot be concluded from linear regressions of summary statistics. Furthermore, many ecologically important properties are functions of size, including carbonate production and linear extension for corals (Carlot *et al.*, 2021). Compositional functional regression will allow us to link predictions about changes in size distributions to changes in these ecologically important properties. For example, given a predicted change in size distribution with respect to an environmental variable (e.g., increasing SST), and the relationship between the property of interest (e.g., carbonate production) and size, we can calculate the predicted population-level change in the value of the property (e.g., mean carbonate production per colony) with respect to the environmental variable. In contrast, generally it is not possible to do such calculations given estimated effects on a summary statistic. Similarly, size distributions, rather than summary statistics, are required for modern demographic techniques such as Integral Projection Models (IPMs) (e.g., Kayal *et al.*, 2018; Cant *et al.*, 2020).

Both linear regression and compositional functional regression results identified fewer but bigger corals in marginal reefs, although the evidence from the latter was weaker. Nevertheless, the observed change in summary statistics such as the median (for which there is strong evidence) imply changes in the size-frequency distribution, so that the combined evidence from both methods suggests an effect. The difference in strength of evidence could simply be methodological, *i.e.*, having to consider the effect of the environmental covariates on the entire size-frequency distribution at each reef in compositional functional regression, as opposed to just a single value (of a summary statistic) in linear

regression. It is possible that there is simply a relatively large amount of (random) variation in the density functions (size distributions) among our twenty sites. Although we did not find strong support for temporal effects considering the results from both methods, there was weak evidence that median coral size was smaller and CV was greater at sites surveyed after the 2016 bleaching event (S7: Model sensitivity to the 2016 bleaching event). This finding suggests that where time series data are available, exploring how major disturbances affect size structure over time will be a worthwhile endeavour. Indices summarising local threat levels from human activity (e.g., Burke *et al.*, 2011) might also explain some of the variation in size distributions.

In addition to the environmental parameters examined, other variables could also have acted on the coral size-frequency distributions. For example, storm waves can differentially overturn corals of different sizes and growth forms (Madin *et al.*, 2014), indicating that high latitude environments could well select for larger, more stable horizontally spreading morphologies in our study region (Sommer *et al.*, 2014); and the morphology, taxonomic identity and life-history of corals (Darling *et al.*, 2012) can determine the sizes to which they could grow. There is already some evidence of this across our sites (Figure A-1, S2: Coral taxonomic identity along the environmental gradient). For example, both the encrusting *Micromussa lordhowensis*, and laminar *Turbinaria* are commonly observed on subtropical reefs in this region, but *M. lordhowensis* colonies are generally much smaller. Recent observations of speciation of endemic corals also indicate that evolutionary processes are at play in this region (Schmidt-Roach *et al.*, 2013b; Baird *et al.*, 2017). Where sample sizes are large enough, it will be meaningful to investigate taxa specific population size structure (e.g., Rich *et al.*, 2022; Bernard *et al.*, 2023) along this environmental gradient. Reefs with higher rugosity and thus complexity could support more smaller corals (Crabbe, 2010), meaning reef topography could also be relevant. Competition for space can also reduce the rate at which corals grow (Chadwick & Morrow, 2011), including competition with other non-coral, sessile benthic organisms like algae, corallimorpharians and zoanthids that are abundant on high-latitude reefs (Abrego *et al.*, 2021; Reimer *et al.*, 2021).

Our work assessing coral population size structure over a large biogeographic scale offers a glimpse into a possible response of coral assemblages to

environmental change. Our main finding of increasingly marginal conditions selecting for fewer but larger coral colonies, echoes previous findings that larger corals remain post-disturbance (Bak & Meesters, 1998; Dietzel *et al.*, 2020; Lachs *et al.*, 2021), but see also Pisapia *et al.* (2020) for examples of colonies becoming smaller. The demographic mechanisms that can lead to the prevalence of fewer but bigger corals are likely a combination of low recruitment, partial mortality and slow growth. As ongoing climate change leads to more variable and extreme environmental conditions (Spady *et al.*, 2022), it is possible that some corals in biogeographic transition zones are adapting to changing conditions. Through this observational study, we hypothesise that on a population level, marginality could select mechanisms that shift the population size structure of reef corals towards a larger proportion of bigger individuals, or towards a composition with species that can reach larger sizes. Such a shift is concerning because coral populations with fewer smaller corals (juveniles) suggest recruitment failure, and thus a lowered recovery potential following further disturbances (Riegl *et al.*, 2012; Pisapia *et al.*, 2019; Dietzel *et al.*, 2020; Lachs *et al.*, 2021). In addition, small coral fragments broken off from mature colonies retain their reproductive capacity (Rapuano *et al.*, 2023), but have a higher relative growth rate compared to the original colony, due to a reduction in size. This indicates that smaller corals (both coral recruits and those fragmented from larger corals by natural processes) could be disproportionately important for population persistence. Thus, we recommend improving our understanding of coral reproduction, dispersal and recruitment dynamics along latitudinal gradients (e.g., Mizerek *et al.*, 2021), as it can provide an insight into how coral populations persist and recover despite suboptimal conditions. Further demographic work in this region would be insightful for continuous monitoring and the ground-truthing of our hypothesis.

Climate change will continue to affect population dynamics worldwide (Lawson *et al.*, 2015). Thus, it remains pertinent for ecologists to examine changes in population size structure at biogeographic scales through time (e.g., Riegl *et al.*, 2012; Dietzel *et al.*, 2021). Advances in compositional functional regression (Talská *et al.*, 2018) provide a comprehensive tool for ecologists to examine population size structure, allowing us to gain insight into how environmental extremes and variabilities affect population dynamics (Kreyling *et al.*, 2014). Collectively, our work on the coral population size structure of reefs in the Eastern

Australian biogeographic transition zone highlights fundamental differences along the ~ 900 km tropical to subtropical gradient, where bigger corals are likely selected for in marginal conditions. While the survival of larger corals allows for the persistence of reef habitats, the lack of smaller corals indicates recruitment failure and could signify a lowered resilience to further disturbances.

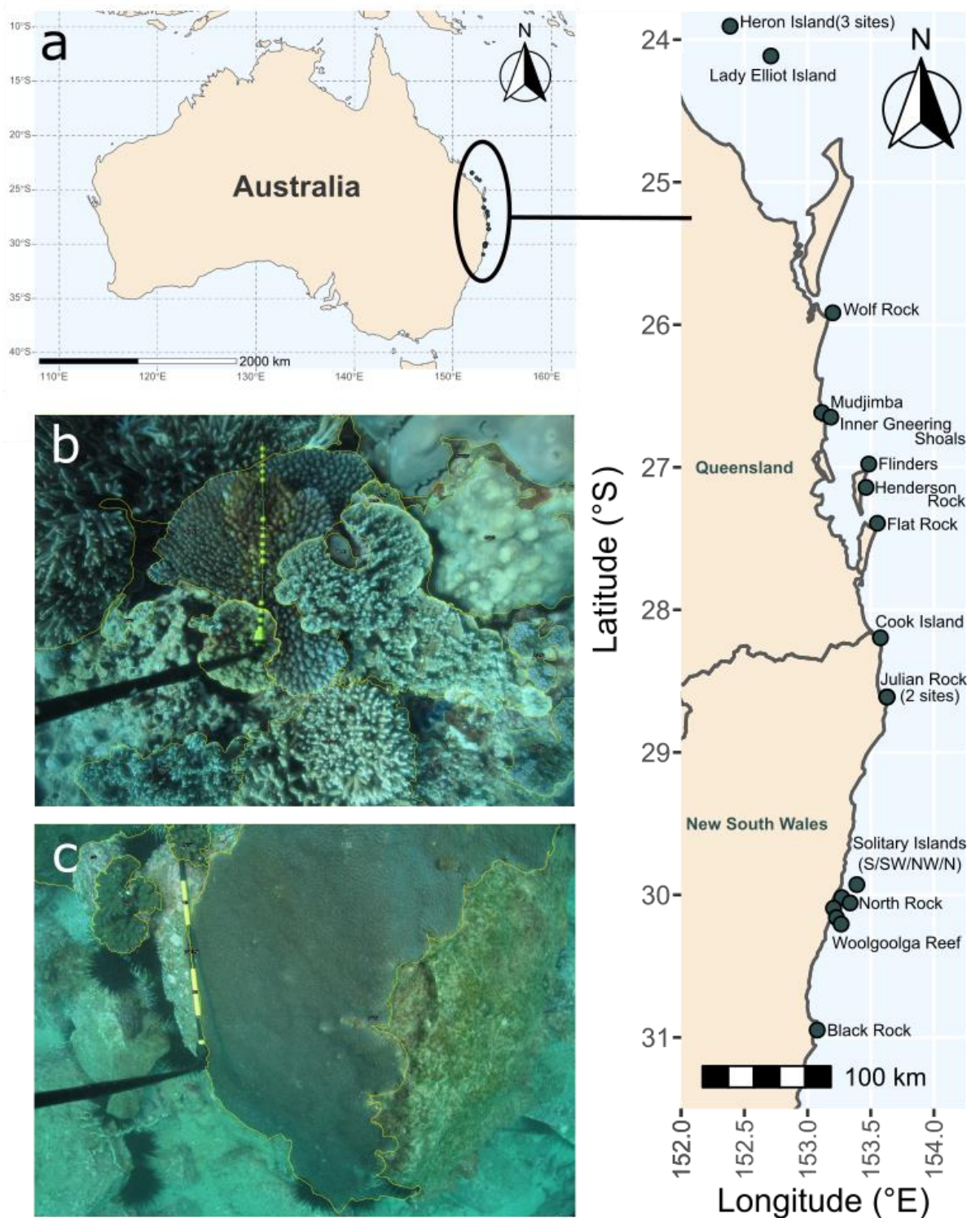


Figure 2.1. Survey design of the study, showing a) the location of the 20 sampling sites in eastern Australia; image examples of the outlined coral communities from b) Lady Elliot Island and c) Black Rock. The 0.5 m black and yellow graduated calibration stick is visible. Corals that were not completely in frame, like the largest one in c) were not included in the final dataset.



Figure 2.2. Biplot showing the PCA ordination of our 20 coral populations (Figure 2.1a) using the 16 environmental variables. Reef names are labelled in grey, the blue arrows are the environmental factors which include the minima (min), maxima (max), means and standard deviations (sd) of chlorophyll a concentration (chla), diffuse attenuation coefficient at 490 nm (kd490), sea surface temperature (sst) and photosynthetically available radiation (PAR). The first and second axes jointly explain 80% of the environmental variation in this region.

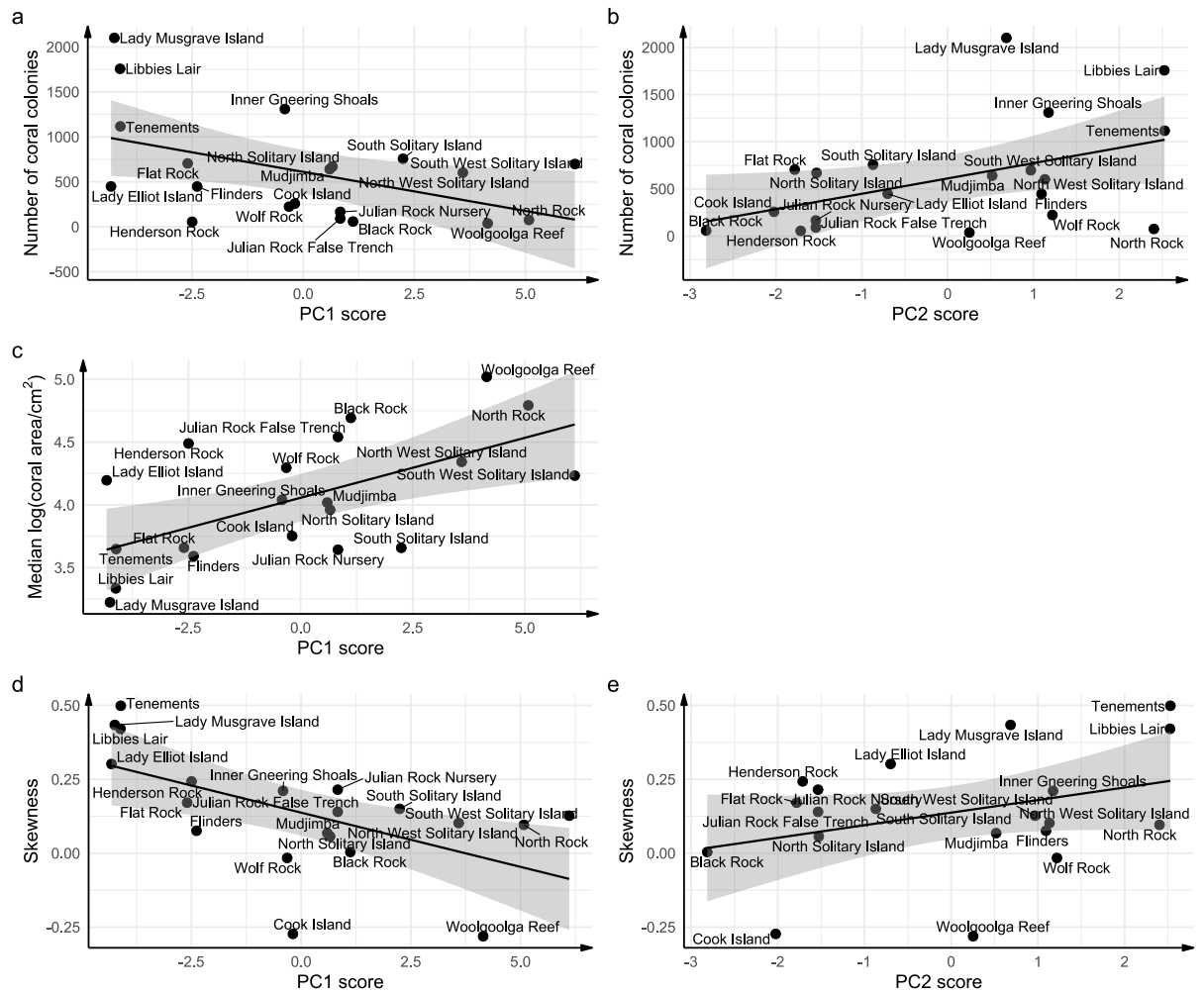
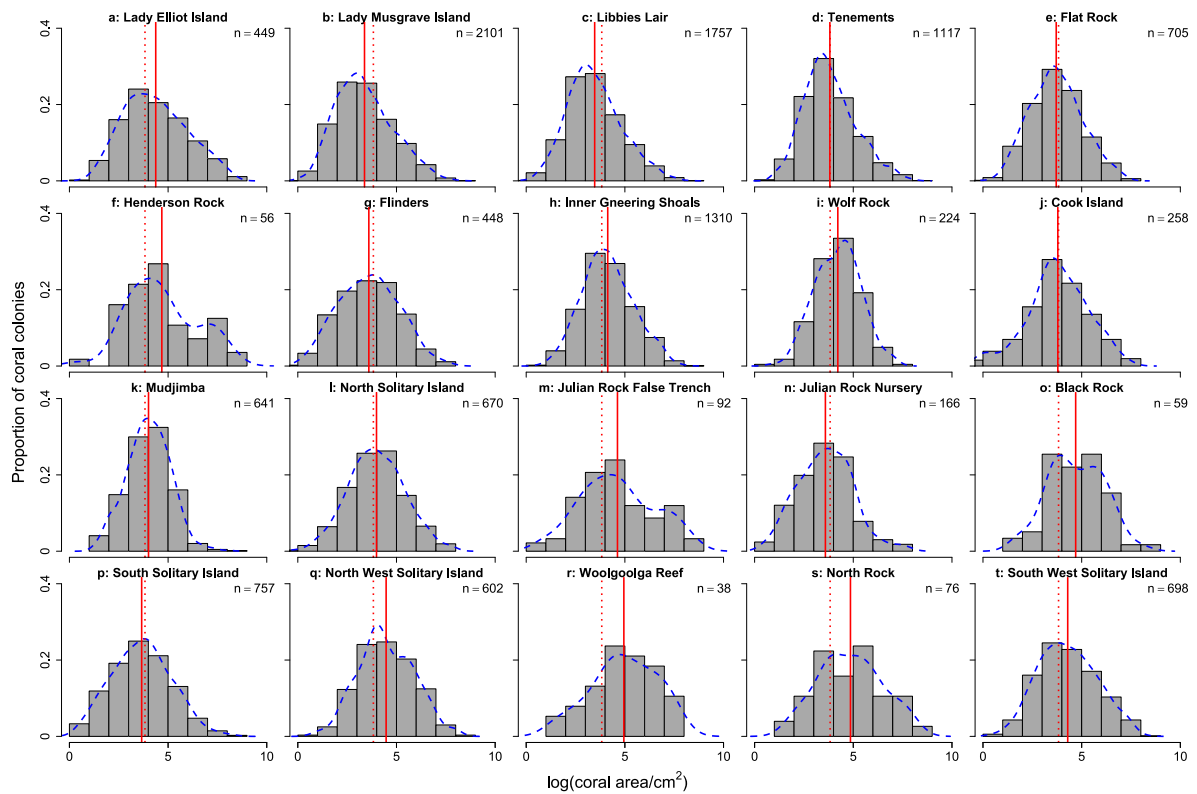


Figure 2.3a) The number of coral colonies decreases with PC1 and b) increases with PC2. c) Median coral colony size increases with PC1. d) Skewness of the coral size-frequency distribution decreases with increasing PC1 and e) increases with PC2. The black line is the line of best fit, and the grey region is the 95% confidence band. The explanatory variables plotted here were chosen based on model selection (Table A-3 to Table A-5). For a), c) and d), more positive PC1 scores represent lower sea surface temperature and photosynthetically available radiation (PAR), *i.e.*, colder and darker, and high chlorophyll *a* concentration and turbidity (kd490), *i.e.*, more productive and more turbid. In b) and e) more positive PC2 scores represent higher minima of chlorophyll *a* concentration and kd490 *i.e.*, lowest turbidity and productivity is least extreme; and lower standard deviations of PAR *i.e.*, more stable light regimes.



1
 2 Figure 2.4. Histograms showing coral colony size structure for each of the 20 reefs.
 3 All plots are on the same scale. Blue dashed lines are density estimates. Red solid
 4 lines are the site-wise mean log coral colony size. Red dotted lines show the global
 5 mean log coral colony size (3.82 log cm²) over all 12,224 coral colonies. Panels (a-t)
 6 are ordered from low to high PC1 scores. Increases in PC1 represents increasingly
 7 marginal conditions (colder, darker, more turbid and productive waters).

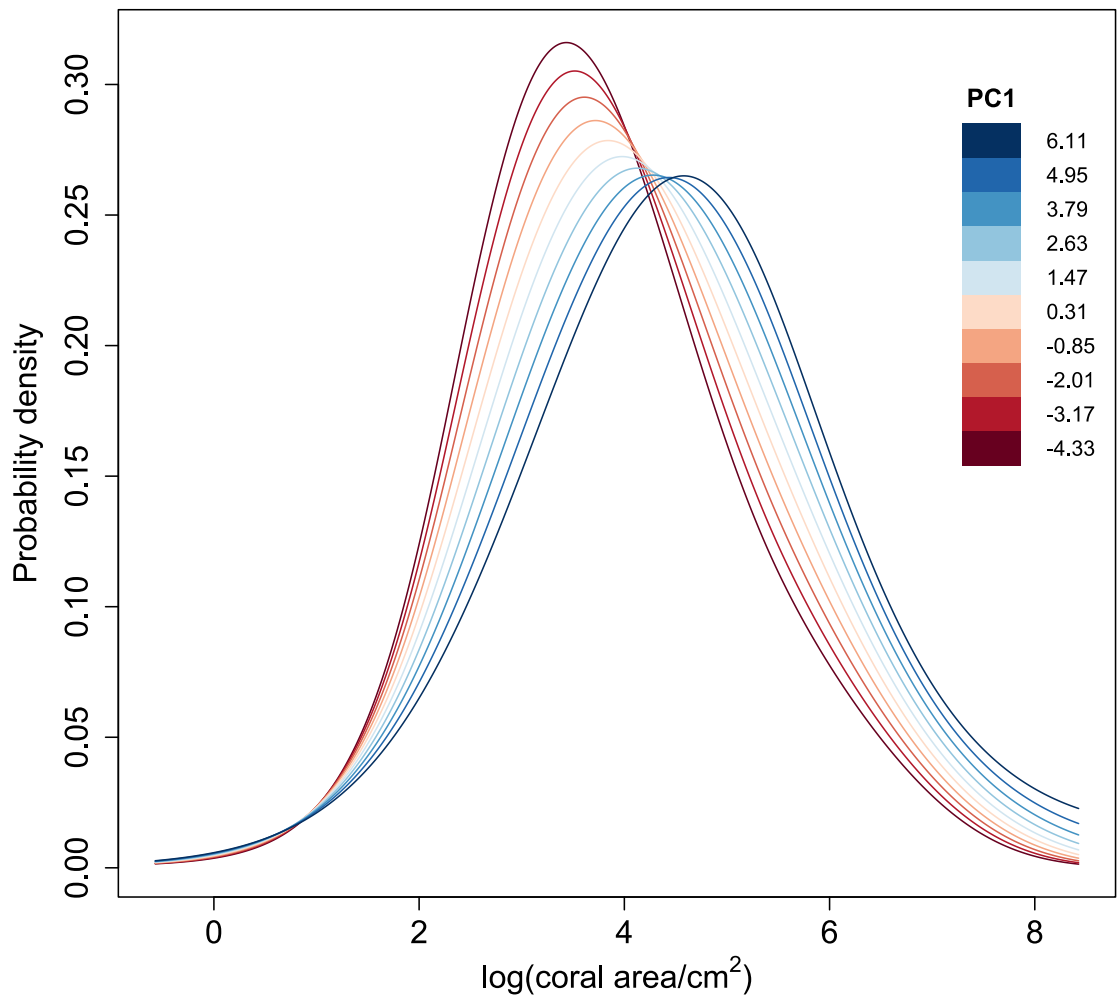


Figure 2.5. As PC1 increases, the predicted distributions of log coral area become broader and flatter, and the mode increases from ~ 3.5 to $5 \log \text{cm}^2$. Increases in PC1 represents increasingly marginal conditions (colder, darker, more turbid and productive waters). Red to blue lines correspond to predicted distributions for ten equally spaced PC1 scores, from the minimum (-4.33, darkest red) to the maximum (6.11, darkest blue). PC2 values are kept constant at 0 (the mean). The coefficient function β_1 determines how the shape of the distribution changes with PC1 but individual distributions are also affected by β_0 (the intercept) and thus by the sampling bias (S3: Size-biased sampling).

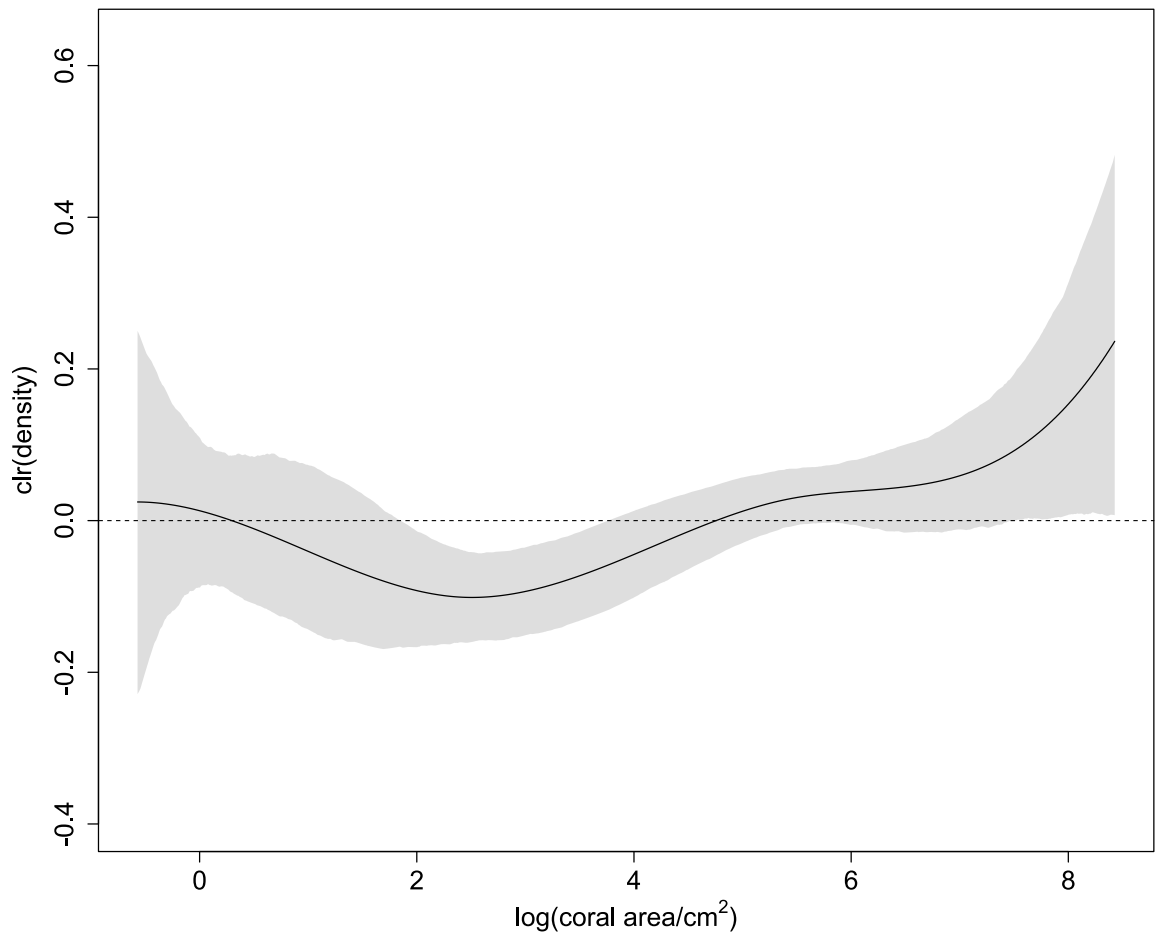


Figure 2.6. Increases in first axis (PC1) scores mean lower densities of corals at ~2-4 log cm². Increases in PC1 represents increasingly marginal conditions (colder, darker, more turbid and productive waters). The black line is the estimated centred log-ratio (clr) transformation of the coefficient function β_1 , which measures the effect of a unit increase in PC1 on the probability density of a given log coral area. Positive values on the y-axis suggest that the corresponding log coral area on the x-axis becomes more likely as PC1 increases, and negative values suggest that the corresponding log coral area becomes less likely. The shaded region is the bootstrap 95% confidence band. The horizontal dashed line represents no effect of PC1 on the probability density of log coral area.

Chapter 3 : Model choice and sampling bias in fish and coral size spectra

3.1 Abstract

Projecting future population growth requires knowledge of population size spectra, because vital rates such as growth, survival and reproduction are size-dependent. An ecological size spectrum is the distribution of body sizes in an ecological community, and is typically assumed to follow a power law distribution. Changes to ecological size spectra are used as indicators for many processes, such as measures of primary productivity and recovery from anthropogenic disturbances. Using coral and fish data from the East Australian biogeographic transition zone, we test if alternative statistical distributions better describe ecological size spectra. We show that bounded power law might not be the best fit for size-abundance data, as it overestimates the abundance of large organisms and that the log-normal distribution is generally a better fit. To examine potential sampling biases of commonly used field methods, we also adjusted for the size-biased sampling of coral colonies from benthic photo transects, which occurs because larger colonies are less likely than smaller colonies to fit entirely in the field of view. Because large organisms have disproportionate influence on the vital rates of a population, such as high fecundity, an overestimation of the largest individuals can lead to overly optimistic conclusions about the community or population of interest. Our results suggest that ecologists should consider the choice of distribution used in their size spectra modelling carefully, and consider multiple model outputs before informing conservation and management decisions.

3.2 Introduction

Organism size is a biological property that is simultaneously a response to the environment, and a consequence of ecological processes happening at individual, population and community levels. Size can be any meaningful measure of organism body extent such as length, area or volume. Because many biological rates scale allometrically with body size, e.g., metabolism (Kjørboe & Hirst, 2014), growth (Dornelas *et al.*, 2017) and reproductive output (Barneche *et al.*, 2018), the abundance-size distribution of communities provides useful insights into demographic processes (Bak & Meesters, 1998), energy fluxes in food webs (Heather *et al.*, 2021) and ecosystem functioning (Yvon-Durocher & Allen, 2012). Understanding what statistical distribution best describes the size spectra is

important for the reconstruction of past population structure (Dietzel, 2020, chapter 4), for example, to understand population trends. Conventionally, the bounded power law and log-normal distributions are used to model the abundance-size distribution of fish (Edwards *et al.*, 2017) and coral (Bak & Meesters, 1998) populations respectively. However, it remains unclear why one was favoured over the other, even though the same properties are modelled.

The size spectrum, or individual size distribution, is a frequency distribution, or probability density function of sizes in a community (White *et al.*, 2007; Edwards *et al.*, 2017). There has been a long history of modelling community size spectra using power law relationships, attributed to physiological rates that are observed to scale with size described by a power law relationship, in which the abundance (N) and body size (M) follow $N \propto M^\lambda$ (Andersen, 2019, chapter 2). However, the exponent λ often varies: stands of competing plants 'self-thin', such that as individual plant biomass increases, the number of plants decreases to the exponent of -1.5 (Yoda *et al.*, 1963; Adler, 1996). Damuth (1981) observed that population density of small herbivorous mammals decreases with increasing body mass with an exponent of -0.75, while marine plankton concentration decreases with increasing cell diameter to the exponent of roughly -2 (Sheldon & Parsons, 1967). The power exponent varies across guilds and communities (Muller-Landau *et al.*, 2006; Hatton *et al.*, 2019; Tekwa *et al.*, 2023), but within a community, the exponent can be used as an indicator of ecosystem health (Jennings & Blanchard, 2004; Petchey & Belgrano, 2010; Gjoni *et al.*, 2024). For example, in fish communities subject to varying fishing intensity (e.g., Graham *et al.*, 2005; Carvalho *et al.*, 2021), removal of larger fish species leads to the steepening of the size spectra and thus a decrease in its exponent. It follows that size spectra changes are useful ecological indicators for processes of interest to ecologists and resource managers alike across the terrestrial, aquatic and marine realms. For example, accurate approximations of size distributions are key to keeping track of population recovery from disturbances and the effectiveness of management strategies (e.g., Coomes *et al.*, 2003; Jennings & Blanchard, 2004).

The analyses of size spectra rely on the assumption that a bounded power law is a good descriptor of the ecological size spectrum (Reuman *et al.*, 2008; Edwards *et al.*, 2017). Power law distributions may be reasonable choices when the data

span a few orders of magnitude (Newman, 2017), which may be the case for cross-phyllum or cross-class body size data. Power law distributions are heavy tailed, not exponentially bounded and have a higher probability for the largest values, i.e., at the upper tail, than the Gaussian or exponential distributions (Pinto *et al.*, 2012). Its cumulative distribution function gives a simple linear relationship when plotted on a log-log scale (White & Kearney, 2014), which makes it easy to identify. The bounded power law is, however, preferable when considering ecological size spectra, because organism size typically has an upper limit. Also, there are usually upper and lower limits to the sizes of organisms sampled (e.g., the mesh size of fishing gear) determined by sampling methods and limitations (Reuman *et al.*, 2008; Edwards *et al.*, 2017). The bounded power law may capture a size distribution elegantly: for a fixed size range x_{min} to x_{max} , a large exponent b indicates a population or a community with more larger individuals. However, the bounded power law might not be the best fit, especially in the upper tail (largest sizes) of the distribution (see model fits in e.g., Robinson *et al.*, 2017; Carvalho *et al.*, 2021; Pomeranz *et al.*, 2022), and questions are raised as to how common (bounded) power law distributions are (Muller-Landau *et al.*, 2006; Stumpf & Porter, 2012). Blindly using a single, potentially poorly-estimated parameter to describe the status of a community could therefore lead to incorrect conclusions about its health, and hide demographic processes and indicators that might be gleaned from assessing changes to the entire size spectrum (Chong *et al.*, 2023; Canty *et al.*, 2024).

The log-normal distribution may also be an appropriate description for size spectra. It has been widely used to understand ecological abundances (Preston, 1962; Pennington, 1996; Talis *et al.*, 2023), and notably also to model coral population size structure (e.g., Bak & Meesters, 1998; Dietzel *et al.*, 2020) which is usually positively skewed (there are usually more smaller corals relative to large ones). Under the log-transformation, coral size frequency often follows a normal distribution. The log-normal distribution has two parameters, the mean μ and the standard deviation σ , which can be tuned independently, affording a higher degree of flexibility than the bounded power law. Despite this, the log-normal distribution is typically not used to model community size spectra in fisheries. This might be because of the apparent ubiquity of power law relationships in biological rates, like the Gill Oxygen Limit Theorem (GOLT)

(Pauly, 2021) in fishes. In addition, within a fixed size range, having one parameter (the exponent b) that describes the distribution might be more convenient than estimating two in the log-normal distribution.

Sampling biases stemming from limitations of commonly used field methodologies also need to be considered when studying size distributions. In particular, sampling biases often affect estimates of size distributions of sessile organisms from quadrat data in ecology (Baddeley, 1998; Zvuloni *et al.*, 2008), yet this issue is rarely acknowledged. For example, larger corals are less likely to fit entirely within quadrat sizes (e.g., 0.5 m x 0.5 m) commonly used in the field, or within a camera's field of view for benthic photo transects. In many cases, organism sizes are only known when the organism fits entirely in the quadrat or sampling unit. Thus, the exclusion of objects that do not fit entirely is often necessary, a process called minus-sampling (Baddeley, 1998, p. 40). Because larger objects are more likely to be excluded, the observed (minus-sampled) size distribution will underestimate the density of larger objects. Applying a minus-sampling correction should therefore improve the data fit.

The distribution chosen to model size spectra influences how we understand, quantify, and predict the viability of populations. Here, we aim to examine the fit of distributions for both sessile and motile marine taxa. Using coral and reef fish data from the East Australian biogeographic transition zone, we ask 1) whether the bounded power law or log-normal distribution is a better description of coral and fish size distributions; 2) for coral data, whether the minus-sampled versions of the two distributions are better fits, since our coral data were affected by a minus-sampling bias; and 3) whether the observed data fit patterns hold across taxa along the entire gradient of tropical to temperate reefs.

3.3 Methods

3.3.1 Data collection

We collected fish and coral data from 20 coral communities along the tropical to temperate transition zone of eastern Australia between 2010-2018 (Table B-1), at 8-10 m water depth. These 20 sites can be characterized by a tropical-to-marginal environmental gradient, from warm, bright environments with low turbidity to darker and colder environments with high turbidity (Chong *et al.*, 2023), which broadly correlates with latitude but is also affected by the East Australian

Current which flows roughly 50km offshore (Archer *et al.*, 2017). At each site, fish assemblages were sampled using underwater visual census (UVCs) along three to five 50 m long x 5 m wide transects. Species identification, abundance and length estimates (to the nearest cm) for all non-cryptic, mobile fish fauna were recorded *in-situ*. We estimated the biomass for each fish following the length-weight equation of $\text{weight} = \alpha \times \text{length}^\beta$, where α is the intercept and β is the slope. We retrieved the parameters α and β for each species from FishBase (Froese & Pauly, 2024). For coral assemblages, downward-facing photos of the benthos were taken at every metre for 30 m, with a 50 cm calibration stick in frame (Sommer *et al.*, 2014). The resulting image sampled approximately 1.4 m² (1.37 m x 1.02 m) of the seabed. We then extracted coral taxa and sizes (2D planar area) using ImageJ (Schindelin *et al.*, 2012) following the SizeExtractR work-flow (Lachs *et al.*, 2022). Only measurements from coral colonies that fitted entirely into the camera field of view were included in the subsequent analyses. Summaries of coral (Figure B-1, Table B-2) and fish abundance and sizes (Figure B-2, Table B-3) are provided.

3.3.2 Fish data from Indonesia

In the interest of using data from more than one UVC observer, we also used fish data from Carvalho *et al.* (2021). We also fitted the log-normal distribution to reef fish biomass data from three regions in Indonesia: Raja Ampat (Eastern Indonesia), Wakatobi (South-East Sulawesi) and Lombok (East of Bali) (for sampling details, see Carvalho *et al.*, 2021). These three regions have varying levels of fishing pressure. Model comparisons and visualisations were performed as described below.

3.3.3 Distributions, the theory on minus-sampling and parameter estimation

For data from each site, we fitted separately: 1) bounded power law and 2) log-normal distributions to fish biomass and coral area data; and 3) minus-sampled bounded power law and 4) minus-sampled log-normal distributions to the coral area data, as the coral data were subject to a minus-sampling bias. Throughout, coral sizes are in cm², fish biomass is in kg, and mentions of log refer to natural logarithm.

3.1.1.1 Bounded power law

The bounded power law distribution has a probability density function $f(x)$ for size x lying between minimum x_{min} and maximum x_{max} , given by

$$f(x) = Cx^b, \quad x_{min} \leq x \leq x_{max}, \quad (1)$$

where

$$C = \begin{cases} \frac{b+1}{x_{max}^{b+1} - x_{min}^{b+1}}, & b \neq -1, \\ \frac{1}{\log x_{max} - \log x_{min}}, & b = -1. \end{cases} \quad (2)$$

(Edwards *et al.*, 2017). We estimated the parameter b by maximum likelihood using R code adapted from Edwards *et al.* (2017), in which the log-likelihood is minimized numerically using the R function `nlm()`. The parameters x_{max} and x_{min} are estimated by the maximum and minimum values of the data (Edwards *et al.*, 2017, supporting information A.1.2). Under the assumption that each coral colony or fish is an independent observation, the log-likelihood $\log L$ is given by

$$\log L = n \log C + \hat{b} \sum_{i=1}^n \log x_i, \quad (3)$$

where n is the number of corals or fish at a given site, C is the normalization constant (Equation 2), \hat{b} is the estimated exponent of the bounded power law, and x_i is the size of the i th coral or fish at a given site (Edwards *et al.*, 2017, supporting information A.1.2). A more negative b , *i.e.*, a steeper slope, indicates a population with a higher proportion of small corals or fish.

3.1.1.2 Log-normal

The probability density function of the log-normal distribution is

$$f(x) = \frac{1}{x\sigma\sqrt{2\pi}} e^{-\frac{(\log(x)-\mu)^2}{2\sigma^2}}, \quad (4)$$

where σ is the scale parameter (standard deviation of log size at the site), and μ is the location parameter (mean log size at a given site) (Forbes *et al.*, 2010, p.

131). Under the assumption that each coral or fish is an independent observation, the log likelihood for a set of n sizes is given by

$$\log L = -\sum_{i=1}^n \log x_i - n \log \hat{\sigma} - \frac{n}{2} \log 2\pi - \frac{1}{2} \sum_{i=1}^n \left(\frac{\log x_i - \hat{\mu}}{\hat{\sigma}} \right)^2, \quad (5)$$

where the maximum likelihood estimate $\hat{\mu}$ of the location parameter is the usual sample mean of the log sizes, and the maximum likelihood estimate $\hat{\sigma}$ of the scale parameter is $\sqrt{\frac{n-1}{n}}$ times the usual sample standard deviation of the log sizes. We used the `dlnorm()` function in R to calculate the log likelihood. For two log-normal size distributions whose $\hat{\sigma}$ are different, the one with the larger $\hat{\sigma}$ predicts a larger proportion of organisms with sizes greater than a given threshold, regardless of their $\hat{\mu}$. This makes $\hat{\sigma}$ a potentially useful parameter to compare the size structure between populations by highlighting the proportion of corals that are greater than a given size.

3.1.1.3 Minus sampling in coral data

As we only observed the sizes of corals that were completely within the frame, the distribution of sizes sampled by our methodology under-samples the larger corals, and will be different from the distribution of all coral sizes. To tackle this issue, we made some simplifying assumptions: 1) corals are circular (Zvuloni *et al.*, 2008), 2) coral colony size does not depend on location, and 3) quadrats are randomly located, so that the probability a coral lies in the frame is a function of size alone.

Let θ be the event that we observe a coral (where the entire colony fits in the frame). It can be shown that the probability an object of area x lies entirely within a randomly-placed rectangular frame with width w and height $v \leq w$ is $\frac{(w-r_1)(v-r_2)}{wv}$, where r_1 and r_2 are the width and height of the smallest rectangle aligned with the frame that contains the object (Baddeley, 1998, p. 50). For a circular colony with area x , the smallest rectangle aligned with the frame that contains the object is a square with side length $2\sqrt{\frac{x}{\pi}}$, so the conditional probability $\mathbb{P}(\theta|x)$ that a coral of area x lies entirely in the frame is

$$\mathbb{P}(\theta|x) = \begin{cases} \frac{\left(w - 2\sqrt{\frac{x}{\pi}}\right)\left(v - 2\sqrt{\frac{x}{\pi}}\right)}{wv}, & \text{if } x < \frac{\pi}{4}v^2, \\ 0, & \text{otherwise.} \end{cases} \quad (6)$$

We assume that $\frac{\pi}{4}v^2$ is the area of the largest coral that can fit in the frame, and that $\frac{\pi}{4}v^2 < x_{max}$ (i.e. that some corals are too big to fit within the frame). Note that v and w are known constants of image dimensions, not parameters estimated from the data (Figure B-3).

Let $f(\theta, x)$ be the joint density of event θ and area x . Then

$$\begin{aligned} f(\theta, x) &= \mathbb{P}(\theta|x)f(x) \\ &= f(x|\theta)\mathbb{P}(\theta), \end{aligned} \quad (7)$$

where $f(x)$ is the underlying size distribution without sampling bias, $\mathbb{P}(\theta)$ is the probability of observing a coral of any area (assumed not to be zero), and $f(x|\theta)$ is the conditional density of observing a coral of area x . We then use Bayes' Theorem to find the conditional density of observed coral area. Dividing both sides of Equation 7 by $\mathbb{P}(\theta)$ gives

$$f(x|\theta) = \frac{\mathbb{P}(\theta|x)f(x)}{\mathbb{P}(\theta)} = \frac{\mathbb{P}(\theta|x)f(x)}{\int \mathbb{P}(\theta|x)f(x)dx}, \quad (8)$$

where the integral in the denominator is over all areas x that could possibly be observed in the given frame of size $w \times v$.

3.1.1.4 Minus-sampled bounded power law

We account for the size bias caused by minus sampling using a 'minus-sampled' bounded power law. Following Equation 7, the conditional density $f(x|\theta)$ is given by

$$f(x|\theta) = f(x) \times g(x), \quad x_{min} \leq x < \frac{\pi}{4}v^2 \quad (9)$$

where $f(x)$ is given by Equation 1 and the factor $g(x) = \frac{\mathbb{P}(\theta|x)}{\int \mathbb{P}(\theta|x)f(x)dx}$ corrects for minus-sampling bias and is given by

$$g(x) = \mathbb{P}(\theta|x) \left[\int_{x_{min}}^{\frac{\pi}{4}v^2} f(x) \times \mathbb{P}(\theta|x) dx \right]^{-1}, \quad (10)$$

where $\mathbb{P}(\theta|x)$ is given by Equation 6. Note that x_{max} from Equations 1 and 2 is no longer a parameter, because of the assumption that there are some corals too large to fit in the frame, so is replaced by the area of the largest observable coral, $\frac{\pi}{4}v^2$. Then the log-likelihood for the minus-sampled bounded power law is the sum of the log of Equation 10 over all observed colonies (S2: Probability density function for the minus-sampled bounded power law). The maximum likelihood estimate of b was found numerically by minimizing the log-likelihood with respect to b over the interval $(-3, 0)$, using the `optimize()` function in R. This interval was chosen because it must be negative and for most real world applications it falls between -2 and -3 (Clauset *et al.*, 2009). As with the bounded power law, the smallest coral observed is the maximum likelihood estimator of x_{min} . This is because the integrand in the denominator is always non-negative, so increasing x_{min} reduces the denominator, up to the point where x_{min} equals the area of the smallest coral.

3.1.1.5 Minus sampled log-normal

We obtained the minus sampled log-normal distributions similarly to minus-sampled bounded power law described in section 3.1.1.4, with $f(x)$ in equations (9) and (10) given by equation (4):

$$f(x|\theta) = \frac{1}{x\sigma\sqrt{2\pi}} \exp\left\{-\frac{(\ln(x)-\mu)^2}{2\sigma^2}\right\} \times g(x) \quad (11),$$

The integral in the denominator of equation (10) was computed numerically using `integrate()` in R. The maximum likelihood estimate of the parameters μ and σ of the minus-sampled log normal was obtained by minimizing the log-likelihood numerically using the `optim()` function in R with the default Nelder-Mead method.

3.3.4 Data visualisation and model comparison

For each site, we plotted histograms of log-transformed data for the size frequency distribution. We used quantile-quantile (Q-Q) plots to visualise model fits for the ordinary bounded power law, ordinary log-normal, and the minus-

sampled versions (for corals only), plotting sample quantiles against theoretical quantiles from each fitted distribution. We obtained theoretical quantiles by inverting the cumulative distribution functions (CDFs) of the respective distributions. We calculated the inverse CDF for the bounded power law analytically as in Edwards *et al.* (2017, Section A.1.3), and the CDF for the log-normal was calculated using the `plnorm()` function in R. For the minus-sampled distributions, we obtained CDFs by integrating the minus-sampled density functions up to the observed area x . We obtained inverse CDFs numerically by finding the zero of the difference between the value of the CDF and the target value, using the `uniroot()` function in R.

We also produced ‘rank plots’ at each site, in which the number of observed fish and coral colonies with size $\geq x$ is plotted against x . Rank plots are a standard approach in size spectra studies to visualize the fitted models. For corals, we showed all four distributions (bounded power law, minus-sampled bounded power law, log-normal and minus-sampled log normal) fitted by maximum likelihood. For fishes, we only fitted and show bounded power law and log-normal distributions. For each fitted distribution, the value on the y -axis is the survival function ($1 - \text{CDF}$) multiplied by the total number of colonies or fish.

3.3.5 Model comparison using log-likelihoods

We used log-likelihoods to measure the performance of each model. A larger log-likelihood indicates a better fit, although it does not account for the number of parameters. In general, adding more parameters is expected to improve the fit of a model. We also calculated the Akaike Information Criterion (AIC) that is commonly used for model comparison and accounts for the number of parameters. For a given dataset, the lower the AIC, the more parsimonious the model. The AIC is given by

$$\text{AIC} = 2k - 2\ln(L)$$

where k is the number of parameters per distribution and L is the maximum likelihood. The value of k is two for log-normal (μ and σ), minus-sampled log-normal (μ and σ) and minus sampled bounded power law (b and x_{min}), and three for bounded power law (b , x_{min} and x_{max}). Although an AIC value can be

calculated for all distributions, it is not valid for the bounded power law, because the assumption that the log-likelihood is locally quadratic (Mitchell *et al.*, 2022) is not met with respect to x_{min} and x_{max} . However, since the other three distributions have the same number of parameters, we made decisions about the best-fitting model amongst those by comparing log-likelihoods and AICs. In cases where the bounded power law has the largest log-likelihood, it is unclear which would be the best-fitting model, because it has one more parameter than the other distributions. In those cases, we rely on visual inspections of the data fit. All analyses were done in R version 4.2.1 (R Core Team, 2022).

3.4 Results

Rank plots showed that for most sites, the (minus-sampled) log-normal distributions more closely tracked the coral (green and purple lines, Figure 3.1) and fish (green lines, Figure 3.2) observations than the power law distributions throughout the sampled size range. Bounded power law and the two minus-sampled models for corals systematically predict more larger organisms than we observed (corals: black and orange lines, Figure 3.1; fish: black lines, Figure 3.2).

The rank plots and log-likelihoods jointly demonstrated (Table 3.1; Figure 3.1) that, with the exception of four sites (Wolf Rock, Cook Island, Woolgoolga Reef and North Rock), the log-normal distribution best described the coral size data (green lines on Figure 3.1; log-likelihood values on Table 1). The minus sampled log-normal distribution was better for Wolf Rock and Cook Island. For Wolf Rock, the differences between minus-sampled and ordinary log-normal AIC were ~ 0.1 and ~ 0.3 respectively; these small differences (< 2) suggest that the log-normal models were comparable (using the rule of thumb in Burnham & Anderson, 2004, p. 271); for Cook Island, the difference in AIC was ~ 3.3 , suggesting the minus-sampled version was comparable to slightly better (Burnham & Anderson, 2004, p. 271) than the ordinary log-normal version. The bounded power law and the minus-sampled bounded power law had the largest log-likelihoods for Woolgoolga Reef and North Rock, respectively, but as noted in the methodology, the best model is therefore unclear for Woolgoolga Reef. Q-Q plots agreed with the model comparison results, in which there were least departures from the theoretical distribution (solid lines, Figure B-4 to Figure B-23) whose log-likelihood was the highest.

Comparing minus-sampled to the ordinary versions for coral data, the minus-sampled bounded power law was almost always better than the ordinary bounded power law (Table 1: 17 out of 20 sites), while the minus sampled log-normal distribution was only better than the ordinary log normal for three out of 20 sites (Table 1). The bounded power law generally predicted more of the largest colonies than observed, even considering minus sampling (Figure 1, black and orange lines generally above the dots in the right tail). The minus-sampled bounded power law gave a less negative estimate of the parameter b (less steep slope) across all sites (Figure 1, numbers), and thus predicted more large corals than the ordinary bounded power law, but fewer of the largest corals (Figure 1, purple lines below green lines in the right tail). This was as expected, because the minus-sampled model deals with the sampling bias against large corals. Compared to the ordinary log-normal, the minus-sampled log-normal also predicted more larger corals, as the estimated standard deviation of the minus-sampled version are all higher than the ordinary log-normal (Table B-4).

For fish community biomass, the log-normal distribution had higher log-likelihoods for all sites but Black Rock (Figure 3.2 and Table 3.2). Black Rock records showed over 700 small *Atypichthys strigatus* estimated to be 1 cm in length, giving large quantities at a small biomass. Q-Q plots agreed with the model comparison results, in which there were least departures from the theoretical distribution (solid lines, Figure B-24 to Figure B-43) whose log-likelihood was the highest. For both bounded power law and log-normal distributions however, there were considerable departures at the lower and upper quantiles.

3.4.1 Fish data from Indonesia

Rank plots showed that neither bounded power law nor log-normal appeared to be great fit for the data from Raja Ampat, Wakatobi and Lombok (Carvalho *et al.*, 2021) (Figure B-44). At Raja Ampat and Lombok (Figure B-44a and c), there were very prominent stacking at fish biomass approx. 5kg and 3kg respectively, which were at the upper tail of the distribution. Bounded power law log-likelihoods were higher for Raja Ampat and Lombok (Table B-5), but because it has one more parameter, it is unclear if it was truly better. Visual examinations of the rank plot (Figure B-44a, c) and Q-Q plots do not support a large improvement for either

distribution choice (Figure B-45Figure B-47). The log-normal log-likelihood was higher for Wakatobi (Table B-5).

3.5 Discussion

Accurately estimating population size spectra is critical for predicting population trends, which has a number of applications, including informing management of fish stocks, and monitoring population recovery from disturbances. Our results demonstrate that the log-normal distribution is generally a better description of coral and fish size distributions, and this result holds for sites across tropical-temperate reef communities. For coral size-abundance data affected by minus-sampling, the minus-sampled bounded power law and log-normal distributions were able to correct for the under sampling of larger corals. The minus-sampled bounded power law generally performed better than the ordinary version, but this adjustment generally did not improve model fit for the log-normal distribution. Ecological size spectra studies commonly employed in fisheries research heavily rely on the assumption of a (bounded) power law relationship between organism abundance and size (Edwards *et al.*, 2017; Andersen, 2019). We showed that there is a need to consider alternative distribution fits to characterise size spectra models for the best descriptor. Notably, the bounded power law tended to overestimate the abundance of the largest organisms, while the log-normal distribution did so to a lesser extent. This has important ecological and conservation implications. For instance, large organisms have disproportionately higher fecundity and reproductive outputs (Álvarez-Noriega *et al.*, 2016; Evans-Powell *et al.*, 2024), and an overestimation of their abundance would lead to an overestimation of reproductive rates. This could affect estimates of stock replenishment and recovery capacity post-disturbance (e.g., Hughes *et al.*, 2019) or sustainability assessments of stocks, which could in turn influence management strategies (Carvalho *et al.*, 2021; Edgar *et al.*, 2024).

For coral and fish data from most sites in the East Australian biogeographic transition zone, the log-normal distribution was generally a better fit compared to bounded power law. In addition to the behavioural differences of the distributions, log-normal has two parameters (σ and μ) that describe the shape and scale of the distribution, allowing more flexible fit around the data, compared to the only

parameter, the exponent b , which controls the slope of the bounded power law distribution for a known size range. A steeper slope b indicates a population or community of interest with fewer larger organisms and/or more smaller organisms, which provides useful biological insights. In a coral population dynamics context, b shows to what extent the community is dominated by larger individuals, which can indicate recruitment or recovery bottlenecks (Lachs *et al.*, 2021; Chong *et al.*, 2023; Sommer *et al.*, 2024). In a fisheries context, b demonstrates the proportion of small to large fish, which mirrors lower to higher trophic level fish (Robinson & Baum, 2016; Heather *et al.*, 2021), and is a useful indicator for energy flow in an ecosystem. Changes to b thus allow the quantification of impact from human overexploitation, and the tracking of recovery (Blanchard *et al.*, 2014; Robinson *et al.*, 2017; Carvalho *et al.*, 2021).

We argue that although b is convenient, its use as a standalone metric without the inspection of model fit is questionable. The two parameters of the log-normal distribution are not intuitive in the same manner, but it is possible to compare the standard deviations (σ) between log-normal distributions (e.g., ordinary and minus-sampled). Generally, a distribution with a larger standard deviation has a higher probability of observing corals above a given size threshold. This was the case for all minus-sampled log-normal distributions compared to the ordinary log-normal distribution for corals, where the former predicted more larger corals. In addition to these distribution parameters, the large fish indicator (LFI; e.g., biomass of fish $> 1\text{kg}$ divided by the total biomass of the fish assemblage) (Greenstreet *et al.*, 2012) might present a more direct measure of large fish/organism quantity in an ecosystem, and could be used in conjunction with size spectra models, without having to reduce entire distributions to a single parameter.

For minus-sampled coral size data from benthic photo quadrats, applying the minus-sampling correction generally improved the fit of the bounded power law distribution to the data, but the correction made little difference to the fit of the log-normal distribution (Figure 3.2). The minus-sampled adjustment improved the model fit by predicting fewer of the largest corals, while increasing the proportion of mid-large corals, thereby flattening the slope (more positive b) of the bounded power law size spectrum. The considerable difference observed in the estimates

of b shows that sampling biases should be considered and incorporated in ecological size spectra studies. However, the lack of improvement in the log-normal distribution suggests that alternative distribution functions and their suitability for size spectra models should be explored. A possible candidate is the gamma distribution, also with two parameters, and is known for its effectiveness in modelling positively skewed, non-negative data. Gamma distributions have been used to model fresh-water stream macroinvertebrate community biomass (Pomeranz *et al.*, 2022) and in global species abundance distributions, because of its flexibility (Callaghan *et al.*, 2023).

Size spectrum models are useful ecological indicators in many ecological contexts. Their ability to link individual level biological processes to population and community level responses to external stressors, such as fishing pressure, is invaluable. However, their assumption of a bounded power law relationship between the abundance and size of organisms needs re-evaluation, as it might over-estimate the sustainability of a population or community, by predicting more large organisms than present. The log-normal distribution more commonly used in the coral population structure literature is generally a better statistical distribution to fit to both coral (sessile) and fish (motile) size-abundance data across tropical to temperate reef communities in eastern Australia. Our findings show that it is important for studies to consider multiple model outputs when using size spectra to inform conservation and management priorities.

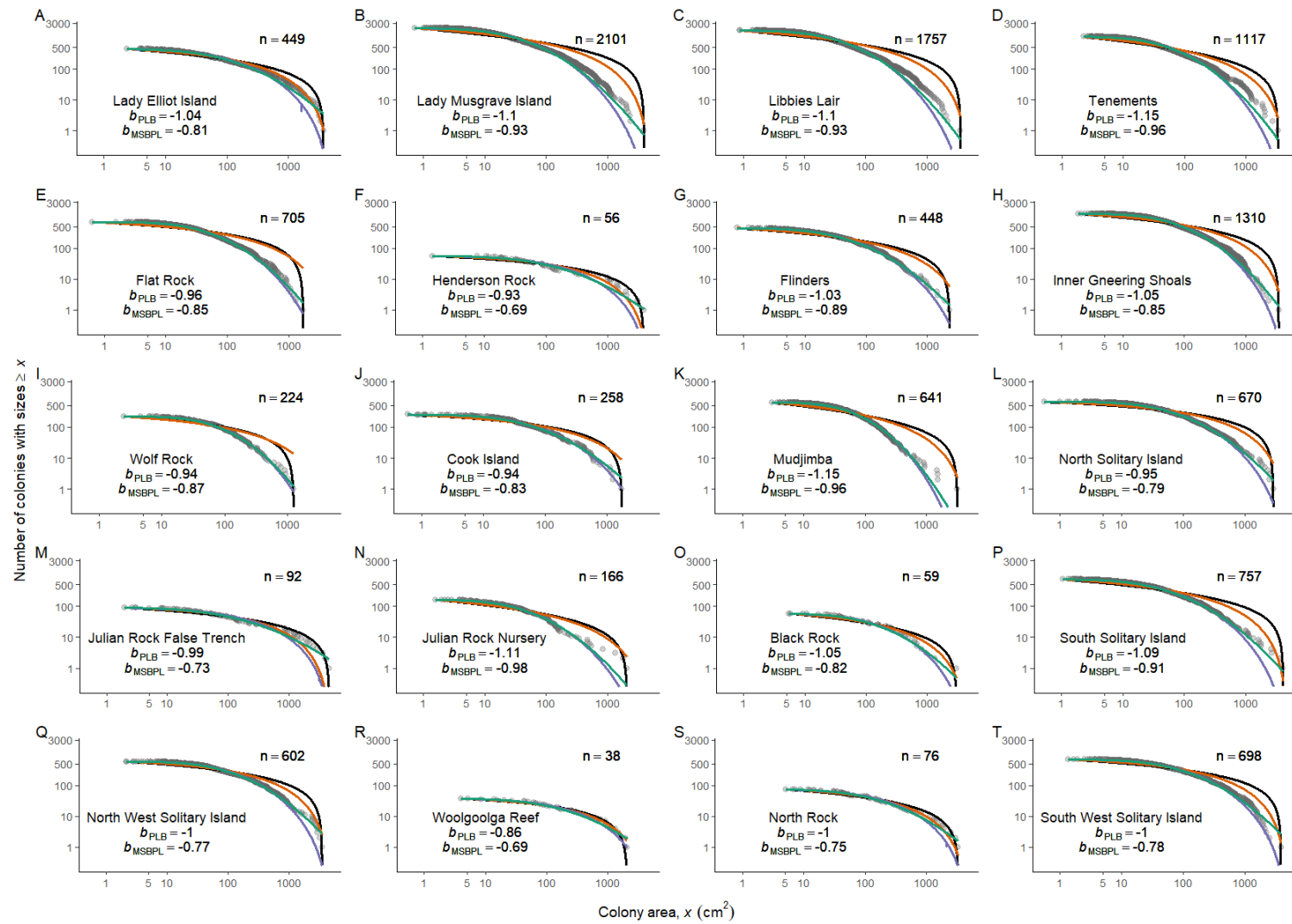


Figure 3.1 The number of colonies with coral area $\geq x$ plotted against coral colony area x on logarithmic scales at each of the 20 sites (A-T). Sites are ordered from tropical (A) to marginal (T) conditions. The number of corals sampled from each site is indicated by “n=”. Dark grey circles are data points. Black lines: bounded power law, orange lines: minus-sampled bounded power law, green lines: log-normal, purple lines: minus-sampled log normal. All lines are fitted by maximum likelihood estimation. The estimated exponent b for the bounded power law (bPLB) and minus-sampled bounded power law (bMSBPL) are also displayed.

Table 3.1. Log-likelihoods and AIC for each distribution fitted to coral size data. BPL: bounded power law; MSBPL: minus-sampled bounded power law; LN: log-normal; MSLN: minus-sampled log-normal. A larger log-likelihood indicate a better model fit. Bold numbers show the better model between ‘ordinary’ and minus-sampled bounded power law. Underlined numbers show the better model between ‘ordinary’ and minus-sampled log-normal. Green-shaded boxes indicate the best overall model for each site. Numbers are rounded to the nearest whole number or to two decimal places.

Site	BPL log-likelihood	MSBPL log-likelihood	LN log-likelihood	MSLN log-likelihood	AICB PL	AICMS BPL	AIClognorm	AICmslognorm
Lady Elliot Island	-2858	-2826	<u>-2809</u>	-2818	5723	5656	5623	5640
Lady Musgrave Island	-11554	-11294	<u>-10848</u>	-10865	2311 5	22593	21700	21735
Libbies Lair	-9767	-9556	<u>-9141</u>	-9156	1954 0	19115	18287	18315
Tenements	-6430	-6323	<u>-6140</u>	-6151	1286 5	12651	12283	12307
Flat Rock	-4072	-4025	<u>-3815</u>	-3816	8150	8054	7633	7636
Henderson Rock	-377	-375	<u>-372</u>	-374	760	754	749	753
Flinders Reef	-2544	-2507	<u>-2436</u>	-2437	5095	5018	4877	4878
Inner Gneering Shoals	-8046	-7877	<u>-7615</u>	-7622	1609 8	15759	15235	15247
Wolf Rock	-1352.32	-1352.97	-1292.46	<u>-1292.34</u>	2711	2710	2589	2589

Cook Island	-1511	-1498	-1457	-1455	3029	3001	2917	2914
Mudjimba Island	-3784	-3713	<u>-3543</u>	<u>-3544</u>	7575	7429	7090	7093
North Solitary Island	-4103	-4017	<u>-3864</u>	<u>-3867</u>	8212	8039	7733	7738
Julian Rock False Trench	-613.85	-613.89	<u>-613.62</u>	<u>-618.72</u>	1234	1232	1231	1241
Julian Rock Nursery	-919	-909	<u>-884</u>	<u>-885</u>	1843	1823	1772	1774
Black Rock	-385.67	-381.65	<u>-380.01</u>	<u>-380.16</u>	777	767	764.02	764.32
South Solitary Island	-4351	-4260	<u>-4158</u>	<u>-4164</u>	8708	8524	8320	8332
North West Solitary Island	-3899	-3828	<u>-3755</u>	<u>-3759</u>	7803	7661	7514	7522
Woolgoolga Reef	-257	-258	<u>-261</u>	<u>-259</u>	519	520	525	523
North Rock	-511	-510	<u>-512</u>	<u>-513</u>	1028	1023	1028	1030
South West Solitary Island	-4441	-4348	<u>-4260</u>	<u>-4263</u>	8888	8699	8525	8531

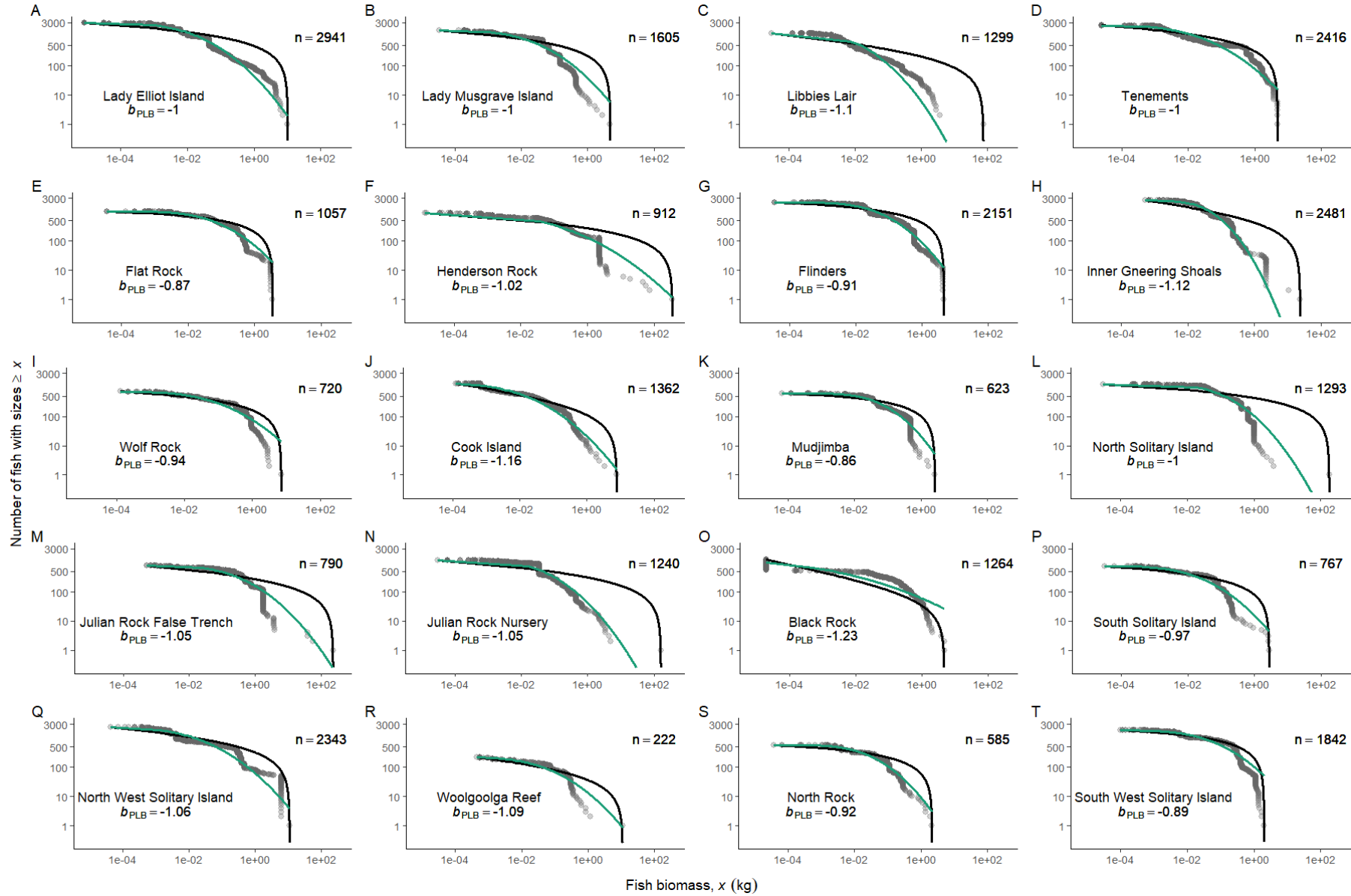


Figure 3.2. The number of fish with biomass $\geq x$ plotted against biomass x in kg on logarithmic scales at each of the 20 sites (A-T). Sites are ordered from tropical to marginal conditions. The number of fish sampled from each site is indicated by “n=”. Dark grey circles are data points. Black lines: bounded power law; green lines: log-normal distribution. All lines are fitted by maximum likelihood estimation. The exponent b for bounded power law is displayed.

Table 3.2. Log-likelihoods for each distribution on fish biomass data. BPL: bounded power law; LN: log-normal. A larger log-likelihood indicate a better model fit. Green-shaded box indicate the better model. Figures rounded to the nearest whole number.

Site	BPL log-likelihood	LN log-likelihood	AICBPL	AIClognorm
Lady Elliot Island	6206	7498	-12407	-14992
Lady Musgrave Island	2952	3396	-5898	-6787
Libbies Lair	2852	3595	-5698	-7186
Tenements	4793	5261	-9579	-10517
Flat Rock	791	1004	-1576	-2004
Henderson Rock	296	586	-586	-1169
Flinders Reef	1897	2654	-3788	-5305

Inner Gneering Shoals	2594	3998	-5183	-7993
Wolf Rock	400	468	-794	-933
Cook Island	3664	3711	-7322	-7418
Mudjimba Island	493	702	-979	-1401
North Solitary Island	-264	665	533	-1326
Julian Rock False Trench	-659	-347	1324	698
Julian Rock Nursery	1059	1831	-2113	-3657
Black Rock	6311	5489	-12615	-10974
South Solitary Island	1487	1679	-2968	-3354
North West Solitary Island	4932	5418	-9859	-10832
Woolgoolga Reef	248	266	-489	-528
North Rock	921	1120	-1835	-2237
South West Solitary Island	2049	2180	-4093	-4355

Chapter 4 : Subtropical specialists dominate a coral range expansion front

4.1 Abstract

Potential range expansion of scleractinian corals in high latitude reefs is critically dependent on the coral host-symbiont relationship that determines coral growth and survival. Although increases in coral cover have been observed at higher latitudes, the identities of habitat-building reef corals and their symbionts are underreported. Here, we examine how scleractinian host and symbiont Symbiodiniaceae diversity changes along a tropical-temperate environmental gradient. We use *Pocillopora* spp. and associated symbiont communities as a model to understand whether they are expanding their range poleward, and the role of symbionts in this process. Along the Kuroshio Current, which carries warm equatorial waters northward along the Pacific coast of Japan, we collected coral tissues from 23 (sub)tropical to temperate reefs, from southern Iriomote in the Ryukyu Islands (24°N) to northernmost Kushimoto on mainland Japan (33°N). We examined host identities through direct sequencing of the mitochondrial open reading frame (mtORF), and symbiont identities with next-generation sequencing of the internal transcribed spacer 2 (ITS2) region of the ribosomal DNA. Our results show a dramatic reduction of *Pocillopora* haplotypes and a marked change in dominant symbiont types northward (poleward) from Cape Sata (30°N), Kagoshima. 'Tropical' *Pocillopora* haplotypes were absent from mainland Japan sites. We also demonstrate high host specificity between the subtropical *Pocillopora* haplotype and *Cladocopium* symbiont types. Our findings question how common 'coral tropicalisation' is, and the location of the coral range expansion front. The specificity of hosts and symbionts in high-latitude corals suggests that high-latitude reefs are unlikely to support the persistence of tropical zooxanthellate corals.

海洋の温暖化に伴った高緯度地域へのサンゴ類の分布拡大は、しばしば「熱帯化」と呼ばれている。イシサンゴ類の成長と生存は、サンゴとその体内に共生する褐虫藻との関係に依存している。日本の高緯度地域において、イシサンゴ類の被度の増加が観察されているが、イシサンゴ類と褐虫類の組成についての報告例は限られている。そこで本研究では、熱帯から温帯の環境勾配に沿って、イシサンゴ類と褐虫類の組成がどのように変化するかを調査した。ハナヤサイサンゴ類と共生する褐虫類をモデル系として、ハナヤサイサンゴ類が分布拡大しているかどうか、またこのプロセスにおける褐虫類の役割を明らかにすることを目的とした。赤道付近の暖かい海水を日本の太平洋岸に沿って流れる

黒潮に沿って、琉球列島の西表島南部（北緯 24 度）から日本本土の串本最北端（北緯 33 度）に至る 23 地点の熱帯のサンゴ礁から温帯のサンゴ群集でサンゴの断片を採集した。ミトコンドリアの open reading frame (mtORF) の塩基配列決定によりサンゴの同定を行い、核リボソーム DNA の internal transcribed spacer 2 (ITS2) 領域を対象に次世代シーケンサーを用いて褐虫藻の組成を把握した。その結果、熱帯域特有のハプロタイプを持つハナヤサイサンゴ類は本州では観察されず、鹿児島県佐多岬（北緯 30°）から北へ向かうにつれて、ハナヤサイサンゴ類のハプロタイプが劇的に減少し、共生する褐虫藻の組成も顕著に変化していることが明らかになった。また、亜熱帯域特有のハプロタイプを持つハナヤサイサンゴ類と褐虫藻の *Cladocopium* との間に高い宿主特異性があることも明らかになった。本研究の結果から、高緯度のサンゴ群集におけるイシサンゴ類と褐虫藻の特異性が明らかになり、高緯度のサンゴ群集は熱帯性の有藻性サンゴの存続を支える可能性は低く、高緯度のサンゴ群集が熱帯性の有藻性サンゴの気候的な避難場所として機能する可能性が低いことが示唆された。

4.2 Introduction

Tropicalisation of marine environments is a relatively recent phenomenon arising from anthropogenic climate change (Zarzyczny *et al.*, 2024), where global warming causes species to shift their distributions as suitable environmental conditions shift. For example, subtropical-temperate regions at high latitudes become increasingly more suited for the growth and survival of tropical species (Kumagai *et al.*, 2018). This process predicts a poleward range expansion of some tropical species, accompanied by a reduction in abundance and extent of temperate species (Vergés *et al.*, 2014; Messer *et al.*, 2020). Areas of prolific tropicalisation are typically biogeographic transition zones associated with western boundary currents (Vergés *et al.*, 2014). These currents carry warm, oligotrophic waters from the equator to temperate latitudes, such as the Kuroshio Current in the North Pacific, and the East Australian Current in the South Pacific (Imawaki *et al.*, 2013; Sen Gupta *et al.*, 2021), extending suitable conditions for some tropical species beyond the tropics. For example, reefs in New South Wales, Australia, now host more tropical herbivorous fish species than in the early 2000s (Smith *et al.*, 2021). In Japan, *Acropora* coral distribution is estimated to have expanded poleward at ~14 km/year since records began in the 1930s (Yamano *et al.*, 2011). However, the extent to which 'tropicalisation by range shift' occurs in scleractinian coral communities remains a contentious topic, as changes in coral community composition could instead be a result of the increased growth (or proliferation, *sensu* Keshavmurthy *et al.* (2023)) of native subtropical/temperate corals that are often cryptic or undescribed (Fifer *et al.*, 2022; Keshavmurthy *et al.*, 2023). This hypothesis is supported by the ongoing discovery and description of subtropical endemic coral species (e.g., coralprojectphoenix.org) with molecular tools (Cowman *et al.*, 2020). In addition, despite having a critical role on the physiology and survival of the coral host (Starko *et al.*, 2023), the identities of symbiotic dinoflagellate Symbiodiniaceae in corals affected by climate change and potential tropicalisation in biogeographic transition zones remains largely unexamined (but see Wicks *et al.*, 2010; Lien *et al.*, 2013).

The tropicalisation of temperate reefs by range expansion is driven by rising ocean temperatures, favouring hard coral growth in previously colder waters, and the deforestation of macroalgal beds by tropical herbivorous fishes (Kumagai *et*

al., 2018; Zarco-Perello *et al.*, 2020), urchins (Ling *et al.*, 2009) or environmental pulses such as storms and heatwaves (Wernberg *et al.*, 2013; Wernberg *et al.*, 2024). The loss of foundation species, such as kelp at higher latitudes, results in more physical space becoming available for other benthic competitors such as turf algae and hard corals (Vergés *et al.*, 2016; Zarco-Perello *et al.*, 2021). Fossil records from the Holocene, where sea surface temperatures were on average 1.5°C warmer than today, demonstrated that high latitude reefs in Tateyama, Japan (~35°N) 6,000 years ago had twice the number of coral species as compared to coral communities in the vicinity today (Veron & Minchin, 1992; Buddemeier *et al.*, 2004). Drawing on this analogue, the observed increase in coral cover at higher latitudes as a result of warming oceans has fueled the debate around the temperate and subtropical reefs acting as climate change refugia for tropical corals (Beger *et al.*, 2014; Muir *et al.*, 2015; Soares, 2020), in which range expansion into marginal environments preserves genetic diversity under climate change.

An alternative to ‘tropicalisation by range shift’ explaining the observed increase in coral cover at high latitudes is the proliferation of subtropical species in their existing range (Keshavmurthy *et al.*, 2023). Range expansion is strongly reliant on the corals’ ability to withstand prolonged periods of low winter temperatures (~13°C), which can cause cold bleaching and subsequent mortality (Suzuki *et al.*, 2013; Higuchi *et al.*, 2015), while proliferation of existing subtropical species relies on individuals that must already have this ability. Range expansion by tropical species also relies on a consistent tropical to temperate larval supply to ensure population connectivity (Mizerek *et al.*, 2021; Nakamura *et al.*, 2021). A growing body of evidence suggests that high latitude reefs host more endemic species than previously thought, and these corals could be responsible for the observed ‘subtropical proliferation’. For example, *Pocillopora aliciae*, *Cyphastrea salae* and *Plesiastrea versipora* (Schmidt-Roach *et al.*, 2013b; Baird *et al.*, 2017; Juszkiwicz *et al.*, 2022) are corals that were originally thought to be subtropical members of different, more cosmopolitan species. In Japan, the same pattern has been observed in the *Acropora hyacinthus* and *Goniopora lobata* species complexes (Nakabayashi *et al.*, 2019; Yasuda *et al.*, 2021; Fifer *et al.*, 2022). Observations of morphologically distinct ‘tropical’ *Acropora* spp. having expanded into previously unrecorded high latitudes (30°S) (Baird *et al.*, 2012) were deemed

inconsequential, as subsequent benthic surveys concluded there was a lack of an overall increase in the abundance of tropical/cosmopolitan corals compared to the coral assemblage in 1992 (Mizerek *et al.*, 2021). Since the growth, survival and recruitment rates of subtropical corals are different to their tropical counterparts (Cant *et al.*, 2023; Chong *et al.*, 2023), range expansion of tropical corals poleward would lead to differential population level responses to environmental disturbances, in turn affecting the persistence and ecological functioning of high latitude reefs. It is therefore important to identify whether habitat forming species in 'tropicalising' biogeographic transition zones consist of poleward range expanding tropical species, or whether they are proliferating subtropical species, in addition to monitoring changes in coral and symbiont diversity and abundances.

Pocillopora is a genus of morphologically-plastic scleractinian corals that are known to adjust their morphological structure based on environmental conditions (Paz-García *et al.*, 2015; De Palmas *et al.*, 2018), making them difficult to visually identify to species level based on morphological features alone. The flexible characteristics of *Pocillopora* corals suggest that they should be good candidates for both range expansion and subtropical proliferation at niche boundaries (Hoogenboom *et al.*, 2008), and are therefore ideal to test between these two alternative hypotheses. However, genetic data are crucial for species delineation. Delineating haplotypes (clusters of genetic material co-located in the genome and are typically inherited together) based on known DNA markers (Gélin *et al.*, 2017) gives intraspecific resolution for the visualization of genealogical relationships. This allows the inference of biogeography and history of coral populations (Leigh & Bryant, 2015). Species in *Pocillopora* span a wide spectrum of coral life-history traits: some are considered weedy and some competitive (Darling *et al.*, 2012; Madin *et al.*, 2016), while some are stress-tolerant (Haryanti *et al.*, 2015; Fox *et al.*, 2021). *Pocillopora* corals are able to recover rapidly after disturbances through high recruitment (Holbrook *et al.*, 2018) and have been observed to dominate settlement panels at high latitude reefs across different ocean basins (Table 1 in Nakamura *et al.* (2021)). The obligate coral-symbiont relationship might also play an important role in ensuring a good nutritional strategy for different environments in which *Pocillopora* corals are found. Photosynthetic Symbiodiniaceae dinoflagellates (hereafter symbionts) are essential for the

growth and survival of corals. One coral colony may harbour several species of symbionts, and may be able to adjust the abundances of their dominant symbionts based on the required thermal, light and oxygen sensitivity (Jones *et al.*, 2008; Putnam *et al.*, 2012; Wang *et al.*, 2022), often with some *Durusdinium* spp. considered to be more beneficial under heightened heat stress. *Pocillopora* are brooders as well as broadcast-spawners (Ward, 1992; Schmidt-Roach *et al.*, 2012), suggesting a mixed transmission mode of symbionts in this genus (both horizontal and vertical) (Baird *et al.*, 2009). This affords a higher degree of flexibility, which might be especially beneficial for coral persistence and survival under changing environmental conditions (Quigley *et al.*, 2018; Quigley *et al.*, 2019; Baird *et al.*, 2021). Indeed, *P. aliciae* (a subtropical endemic), previously thought to be *P. damicornis*, has proliferated at higher latitudes (33°S) off Sydney, Australia (O'Connell *et al.*, 2023), and hosts endemic symbiont lineages (Schmidt-Roach *et al.*, 2013a). Understanding *Pocillopora* range expansion and/or proliferation in other regions, such as the Kuroshio Current region in the northern Pacific Ocean, will therefore help promote better understanding of mechanisms of coral persistence at high latitudes under global climate change.

Despite being one of the most well studied genera of scleractinian corals, there is limited work linking the identities of *Pocillopora* host and symbionts (but see Wicks *et al.* (2010); Johnston *et al.* (2022)) to how tropical-temperate populations respond to increasing environmental stress: either by the range expansion of tropical lineages, or by the proliferation of subtropical specialists. For any group of zooxanthellate corals, range expansion versus existing proliferation should show different genetic signatures in common coral genetic markers. The hypothesis of tropicalisation by recent range expansion predicts closely related haplotypes along the range expansion front, while range increasing via proliferation is expected to show a longer history of mutation accumulation and population structure (Slatkin & Hudson, 1991). These patterns are likely to also be reflected in their dinoflagellate symbionts in co-phylogeny and host specificity (Johnston *et al.*, 2022). Because of the symbionts' crucial role in facilitating the survival of coral hosts, we expected corals that inhabit high-latitude range limits to harbour distinctly different Symbiodiniaceae communities to those at lower latitudes. Here, we genotyped *Pocillopora* and its symbionts along a ~1500 km environmental gradient (24.3-33.5°N), from Iriomote Island in southern Japan, to

Kushimoto, Wakayama on the Pacific coast of mainland Japan, following the Kuroshio Current. We aimed to 1) understand the identity of *Pocillopora* host and symbiont diversity along the environmental gradient, and 2) test whether the genetic structure of *Pocillopora* and symbionts imply a range-expansion poleward, or a proliferation of subtropical lineages. Our results facilitate understanding and accurately projecting change in high-latitude coral assemblages under climate change.

4.3 Material and Methods

4.3.1 Specimen collection

We collected coral tissues from 332 *Pocillopora* colonies from June to August 2023 from 26 sites: from the tropical coral reefs in Iriomote, Okinawa in southern Japan to the subtropical communities of Kushimoto, Wakayama (Figure 4.1, Table C-1). At each site, following three 30 m transects at 5-10 m water depth, we aimed to sample at least five colonies per transect. Colonies sampled were at least 1 m away from each other in an attempt to avoid sampling clones. However, this was not always possible at sites where *Pocillopora* corals were not common. At those sites, fewer samples were obtained at similar water depths opportunistically. For each coral, we removed three to five verrucae from the branches using a bone cutter, avoiding growing tips. We also took two scaled photographs of each sampled colony: one showing the details of the corallites and one showing the gross morphology of the coral colony, using an Olympus Tough TG-6 camera (Olympus Corporation, Tokyo, Japan). We stored coral tissue samples in 99.1% ethanol until DNA extraction in October 2023.

4.3.2 Characterising the Kuroshio Current environmental gradient

In Japan, the Kuroshio Current is a directional driver of the extension of tropical reef environments. We characterised the environmental gradient of all sites with a focus on seawater temperature and turbidity, due to their known influences on coral physiology which might drive coral distribution (Sully & van Woesik, 2020; Abrego *et al.*, 2021). We extracted monthly 1km-resolution sea surface temperature (SST) ('jplMURSST41mday'; Nasa/Jpl, 2015) and 4km-resolution kd490 (diffuse attenuation coefficient at 490 nm) as a proxy for turbidity ('nesdisVHNSQkd490Monthly'; NOAA, 2012b), from CoastWatch using the packages 'rerddap' (Chamberlain, 2024) and 'rerddapXtracto' (Mendelssohn, 2024). We calculated the minima, maxima, means, and standard deviations for

the monthly SST and kd490 over the period January 2012 to July 2023. We performed a principal component analysis (PCA) on these eight variables for dimension reduction (Figure 4.2). The first axis (PC1) explained 50.3% of the observed variance, where positive scores reflect warmer sites that experienced less temperature fluctuations than colder, more variable sites. The second axis (PC2) explained 35.0% of the variance and captured a turbidity gradient. Positive PC2 scores indicated sites with murkier waters that also experienced higher variations in turbidity (Figure 4.2). The PC1 and PC2 scores were then extracted for subsequently statistical analyses.

4.3.3 DNA extraction, *Pocillopora* host sequencing & Symbiodiniaceae NGS

We extracted total genomic DNA from tissue using the DNeasy Blood & Tissue Kit (Qiagen, Hilden, Germany) following the manufacturer's instructions. Using a NanoDrop ND-1000 spectrophotometer (Thermo Scientific), we quantified the quality and the concentrations of extractions, and diluted each sample to a concentration of 1 ng/μl using UltraPure™ DNase/RNase free water (Invitrogen). We amplified the mitochondrial open reading frame (ORF) gene of the *Pocillopora* hosts with the FATP6.1 (forward) and RORF (reverse) markers, following the recommended Polymerase Chain Reaction (PCR) cycles (Flot *et al.*, 2008) (Table C-2). DNA from 311 samples were successfully amplified and sent to FASMAC (Kanagawa) to be Sanger sequenced in both directions with 3730xl DNA Analyzer (Applied Biosystems, Thermofisher) in December 2023 and January 2024.

For the symbionts, we amplified the internal transcribed space 2 region of ribosomal DNA (ITS2 rDNA) from the same DNA extractions, with the primer pair SYM_VAR_5.8S2/SYM_VAR_REV, following the recommended PCR cycles (Hume *et al.*, 2018) (Table C-3), using TaKaRa *ExTaq*® Hot Start version (Takara Bio Inc., Shiga, Japan). After purification using Ampure XP beads (Beckman Coulter, Brea, CA, USA), we sequenced the amplified and indexed PCR products on the Illumina MiSeq platform at the National Institute of Advanced Industrial Science and Technology (AIST; Tsukuba, Japan), using a MiSeq Reagent Nano (v2-500 cycle) kit to generate 2 × 250 bp paired-end reads. We processed the obtained FASTQ files using the SymPortal analytical framework version 0.3.20 to determine Symbiodiniaceae genotypes (Hume *et al.*, 2019). Briefly, individual corals may host Symbiodiniaceae from more than one genus, as well as different

species and types from the same genus. Each Symbiodiniaceae cell contains multiple copies of the ITS2 gene, giving high intragenomic diversity. In SymPortal, recurring sets of ITS2 sequences are called defining intragenomic variants (DIVs) and their abundances are catalogued. The relative abundance and combinations of DIVs then contribute to the definition of unique ITS2 profiles, which can be considered symbiont 'taxa' (Hume *et al.*, 2019). In SymPortal, sequence quality control is performed using mothur, the BLAST + suite, and minimum entropy decomposition (MED). The sequences obtained here are deposited in GenBank under the submission number DRA019949.

4.3.4 Haplotype network and Phylogenetic tree of *Pocillopora* ORF haplotypes

We trimmed and aligned 311 forward and reverse sequences of *Pocillopora* using MUSCLE on Geneious 11.0.5 (<https://www.geneious.com>), inspecting single nucleotide changes manually to verify sequence base calling. We drew a haplotype network with median joining network (Bandelt *et al.*, 1999) using PopART (Leigh & Bryant, 2015). Using the Geneious Tree Builder, we built a phylogenetic tree (HKY Model, neighbor-joining tree build method, with bootstrap resampling (random seed) and 100 replicates to create consensus trees), to examine the relationship amongst mitochondrial ORFs found in our study region (Figure C-1). The GenBank accession numbers of the haplotypes are PQ766765-PQ767075.

4.3.5 Testing the effect of the environmental gradient on coral and symbiont diversity

To understand the effect of environmental conditions on the number of haplotypes present at a given site, we ran an ordinal logistical regression using the function `polr()` from the 'MASS' package (Venables, 2002). We used PC1 and PC2 scores as predictor variables, and the number of *Pocillopora* haplotypes as a categorical response variable to predict the probability of finding a given number of haplotypes at a site. Using `chisq.test()` and the option to simulate p-values, we checked the goodness of fit, and generated a Nagelkerke pseudo R2 value using `PseudoR2()` from the package 'DescTools' (Signorell, 2024). We also calculated p-values and confidence intervals for each parameter estimate (Table C-5). Holding PC2 scores at the mean, we predicted the probabilities of the number of haplotypes found over the range of PC1 scores.

Similarly, to test the effect of environmental conditions (PC1 and PC2 scores) on the diversity and abundance of symbiont communities (DIVs) at each site, we ran a distance-based redundancy analysis (dbRDA) using `capscale()` with Bray-Curtis distance from the package 'vegan' (Oksanen *et al.*, 2022). The model significance was tested using `anova()`.

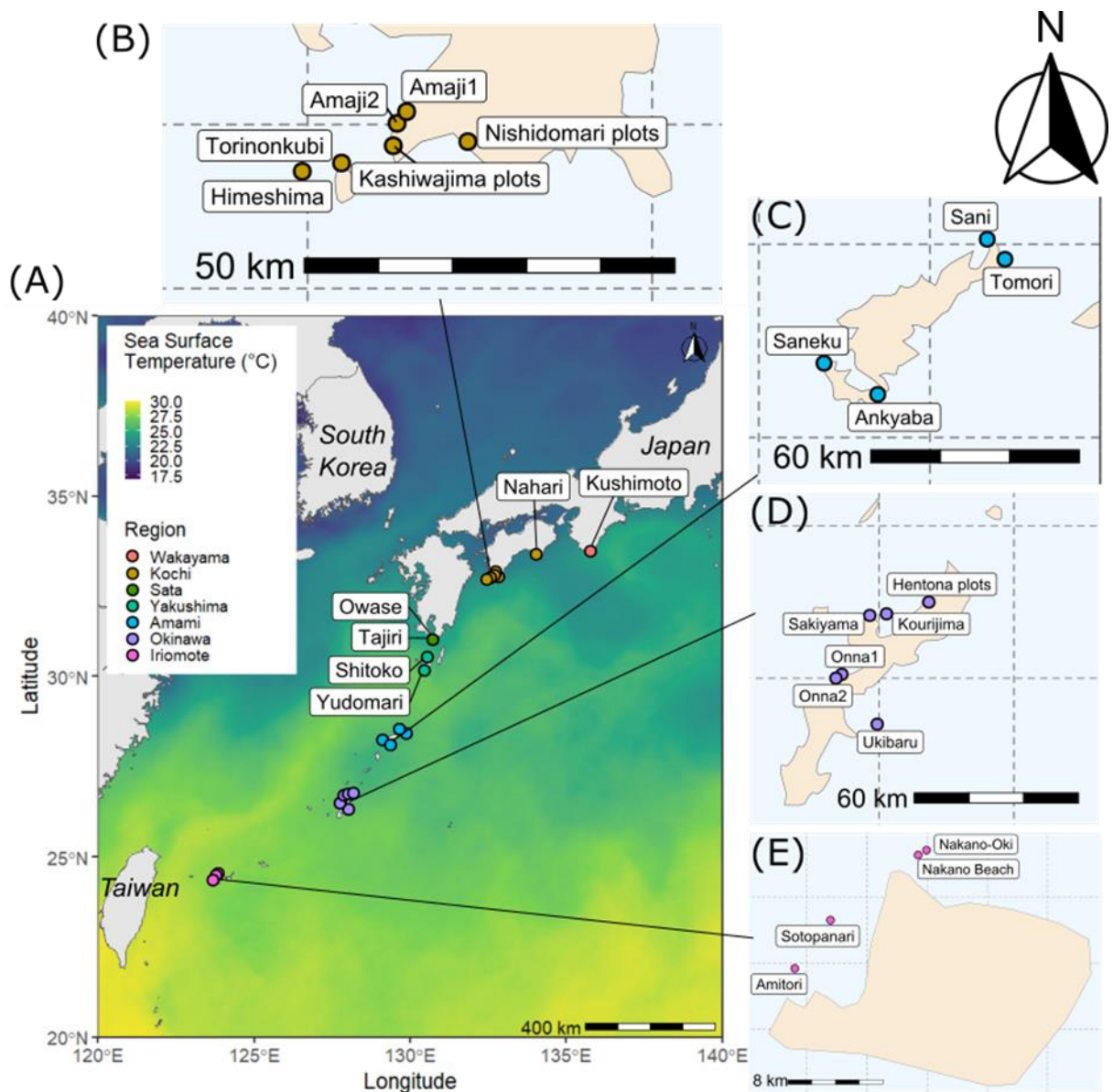


Figure 4.1. (A) The 26 sample sites superimposed on sea surface temperature (SST) data from 16 June 2023 (CoastWatch, Nasa/Jpl, 2015). The Kuroshio Current can be traced northwards following the warmer temperatures (yellow) along the Ryukyu Islands and the coast of Japan. Country names are in italics. Sample site circles are coloured by region / major island with a total of seven regions from north to south: Wakayama, Kochi, Sata, Yakushima, Amami, Okinawa, Iriomote. Insets (B-E) show sampling sites that are too close to see

clearly in (A). (B): Kochi, (C): Amami, (D): Okinawa, (E): Iriomote. For more information see Supplementary Information.

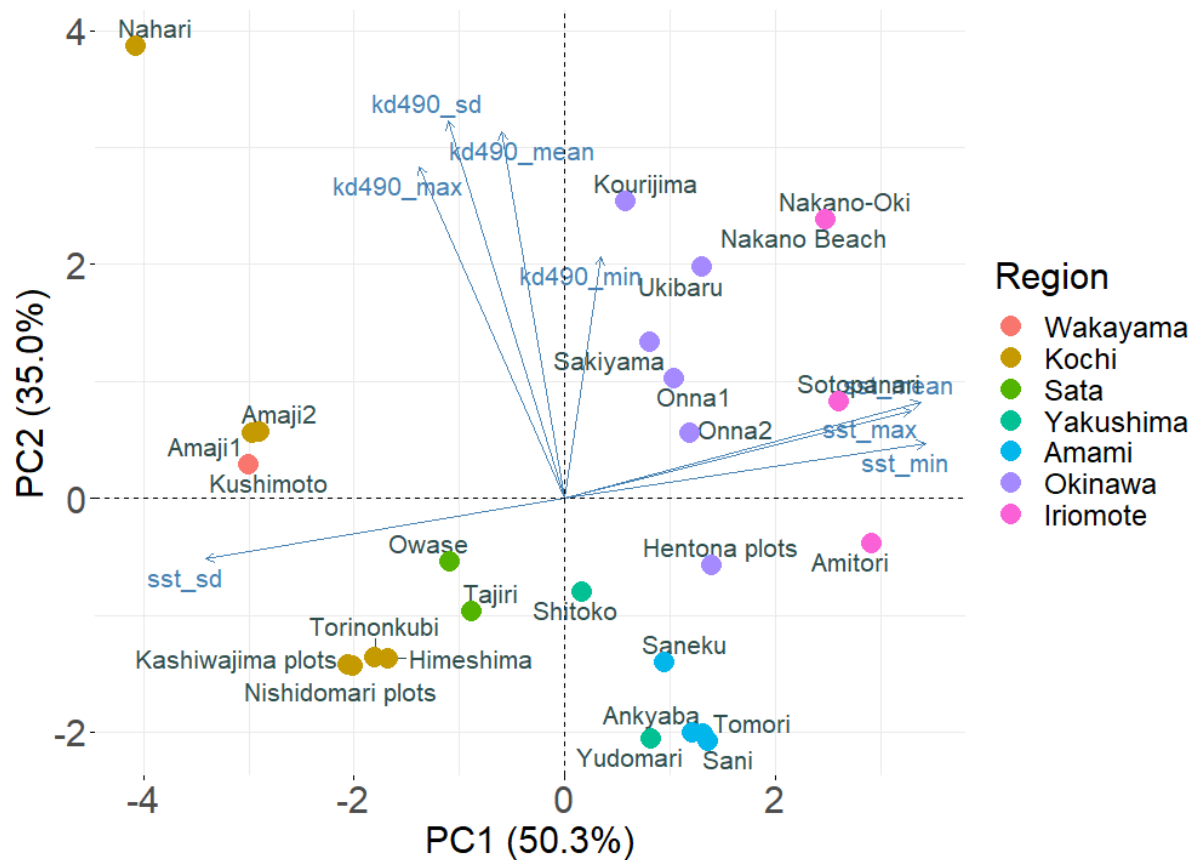


Figure 4.2. Principal component analysis of environmental conditions along the tropical to temperate transition in Japan. The eight environmental variables (blue arrows): sea surface temperature (sst) and turbidity (kd490) variables (minima, maxima, mean, standard deviation) on two principal component axes, which jointly explained 85.3% of the temperature-turbidity regime along this gradient. Site names (dots) coloured by geographic region as in Fig. 1. Positive PC1 scores represent hotter and less variable sites, while positive PC2 scores represent sites with more turbid waters that experienced high variability in turbidity.

4.4 Results

4.4.1 Haplotype diversity and changes along the environmental gradient

We found a total of fifteen *Pocillopora* haplotypes, of which ten have previously been recorded (Gélin *et al.*, 2017) (Figure 4.3). ORF09 and ORF53 were the two haplotypes found with the highest frequencies, while ORF53 was found exclusively in the southern islands (Iriomote, Okinawa, Amami and Yakushima).

These two haplotypes were separated by 22 base pair differences, which corresponded to a separation of over 1.16 million years (average time for a mitochondrial genome mutation to occur is approximately 53,000 years in *Pocillopora* corals; (Palumbi *et al.*, 2023)). The southern island sites had high haplotype diversity (n=15), while mainland Japanese sites (Sata, Kochi and Wakayama) only had one haplotype (ORF09; Figure 4.4). On Yakushima Island (the island closest to mainland Japan), the site Yudomari also hosted mostly ORF09, with one sample of ORF18. According to G lin *et al.* (2017)'s primary species hypothesis (PSH) species delimitation method, the ten known haplotypes constituted seven 'PSH's (species), with a range of possible morphological classifications (Table C-4). Specifically, ORF09 was considered to be *damicornis*-like, while ORF53 had at least five different morphotypes including *verrucosa*-like morphotypes.

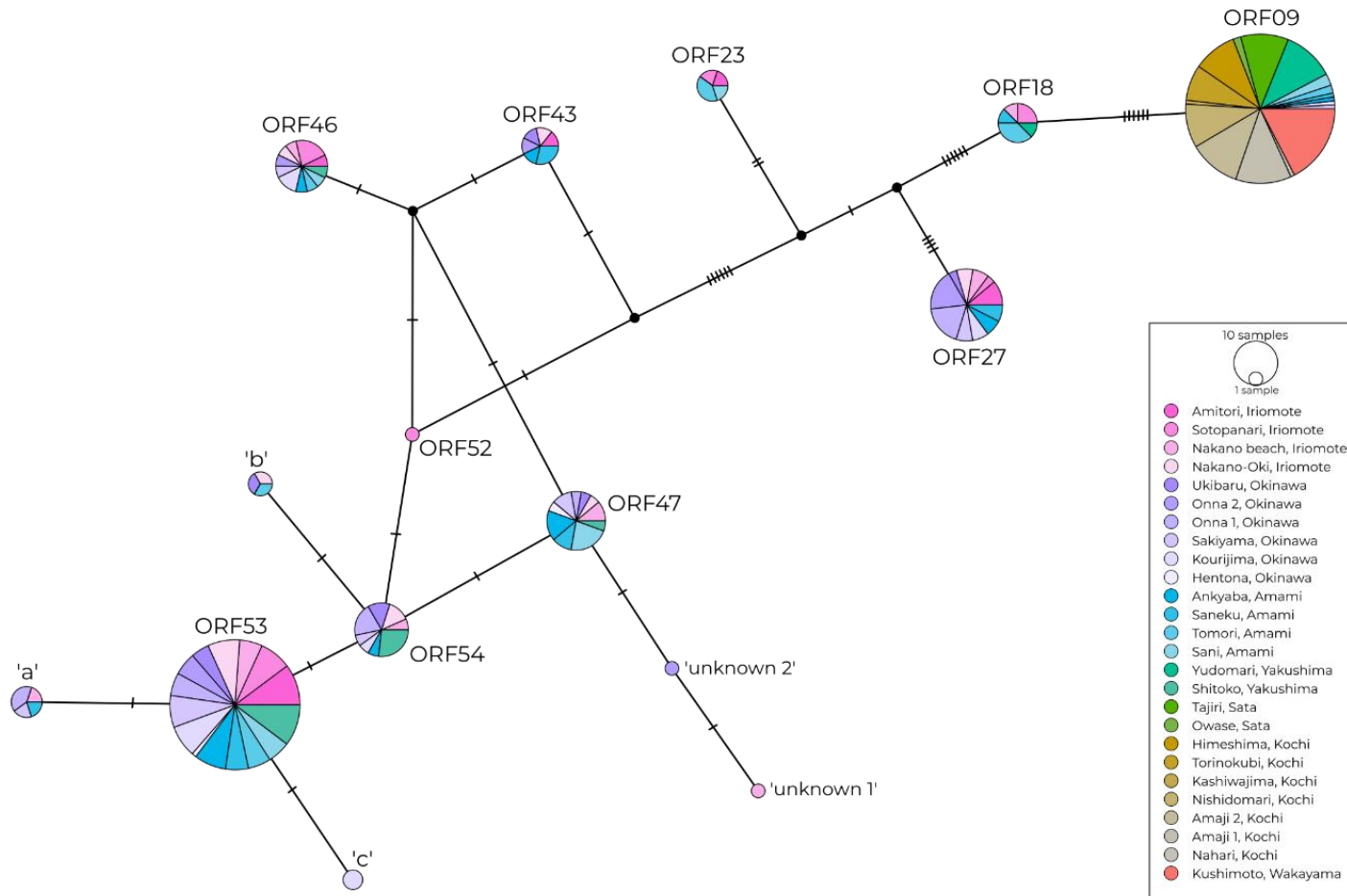
The number of *Pocillopora* haplotypes decreased with increasingly colder and more variable environments (negative PC1 scores) (Figure 4.5). Ordinal logistic regression showed that PC1 scores, reflecting a sea surface temperature gradient, was a significant predictor of the number of haplotypes, while PC2 scores (capturing a turbidity gradient) was not significant (Nagelkerke pseudo R² = 0.726, Table C-5). Most changes in the number of haplotypes were predicted to occur at sites with PC1 values around 0-2, (*i.e.*, the islands of Okinawa, Amami and Yakushima), where the probability of finding only one haplotype fell dramatically, and finding two to six haplotypes peaks. At the warmest sites (PC1 scores of > 2; Iriomote island), there was a higher probability of finding seven or more haplotypes.

4.4.2 Symbiont defining intragenomic variants (DIVs) & ITS2 type profile along the Kuroshio

Symbiont DIVs were different between the southern islands and mainland Japan. While the lower latitude sites had more *Cladocopium* C1d and C1bi, mainland reefs mainly hosted unnamed *Cladocopium* species with the unique identifiers 6597_C and 6601_C (Figure 4.6A). The corresponding ITS2 type profiles also mirrored the pattern observed for DIVs (Figure 4.6B). Only two ITS2 type profiles were found on mainland Japan with UIDs 89 and 94, and were both *Cladocopium* 6597_C and 6601_C dominant; while 11 other ITS2 type profiles were found on

the southern islands, mostly consisting of combinations of DIVs *Cladocopium* C1b, C1d, C42a, C1 (for the dominant DIVs of each ITS2 type profile, see Table C-6). *Durusdinium glynnii*, a heat adapted species (93), was found at Nakano Beach on Iriomote. Yudomari (Yakushima) corals hosted a unique ITS2 type profile (84) made up of a majority sequence of an unnamed *Cladocopium* DIV 25378_C and C1c. dbRDA showed that both PC1 and PC2 (SST and turbidity) were significant predictors for the symbiont DIV community composition with an adjusted $R^2 = 0.354$ (Figure 4.7). Higher SSTs (positive PC1) increased the proportion of *Cladocopium* C1d, C1bi, C1, C42a and C42.2, but limited *Cladocopium* 6597_C, while the remaining 932 DIVS were clustered near the origin with a high degree of overlap (See supplementary data for all DIVs).

1



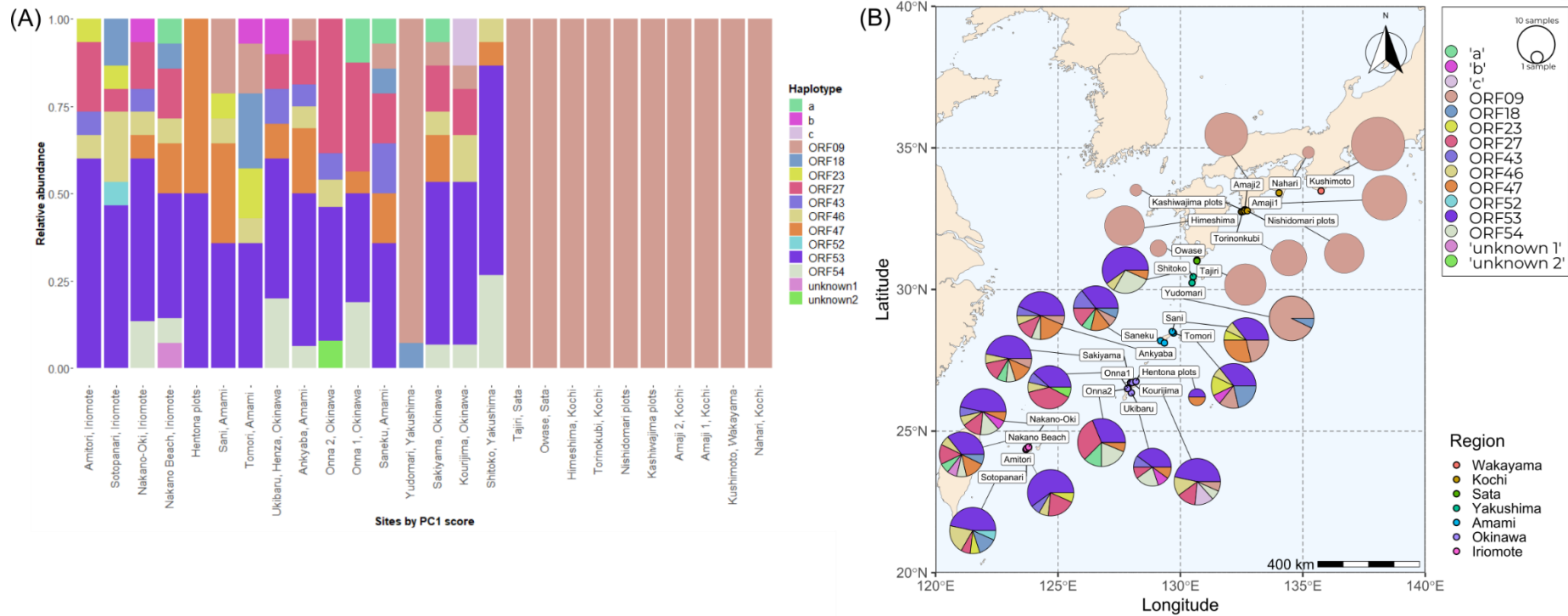
2

3 Figure 4.3. Haplotype network (Median Joining Network: MJN) of *Pocillopora* ORF haplotypes (n=311). Vertical bars (hatches)

4 represent the number of base pair differences between haplotypes. Black circles are unsampled ancestors inferred by the MJN

5 algorithm. The size of each pie indicates the number of samples found to have that haplotype. The colours correspond to the seven
 6 regions as in Fig.1: Iriomote, Okinawa, Amami, Yakushima, Sata, Kochi and Wakayama.

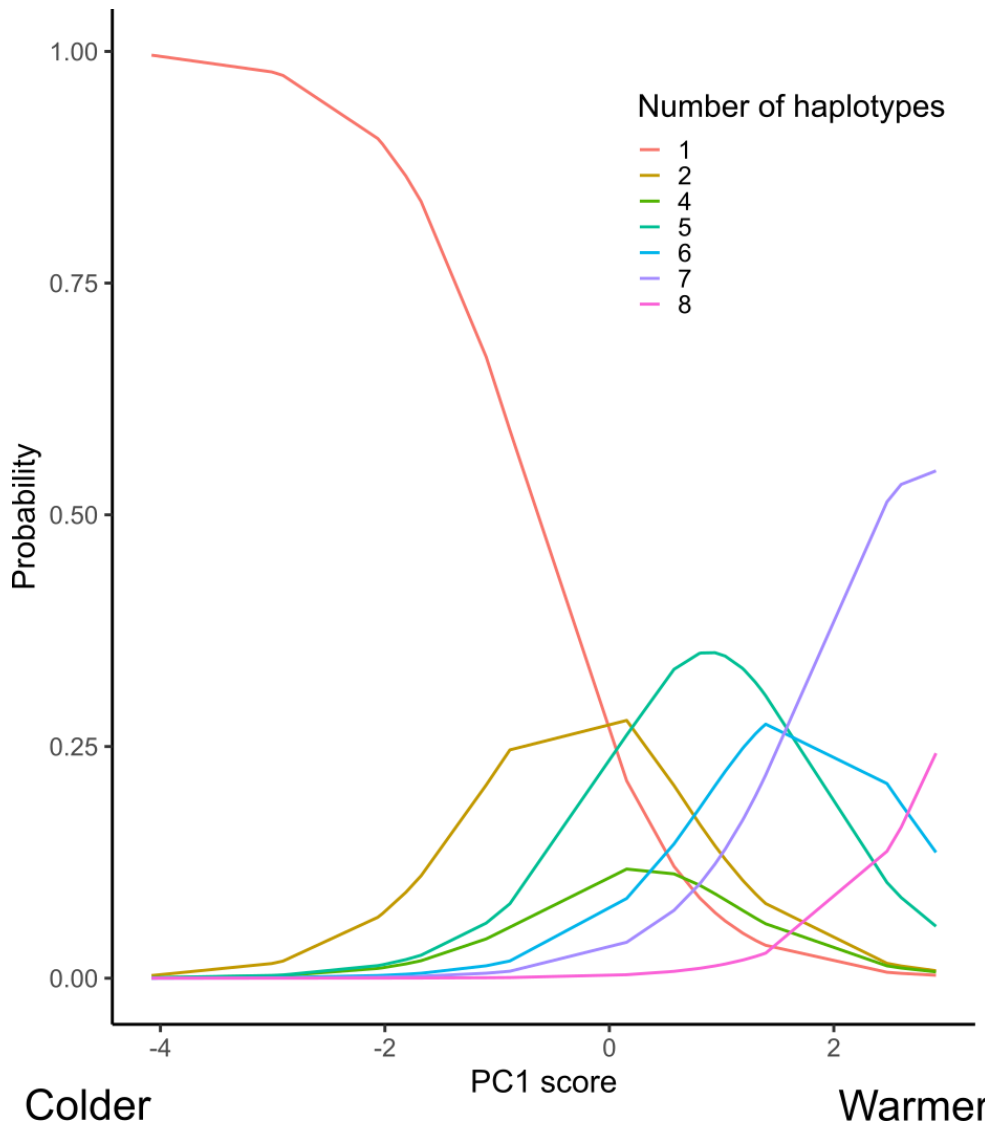
7



8

9 Figure 4.4. (A) The relative abundances of Pocillopora mtORF haplotype at each site, ordered by PC1 score (left to right: high to low
 10 PC1; high PC1 means higher SST). Haplotype nomenclature follows (Gélin *et al.*, 2017). New sequences identified in this study ‘a’,
 11 ‘b’, ‘c’ were found in more than one coral sample, while ‘unknown1’ and ‘unknown2’ are sequences found only in one sample (n=311).

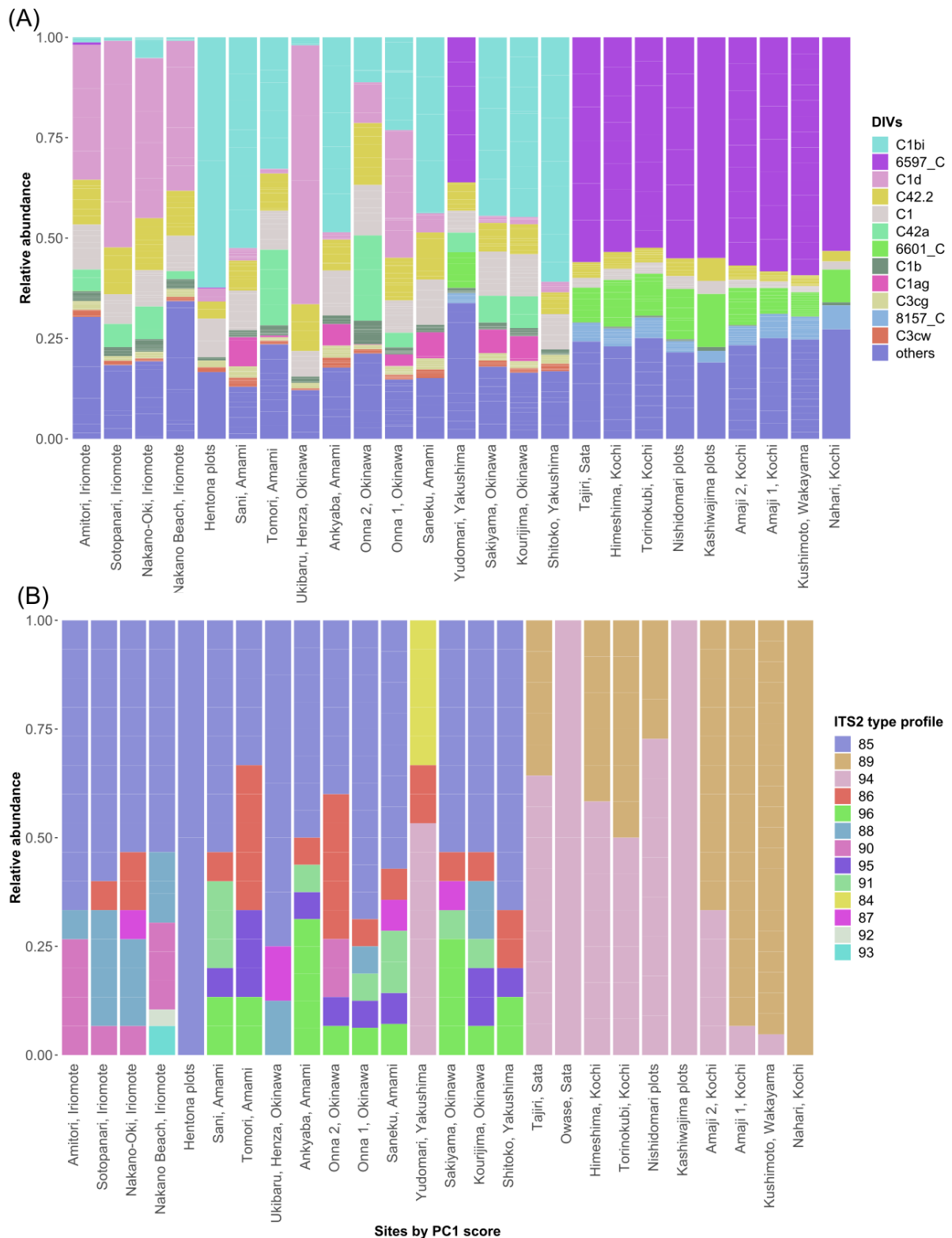
- 12 (B) The haplotypes and abundances are displayed by sampling location on a map, with sample sites coloured by region as in Fig 1.
- 13 Haplotypes are coloured as in (A).



14

15 Figure 4.5. Predicted probability of a given number of *Pocillopora* haplotypes at a site
 16 along the temperature gradient: more positive PC1 scores represent warmer water
 17 temperatures and less variability in water temperatures. PC2 score was held at its
 18 mean value for the regression. Number of haplotypes are 1-2, 4-8, because there were
 19 no sites with three haplotypes in our dataset.

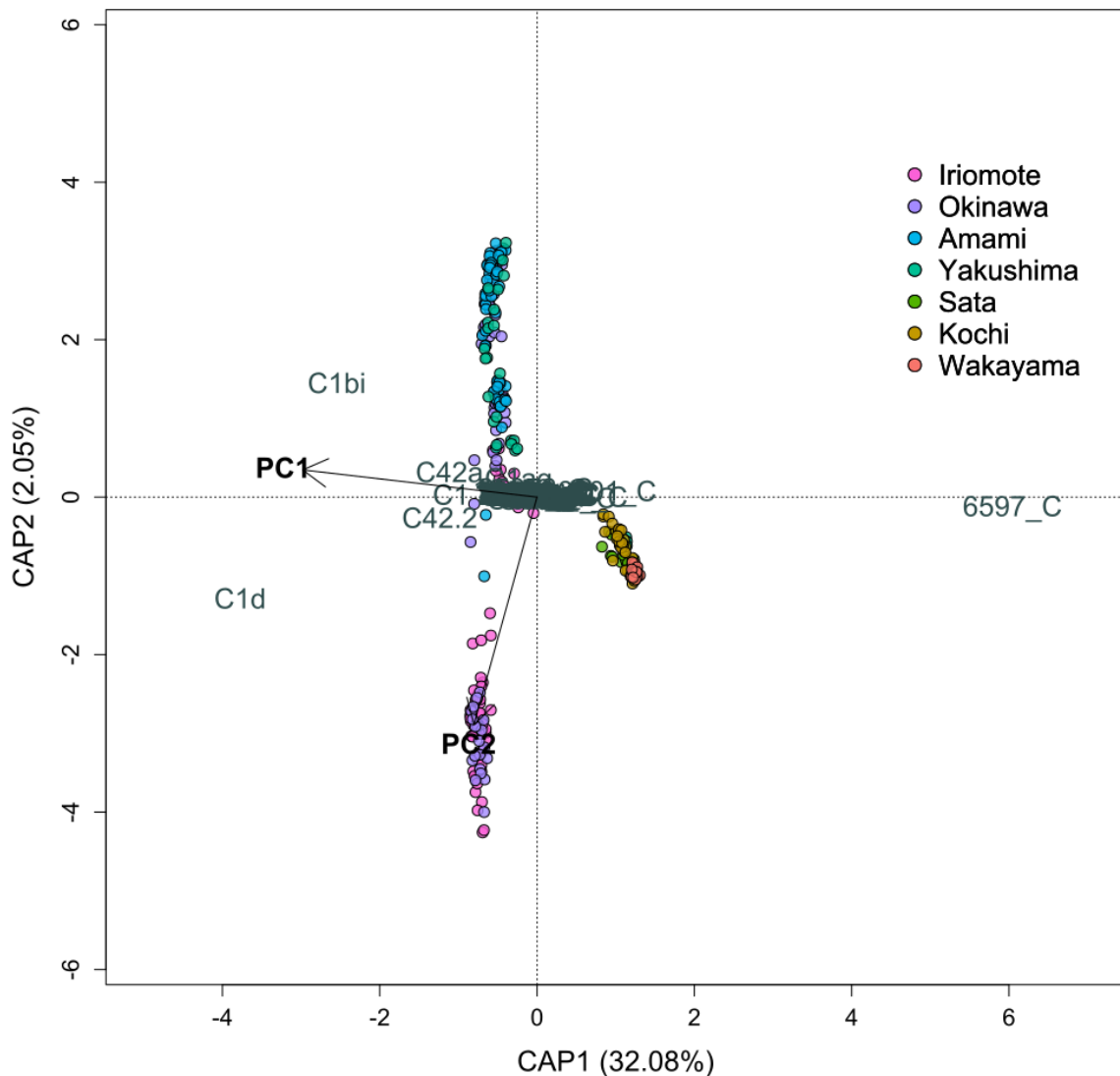
20



21

22 Figure 4.6. (A) The relative abundances of the top 12 most abundant Symbiodiniaceae
 23 defining intragenomic variants (DIVs), ordered by PC1 score (left to right: high to low
 24 PC1; high PC1 means higher SST). The remainder DIVs were all classified under the
 25 group 'others'. The most abundant DIVs were all of the genus *Cladocopium*. A number

26 followed by _C e.g., 6598_C are unnamed species of *Cladocopium*. (B) The relative
 27 abundances of the dominant ITS2 type profiles, ordered by PC1 score (left to right:
 28 high to low PC1; high PC1 means higher SST). For the DIVs that make up each ITS2
 29 type profile, see Table C-6. All ITS2 type profiles are dominated by *Cladocopium*,
 30 except for 93, which was *Durusdinium glynii* dominant.



31
 32 Figure 4.7. Distance-based redundancy analysis (dbRDA) (Bray-Curtis distance,
 33 `capscale()`) triplot showing the symbiont DIVs (response variables) against PC1
 34 and PC2 scores (predictor variables). The circles are coral samples coloured by the
 35 geographic region that they were collected from along the tropical-to-temperate
 36 transition in Japan.

4.5 Discussion

Tropicalisation and the resultant reorganisation of benthic communities could transform ecological processes and interactions at tropical-temperate biogeographic transition zones. While benthic changes have been recorded along western boundary currents at tropicalisation hotspots (Vergés *et al.*, 2014; Vergés *et al.*, 2016; Kumagai *et al.*, 2018), the identity of scleractinian corals that have the potential to expand and proliferate has not often been clearly ascertained, leading to claims that tropical corals could find refugia at higher latitudes (Soares, 2020). In this study, we established that *Pocillopora* corals and their symbionts along the Kuroshio Current are different in the southern Ryukyu Islands compared those at mainland Japan sites, which has only one *Pocillopora* haplotype and a distinct symbiont profile. Our results are consistent with the idea that temperate coral communities may largely consist of subtropical endemics and specialists, rather than representing extensions of tropical species that are expanding their range (*i.e.*, tropicalisation) due to anthropogenic climate change (Keshavmurthy *et al.*, 2023). Indeed, *Pocillopora* corals have been recorded on mainland Japan since the 1930s (Yabe & Sugiyama, 1935). As climate change leads to ocean warming, it is unclear how subtropical endemics and specialists will fare, due to their lower thermal threshold for high temperatures and thus increased susceptibility to bleaching (Kim *et al.*, 2019). We find no evidence that other haplotypes of *Pocillopora* can tolerate the colder and more variable conditions in subtropical/temperate regions along the Kuroshio Current off mainland Japan, adding nuance to the general marine tropicalisation discussion.

The subtropical *Pocillopora* haplotype ORF09 was the only haplotype found in the colder waters of mainland Japan, although they were also present in much lower relative abundances at the southern island sites of this study. We hypothesise that the warmer and milder sea conditions from Yakushima Island southwards benefit more competitive *Pocillopora* haplotypes and their associated symbionts, allowing them to outcompete ORF09, which might be more cold stress-tolerant and is thus the only haplotype that persists in high-latitude marginal reefs. Our evidence also points towards a mis-match between the location of the 'Tokara Gap' (a biogeographic boundary) and coral diversity in this region, and we join the call for more careful examination of biodiversity in biogeographic transition zones (Komaki, 2021). Our haplotype network did not

form a single “starburst” as would be expected if a single population had recently evolved and rapidly expanded along an increasingly suitable environmental gradient (Slatkin & Hudson, 1991). ORF09 is genetically different to its closest relative ORF18 by six base pairs, suggesting that the populations of these haplotypes have been separated for approximately 318,000 years (53,000 years/mitochondrial mutation in corals, at 0.1% per million years (Palumbi *et al.*, 2023)), while haplotypes found in the southern islands are more closely related, many with only one base pair difference between them. ORF09 is also host to subtropical unnamed *Cladocopium* symbiont DIVs 6597_C and 6601_C, whose dominance in the DIV composition gave unique subtropical combinations of ITS2 types. This finding is in broad agreement with Lien *et al.* (2013, Figure 5), who had previously found distinctly different symbiont ITS2 types in *P. damicornis* colonies sampled from Shirahama on mainland Japan, and the southern islands of Amami and Sesoko. Symbiodiniaceae differences along the Kuroshio current have also been observed in other zooxanthellate anthozoans (Reimer *et al.*, 2006).

As one would expect to find many closely related haplotypes on a range expansion front, it is possible that tropicalisation of *Pocillopora* is happening, but has not yet reached the subtropical/temperate reefs of mainland Japan. It is theoretically possible that the southern islands (*e.g.*, Okinawa, Amami) hosted fewer *Pocillopora* haplotypes until recently, and might host different symbiont communities. If historical samples are available, it will be worthwhile to extract, amplify and sequence ‘ancient’ DNA to understand the effect of anthropogenic environmental change (Baker *et al.*, 2013). Continual monitoring in the entire Kuroshio region would improve our understanding of the mechanisms of coral population persistence along biogeographic transition zones. From our results, Yakushima Island might represent the best location to monitor for tropical haplotype expansion. Of the two Yakushima sites visited, Yudomari hosted predominantly the subtropical haplotype (ORF09) and a unique symbiont ITS2 type profile (84) dominated by 25378_C and C1c, while Shitoko hosted no ORF09, but other haplotypes that were found in the southern island groups, with symbiont ITS2 profiles that resemble those from Okinawa. Reefs on Yakushima Island thus may be one of the potential stepping stones (Saura *et al.*, 2014) for poleward

northward expansion of the 'tropical' *Pocillopora* haplotypes and associated symbionts under climate change.

Although we did not explicitly test the physiological performance of the different haplotypes and their symbionts (e.g., Edmunds *et al.*, 2024), environmental differences clearly predict haplotype diversity and distribution (e.g., Figure 4.5, Figure 4.7). The subtropical symbiont DIVs recorded in this study demonstrate that there are specific coral symbiont types and communities that are better suited to colder and more turbid temperate sites. In addition to heat stress experiments that are more commonly employed to understand coral-symbiont physiology, low temperature, light availability and salinity stress experiments (e.g., Kerswell & Jones, 2003; Jones *et al.*, 2020) with different symbiont communities could be a worthy endeavor in understanding the physiology of corals in marginal reefs. For instance, it would be useful to establish the survival rates of tropical-subtropical symbionts in the water column to see if they remain viable under different environmental conditions, to be taken up by prospective coral hosts. It is also pertinent to understand the reproductive and survival strategies of these different *Pocillopora* haplotypes on the range expansion front, to predict if beneficial symbionts can be taken up from the environment (horizontal transmission) as well as inherited from the mother (vertical transmission). Although we show that there is host specificity between *Pocillopora* haplotype and associated symbionts, poleward range expansion of tropical haplotypes might be promoted if there can be an active uptake of subtropical symbiont communities from the environment. Understanding these physiological differences could improve our ability to project population performances under climate change (Cant *et al.*, 2022).

To our knowledge, Wakayama is the most northern location that *Pocillopora* has been observed in Japan. But based on environmental parameters, coastal locations are likely to experience more marginal (colder, more turbid) conditions. For example, in Nahari, Kochi, coral communities experienced heavy mortality in a 2018 cold bleaching event, when the Kuroshio Current meandered away from the coast (Lerriorato & Nakamura, 2019). Climate change is expected to affect the strength of western boundary currents (WBCs), and the Kuroshio Current is projected to weaken (Sen Gupta *et al.*, 2021). It is therefore possible that extremely cold winter conditions could appear in sites on mainland Japan in the future, leading to heavy coral mortality that could take years to recover from. This

further hampers the likelihood of tropicalisation by range expansion of tropical lineages at poleward limits. Adding genetic data from more tropical sites, such as in Taiwan (Hsiao *et al.*, in review) and the Philippines (Torres & Ravago-Gotanco, 2018) could improve our understanding of the level of connectivity, diversity and distribution of *Pocillopora* along the Kuroshio environmental gradient. Such research would help identify regions of high genetic diversity, or potential stepping stones of any poleward range expansion. In other parts of the world, WBCs such as the Brazil Current and the East Australian Extension are predicted to strengthen (Sen Gupta *et al.*, 2021). The increased transport of warmer waters poleward could encourage the range expansion of coral taxa in those regions. This process could have unknown or potentially negative effects on native subtropical and temperate endemics (Martello *et al.*, 2024) by augmenting benthic composition with knock-on effects on ecosystem functioning of high latitude reefs.

Climate change and ocean warming will continue to affect ecological communities, including via tropicalisation, where tropical taxa expand their range poleward for more favourable environmental conditions. Although frequently observed in mobile taxa such as marine fish (Vergés *et al.*, 2016; Miller *et al.*, 2023; O'Connell *et al.*, 2023), there is mixed evidence for tropicalisation by range expansion in zooxanthellate reef corals, likely due to cold extremes during winter months in poleward locations, making those sites unviable even for subtropical corals, let alone tropical lineages. Recent observations of coral expansion in the subtropics could be due to the scientific community's increased awareness of (subtropical endemic) corals at high latitudes, and/or increasingly favourable conditions for subtropical coral proliferation due to warming. Our study of *Pocillopora* spp. and their symbionts in the Kuroshio region highlights the taxonomic distinctness of subtropical endemics, and their long evolutionary history adapting to local environments (Thomas *et al.*, 2017). It is unclear whether high latitude regions can support tropical corals and act as climate refugia for tropical coral reef biodiversity, but we show that the evolutionary distinctness of subtropical communities (Budd & Pandolfi, 2010) underpins fundamental differences to their tropical counterparts.

Chapter 5 : General Discussion

Anthropogenic climate change continues to threaten the existence of coral reef ecosystems (Hoegh-Guldberg *et al.*, 2017). In many parts of the world, the effects of mass bleaching events due to warming ocean temperatures, as well as local stressors have led to coral cover declining dramatically over the last few decades, affecting adult brood stock levels, which threatens recruitment and thus population recovery (Hughes *et al.*, 2019). These extreme thermal conditions are projected to continue until the end of this century, even if carbon emissions reached net zero today (Palazzo Corner *et al.*, 2023; Summerhayes *et al.*, 2024). While ecological processes underpinning tropical coral reef ecosystems are well-understood, relatively little is known about the coral communities at high latitude range limits. Specifically, how do they differ in their genetic identity, species composition, biological and population level responses to environmental stress, when compared to their tropical counterparts? Anthropogenic climate change effects are pronounced in biogeographic transition zones (Mieszkowska & Sugden, 2016; Zarzyczny *et al.*, 2024) with little-known changes affecting its resident population dynamics. Since climate change effects are not isolated, and affect all coral populations, there is an urgent need for large-scale, macroecological approaches to coral reef demography to understand population persistence and the dynamics of coral communities in biogeographic transition zones.

This thesis explored population dynamics along environmental gradients from tropical coral reefs to high latitude coral communities, and filled gaps in our understanding of population size structure. I highlighted macroecological patterns and evaluated statistical assumptions that underpin community size spectra models. I also investigated the extent to which tropicalisation by range shift is occurring in scleractinian corals, using the *Pocillopora* species complex and their Symbiodiniaceae endosymbiotic algae as a model.

I first focused on the coral reefs and marginal reef communities off the east coast of Australia, following the East Australian Current. I demonstrated that the population size structure of coral communities differed along a tropical to marginal environmental gradient (chapter 2). Coral communities in colder, more turbid and productive waters (thus more marginal environments) had a higher proportion of

larger individuals, which could be indicative of recruitment bottlenecks in an ageing population (Sommer *et al.*, 2024). To further tease out differences in population dynamics, I explored individual size distributions, or size spectrum models, a method favoured in fishery science (chapter 3). I explored the assumption that the size-abundance relationship is a bounded power law distribution. I found that the log-normal distribution, commonly used in coral population studies, better describes both coral and reef fish size abundance data than the power law. A bounded power law fit might lead to inaccurate inferences about population dynamics. Finally, to understand the extent of coral tropicalisation under climate change, I used genetic sequencing to examine the diversity and distribution of corals along the Pacific coast of Japan, following the Kuroshio current (chapter 4). I found that these high latitude temperate reefs have unique, specialist coral populations associated with endosymbiont communities distinctly different to the more genetically diverse populations in the tropical reefs, which is in broad agreement with other studies discovering endemics in high latitude reefs.

5.1 Ecological findings and implications

The findings of this thesis highlight fundamental differences between the population dynamics of coral communities at the low latitude tropical environments and the high latitude marginal reefs. Population size structure is more informative than coral cover because allometric scaling relationships are biologically important – survival, growth and reproduction rates are all size dependent. Previous work found that post-disturbance, e.g., thermal stress driven bleaching events (Dietzel *et al.*, 2020; Lachs *et al.*, 2021), coral population structure becomes more left-skewed, where the population contains more large individuals (Bak & Meesters, 1998). This suggests that high latitude marginal reefs might be persisting under relative stress: although there were more bigger corals, there were fewer corals all together (Chong *et al.*, 2023, chapter 2 of this thesis). The persistence of marginal coral populations is thus reliant on the survival of these larger individuals and their capacity to act as brood stock for recruitment (Hughes *et al.*, 2019). Due to apparently different life-histories and demographic responses to a changing environment (Cant *et al.*, 2022; Cant *et al.*, 2023), questions are raised as to the genetic relatedness of corals that appear to inhabit both tropical and subtropical reefs. Because marine organisms live close

to their thermal limits, they are highly sensitive to ocean warming, and are expected to experience range contraction if unable to track the rate of warming (Pinsky *et al.*, 2020). Although benthic community changes from kelp reefs to turf algae/hard coral dominant reefs indicate tropicalisation is occurring to some extent (Fujita, 2010; Vergés *et al.*, 2014), I showed that the scleractinian coral species at high latitudes in Japan are specialists with distinctly different endosymbiont communities (Chapter 4). Our genetic examination of *Pocillopora* corals and their endosymbionts along the Kuroshio current confirmed that coral populations found in the tropics are phylogenetically distinct from their high latitude counterparts, despite the current transporting warm water and genetic materials poleward. Despite ongoing ocean warming, there is a clear biogeographic break that separates the southern islands and mainland Japan, implying that abiotic conditions at high latitude range limits (low winter temperatures, high turbidity) continue to exert control on the poleward range limits of tropical coral taxa. Altogether, the demographic and genetic differences suggest that high latitude marginal reefs are unique entities, with corals that are vulnerable to climate change effects, due to the suite of physiological adaptations that is required for survival at high latitudes. As such, these reefs are unlikely to serve as refugia for tropical taxa (Soares, 2020).

5.2 Methods progress and implications

The approaches used in this thesis sought to improve our ability in detecting changes in population size structure (size distributions) of ecological communities. Most studies calculate, compare and regress summary statistics (e.g., the geometric mean) against some predictor variable to assess how size distributions differ, reducing entire probability density functions to single numbers. This means that valuable, nuanced information such as multimodality in a distribution is lost. In chapter 2, I used compositional functional regression (Talská *et al.*, 2018) to predict how entire size distributions change along the East Australian coast, providing direct estimates of coral sizes that appear most affected by abiotic differences along the environmental gradient along the east coast of Australia. Beyond demographic inferences and insights that can be gained from using size distributions (e.g., Kayal *et al.*, 2018; Pisapia *et al.*, 2020), this method allows other size-dependent rates, such as photosynthesis, respiration and calcification rates to be estimated at a population/community level (Carlot *et al.*, 2021; Carlot

et al., 2022). Size spectrum modelling is another cost-effective way of summarizing and assessing population states under different conditions, typically used in fishery assessments (Blanchard *et al.*, 2005). With the assumption of an underlying bounded power law distribution (Edwards *et al.*, 2017), the value of exponent b of the distribution can indicate the proportion of small to larger individuals in a population or assemblage. However, my findings in chapter 3 indicate that the log-normal distribution describes reef fish and coral abundance data much better. BPL also systematically over-estimates the sizes of the largest individuals in a population. Because large individuals have disproportionate effects on vital rates such as fecundity and reproductive output, skewed estimates of the largest sizes could propagate serious errors and result in excessively positive assessment of stock status, wrongly informing fisheries recommendations (Edgar *et al.*, 2024), in assessing the impact of human activities on populations (Carvalho *et al.*, 2021), or in estimating recovery potential of populations (Pisapia *et al.*, 2020). I add evidence to the call for using ensemble techniques that compare outputs of multiple models (Edgar *et al.*, 2018).

5.3 Future research directions

This thesis uses the strength of a dataset that covers a large spatial scale to answer demographic questions using a macroecological approach. While a snapshot of the population size structure of coral and fish provides insight into the main drivers of biodiversity patterns, capturing long-term patterns through repeated monitoring, especially pre- and post- disturbance to track population recovery would be critical following projected back-to-back mass bleaching events. In addition, repeated monitoring could also be used in other applications to assess the effectiveness of various large-scale interventions and mitigations (Anthony *et al.*, 2020; Voolstra *et al.*, 2023), such as regional scale cloud brightening, which might be employed to keep solar radiation low, and crown-of-thorns starfish control to reduce the extent of coral mortality from predation (Condie *et al.*, 2021). The effectiveness of these interventions would be especially suitable for testing using a demographic approach, as outlined in chapter 2. However, some limitations must be considered to make large-scale investigations realistic and achievable. Firstly, coral size abundance data is collected through benthic photo transects, which means that the data collected is subject to a minus

sampling bias, in which large corals are less likely to be sampled (chapters 2 and 3). Secondly, I do not currently differentiate between coral taxa. Challenges in field taxonomy needs to be overcome by having enough individuals – thus data points – to compare across the entire environmental gradient. A solution to both issues would be to employ photogrammetry (Ferrari *et al.*, 2021) to survey reefs along environmental gradients by building 3D photo-mosaics, and to incorporate machine learning techniques (e.g., ReefCloud, reefcloud.ai; TagLab, taglab.isti.cnr.it) for image annotation and data analysis. Photo-mosaics would capture more data, as well as more accurate sizes/volumes of entire colonies, reducing the likelihood of sampling biases across size spectra. Having more data across taxa allows for conducting population level studies that are taxa specific. Although the initial cost and time investment of photogrammetry techniques might be higher, a semi-automated procedure that can be improved incrementally would make long-term monitoring easier better and scalable (e.g., Lange & Perry, 2020; Sauder *et al.*, 2024). Efforts should also be put into understanding the error margins associated with transforming 2D planar areas to 3D volumes across all coral taxa (House *et al.*, 2018), to ensure continuity and that historical data are not lost due to a change in methodology.

A limitation to macroecological approaches is that it is generally difficult to tease out processes from observable patterns, especially since multiple processes can give the same pattern (Beck *et al.*, 2012; Damgaard, 2019). Biological processes and their effects on population dynamics, e.g., density dependence and competition between taxa, have not been addressed in this thesis, but would be a worthy endeavour. For example, Kayal and Adjeroud (2022) hypothesised that differences in coral competitive performance across environment gradients can indicate their ecological niches and windows, which could aid the prediction of response to environmental stressors. Similarly, using static co-occurrence and abundance data of coral communities along gradients could highlight species pairs that show facilitative interactions, which might allow the prediction of diversity and distributions with increasing environmental stress (Gallien *et al.*, 2018). Efforts to quantify and understand the intra- and inter-specific density dependence would provide important insights into the recruitment and survival dynamics of corals (Cameron & Harrison, 2020; Fundakowski *et al.*, 2024), and

potentially aid any human interventions, such as coral restoration efforts (Suggett & van Oppen, 2022).

Finally, while there is currently no strong evidence for coral tropicalisation in *Pocillopora*, this could change in the near future. It will be worthwhile to resample and examine likelihood and progress of coral poleward range expansion, as well as to link genetic diversity to population size structure. As techniques such as Oxford Nanopore Technologies mature and costs reduce, in-situ molecular characterisation of coral holobionts (Carradec *et al.*, 2020) could become commonplace, guiding sampling efforts in research programmes by clarifying the genetic identity of cryptic species and/or species complexes of interest. Understanding spatial and temporal patterns of genetic variation can reveal the driving forces of genetic turnover, mechanisms of divergent selection, local adaptation and population viability (Wogan & Wang, 2018).

Linking genetics and demography should be at the centre of understanding population resilience to climate change. Careful quantitative analyses of size spectra, such as those outlined in this thesis, provide the most holistic insight into the growth, survival and recruitment dynamics of a population. Genetic data at an appropriate resolution provides an ecological baseline to understand the effect of demographic changes at different levels of organisation: from individual, species, population to community (Capdevila *et al.*, 2021). Where resources are available, the development and upscaling of demographic research programmes that combine developments in genetics and quantitative techniques could give better predictions of population viability than current methods, which still strongly relies on expert opinion, e.g., the IUCN SSC Coral Specialist Group (Carpenter *et al.*, 2008).

5.4 Conclusions

To summarise, this thesis provides 1) new ecological insights into the population dynamics of reef coral communities in two biogeographic transition zones in the western Pacific, one along the east coast of Australia, and one on the Pacific coast of Japan, and 2) methodological improvements in detecting changes in population size structure. At these large spatial scales, I highlight fundamental demographic and genetic differences in reef corals along environmental gradients spanning approximately 1000 km. Fewer but larger corals are found at

high latitude reefs, in which the genetic diversity is low and unique. Methods currently used to quantify differences in population structure could be improved by considering entire probability distributions, and acknowledging poor model fits where they exist. Anthropogenic climate change will continue to threaten coral reef communities along environmental gradients. In addition to curbing carbon emissions to allow for longer windows of recovery from heat stress, continual monitoring of population structure, organismal diversity and distribution using modern technological advances is paramount to understanding the resilience of populations, and the recovery potential of affected reef communities.

References

- Abrego, D., Howells, E. J., Smith, S. D. A., Madin, J. S., Sommer, B., Schmidt-Roach, S., Cumbo, V. R., Thomson, D. P., Rosser, N. L., & Baird, A. H. (2021). Factors Limiting the Range Extension of Corals into High-Latitude Reef Regions. *Diversity*, 13(12), 632. <https://doi.org/10.3390/d13120632>
- Adjeroud, M., Pratchett, M. S., Kospartov, M. C., Lejeusne, C., & Penin, L. (2007). Small-scale variability in the size structure of scleractinian corals around Moorea, French Polynesia: patterns across depths and locations. *Hydrobiologia*, 589(1), 117-126. <https://doi.org/10.1007/s10750-007-0726-2>
- Adler, F. R. (1996). A model of self-thinning through local competition. *Proceedings of the National Academy of Sciences*, 93(18), 9980-9984. <https://doi.org/doi:10.1073/pnas.93.18.9980>
- AIMS. (2024a). *Coral cover remains high while impacts of mass coral bleaching yet to be determined*. Australian Institute of Marine Science. (Annual Summary Report of the Great Barrier Reef Coral Reef Condition, Issue. <https://www.aims.gov.au/monitoring-great-barrier-reef/gbr-condition-summary-2023-24>
- AIMS. (2024b). *Unfolding global bleaching calls for collaboration and solutions*. Retrieved 27th September from <https://www.aims.gov.au/information-centre/news-and-stories/unfolding-global-bleaching-calls-collaboration-and-solutions>
- Ainsworth, T. D., & Brown, B. E. (2021). Coral bleaching. *Current Biology*, 31(1), R5-R6. <https://doi.org/10.1016/j.cub.2020.10.048>
- Álvarez-Noriega, M., Baird, A. H., Dornelas, M., Madin, J. S., Cumbo, V. R., & Connolly, S. R. (2016). Fecundity and the demographic strategies of coral morphologies. *Ecology*, 97(12), 3485-3493. <https://doi.org/10.1002/ecy.1588>
- Andersen, K. H. (2019). *Fish Ecology, Evolution, and Exploitation: A New Theoretical Synthesis*. Princeton University Press. <https://doi.org/10.23943/princeton/9780691192956.001.0001>
- Anderson, K. D., & Pratchett, M. S. (2014). Variation in size-frequency distributions of branching corals between a tropical versus sub-tropical reef. *Marine Ecology Progress Series*, 502, 117-128. <https://www.int-res.com/abstracts/meps/v502/p117-128/>
- Anthony, K. R. N., Helmstedt, K. J., Bay, L. K., Fidelman, P., Hussey, K. E., Lundgren, P., Mead, D., McLeod, I. M., Mumby, P. J., Newlands, M., Schaffelke, B., Wilson, K. A., & Hardisty, P. E. (2020). Interventions to help coral reefs under global change—A complex decision challenge. *PLOS ONE*, 15(8), e0236399. <https://doi.org/10.1371/journal.pone.0236399>
- Archer, M. R., Roughan, M., Keating, S. R., & Schaeffer, A. (2017). On the Variability of the East Australian Current: Jet Structure, Meandering, and Influence on Shelf Circulation. *Journal of Geophysical Research: Oceans*, 122(11), 8464-8481. <https://doi.org/https://doi.org/10.1002/2017JC013097>
- Baddeley, A. J. (1998). Spatial sampling and censoring. In O. E. Barndorff-Nielsen, W. S. Kendall, & M. N. M. van Lieshout (Eds.), *Stochastic Geometry: Likelihood and Computation* (1st ed.). Routledge.

- Baird, A. H., Guest, J. R., & Willis, B. L. (2009). Systematic and Biogeographical Patterns in the Reproductive Biology of Scleractinian Corals. *Annual Review of Ecology, Evolution and Systematics*, 40(Volume 40, 2009), 551-571.
<https://doi.org/https://doi.org/10.1146/annurev.ecolsys.110308.120220>
- Baird, A. H., Hoogenboom, M. O., & Huang, D. (2017). *Cyphastrea salae*, a new species of hard coral from Lord Howe Island, Australia (Scleractinia, Merulinidae). *ZooKeys*, 662, 49-66.
<https://doi.org/10.3897/zookeys.662.11454>
- Baird, A. H., Sommer, B., & Madin, J. S. (2012). Pole-ward range expansion of *Acropora* spp. along the east coast of Australia. *Coral Reefs*, 31(4), 1063-1063. <https://doi.org/10.1007/s00338-012-0928-6>
- Baird, A. H., Yakovleva, I. M., Harii, S., Sinniger, F., & Hidaka, M. (2021). Environmental constraints on the mode of symbiont transmission in corals. *Journal of Experimental Marine Biology and Ecology*, 538, 151499. <https://doi.org/https://doi.org/10.1016/j.jembe.2020.151499>
- Baird, M. E., Timko, P. G., Middleton, J. H., Mullaney, T. J., Cox, D. R., & Suthers, I. M. (2008). Biological properties across the Tasman Front off southeast Australia. *Deep Sea Research Part I: Oceanographic Research Papers*, 55(11), 1438-1455.
<https://doi.org/https://doi.org/10.1016/j.dsr.2008.06.011>
- Bak, R. P. M., & Meesters, E. H. (1998). Coral population structure: the hidden information of colony size-frequency distributions. *Marine Ecology Progress Series*, 162, 301-306. <http://www.jstor.org/stable/24859064>
- Bak, R. P. M., & Meesters, E. H. (1999). Population Structure as a Response of Coral Communities to Global Change. *American Zoologist*, 39(1), 56-65.
<https://doi.org/10.1093/icb/39.1.56>
- Baker, D. M., Weigt, L., Fogel, M., & Knowlton, N. (2013). Ancient DNA from Coral-Hosted Symbiodinium Reveal a Static Mutualism over the Last 172 Years. *PLOS ONE*, 8(2), e55057.
<https://doi.org/10.1371/journal.pone.0055057>
- Bandelt, H. J., Forster, P., & Röhl, A. (1999). Median-joining networks for inferring intraspecific phylogenies. *Mol Biol Evol*, 16(1), 37-48.
<https://doi.org/10.1093/oxfordjournals.molbev.a026036>
- Barneche, D. R., Robertson, D. R., White, C. R., & Marshall, D. J. (2018). Fish reproductive-energy output increases disproportionately with body size. *Science*, 360(6389), 642-645.
<https://doi.org/doi:10.1126/science.aao6868>
- Beck, J., Ballesteros-Mejia, L., Buchmann, C. M., Dengler, J., Fritz, S. A., Gruber, B., Hof, C., Jansen, F., Knapp, S., Kreft, H., Schneider, A.-K., Winter, M., & Dormann, C. F. (2012). What's on the horizon for macroecology? *Ecography*, 35(8), 673-683.
<https://doi.org/https://doi.org/10.1111/j.1600-0587.2012.07364.x>
- Beger, M., Sommer, B., Harrison, P. L., Smith, S. D. A., & Pandolfi, J. M. (2014). Conserving potential coral reef refuges at high latitudes. *Diversity and Distributions*, 20(3), 245-257.
<https://doi.org/https://doi.org/10.1111/ddi.12140>
- Beier, C., Beierkuhnlein, C., Wohlgemuth, T., Penuelas, J., Emmett, B., Körner, C., De Boeck, H., Christensen, J. H., Leuzinger, S., Janssens, I. A., & Hansen, K. (2012). Precipitation manipulation experiments - challenges and recommendations for the future. *Ecology Letters*, 15(8), 899-911.
<https://doi.org/10.1111/j.1461-0248.2012.01793.x>

- Bernard, C. D., Bonsall, M. B., & Salguero-Gómez, R. (2024). Life Histories and Study Duration matter less than Prior Knowledge of Vital Rates to Inverse Integral Projection Models. *bioRxiv*, 2024.2004.2006.588423. <https://doi.org/10.1101/2024.04.06.588423>
- Bernard, G. G. R., Kellam, A. L., & Szereday, S. (2023). Differential size frequency distribution of hard coral colonies across physical reef health gradients in Northeast Peninsula Malaysia. *Regional Studies in Marine Science*, 61, 102872.
- Blanchard, J. L., Andersen, K. H., Scott, F., Hintzen, N. T., Piet, G., & Jennings, S. (2014). Evaluating targets and trade-offs among fisheries and conservation objectives using a multispecies size spectrum model. *Journal of Applied Ecology*, 51(3), 612-622. <https://doi.org/https://doi.org/10.1111/1365-2664.12238>
- Blanchard, J. L., Dulvy, N. K., Jennings, S., Ellis, J. R., Pinnegar, J. K., Tidd, A., & Kell, L. T. (2005). Do climate and fishing influence size-based indicators of Celtic Sea fish community structure? *ICES Journal of Marine Science*, 62(3), 405-411. <https://doi.org/10.1016/j.icesjms.2005.01.006>
- Bongaerts, P., Ridgway, T., Sampayo, E. M., & Hoegh-Guldberg, O. (2010). Assessing the 'deep reef refugia' hypothesis: focus on Caribbean reefs. *Coral Reefs*, 29(2), 309-327. <https://doi.org/10.1007/s00338-009-0581-x>
- Brown, J. H. (1995). *Macroecology*. University of Chicago Press.
- Brown, K. T., Lenz, E. A., Glass, B. H., Kruse, E., McClintock, R., Drury, C., Nelson, C. E., Putnam, H. M., & Barott, K. L. (2023). Divergent bleaching and recovery trajectories in reef-building corals following a decade of successive marine heatwaves. *Proceedings of the National Academy of Sciences*, 120(52), e2312104120. <https://doi.org/doi:10.1073/pnas.2312104120>
- Brunner, C. A., Uthicke, S., Ricardo, G. F., Hoogenboom, M. O., & Negri, A. P. (2021). Climate change doubles sedimentation-induced coral recruit mortality. *Science of The Total Environment*, 768, 143897. <https://doi.org/https://doi.org/10.1016/j.scitotenv.2020.143897>
- Budd, A. F., & Pandolfi, J. M. (2010). Evolutionary novelty is concentrated at the edge of coral species distributions. *Science*, 328(5985), 1558-1561. <https://doi.org/10.1126/science.1188947>
- Buddemeier, R., Kleypas, J., & Aronson, R. (2004). *Coral Reefs & Global Climate Change: Potential Contributions of Climate Change to Stresses on Coral Reef Ecosystems*. Pew Center on Global Climate Change Virginia.
- Burke, L., Reytar, K., Spalding, M., & Perry, A. (2011). *Reefs At Risk Revisited*. World Resources Institute. Washington. <http://www.wri.org/publication/reefs-risk-revisited>
- Burnham, K. P., & Anderson, D. R. (2004). Multimodel Inference: Understanding AIC and BIC in Model Selection. *Sociological Methods & Research*, 33(2), 261-304. <https://doi.org/10.1177/0049124104268644>
- Callaghan, C. T., Borda-de-Água, L., van Klink, R., Rozzi, R., & Pereira, H. M. (2023). Unveiling global species abundance distributions. *Nature Ecology & Evolution*, 7(10), 1600-1609. <https://doi.org/10.1038/s41559-023-02173-y>
- Cameron, K. A., & Harrison, P. L. (2020). Density of coral larvae can influence settlement, post-settlement colony abundance and coral cover in larval

- restoration. *Scientific Reports*, 10(5488).
<https://doi.org/https://doi.org/10.1038/s41598-020-62366-4>
- Cant, J., Cook, K., Reimer, J., Takuma, M., Masako, N., O'Flaherty, C., Salguero-Gómez, R., & Beger, M. (2022). Transient amplification enhances the persistence of tropicalising coral assemblages in marginal high latitude environments. *Ecography*.
- Cant, J., Reimer, J. D., Sommer, B., Cook, K. M., Kim, S. W., Sims, C. A., Mezaki, T., O'Flaherty, C., Brooks, M., Malcolm, H. A., Pandolfi, J. M., Salguero-Gómez, R., & Beger, M. (2023). Coral assemblages at higher latitudes favor short-term potential over long-term performance. *Ecology*, 104(9), e4138. <https://doi.org/https://doi.org/10.1002/ecy.4138>
- Cant, J., Salguero-Gómez, R., Kim, S. W., Sims, C. A., Sommer, B., Brooks, M., Malcolm, H. A., Pandolfi, J. M., & Beger, M. (2020). The projected degradation of subtropical coral assemblages by recurrent thermal stress. *Journal of Animal Ecology*, 00, 1-15. <https://doi.org/10.1111/1365-2656.13340>
- Canty, S. W. J., Nowakowski, A. J., Cox, C. E., Valdivia, A., Holstein, D. M., Limer, B., Lefcheck, J. S., Craig, N., Drysdale, I., Giro, A., Soto, M., & McField, M. (2024). Interplay of management and environmental drivers shifts size structure of reef fish communities. *Global Change Biology*, 30(4), e17257. <https://doi.org/https://doi.org/10.1111/gcb.17257>
- Capdevila, P., Stott, I., Beger, M., & Salguero-Gómez, R. (2020). Towards a Comparative Framework of Demographic Resilience. *Trends in Ecology & Evolution*, 35(9), 776-786.
<https://doi.org/https://doi.org/10.1016/j.tree.2020.05.001>
- Capdevila, P., Stott, I., Oliveras Menor, I., Stouffer, D. B., Raimundo, R. L. G., White, H., Barbour, M., & Salguero-Gómez, R. (2021). Reconciling resilience across ecological systems, species and subdisciplines. *Journal of Ecology*, 109(9), 3102-3113.
<https://doi.org/https://doi.org/10.1111/1365-2745.13775>
- Carlot, J., Kayal, M., Lenihan, H. S., Brandl, S. J., Casey, J. M., Adjeroud, M., Cardini, U., Merciere, A., Espiau, B., Barneche, D. R., Rovere, A., Hédouin, L., & Parravicini, V. (2021). Juvenile corals underpin coral reef carbonate production after disturbance. *Global Change Biology*, 27(11), 2623-2632. <https://doi.org/https://doi.org/10.1111/gcb.15610>
- Carlot, J., Rouzé, H., Barneche, D. R., Mercière, A., Espiau, B., Cardini, U., Brandl, S. J., Casey, J. M., Pérez-Rosales, G., Adjeroud, M., Hédouin, L., & Parravicini, V. (2022). Scaling up calcification, respiration, and photosynthesis rates of six prominent coral taxa. *Ecology and Evolution*, 12(3), e8613. <https://doi.org/https://doi.org/10.1002/ece3.8613>
- Carpenter, K. E., Abrar, M., Aeby, G., Aronson, R. B., Banks, S., Bruckner, A., Chiriboga, A., Cortés, J., Delbeek, J. C., DeVantier, L., Edgar, G. J., Edwards, A. J., Fenner, D., Guzmán, H. M., Hoeksema, B. W., Hodgson, G., Johan, O., Licuanan, W. Y., Livingstone, S. R., Lovell, E. R., Moore, J. A., Obura, D. O., Ochavillo, D., Polidoro, B. A., Precht, W. F., Quibilan, M. C., Reboton, C., Richards, Z. T., Rogers, A. D., Sanciangco, J., Sheppard, A., Sheppard, C., Smith, J., Stuart, S., Turak, E., Veron, J. E. N., Wallace, C., Weil, E., & Wood, E. (2008). One-Third of Reef-Building Corals Face Elevated Extinction Risk from Climate Change and Local Impacts. *Science*, 321(5888), 560-563.
<https://doi.org/doi:10.1126/science.1159196>

- Carradec, Q., Poulain, J., Boissin, E., Hume, B. C. C., Voolstra, C. R., Ziegler, M., Engelen, S., Cruaud, C., Planes, S., & Wincker, P. (2020). A framework for in situ molecular characterization of coral holobionts using nanopore sequencing. *Scientific Reports*, *10*(1), 15893. <https://doi.org/10.1038/s41598-020-72589-0>
- Carvalho, P. G., Setiawan, F., Fahlevy, K., Subhan, B., Madduppa, H., Zhu, G., & Humphries, A. T. (2021). Fishing and habitat condition differentially affect size spectra slopes of coral reef fishes. *Ecological Applications*, *31*(5), e02345. <https://doi.org/https://doi.org/10.1002/eap.2345>
- Caswell, H. (2001). *Matrix Population Models: Construction, Analysis and Interpretation* (2nd ed.). Oxford University Press.
- Ceccarelli, D. M., Evans, R. D., Logan, M., Mantel, P., Puotinen, M., Petus, C., Russ, G. R., & Williamson, D. H. (2020). Long-term dynamics and drivers of coral and macroalgal cover on inshore reefs of the Great Barrier Reef Marine Park. *Ecological Applications*, *30*(1), e02008. <https://doi.org/https://doi.org/10.1002/eap.2008>
- Chadwick, N. E., & Morrow, K. M. (2011). Competition Among Sessile Organisms on Coral Reefs. In Z. Dubinsky & N. Stambler (Eds.), *Coral Reefs: An Ecosystem in Transition* (pp. 347-371). Springer Netherlands. https://doi.org/10.1007/978-94-007-0114-4_20
- Chamberlain, S. (2024). *rerddap: General Purpose Client for 'ERDDAP' Servers*. In (Version R package version 1.1.0) <https://CRAN.R-project.org/package=rerddap>
- Chan, Y. K. S., Affendi, Y. A., Ang, P. O., Baria-Rodriguez, M. V., Chen, C. A., Chui, A. P. Y., Giyanto, Glue, M., Huang, H., Kuo, C. Y., Kim, S. W., Lam, V. Y. Y., Lane, D. J. W., Lian, J. S., Lin, S. M. N. N., Lunn, Z., Nañola, C. L., Nguyen, V. L., Park, H. S., Suharsono, Sutthacheep, M., Vo, S. T., Vibol, O., Waheed, Z., Yamano, H., Yeemin, T., Yong, E., Kimura, T., Tun, K., Chou, L. M., & Huang, D. (2023). Decadal stability in coral cover could mask hidden changes on reefs in the East Asian Seas. *Communications Biology*, *6*(1), 630. <https://doi.org/10.1038/s42003-023-05000-z>
- Charbonneau, J. A., Keith, D. M., & Hutchings, J. A. (2018). Trends in the size and age structure of marine fishes. *ICES Journal of Marine Science*, *76*(4), 938-945. <https://doi.org/10.1093/icesjms/fsy180>
- Chong, F., Sommer, B., Stant, G., Verano, N., Cant, J., Lachs, L., Johnson, M. L., Parsons, D. R., Pandolfi, J. M., Salguero-Gómez, R., Spencer, M., & Beger, M. (2023). High-latitude marginal reefs support fewer but bigger corals than their tropical counterparts. *Ecography*, *2023*(12), e06835. <https://doi.org/https://doi.org/10.1111/ecog.06835>
- Cinner, J. E., Huchery, C., MacNeil, M. A., Graham, N. A. J., McClanahan, T. R., Maina, J., Maire, E., Kittinger, J. N., Hicks, C. C., Mora, C., Allison, E. H., D'Agata, S., Hoey, A., Feary, D. A., Crowder, L., Williams, I. D., Kulbicki, M., Vigliola, L., Wantiez, L., Edgar, G., Stuart-Smith, R. D., Sandin, S. A., Green, A. L., Hardt, M. J., Beger, M., Friedlander, A., Campbell, S. J., Holmes, K. E., Wilson, S. K., Brokovich, E., Brooks, A. J., Cruz-Motta, J. J., Booth, D. J., Chabanet, P., Gough, C., Tupper, M., Ferse, S. C. A., Sumaila, U. R., & Mouillot, D. (2016). Bright spots among the world's coral reefs. *Nature*, *535*(7612), 416-419. <https://doi.org/10.1038/nature18607>

- Clauset, A., Shalizi, C. R., & Newman, M. E. J. (2009). Power-law distributions in empirical data. *SIAM review*, 51(4), 661-703.
<https://doi.org/https://doi.org/10.1137/070710111>
- Condie, S. A., Anthony, K. R. N., Babcock, R. C., Baird, M. E., Beeden, R., Fletcher, C. S., Gorton, R., Harrison, D., Hobday, A. J., Plagányi, É. E., & Westcott, D. A. (2021). Large-scale interventions may delay decline of the Great Barrier Reef. *Royal Society Open Science*, 8(4), 201296.
<https://doi.org/doi:10.1098/rsos.201296>
- Connell, J. H. (1973). Population ecology of reef-building corals. In O. A. Jones & R. Endean (Eds.), *Biology and geology of coral reefs* (Vol. 2, pp. 205-245). Academic Press.
- Connell, J. H. (1978). Diversity in Tropical Rain Forests and Coral Reefs. *Science*, 199(4335), 1302-1310.
<https://doi.org/doi:10.1126/science.199.4335.1302>
- Coomes, D. A., Duncan, R. P., Allen, R. B., & Truscott, J. (2003). Disturbances prevent stem size-density distributions in natural forests from following scaling relationships. *Ecology Letters*, 6(11), 980-989.
<https://doi.org/https://doi.org/10.1046/j.1461-0248.2003.00520.x>
- Cousins, S. R., Witkowski, E. T. F., & Pfab, M. F. (2014). Elucidating patterns in the population size structure and density of *Aloe plicatilis*, a tree aloe endemic to the Cape fynbos, South Africa. *South African Journal of Botany*, 90, 20-36.
<https://doi.org/https://doi.org/10.1016/j.sajb.2013.09.012>
- Cowman, P. F., Quattrini, A. M., Bridge, T. C. L., Watkins-Colwell, G. J., Fadli, N., Grinblat, M., Roberts, T. E., McFadden, C. S., Miller, D. J., & Baird, A. H. (2020). An enhanced target-enrichment bait set for Hexacorallia provides phylogenomic resolution of the staghorn corals (Acroporidae) and close relatives. *Molecular Phylogenetics and Evolution*, 153, 106944.
<https://doi.org/https://doi.org/10.1016/j.ympev.2020.106944>
- Crabbe, M. J. C. (2010). Topography and spatial arrangement of reef-building corals on the fringing reefs of North Jamaica may influence their response to disturbance from bleaching. *Marine Environmental Research*, 69(3), 158-162.
<https://doi.org/10.1016/j.marenvres.2009.09.007>
- Cramer, K. L., Jackson, J. B. C., Donovan, M. K., Greenstein, B. J., Korpanty, C. A., Cook, G. M., & Pandolfi, J. M. (2020). Widespread loss of Caribbean acroporid corals was underway before coral bleaching and disease outbreaks. *Science Advances*, 6(17), eaax9395.
<https://doi.org/doi:10.1126/sciadv.aax9395>
- Crutzen, P. J. (2006). The “Anthropocene”. In E. Ehlers & T. Krafft (Eds.), *Earth System Science in the Anthropocene* (pp. 13-18). Springer Berlin Heidelberg.
https://doi.org/10.1007/3-540-26590-2_3
- Damgaard, C. (2019). A Critique of the Space-for-Time Substitution Practice in Community Ecology. *Trends in Ecology & Evolution*, 34.
<https://doi.org/https://doi.org/10.1016/j.tree.2019.01.013>
- Damuth, J. (1981). Population density and body size in mammals. *Nature*, 290, 699-700.
- Darling, E. S., Alvarez-Filip, L., Oliver, T. A., McClanahan, T. R., & Côté, I. M. (2012). Evaluating life-history strategies of reef corals from species traits. *Ecology Letters*, 15(12), 1378-1386.
<https://doi.org/https://doi.org/10.1111/j.1461-0248.2012.01861.x>

- Darling, E. S., McClanahan, T. R., & Côté, I. M. (2013). Life histories predict coral community disassembly under multiple stressors. *Global Change Biology*, 19(6), 1930-1940. <https://doi.org/https://doi.org/10.1111/gcb.12191>
- De Palmas, S., Soto, D., Denis, V., Ho, M., & Chen, C. (2018). Molecular assessment of *Pocillopora verrucosa* (Scleractinia; Pocilloporidae) distribution along a depth gradient in Ludao, Taiwan. *PeerJ* 6, 6(e5797). <https://doi.org/https://doi.org/10.7717/peerj.5797>
- De'ath, G., Fabricius, K. E., Sweatman, H., & Puotinen, M. (2012). The 27-year decline of coral cover on the Great Barrier Reef and its causes. *Proceedings of the National Academy of Sciences*, 109(44), 17995-17999. <https://doi.org/doi:10.1073/pnas.1208909109>
- Deaker, D. J., & Byrne, M. (2022). Crown of thorns starfish life-history traits contribute to outbreaks, a continuing concern for coral reefs. *Emerg Top Life Sci*, 6(1), 67-79. <https://doi.org/10.1042/etls20210239>
- Dietzel, A. (2020). *The viability of coral populations in the Anthropocene* [James Cook University].
- Dietzel, A., Bode, M., Connolly, S. R., & Hughes, T. P. (2020). Long-term shifts in the colony size structure of coral populations along the Great Barrier Reef. *Proceedings of the Royal Society B: Biological Sciences*, 287(1936), 20201432. <https://doi.org/doi:10.1098/rspb.2020.1432>
- Dietzel, A., Bode, M., Connolly, S. R., & Hughes, T. P. (2021). The population sizes and global extinction risk of reef-building coral species at biogeographic scales. *Nature Ecology & Evolution*, 5(5), 663-669. <https://doi.org/10.1038/s41559-021-01393-4>
- Dixon, A. M., Forster, P. M., & Beger, M. (2021). Coral conservation requires ecological climate - change vulnerability assessments. *Frontiers in Ecology and the Environment*, 19(4), 243-250. <https://doi.org/10.1002/fee.2312>
- Dixon, A. M., Forster, P. M., Heron, S. F., Stoner, A. M. K., & Beger, M. (2022). Future loss of local-scale thermal refugia in coral reef ecosystems. *PLOS Climate*, 1(2), e0000004. <https://doi.org/10.1371/journal.pclm.0000004>
- Dornelas, M., Chase, J. M., Gotelli, N. J., Magurran, A. E., McGill, B. J., Antão, L. H., Blowes, S. A., Daskalova, G. N., Leung, B., Martins, I. S., Moyes, F., Myers-Smith, I. H., Thomas, C. D., & Vellend, M. (2023). Looking back on biodiversity change: lessons for the road ahead. *Philosophical Transactions of the Royal Society B: Biological Sciences*, 378(1881), 20220199. <https://doi.org/doi:10.1098/rstb.2022.0199>
- Dornelas, M., Madin, J. S., Baird, A. H., & Connolly, S. R. (2017). Allometric growth in reef-building corals. *Proceedings of the Royal Society B: Biological Sciences*, 284(1851), 20170053. <https://doi.org/doi:10.1098/rspb.2017.0053>
- Dubinsky, Z., & Stambler, N. (1996). Marine pollution and coral reefs. *Global Change Biology*, 2(6), 511-526. <https://doi.org/https://doi.org/10.1111/j.1365-2486.1996.tb00064.x>
- Easterling, M. R., Ellner, S. P., & Dixon, P. M. (2000). SIZE-SPECIFIC SENSITIVITY: APPLYING A NEW STRUCTURED POPULATION MODEL. *Ecology*, 81(3), 694-708. [https://doi.org/https://doi.org/10.1890/0012-9658\(2000\)081\[0694:SSSAAN\]2.0.CO;2](https://doi.org/https://doi.org/10.1890/0012-9658(2000)081[0694:SSSAAN]2.0.CO;2)
- Edgar, G. J., Bates, A. E., Krueck, N. C., Baker, S. C., Stuart-Smith, R. D., & Brown, C. J. (2024). Stock assessment models overstate sustainability of

- the world's fisheries. *Science*, 385(6711), 860-865.
<https://doi.org/doi:10.1126/science.adl6282>
- Edgar, G. J., Ward, T. J., & Stuart-Smith, R. D. (2018). Rapid declines across Australian fishery stocks indicate global sustainability targets will not be achieved without an expanded network of 'no-fishing' reserves. *Aquatic Conservation: Marine and Freshwater Ecosystems*, 28(6), 1337-1350.
<https://doi.org/https://doi.org/10.1002/aqc.2934>
- Edmunds, P. J. (2021). Vital rates of small reef corals are associated with variation in climate. *Limnology and Oceanography*, 66(3), 901-913.
<https://doi.org/https://doi.org/10.1002/lno.11650>
- Edmunds, P. J., Adjeroud, M., Baskett, M. L., Baums, I. B., Budd, A. F., Carpenter, R. C., Fabina, N. S., Fan, T.-Y., Franklin, E. C., Gross, K., Han, X., Jacobson, L., Klaus, J. S., McClanahan, T. R., O'Leary, J. K., van Oppen, M. J. H., Pochon, X., Putnam, H. M., Smith, T. B., Stat, M., Sweatman, H., van Woesik, R., & Gates, R. D. (2014). Persistence and Change in Community Composition of Reef Corals through Present, Past, and Future Climates. *PLOS ONE*, 9(10), e107525.
<https://doi.org/10.1371/journal.pone.0107525>
- Edmunds, P. J., Combsch, D. J., Torrado, H., Sakai, K., Sinniger, F., & Burgess, S. C. (2024). Latitudinal variation in thermal performance of the common coral *Pocillopora* spp. *Journal of Experimental Biology*, 227(11).
<https://doi.org/10.1242/jeb.247090>
- Edmunds, P. J., & Riegl, B. (2020). Urgent need for coral demography in a world where corals are disappearing. *Marine Ecology Progress Series*, 635, 233-242. <https://www.int-res.com/abstracts/meps/v635/p233-242/>
- Edwards, A. M., Robinson, J. P. W., Plank, M. J., Baum, J. K., & Blanchard, J. L. (2017). Testing and recommending methods for fitting size spectra to data. *Methods in Ecology and Evolution*, 8(1), 57-67.
<https://doi.org/10.1111/2041-210x.12641>
- Egozcue, J. J., Díaz-Barrero, J. L., & Pawlowsky-Glahn, V. (2006). Hilbert Space of Probability Density Functions Based on Aitchison Geometry. *Acta Mathematica Sinica*, 22(4), 1175-1182.
<https://doi.org/10.1007/s10114-005-0678-2>
- Egozcue, J. J., Pawlowsky-Glahn, V., Tolosana-Delgado, R., Ortego, M. I., & Van Den Boogaart, K. G. (2013). Bayes spaces: use of improper distributions and exponential families. *Revista de la Real Academia de Ciencias Exactas, Físicas y Naturales. Serie A. Matemáticas*, 107(2), 475-486. <https://doi.org/10.1007/s13398-012-0082-6>
- Elmendorf, S. C., Henry, G. H. R., Hollister, R. D., Fosaa, A. M., Gould, W. A., Hermanutz, L., Hofgaard, A., Jónsdóttir, I. S., Jorgenson, J. C., Lévesque, E., Magnusson, B., Molau, U., Myers-Smith, I. H., Oberbauer, S. F., Rixen, C., Tweedie, C. E., & Walker, M. D. (2015). Experiment, monitoring, and gradient methods used to infer climate change effects on plant communities yield consistent patterns. *Proceedings of the National Academy of Sciences*, 112(2), 448-452.
<https://doi.org/doi:10.1073/pnas.1410088112>
- Emslie, M. J., Logan, M., Bray, P., Ceccarelli, D. M., Cheal, A. J., Hughes, T. P., Johns, K. A., Jonker, M. J., Kennedy, E. V., Kerry, J. T., Mellin, C., Miller, I. R., Osborne, K., Puotinen, M., Sinclair-Taylor, T., & Sweatman, H. (2024). Increasing disturbance frequency undermines coral reef recovery. *Ecological Monographs*, 94(3), e1619.
<https://doi.org/https://doi.org/10.1002/ecm.1619>

- Evans-Powell, R., Hesp, S. A., Denham, A. M., & Beckley, L. E. (2024). Implications of big, old, fat, fecund, female fish (BOFFFFs) for the reproductive potential of a demersal teleost stock. *Fisheries Research*, 272(106934). <https://doi.org/https://doi.org/10.1016/j.fishres.2023.106934>
- Evers, S. M., Knight, T. M., Inouye, D. W., Miller, T. E. X., Salguero-Gómez, R., Iler, A. M., & Compagnoni, A. (2021). Lagged and dormant season climate better predict plant vital rates than climate during the growing season. *Global Change Biology*, 27(9), 1927-1941. <https://doi.org/https://doi.org/10.1111/gcb.15519>
- Eyal, G., Laverick, J. H., Bongaerts, P., Levy, O., & Pandolfi, J. M. (2021). Mesophotic Coral Ecosystems of the Great Barrier Reef Are Understudied and Underexplored [Perspective]. *Frontiers in Marine Science*, 8. <https://doi.org/10.3389/fmars.2021.622856>
- Ferrari, R., Lachs, L., Pygas, D. R., Humanes, A., Sommer, B., Figueira, W. F., Edwards, A. J., Bythell, J. C., & Guest, J. R. (2021). Photogrammetry as a tool to improve ecosystem restoration. *Trends in Ecology & Evolution*, 36(12), 1093-1101. <https://doi.org/https://doi.org/10.1016/j.tree.2021.07.004>
- Ferro, I., & Morrone, J. J. (2014). Biogeographical transition zones: a search for conceptual synthesis. *Biological Journal of the Linnean Society*, 113(1), 1-12. <https://doi.org/10.1111/bij.12333>
- Fifer, J. E., Yasuda, N., Yamakita, T., Bove, C. B., & Davies, S. W. (2022). Genetic divergence and range expansion in a western North Pacific coral. *Science of The Total Environment*, 813, 152423. <https://doi.org/https://doi.org/10.1016/j.scitotenv.2021.152423>
- Flot, J.-F., Magalon, H., Cruaud, C., Couloux, A., & Tillier, S. (2008). Patterns of genetic structure among Hawaiian corals of the genus Pocillopora yield clusters of individuals that are compatible with morphology. *Comptes Rendus. Biologies*, 331(3), 239-247. <https://doi.org/10.1016/j.crvi.2007.12.003>
- Forbes, C., Evans, M., Hastings, N., & Peacock, B. (2010). Lognormal Distribution. In C. Forbes, M. Evans, N. Hastings, & B. Peacock (Eds.), *Statistical Distributions* (pp. 131-134). <https://doi.org/https://doi.org/10.1002/9780470627242.ch29>
- Fox, M. D., Nelson, C. E., Oliver, T. A., Quinlan, Z. A., Remple, K., Glanz, J., Smith, J. E., & Putnam, H. M. (2021). Differential resistance and acclimation of two coral species to chronic nutrient enrichment reflect life-history traits. *Functional Ecology*, 35(5), 1081-1093. <https://doi.org/https://doi.org/10.1111/1365-2435.13780>
- Froese, R., & Pauly, D. (2024). *FishBase* www.fishbase.org
- Fujita, D. (2010). Current status and problems of isoyake in Japan. *Bulletin of Fisheries Research Agency*, 32, 33-42.
- Fundakowski, G., Carroll, T., Chapeau, M., Edelaar, P., Lala, K., Madin, J. S., Schiettekatte, N., & Dornelas, M. (2024). Positive and negative effects of coral structure on survival and growth of coral fragments. European Coral Reef Symposium, Naples, Italy.
- Gallien, L., Zurell, D., & Zimmermann, N. E. (2018). Frequency and intensity of facilitation reveal opposing patterns along a stress gradient. *Ecology and Evolution*, 8(4), 2171-2181. <https://doi.org/https://doi.org/10.1002/ece3.3855>

- Gardner, T. A., Côté, I. M., Gill, J. A., Grant, A., & Watkinson, A. R. (2003). Long-Term Region-Wide Declines in Caribbean Corals. *Science*, 301(5635), 958-960. <https://doi.org/doi:10.1126/science.1086050>
- Gélin, P., Postaire, B., Fauvelot, C., & Magalon, H. (2017). Reevaluating species number, distribution and endemism of the coral genus *Pocillopora* Lamarck, 1816 using species delimitation methods and microsatellites. *Mol Phylogenet Evol*, 109, 430-446. <https://doi.org/10.1016/j.ympev.2017.01.018>
- Giglio, V. J., Luiz, O. J., & Ferreira, C. E. L. (2020). Ecological impacts and management strategies for recreational diving: A review. *Journal of Environmental Management*, 256, 109949. <https://doi.org/https://doi.org/10.1016/j.jenvman.2019.109949>
- Gjoni, V., Pomeranz, J. P. F., Junker, J. R., & Wesner, J. S. (2024). Size spectra in freshwater streams are consistent across temperature and resource supply. *bioRxiv*, 2024.2001.2009.574822. <https://doi.org/10.1101/2024.01.09.574822>
- Graham, N. A. J., Dulvy, N. K., Jennings, S., & Polunin, N. V. C. (2005). Size-spectra as indicators of the effects of fishing on coral reef fish assemblages. *Coral Reefs*, 24(1), 118-124. <https://doi.org/10.1007/s00338-004-0466-y>
- Greenstreet, S. P. R., Rogers, S. I., Rice, J. C., Piet, G. J., Guirey, E. J., Fraser, H. M., & Fryer, R. J. (2012). A reassessment of trends in the North Sea Large Fish Indicator and a re-evaluation of earlier conclusions. *ICES Journal of Marine Science*, 69(2), 343-345. <https://doi.org/10.1093/icesjms/fsr201>
- Hadj-Hammou, J., Cinner, J. E., Barneche, D. R., Caldwell, I. R., Mouillot, D., Robinson, J. P. W., Schiettekatte, N. M. D., Siqueira, A. C., Taylor, B. M., & Graham, N. A. J. (2024). Global patterns and drivers of fish reproductive potential on coral reefs. *Nature Communications*, 15(1), 6105. <https://doi.org/10.1038/s41467-024-50367-0>
- Harriott, V., & Banks, S. (1995). Recruitment of scleractinian corals in the Solitary Islands Marine Reserve, a high latitude coral-dominated community in Eastern Australia. *Marine Ecology Progress Series*, 123, 155-161. <https://doi.org/10.3354/meps123155>
- Harriott, V. J., Smith, S. D., & Harrison, P. L. (1994). Patterns of coral community structure of subtropical reefs in the Solitary Islands Marine Reserve, Eastern Australia. *Marine Ecology Progress Series*, 109, 67-76.
- Harriott, V. J., & Smith, S. D. A. (2000). Coral population dynamics in a subtropical coral community, Solitary Islands Marine Park, Australia. Proceedings 9th International Coral Reef Symposium, Bali, Indonesia.
- Harrison, H. B., Williamson, D. H., Evans, R. D., Almany, G. R., Thorrold, S. R., Russ, G. R., Feldheim, K. A., van Herwerden, L., Planes, S., Srinivasan, M., Berumen, M. L., & Jones, G. P. (2012). Larval export from marine reserves and the recruitment benefit for fish and fisheries. *Curr Biol*, 22(11), 1023-1028. <https://doi.org/10.1016/j.cub.2012.04.008>
- Haryanti, D., Yasuda, N., Harii, S., & Hidaka, M. (2015). High tolerance of symbiotic larvae of *Pocillopora damicornis* to thermal stress. *Zoological Studies*, 54(1), 52. <https://doi.org/10.1186/s40555-015-0134-7>
- Hatton, I. A., Dobson, A. P., Storch, D., Galbraith, E. D., & Loreau, M. (2019). Linking scaling laws across eukaryotes. *Proceedings of the National Academy of Sciences*, 116(43), 21616-21622. <https://doi.org/doi:10.1073/pnas.1900492116>

- Heather, F. J., Blanchard, J. L., Edgar, G. J., Trebilco, R., & Stuart - Smith, R. D. (2021). Globally consistent reef size spectra integrating fishes and invertebrates. *Ecology Letters*, 24(3), 572-579. <https://doi.org/10.1111/ele.13661>
- Henley, B. J., McGregor, H. V., King, A. D., Hoegh-Guldberg, O., Arzey, A. K., Karoly, D. J., Lough, J. M., DeCarlo, T. M., & Linsley, B. K. (2024). Highest ocean heat in four centuries places Great Barrier Reef in danger. *Nature*, 632(8024), 320-326. <https://doi.org/10.1038/s41586-024-07672-x>
- Higuchi, T., Agostini, S., Casareto, B. E., Suzuki, Y., & Yuyama, I. (2015). The northern limit of corals of the genus *Acropora* in temperate zones is determined by their resilience to cold bleaching. *Scientific Reports*, 5(1), 18467. <https://doi.org/10.1038/srep18467>
- Hoegh-Guldberg, O. (1999). Climate change, coral bleaching and the future of the world's coral reefs. *Marine and Freshwater Research*, 50(8), 839-866. <https://doi.org/https://doi.org/10.1071/MF99078>
- Hoegh-Guldberg, O., Poloczanska, E. S., Skirving, W., & Dove, S. (2017). Coral Reef Ecosystems under Climate Change and Ocean Acidification [Review]. *Frontiers in Marine Science*, 4(158). <https://doi.org/10.3389/fmars.2017.00158>
- Holbrook, S. J., Adam, T. C., Edmunds, P. J., Schmitt, R. J., Carpenter, R. C., Brooks, A. J., Lenihan, H. S., & Briggs, C. J. (2018). Recruitment Drives Spatial Variation in Recovery Rates of Resilient Coral Reefs. *Scientific Reports*, 8(1), 7338. <https://doi.org/10.1038/s41598-018-25414-8>
- Hoogenboom, M. O., Connolly, S. R., & Anthony, K. R. N. (2008). Interactions between morphological and physiological plasticity optimise energy acquisition in corals. *Ecology*, 89(4), 1144-1154. <https://doi.org/https://doi.org/10.1890/07-1272.1>
- House, J. E., Brambilla, V., Bidaut, L. M., Christie, A. P., Pizarro, O., Madin, J. S., & Dornelas, M. (2018). Moving to 3D: relationships between coral planar area, surface area and volume. *PeerJ*, 6, e4280. <https://doi.org/10.7717/peerj.4280>
- Hsiao, W. V., Denis, V., De Palmas, S., & Beger, M. (in review). The ecological importance of taxonomic resolution: A case study on *Pocillopora* demographics. *Ecology and Evolution* (in review).
- Hughes, Terry P., Baird, Andrew H., Dinsdale, Elizabeth A., Moltschaniwskyj, Natalie A., Pratchett, Morgan S., Tanner, Jason E., & Willis, Bette L. (2012). Assembly Rules of Reef Corals Are Flexible along a Steep Climatic Gradient. *Current Biology*, 22(8), 736-741. <https://doi.org/https://doi.org/10.1016/j.cub.2012.02.068>
- Hughes, T. P., Barnes, M. L., Bellwood, D. R., Cinner, J. E., Cumming, G. S., Jackson, J. B. C., Kleypas, J., Van De Leemput, I. A., Lough, J. M., Morrison, T. H., Palumbi, S. R., Van Nes, E. H., & Scheffer, M. (2017a). Coral reefs in the Anthropocene. *Nature*, 546(7656), 82-90. <https://doi.org/10.1038/nature22901>
- Hughes, T. P., & Connell, J. H. (1987). Population Dynamics Based on Size or Age? A Reef-Coral Analysis. *The American Naturalist*, 129(6), 818-829. <https://doi.org/10.1086/284677>
- Hughes, T. P., Kerry, J. T., Álvarez-Noriega, M., Álvarez-Romero, J. G., Anderson, K. D., Baird, A. H., Babcock, R. C., Beger, M., Bellwood, D. R., Berkelmans, R., Bridge, T. C., Butler, I. R., Byrne, M., Cantin, N. E., Comeau, S., Connolly, S. R., Cumming, G. S., Dalton, S. J., Diaz-Pulido, G., Eakin, C. M., Figueira, W. F., Gilmour, J. P., Harrison, H. B., Heron,

- S. F., Hoey, A. S., Hobbs, J.-P. A., Hoogenboom, M. O., Kennedy, E. V., Kuo, C.-y., Lough, J. M., Lowe, R. J., Liu, G., McCulloch, M. T., Malcolm, H. A., McWilliam, M. J., Pandolfi, J. M., Pears, R. J., Pratchett, M. S., Schoepf, V., Simpson, T., Skirving, W. J., Sommer, B., Torda, G., Wachenfeld, D. R., Willis, B. L., & Wilson, S. K. (2017b). Global warming and recurrent mass bleaching of corals. *Nature*, *543*(7645), 373-377. <https://doi.org/10.1038/nature21707>
- Hughes, T. P., Kerry, J. T., Baird, A. H., Connolly, S. R., Chase, T. J., Dietzel, A., Hill, T., Hoey, A. S., Hoogenboom, M. O., Jacobson, M., Kerswell, A., Madin, J. S., Mieog, A., Paley, A. S., Pratchett, M. S., Torda, G., & Woods, R. M. (2019). Global warming impairs stock–recruitment dynamics of corals. *Nature*, *568*(7752), 387-390. <https://doi.org/10.1038/s41586-019-1081-y>
- Hughes, T. P., Kerry, J. T., Baird, A. H., Connolly, S. R., Dietzel, A., Eakin, C. M., Heron, S. F., Hoey, A. S., Hoogenboom, M. O., Liu, G., McWilliam, M. J., Pears, R. J., Pratchett, M. S., Skirving, W. J., Stella, J. S., & Torda, G. (2018). Global warming transforms coral reef assemblages. *Nature*, *556*(7702), 492-496. <https://doi.org/10.1038/s41586-018-0041-2>
- Hughes, T. P., & Tanner, J. E. (2000). Recruitment Failure, Life Histories, and Long-Term Decline of Caribbean Corals. *Ecology*, *81*(8), 2250-2263. <https://doi.org/10.2307/177112>
- Hume, B., Ziegler, M., Poulain, J., Pochon, X., Romac, S., Boissin, E., de Vargas, C., Planes, S., Wincker, P., & Voolstra, C. (2018). An improved primer set and amplification protocol with increased specificity and sensitivity targeting the Symbiodinium ITS2 region. *PeerJ* *6*, e4816. <https://doi.org/https://doi.org/10.7717/peerj.4816>
- Hume, B. C. C., Smith, E. G., Ziegler, M., Warrington, H. J. M., Burt, J. A., LaJeunesse, T. C., Wiedenmann, J., & Voolstra, C. R. (2019). SymPortal: A novel analytical framework and platform for coral algal symbiont next-generation sequencing ITS2 profiling. *Molecular Ecology Resources*, *19*(4), 1063-1080. <https://doi.org/https://doi.org/10.1111/1755-0998.13004>
- Hunter, C. M., Caswell, H., Runge, M. C., Regehr, E. V., Amstrup, S. C., & Stirling, I. (2010). Climate change threatens polar bear populations: a stochastic demographic analysis. *Ecology*, *91*(10), 2883-2897. <https://doi.org/10.1890/09-1641.1>
- Imawaki, S., Bower, A. S., Beal, L., & Qiu, B. (2013). Chapter 13 - Western Boundary Currents. In G. Siedler, S. M. Griffies, J. Gould, & J. A. Church (Eds.), *International Geophysics* (Vol. 103, pp. 305-338). Academic Press. <https://doi.org/https://doi.org/10.1016/B978-0-12-391851-2.00013-1>
- Jennings, S., & Blanchard, J. L. (2004). Fish abundance with no fishing: predictions based on macroecological theory. *Journal of Animal Ecology*, *73*(4), 632-642. <https://doi.org/10.1111/j.0021-8790.2004.00839.x>
- Johnston, E. C., Cunning, R., & Burgess, S. C. (2022). Cophylogeny and specificity between cryptic coral species (*Pocillopora* spp.) at Mo'orea and their symbionts (Symbiodiniaceae). *Molecular Ecology*, *31*(20), 5368-5385. <https://doi.org/https://doi.org/10.1111/mec.16654>
- Jones, A. M., Berkelmans, R., van Oppen, M. J. H., Mieog, J. C., & Sinclair, W. (2008). A community change in the algal endosymbionts of a scleractinian coral following a natural bleaching event: field evidence of

- acclimatization. *Proceedings of the Royal Society B: Biological Sciences*, 275(1641), 1359-1365. <https://doi.org/doi:10.1098/rspb.2008.0069>
- Jones, R., Giofre, N., Luter, H. M., Neoh, T. L., Fisher, R., & Duckworth, A. (2020). Responses of corals to chronic turbidity. *Scientific Reports*, 10(1), 4762. <https://doi.org/10.1038/s41598-020-61712-w>
- Juszkiewicz, D. J., White, N. E., Stolarski, J., Benzoni, F., Arrigoni, R., Hoeksema, B. W., Wilson, N. G., Bunce, M., & Richards, Z. T. (2022). Phylogeography of recent *Plesiastrea* (Scleractinia: Plesiastreidae) based on an integrated taxonomic approach. *Molecular Phylogenetics and Evolution*, 172, 107469. <https://doi.org/https://doi.org/10.1016/j.ympev.2022.107469>
- Kayal, M., & Adjeroud, M. (2022). The war of corals: patterns, drivers and implications of changing coral competitive performances across reef environments. *Royal Society Open Science*, 9(220003). <https://doi.org/https://doi.org/10.1098/rsos.220003>
- Kayal, M., Lenihan, H. S., Brooks, A. J., Holbrook, S. J., Schmitt, R. J., & Kendall, B. E. (2018). Predicting coral community recovery using multi-species population dynamics models. *Ecology Letters*, 21(12), 1790-1799. <https://doi.org/https://doi.org/10.1111/ele.13153>
- Keith, S. A., Webb, T. J., Böhning-Gaese, K., Connolly, S. R., Dulvy, N. K., Eigenbrod, F., Jones, K. E., Price, T., Redding, D. W., Owens, I. P. F., & Isaac, N. J. B. (2012). What is macroecology? *Biology Letters*, 8(6), 904-906. <https://doi.org/doi:10.1098/rsbl.2012.0672>
- Kelley, R. (2021). *Coral Finder 2021*. BYOGUIDES. <https://byoguides.com/products/coral-finder-2021>
- Kerswell, A. P., & Jones, R. J. (2003). Effects of hypo-osmosis on the coral *Stylophora pistillata*: nature and cause of 'low-salinity bleaching'. *Marine Ecology Progress Series*, 253, 145-154.
- Keshavmurthy, S., Mezaki, T., Reimer, J. D., Choi, K.-S., & Chen, C. A. (2023). Succession and Emergence of Corals in High-Latitude (Temperate) Areas of Eastern Asia into the Future. In I. Takeuchi & H. Yamashiro (Eds.), *Coral Reefs of Eastern Asia under Anthropogenic Impacts* (pp. 53-71). Springer International Publishing. https://doi.org/10.1007/978-3-031-27560-9_4
- Kim, S. W., Sampayo, E. M., Sommer, B., Sims, C. A., Gómez-Cabrera, M. d. C., Dalton, S. J., Beger, M., Malcolm, H. A., Ferrari, R., Fraser, N., Figueira, W. F., Smith, S. D. A., Heron, S. F., Baird, A. H., Byrne, M., Eakin, C. M., Edgar, R., Hughes, T. P., Kyriacou, N., Liu, G., Matis, P. A., Skirving, W. J., & Pandolfi, J. M. (2019). Refugia under threat: Mass bleaching of coral assemblages in high-latitude eastern Australia. *Global Change Biology*, 25(11), 3918-3931. <https://doi.org/https://doi.org/10.1111/gcb.14772>
- Kjørboe, T., & Hirst, A. G. (2014). Shifts in Mass Scaling of Respiration, Feeding, and Growth Rates across Life-Form Transitions in Marine Pelagic Organisms. *The American Naturalist*, 183(4), E118-E130. <https://doi.org/10.1086/675241>
- Komaki, S. (2021). Widespread misperception about a major East Asian biogeographic boundary exposed through bibliographic survey and biogeographic meta-analysis. *Journal of Biogeography*, 48(9), 2375-2386. <https://doi.org/https://doi.org/10.1111/jbi.14210>
- Kramer, N., Tamir, R., Eyal, G., & Loya, Y. (2020). Coral Morphology Portrays the Spatial Distribution and Population Size-Structure Along a 5–100 m

- Depth Gradient [Original Research]. *Frontiers in Marine Science*, 7. <https://doi.org/10.3389/fmars.2020.00615>
- Kreyling, J., Jentsch, A., & Beier, C. (2014). Beyond realism in climate change experiments: gradient approaches identify thresholds and tipping points. *Ecology Letters*, 17(1), 125-e121. <https://doi.org/10.1111/ele.12193>
- Kumagai, N. H., García Molinos, J., Yamano, H., Takao, S., Fujii, M., & Yamanaka, Y. (2018). Ocean currents and herbivory drive macroalgae-to-coral community shift under climate warming. *Proceedings of the National Academy of Sciences*, 115(36), 8990-8995. <https://doi.org/doi:10.1073/pnas.1716826115>
- Lachs, L., Chong, F., Beger, M., East, H. K., Guest, J. R., & Sommer, B. (2022). SizeExtractR: A workflow for rapid reproducible extraction of object size metrics from scaled images. *Ecology and Evolution*, 12(3), e8724. <https://doi.org/https://doi.org/10.1002/ece3.8724>
- Lachs, L., Sommer, B., Cant, J., Hodge, J. M., Malcolm, H. A., Pandolfi, J. M., & Beger, M. (2021). Linking population size structure, heat stress and bleaching responses in a subtropical endemic coral. *Coral Reefs*, 40(3), 777-790. <https://doi.org/10.1007/s00338-021-02081-2>
- Lange, I. D., & Perry, C. T. (2020). A quick, easy and non-invasive method to quantify coral growth rates using photogrammetry and 3D model comparisons. *Methods in Ecology and Evolution*, 11(6), 714-726. <https://doi.org/https://doi.org/10.1111/2041-210X.13388>
- Lawson, C. R., Vindenes, Y., Bailey, L., & Van De Pol, M. (2015). Environmental variation and population responses to global change. *Ecology Letters*, 18(7), 724-736. <https://doi.org/10.1111/ele.12437>
- Leigh, J. W., & Bryant, D. (2015). popart: full-feature software for haplotype network construction. *Methods in Ecology and Evolution*, 6(9), 1110-1116. <https://doi.org/https://doi.org/10.1111/2041-210X.12410>
- Leriorato, J. C., & Nakamura, Y. (2019). Unpredictable extreme cold events: a threat to range-shifting tropical reef fishes in temperate waters. *Marine Biology*, 166(8), 110. <https://doi.org/10.1007/s00227-019-3557-6>
- Lien, Y.-T., Fukami, H., & Yamashita, Y. (2013). Genetic variations within Symbiodinium clade C among zooxanthellate corals (Scleractinia) in the temperate zone of Japan. *Fisheries Science*, 79, 579-591. <https://doi.org/10.1007/s12562-013-0623-8>
- Ling, S. D., Johnson, C. R., Frusher, S. D., & Ridgway, K. R. (2009). Overfishing reduces resilience of kelp beds to climate-driven catastrophic phase shift. *Proceedings of the National Academy of Sciences*, 106(52), 22341-22345. <https://doi.org/doi:10.1073/pnas.0907529106>
- Machalová, J., Talská, R., Hron, K., & Gába, A. (2021). Compositional splines for representation of density functions. *Computational Statistics*, 36(2), 1031-1064. <https://doi.org/10.1007/s00180-020-01042-7>
- Madin, J. S., Anderson, K. D., Andreasen, M. H., Bridge, T. C. L., Cairns, S. D., Connolly, S. R., Darling, E. S., Diaz, M., Falster, D. S., Franklin, E. C., Gates, R. D., Harmer, A. M. T., Hoogenboom, M. O., Huang, D., Keith, S. A., Kosnik, M. A., Kuo, C.-Y., Lough, J. M., Lovelock, C. E., Luiz, O., Martinelli, J., Mizerek, T., Pandolfi, J. M., Pochon, X., Pratchett, M. S., Putnam, H. M., Roberts, T. E., Stat, M., Wallace, C. C., Widman, E., & Baird, A. H. (2016). The Coral Trait Database, a curated database of trait information for coral species from the global oceans. *Scientific Data*, 3(1), 160017. <https://doi.org/10.1038/sdata.2016.17>

- Madin, J. S., Baird, A. H., Baskett, M. L., Connolly, S. R., & Dornelas, M. A. (2020). Partitioning colony size variation into growth and partial mortality. *Biology Letters*, 16(1), 20190727. <https://doi.org/10.1098/rsbl.2019.0727>
- Madin, J. S., Baird, A. H., Dornelas, M., & Connolly, S. R. (2014). Mechanical vulnerability explains size - dependent mortality of reef corals. *Ecology Letters*, 17(8), 1008-1015. <https://doi.org/10.1111/ele.12306>
- Malcolm, H. A., Davies, P. L., Jordan, A., & Smith, S. D. A. (2011). Variation in sea temperature and the East Australian Current in the Solitary Islands region between 2001–2008. *Deep Sea Research Part II: Topical Studies in Oceanography*, 58(5), 616-627. <https://doi.org/https://doi.org/10.1016/j.dsr2.2010.09.030>
- Martello, M. F., Bleuel, J., Pennino, M. G., & Longo, G. O. (2024). Projected climate-driven shifts in coral distribution indicate tropicalisation of Southwestern Atlantic reefs. *Diversity and Distributions*, n/a(n/a), e13851. <https://doi.org/https://doi.org/10.1111/ddi.13851>
- Martín-Fernández, J. A., Barceló-Vidal, C., & Pawlowsky-Glahn, V. (2003). Dealing with Zeros and Missing Values in Compositional Data Sets Using Nonparametric Imputation. *Mathematical Geology*, 35(3), 253-278. <https://doi.org/10.1023/A:1023866030544>
- McClanahan, T. R., Ateweberhan, M., & Omukoto, J. (2008). Long-term changes in coral colony size distributions on Kenyan reefs under different management regimes and across the 1998 bleaching event. *Marine Biology*, 153(5), 755-768. <https://doi.org/10.1007/s00227-007-0844-4>
- McGill, B. J., Chase, J. M., Hortal, J., Overcast, I., Rominger, A. J., Rosindell, J., Borges, P. A. V., Emerson, B. C., Etienne, R. S., Hickerson, M. J., Mahler, D. L., Massol, F., McGaughan, A., Neves, P., Parent, C., Patiño, J., Ruffley, M., Wagner, C. E., & Gillespie, R. (2019). Unifying macroecology and macroevolution to answer fundamental questions about biodiversity. *Global Ecology and Biogeography*, 28(12), 1925-1936. <https://doi.org/https://doi.org/10.1111/geb.13020>
- Mendelssohn, R. (2024). *rerddapXtracto: Extracts Environmental Data from 'ERDDAP' Web Services*. In (Version R package version 1.2.0) <https://CRAN.R-project.org/package=rerddapXtracto>
- Merow, C., Dahlgren, J. P., Metcalf, C. J. E., Childs, D. Z., Evans, M. E. K., Jongejans, E., Record, S., Rees, M., Salguero-Gómez, R., & McMahon, S. M. (2014). Advancing population ecology with integral projection models: a practical guide. *Methods in Ecology and Evolution*, 5(2), 99-110. <https://doi.org/https://doi.org/10.1111/2041-210X.12146>
- Messer, L. F., Ostrowski, M., Doblin, M. A., Petrou, K., Baird, M. E., Ingleton, T., Bissett, A., Van de Kamp, J., Nelson, T., Paulsen, I., Bodrossy, L., Fuhrman, J. A., Seymour, J. R., & Brown, M. V. (2020). Microbial tropicalization driven by a strengthening western ocean boundary current. *Global Change Biology*, 26(10), 5613-5629. <https://doi.org/https://doi.org/10.1111/gcb.15257>
- Mieszowska, N., & Sugden, H. E. (2016). Chapter Seven - Climate-Driven Range Shifts Within Benthic Habitats Across a Marine Biogeographic Transition Zone. In A. J. Dumbrell, R. L. Kordas, & G. Woodward (Eds.), *Advances in Ecological Research* (Vol. 55, pp. 325-369). Academic Press. <https://doi.org/https://doi.org/10.1016/bs.aecr.2016.08.007>
- Miller, M. G. R., Reimer, J. D., Sommer, B., Cook, K. M., Pandolfi, J. M., Obuchi, M., & Beger, M. (2023). Temperate functional niche availability not resident-invader competition shapes tropicalisation in reef fishes.

- Nature Communications*, 14(1), 2181. <https://doi.org/10.1038/s41467-023-37550-5>
- Mitchell, J. D., Allman, E. S., & Rhodes, J. A. (2022). A generalized AIC for models with singularities and boundaries. *arXivarXiv preprint arXiv:2211.04136*. <https://arxiv.org/abs/2211.04136>
- Mizerek, T. L., Madin, J. S., Benzoni, F., Huang, D., Luiz, O. J., Mera, H., Schmidt-Roach, S., Smith, S. D. A., Sommer, B., & Baird, A. H. (2021). No evidence for tropicalization of coral assemblages in a subtropical climate change hot spot. *Coral Reefs*. <https://doi.org/10.1007/s00338-021-02167-x>
- Muenzel, D., Critchell, K., Cox, C., Campbell, S. J., Jakub, R., Suherfian, W., Sara, L., Chollett, I., Trembl, E. A., & Beger, M. (2023). Integrating larval connectivity into the marine conservation decision-making process across spatial scales. *Conservation Biology*, 37(3), e14038. <https://doi.org/https://doi.org/10.1111/cobi.14038>
- Muir, P. R., Obura, D. O., Hoeksema, B. W., Sheppard, C., Pichon, M., & Richards, Z. T. (2022). Conclusions of low extinction risk for most species of reef-building corals are premature. *Nature Ecology & Evolution*, 6(4), 357-358. <https://doi.org/10.1038/s41559-022-01659-5>
- Muir, P. R., Wallace, C. C., Done, T., & Aguirre, J. D. (2015). Limited scope for latitudinal extension of reef corals. *Science*, 348(6239), 1135-1138. <https://doi.org/doi:10.1126/science.1259911>
- Muller-Landau, H. C., Condit, R. S., Harms, K. E., Marks, C. O., Thomas, S. C., Bunyavejchewin, S., Chuyong, G., Co, L., Davies, S., Foster, R., Gunatilleke, S., Gunatilleke, N., Hart, T., Hubbell, S. P., Itoh, A., Kassim, A. R., Kenfack, D., LaFrankie, J. V., Lagunzad, D., Lee, H. S., Losos, E., Makana, J.-R., Ohkubo, T., Samper, C., Sukumar, R., Sun, I.-F., Nur Supardi, M. N., Tan, S., Thomas, D., Thompson, J., Valencia, R., Vallejo, M. I., Muñoz, G. V., Yamakura, T., Zimmerman, J. K., Dattaraja, H. S., Esufali, S., Hall, P., He, F., Hernandez, C., Kiratiprayoon, S., Suresh, H. S., Wills, C., & Ashton, P. (2006). Comparing tropical forest tree size distributions with the predictions of metabolic ecology and equilibrium models. *Ecology Letters*, 9(5), 589-602. <https://doi.org/https://doi.org/10.1111/j.1461-0248.2006.00915.x>
- Nakabayashi, A., Yamakita, T., Nakamura, T., Aizawa, H., Kitano, Y. F., Iguchi, A., Yamano, H., Nagai, S., Agostini, S., Teshima, K. M., & Yasuda, N. (2019). The potential role of temperate Japanese regions as refugia for the coral *Acropora hyacinthus* in the face of climate change. *Scientific Reports*, 9(1), 1892. <https://doi.org/10.1038/s41598-018-38333-5>
- Nakamura, M., Nomura, K., Hirabayashi, I., Nakajima, Y., Nakajima, T., Mitarai, S., & Yokochi, H. (2021). Management of scleractinian coral assemblages in temperate non-reefal areas: insights from a long-term monitoring study in Kushimoto, Japan (33°N). *Marine Biology*, 168(9), 140. <https://doi.org/10.1007/s00227-021-03948-2>
- Nasa/Jpl. (2015). *GHRSSST Level 4 MUR Global Foundation Sea Surface Temperature Analysis (v4.1)* NASA Physical Oceanography Distributed Active Archive Center. <https://doi.org/10.5067/GHGMR-4FJ04>
- Neuheimer, A. B., & Grønkvær, P. (2012). Climate effects on size-at-age: growth in warming waters compensates for earlier maturity in an exploited marine fish. *Global Change Biology*, 18(6), 1812-1822. <https://doi.org/https://doi.org/10.1111/j.1365-2486.2012.02673.x>

- Newman, M. (2017). Power-law distribution. *Significance*, 14(4), 10-11.
<https://doi.org/https://doi.org/10.1111/j.1740-9713.2017.01050.x>
- NOAA. (2012a). *Chlorophyll, NOAA S-NPP VIIRS, Science Quality, Global 4km, Level 3, 2012-present, Monthly NOAA NESDIS CoastWatch*.
- NOAA. (2012b). *Kd490, NOAA S-NPP VIIRS, Science Quality, Global 4km, Level 3, 2012-present, Monthly NOAA NESDIS STAR*.
<https://polarwatch.noaa.gov/erddap/info/neddisVHNSQkd490Monthly/index.html>
- NOAA. (2022). "Multi-scale Ultra-high Resolution (MUR) SST Analysis fv04.1, Global, 0.01°, 2002-present, Monthly". NOAA NMFS SWFSC ERD and NOAA NESDIS CoastWatch WCRN. Retrieved 15th June from
<https://coastwatch.pfeg.noaa.gov/erddap/info/jplMURSST41mday/index.html>
- NOAA. (2024). *NOAA confirms 4th global coral bleaching event*. Retrieved 27th September from <https://www.noaa.gov/news-release/noaa-confirms-4th-global-coral-bleaching-event>
- Nyström, M., Folke, C., & Moberg, F. (2000). Coral reef disturbance and resilience in a human-dominated environment. *Trends in Ecology & Evolution*, 15(10), 413-417. [https://doi.org/https://doi.org/10.1016/S0169-5347\(00\)01948-0](https://doi.org/https://doi.org/10.1016/S0169-5347(00)01948-0)
- O'Connell, M. J., Fowler, A. M., Allan, S. J., Beretta, G. A., & Booth, D. J. (2023). Subtropical coral expansion into SE Australia: a haven for both temperate and expatriating tropical reef fishes. *Coral Reefs*, 42(6), 1257-1262. <https://doi.org/10.1007/s00338-023-02429-w>
- Oksanen, J., Simpson, G., Blanchet, F., Kindt, R., Legendre, P., Minchin, P., O'Hara, R., Solymos, P., Stevens, M., Szoecs, E., Wagner, H., Barbour, M., Bedward, M., Bolker, B., Borcard, D., Carvalho, G., Chirico, M., De Caceres, M., Durand, S., Evangelista, H., FitzJohn, R., Friendly, M., Furneaux, B., Hannigan, G., Hill, M., Lahti, L., McGlinn, D., Ouellette, M., Ribeiro Cunha, E., Smith, T., Stier, A., Ter Braak, C., & Weedon, J. (2022). *vegan: Community Ecology Package*. In (Version R package version 2.6-4) <https://CRAN.R-project.org/package=vegan>
- Palazzo Corner, S., Siegert, M., Ceppi, P., Fox-Kemper, B., Frölicher, T. L., Gallego-Sala, A., Haigh, J., Hegerl, G. C., Jones, C. D., Knutti, R., Koven, C. D., MacDougall, A. H., Meinshausen, M., Nicholls, Z., Sallée, J. B., Sanderson, B. M., Séférian, R., Turetsky, M., Williams, R. G., Zaehle, S., & Rogelj, J. (2023). The Zero Emissions Commitment and climate stabilization [Frontiers in Science Lead Article]. *Frontiers in Science*, 1. <https://doi.org/10.3389/fsci.2023.1170744>
- Palumbi, S. R., Walker, N. S., Hanson, E., Armstrong, K., Lippert, M., Cornwell, B., Nestor, V., & Golbuu, Y. (2023). Small-scale genetic structure of coral populations in Palau based on whole mitochondrial genomes: Implications for future coral resilience. *Evolutionary Applications*, 16(2), 518-529. <https://doi.org/https://doi.org/10.1111/eva.13509>
- Pandolfi, J. M. (2015). Incorporating Uncertainty in Predicting the Future Response of Coral Reefs to Climate Change. *Annual Review of Ecology, Evolution, and Systematics*, 46(1), 281-303.
<https://doi.org/10.1146/annurev-ecolsys-120213-091811>
- Pauly, D. (2021). The gill-oxygen limitation theory (GOLT) and its critics. *Science Advances*, 7(2), eabc6050.
<https://doi.org/doi:10.1126/sciadv.abc6050>

- Paz-García, D. A., Hellberg, M. E., García-de-León, F. J., & Balart, E. F. (2015). Switch between Morphospecies of Pocillopora Corals. *The American Naturalist*, 186(3), 434-440. <https://doi.org/10.1086/682363>
- Pennington, M. (1996). Estimating the mean and variance from highly skewed marine data. *Fishery Bulletin*, 94, 498-505.
- Pepler, A., & Coutts-Smith, A. (2013). A new, objective, database of East Coast Lows. *Australian Meteorological and Oceanographic Journal*, 63, 461-472. <https://doi.org/10.1071/es13035>
- Petchey, O. L., & Belgrano, A. (2010). Body-size distributions and size-spectra: universal indicators of ecological status? *Biology Letters*, 6(4), 434-437. <https://doi.org/doi:10.1098/rsbl.2010.0240>
- Petersen, A., Zhang, C., & Kokoszka, P. (2022). Modeling Probability Density Functions as Data Objects. *Econometrics and Statistics*, 21, 159-178. <https://doi.org/https://doi.org/10.1016/j.ecosta.2021.04.004>
- Pigot, A. L., Merow, C., Wilson, A., & Trisos, C. H. (2023). Abrupt expansion of climate change risks for species globally. *Nature Ecology & Evolution*, 7(7), 1060-1071. <https://doi.org/10.1038/s41559-023-02070-4>
- Pinsky, M. L., Eikeset, A. M., McCauley, D. J., Payne, J. L., & Sunday, J. M. (2019). Greater vulnerability to warming of marine versus terrestrial ectotherms. *Nature*, 569(7754), 108-111. <https://doi.org/10.1038/s41586-019-1132-4>
- Pinsky, M. L., Selden, R. L., & Kitchel, Z. J. (2020). Climate-Driven Shifts in Marine Species Ranges: Scaling from Organisms to Communities. *Annual Review of Marine Science*, 12(Volume 12, 2020), 153-179. <https://doi.org/https://doi.org/10.1146/annurev-marine-010419-010916>
- Pinto, C. M. A., Mendes Lopes, A., & Machado, J. A. T. (2012). A review of power laws in real life phenomena. *Communications in Nonlinear Science and Numerical Simulation*, 17(9), 3558-3578. <https://doi.org/https://doi.org/10.1016/j.cnsns.2012.01.013>
- Pisapia, C., Burn, D., & Pratchett, M. S. (2019). Changes in the population and community structure of corals during recent disturbances (February 2016-October 2017) on Maldivian coral reefs. *Scientific Reports*, 9(1), 8402. <https://doi.org/10.1038/s41598-019-44809-9>
- Pisapia, C., Edmunds, P. J., Moeller, H. V., M. Riegl, B., McWilliam, M., Wells, C. D., & Pratchett, M. S. (2020). Chapter Two - Projected shifts in coral size structure in the Anthropocene. In B. M. Riegl (Ed.), *Advances in Marine Biology* (Vol. 87, pp. 31-60). Academic Press. <https://doi.org/https://doi.org/10.1016/bs.amb.2020.07.003>
- Pomeranz, J. P. F., Junker, J. R., & Wesner, J. S. (2022). Individual size distributions across North American streams vary with local temperature. *Global Change Biology*, 28(3), 848-858. <https://doi.org/https://doi.org/10.1111/gcb.15862>
- Preston, F. W. (1962). The Canonical Distribution of Commonness and Rarity: Part I. *Ecology*, 43(2), 185-215. <https://doi.org/10.2307/1931976>
- Putnam, H. M., Stat, M., Pochon, X., & Gates, R. D. (2012). Endosymbiotic flexibility associates with environmental sensitivity in scleractinian corals. *Proceedings of the Royal Society B: Biological Sciences*, 279(1746), 4352-4361. <https://doi.org/doi:10.1098/rspb.2012.1454>
- Quigley, K. M., Warner, P. A., Bay, L. K., & Willis, B. L. (2018). Unexpected mixed-mode transmission and moderate genetic regulation of Symbiodinium communities in a brooding coral. *Heredity*, 121(6), 524-536. <https://doi.org/10.1038/s41437-018-0059-0>

- Quigley, K. M., Willis, B. L., & Kenkel, C. D. (2019). Transgenerational inheritance of shuffled symbiont communities in the coral *Montipora digitata*. *Scientific Reports*, 9(1), 13328. <https://doi.org/10.1038/s41598-019-50045-y>
- R Core Team. (2021). *R: A language and environment for statistical computing*. In (Version 4.1.2) R Foundation for Statistical Computing. <http://www.r-project.org/index.html>
- R Core Team. (2022). *R: A Language and Environment for Statistical Computing*. In (Version 4.2.1) R Foundation for Statistical Computing. <https://www.R-project.org/>
- Radchuk, V., Turlure, C., & Schtickzelle, N. (2013). Each life stage matters: the importance of assessing the response to climate change over the complete life cycle in butterflies. *Journal of Animal Ecology*, 82(1), 275-285. <https://doi.org/10.1111/j.1365-2656.2012.02029.x>
- Ramsay, J., Hooker, G., & Graves, S. (2009). *Functional data analysis with R and MATLAB*. Springer International Publishing.
- Rapacciuolo, G. (2019). Strengthening the contribution of macroecological models to conservation practice. *Global Ecology and Biogeography*, 28(1), 54-60. <https://doi.org/https://doi.org/10.1111/geb.12848>
- Rapuano, H., Shlesinger, T., Roth, L., Bronstein, O., & Loya, Y. (2023). Coming of age: Annual onset of coral reproduction is determined by age rather than size. *iScience*, 26(5), 106533. <https://doi.org/https://doi.org/10.1016/j.isci.2023.106533>
- Reguero, B. G., Losada, I. J., & Méndez, F. J. (2019). A recent increase in global wave power as a consequence of oceanic warming. *Nature Communications*, 10(1), 205. <https://doi.org/10.1038/s41467-018-08066-0>
- Reimer, J. D., Takishita, K., Ono, S., Maruyama, T., & Tsukahara, J. (2006). Latitudinal and intracolony ITS-rDNA sequence variation in the symbiotic dinoflagellate genus *Symbiodinium* (Dinophyceae) in *Zoanthus sansibaricus* (Anthozoa: Hexacorallia). *Phycological Research*, 54(2), 122-132. <https://doi.org/https://doi.org/10.1111/j.1440-1835.2006.00419.x>
- Reimer, J. D., Wee, H. B., López, C., Beger, M., & Cruz, I. C. S. (2021). Widespread *Zoanthus* and *Palythoa* Dominance, Barrens, and Phase Shifts in Shallow Water Subtropical and Tropical Marine Ecosystems. In (pp. 533-557). CRC Press. <https://doi.org/10.1201/9781003138846-7>
- Reuman, D. C., Mulder, C., Raffaelli, D., & Cohen, J. E. (2008). Three allometric relations of population density to body mass: theoretical integration and empirical tests in 149 food webs. *Ecology Letters*, 11(11), 1216-1228. <https://doi.org/https://doi.org/10.1111/j.1461-0248.2008.01236.x>
- Rich, W. A., Carvalho, S., Cadiz, R., Gil, G., Gonzalez, K., & Berumen, M. L. (2022). Size structure of the coral *Stylophora pistillata* across reef flat zones in the central Red Sea. *Scientific Reports*, 12(1). <https://doi.org/10.1038/s41598-022-17908-3>
- Riegl, B. M., Bruckner, A. W., Rowlands, G. P., Purkis, S. J., & Renaud, P. (2012). Red Sea Coral Reef Trajectories over 2 Decades Suggest Increasing Community Homogenization and Decline in Coral Size. *PLOS ONE*, 7(5), e38396. <https://doi.org/10.1371/journal.pone.0038396>
- Robinson, J. P. W., & Baum, J. K. (2016). Trophic roles determine coral reef fish community size structure. *Canadian Journal of Fisheries and Aquatic Sciences*, 73(4), 496-505. <https://doi.org/10.1139/cjfas-2015-0178>

- Robinson, J. P. W., Williams, I. D., Edwards, A. M., McPherson, J., Yeager, L., Vigliola, L., Brainard, R. E., & Baum, J. K. (2017). Fishing degrades size structure of coral reef fish communities. *Global Change Biology*, 23(3), 1009-1022. <https://doi.org/https://doi.org/10.1111/gcb.13482>
- Rocha, L. A., Pinheiro, H. T., Shepherd, B., Papastamatiou, Y. P., Luiz, O. J., Pyle, R. L., & Bongaerts, P. (2018). Mesophotic coral ecosystems are threatened and ecologically distinct from shallow water reefs. *Science*, 361(6399), 281-284. <https://doi.org/doi:10.1126/science.aag1614>
- Rogers, A., Harborne, A. R., Brown, C. J., Bozec, Y.-M., Castro, C., Chollett, I., Hock, K., Knowland, C. A., Marshall, A., Ortiz, J. C., Razak, T., Roff, G., Samper-Villarreal, J., Saunders, M. I., Wolff, N. H., & Mumby, P. J. (2015). Anticipative management for coral reef ecosystem services in the 21st century. *Global Change Biology*, 21(2), 504-514. <https://doi.org/https://doi.org/10.1111/gcb.12725>
- Santana, E. F. C., Mies, M., Longo, G. O., Menezes, R., Aued, A. W., Luza, A. L., Bender, M. G., Segal, B., Floeter, S. R., & Francini-Filho, R. B. (2023). Turbidity shapes shallow Southwestern Atlantic benthic reef communities. *Marine Environmental Research*, 183, 105807. <https://doi.org/https://doi.org/10.1016/j.marenvres.2022.105807>
- Sauder, J., Banc-Prandi, G., Meibom, A., & Tuia, D. (2024). Scalable semantic 3D mapping of coral reefs with deep learning. *Methods in Ecology and Evolution*, 15(5), 916-934. <https://doi.org/https://doi.org/10.1111/2041-210X.14307>
- Saura, S., Bodin, Ö., & Fortin, M.-J. (2014). EDITOR'S CHOICE: Stepping stones are crucial for species' long-distance dispersal and range expansion through habitat networks. *Journal of Applied Ecology*, 51(1), 171-182. <https://doi.org/https://doi.org/10.1111/1365-2664.12179>
- Schindelin, J., Arganda-Carreras, I., Frise, E., Kaynig, V., Longair, M., Pietzsch, T., Preibisch, S., Rueden, C., Saalfeld, S., Schmid, B., Tinevez, J.-Y., White, D. J., Hartenstein, V., Eliceiri, K., Tomancak, P., & Cardona, A. (2012). Fiji: an open-source platform for biological-image analysis. *Nature Methods*, 9(7), 676-682. <https://doi.org/10.1038/nmeth.2019>
- Schmidt-Roach, S., Lundgren, P., Miller, K. J., Gerlach, G., Noreen, A. M. E., & Andreakis, N. (2013a). Assessing hidden species diversity in the coral *Pocillopora damicornis* from Eastern Australia. *Coral Reefs*, 32(1), 161-172. <https://doi.org/10.1007/s00338-012-0959-z>
- Schmidt-Roach, S., Miller, K. J., & Andreakis, N. (2013b). *Pocillopora aliciae*: a new species of scleractinian coral (Scleractinia, Pocilloporidae) from subtropical Eastern Australia. *Zootaxa*, 3626, 576-582. <https://doi.org/10.11646/zootaxa.3626.4.11>
- Schmidt-Roach, S., Miller, K. J., Woolsey, E., Gerlach, G., & Baird, A. H. (2012). Broadcast Spawning by *Pocillopora* Species on the Great Barrier Reef. *PLOS ONE*, 7(12), e50847. <https://doi.org/10.1371/journal.pone.0050847>
- Sen Gupta, A., Stellema, A., Pontes, G. M., Taschetto, A. S., Vergés, A., & Rossi, V. (2021). Future changes to the upper ocean Western Boundary Currents across two generations of climate models. *Scientific Reports*, 11(1), 9538. <https://doi.org/10.1038/s41598-021-88934-w>
- Shaffer, M. L. (1981). Minimum Population Sizes for Species Conservation. *BioScience*, 31(2), 131-134. <https://doi.org/10.2307/1308256>

- Sheldon, R. W., & Parsons, T. R. (1967). A Continuous Size Spectrum for Particulate Matter in the Sea. *Journal of the Fisheries Research Board of Canada*, 24(5), 909-915. <https://doi.org/10.1139/f67-081>
- Signorell, A. (2024). *DescTools: Tools for Descriptive Statistics* In (Version R package version 0.99.54) <https://CRAN.R-project.org/package=DescTools>
- Slatkin, M., & Hudson, R. R. (1991). Pairwise comparisons of mitochondrial DNA sequences in stable and exponentially growing populations. *Genetics*, 129(2), 555-562. <https://doi.org/10.1093/genetics/129.2.555>
- Smith, S. M., Malcolm, H. A., Marzinelli, E. M., Schultz, A. L., Steinberg, P. D., & Vergés, A. (2021). Tropicalization and kelp loss shift trophic composition and lead to more winners than losers in fish communities. *Global Change Biology*, 27(11), 2537-2548. <https://doi.org/https://doi.org/10.1111/gcb.15592>
- Soares, M. d. O. (2020). Marginal reef paradox: A possible refuge from environmental changes? *Ocean & Coastal Management*, 185, 105063. <https://doi.org/https://doi.org/10.1016/j.ocecoaman.2019.105063>
- Sommer, B., Beger, M., Harrison, P. L., Babcock, R. C., & Pandolfi, J. M. (2018). Differential response to abiotic stress controls species distributions at biogeographic transition zones. *Ecography*, 41(3), 478-490. <https://doi.org/https://doi.org/10.1111/ecog.02986>
- Sommer, B., Butler, I. R., & Pandolfi, J. M. (2021). Trait-based approach reveals how marginal reefs respond to acute and chronic disturbance. *Coral Reefs*, 40(3), 735-749. <https://doi.org/10.1007/s00338-021-02077-y>
- Sommer, B., Harrison, P. L., Beger, M., & Pandolfi, J. M. (2014). Trait-mediated environmental filtering drives assembly at biogeographic transition zones. *Ecology*, 95(4), 1000-1009. <https://doi.org/https://doi.org/10.1890/13-1445.1>
- Sommer, B., Harrison, P. L., Brooks, L., & Scheffers, S. R. (2011). Coral Community Decline at Bonaire, Southern Caribbean. *Bulletin of Marine Science*, 87(3), 541-565. <https://doi.org/10.5343/bms.2010.1046>
- Sommer, B., Hodge, J. M., Lachs, L., Cant, J., Pandolfi, J. M., & Beger, M. (2024). Decadal demographic shifts and size-dependent disturbance responses of corals in a subtropical warming hotspot. *Scientific Reports*, 14(1), 6327. <https://doi.org/10.1038/s41598-024-56890-w>
- Soong, K., & Lang, J. C. (1992). Reproductive Integration in Reef Corals. *The Biological Bulletin*, 183(3), 418-431. <https://doi.org/10.2307/1542018>
- Spady, B. L., Skirving, W. J., Liu, G., De La Cour, J. L., McDonald, C. J., & Manzello, D. P. (2022). Unprecedented early-summer heat stress and forecast of coral bleaching on the Great Barrier Reef, 2021-2022. *F1000Research*, 11, 127. <https://doi.org/10.12688/f1000research.108724.3>
- Starko, S., Fifer, J. E., Claar, D. C., Davies, S. W., Cunning, R., Baker, A. C., & Baum, J. K. (2023). Marine heatwaves threaten cryptic coral diversity and erode associations among coevolving partners. *Sci Adv*, 9(32), eadf0954. <https://doi.org/10.1126/sciadv.adf0954>
- Stumpf, M. P. H., & Porter, M. A. (2012). Critical Truths About Power Laws. *Science*, 335(6069), 665-666. <https://doi.org/doi:10.1126/science.1216142>
- Sturges, H. A. (1926). The Choice of a Class Interval. *Journal of the American Statistical Association*, 21(153), 65-66. <https://doi.org/10.1080/01621459.1926.10502161>

- Suggett, D. J., & van Oppen, M. J. H. (2022). Horizon scan of rapidly advancing coral restoration approaches for 21st century reef management *Emerging Topics in Life Sciences*, 6(1), 125-136. <https://doi.org/https://doi.org/10.1042/ETLS20210240>
- Sully, S., & van Woesik, R. (2020). Turbid reefs moderate coral bleaching under climate-related temperature stress. *Glob Chang Biol*, 26(3), 1367-1373. <https://doi.org/10.1111/gcb.14948>
- Summerhayes, C. P., Zalasiewicz, J., Head, M. J., Syvitski, J., Barnosky, A. D., Cearreta, A., Fiałkiewicz-Kozieł, B., Grinevald, J., Leinfelder, R., McCarthy, F. M. G., McNeill, J. R., Saito, Y., Wagleich, M., Waters, C. N., Williams, M., & Zinke, J. (2024). The future extent of the Anthropocene epoch: A synthesis. *Global and Planetary Change*, 242, 104568. <https://doi.org/https://doi.org/10.1016/j.gloplacha.2024.104568>
- Suzuki, G., Yatsuya, K., & Muko, S. (2013). Bleaching of tabular *Acropora* corals during the winter season in a high-latitude community (Nagasaki, Japan). *Galaxea, Journal of Coral Reef Studies*, 15(2), 43-44. <https://doi.org/10.3755/galaxea.15.43>
- Talis, E. J., Che-Castaldo, C., & Lynch, H. J. (2023). Difficulties in summing log-normal distributions for abundance and potential solutions. *PLOS ONE*, 18(1), e0280351. <https://doi.org/10.1371/journal.pone.0280351>
- Talská, R., Menafoglio, A., Machalová, J., Hron, K., & Fišerová, E. (2018). Compositional regression with functional response. *Computational Statistics & Data Analysis*, 123, 66-85. <https://doi.org/https://doi.org/10.1016/j.csda.2018.01.018>
- Tavecchia, G., Tenan, S., Pradel, R., Igual, J.-M., Genovart, M., & Oro, D. (2016). Climate-driven vital rates do not always mean climate-driven population. *Global Change Biology*, 22(12), 3960-3966. <https://doi.org/https://doi.org/10.1111/gcb.13330>
- Tebbett, S. B., Connolly, S. R., & Bellwood, D. R. (2023). Benthic composition changes on coral reefs at global scales. *Nature Ecology & Evolution*, 7(1), 71-81. <https://doi.org/10.1038/s41559-022-01937-2>
- Tekwa, E. W., Catalano, K. A., Bazzicalupo, A. L., O'Connor, M. I., & Pinsky, M. L. (2023). The sizes of life. *PLOS ONE*, 18(3), e0283020. <https://doi.org/10.1371/journal.pone.0283020>
- Thomas, L., Kennington, W. J., Evans, R. D., Kendrick, G. A., & Stat, M. (2017). Restricted gene flow and local adaptation highlight the vulnerability of high-latitude reefs to rapid environmental change. *Global Change Biology*, 23(6), 2197-2205. <https://doi.org/https://doi.org/10.1111/gcb.13639>
- Torres, A. F., & Ravago-Gotanco, R. (2018). Rarity of the “common” coral *Pocillopora damicornis* in the western Philippine archipelago. *Coral Reefs*, 37(4), 1209-1216. <https://doi.org/10.1007/s00338-018-1729-3>
- Toth, L. T., Precht, W. F., Modys, A. B., Stathakopoulos, A., Robbart, M. L., Hudson, J. H., Oleinik, A. E., Riegl, B. M., Shinn, E. A., & Aronson, R. B. (2021). Climate and the latitudinal limits of subtropical reef development. *Scientific Reports*, 11(1), 13044. <https://doi.org/10.1038/s41598-021-87883-8>
- Tu, C.-Y., Chen, K.-T., & Hsieh, C.-h. (2018). Fishing and temperature effects on the size structure of exploited fish stocks. *Scientific Reports*, 8(1), 7132. <https://doi.org/10.1038/s41598-018-25403-x>

- van den Boogaart, K. G., Egozcue, J. J., & Pawlowsky-Glahn, V. (2014). Bayes Hilbert Spaces. *Australian & New Zealand Journal of Statistics*, 56(2), 171-194. <https://doi.org/https://doi.org/10.1111/anzs.12074>
- van Woessik, R., Shlesinger, T., Grotoli, A. G., Toonen, R. J., Vega Thurber, R., Warner, M. E., Marie Hulver, A., Chapron, L., McLachlan, R. H., Albright, R., Crandall, E., DeCarlo, T. M., Donovan, M. K., Eirin-Lopez, J., Harrison, H. B., Heron, S. F., Huang, D., Humanes, A., Krueger, T., Madin, J. S., Manzello, D., McManus, L. C., Matz, M., Muller, E. M., Rodriguez-Lanetty, M., Vega-Rodriguez, M., Voolstra, C. R., & Zaneveld, J. (2022). Coral-bleaching responses to climate change across biological scales. *Global Change Biology*, 28(14), 4229-4250. <https://doi.org/https://doi.org/10.1111/gcb.16192>
- Venables, W. N. R., B. D. (2002). *Modern Applied Statistics with S*. (4th ed.). Springer.
- Vergés, A., Doropoulos, C., Malcolm, H. A., Skye, M., Garcia-Pizá, M., Marzinelli, E. M., Campbell, A. H., Ballesteros, E., Hoey, A. S., Vila-Concejo, A., Bozec, Y. M., & Steinberg, P. D. (2016). Long-term empirical evidence of ocean warming leading to tropicalization of fish communities, increased herbivory, and loss of kelp. *Proc Natl Acad Sci U S A*, 113(48), 13791-13796. <https://doi.org/10.1073/pnas.1610725113>
- Vergés, A., McCosker, E., Mayer-Pinto, M., Coleman, M. A., Wernberg, T., Ainsworth, T., & Steinberg, P. D. (2019). Tropicalisation of temperate reefs: Implications for ecosystem functions and management actions. *Functional Ecology*, 33(6), 1000-1013. <https://doi.org/https://doi.org/10.1111/1365-2435.13310>
- Vergés, A., Steinberg, P. D., Hay, M. E., Poore, A. G. B., Campbell, A. H., Ballesteros, E., Heck, K. L., Booth, D. J., Coleman, M. A., Feary, D. A., Figueira, W., Langlois, T., Marzinelli, E. M., Mizerek, T., Mumby, P. J., Nakamura, Y., Roughan, M., van Sebille, E., Gupta, A. S., Smale, D. A., Tomas, F., Wernberg, T., & Wilson, S. K. (2014). The tropicalization of temperate marine ecosystems: climate-mediated changes in herbivory and community phase shifts. *Proceedings of the Royal Society B: Biological Sciences*, 281(1789), 20140846. <https://doi.org/doi:10.1098/rspb.2014.0846>
- Veron, J. E. N., & Minchin, P. R. (1992). Correlations between sea surface temperature, circulation patterns and the distribution of hermatypic corals of Japan. *Continental Shelf Research*, 12(7), 835-857. [https://doi.org/https://doi.org/10.1016/0278-4343\(92\)90047-N](https://doi.org/https://doi.org/10.1016/0278-4343(92)90047-N)
- Veron, J. E. N., Stafford-Smith, M. G., Turak, E., & DeVantier, L. M. (2016). *Corals of the World*. Retrieved 21 February from <http://www.coralsoftheworld.org/page/home/>
- Vetter, S. G., Puskas, Z., Bieber, C., & Ruf, T. (2020). How climate change and wildlife management affect population structure in wild boars. *Scientific Reports*, 10(1). <https://doi.org/10.1038/s41598-020-64216-9>
- Vitousek, S., Barnard, P. L., Fletcher, C. H., Frazer, N., Erikson, L., & Storlazzi, C. D. (2017). Doubling of coastal flooding frequency within decades due to sea-level rise. *Scientific Reports*, 7(1). <https://doi.org/10.1038/s41598-017-01362-7>
- Voolstra, C. R., Peixoto, R. S., & Ferrier - Pagès, C. (2023). Mitigating the ecological collapse of coral reef ecosystems. *EMBO reports*, 24(4), e56826. <https://doi.org/https://doi.org/10.15252/embr.202356826>

- Wang, C., Zheng, X., Li, Y., Sun, D., Huang, W., & Shi, T. (2022). Symbiont shuffling dynamics associated with photodamage during temperature stress in coral symbiosis. *Ecological Indicators*, 145, 109706. <https://doi.org/https://doi.org/10.1016/j.ecolind.2022.109706>
- Ward, S. (1992). Evidence for broadcast spawning as well as brooding in the scleractinian coral *Pocillopora damicornis*. *Marine Biology*, 112(4), 641-646. <https://doi.org/10.1007/BF00346182>
- Wernberg, T., Smale, D. A., Tuya, F., Thomsen, M. S., Langlois, T. J., de Bettignies, T., Bennett, S., & Rousseaux, C. S. (2013). An extreme climatic event alters marine ecosystem structure in a global biodiversity hotspot. *Nature Climate Change*, 3(1), 78-82. <https://doi.org/10.1038/nclimate1627>
- Wernberg, T., Thomsen, M. S., Baum, J. K., Bishop, M. J., Bruno, J. F., Coleman, M. A., Filbee-Dexter, K., Gagnon, K., He, Q., Murdiyarso, D., Rogers, K., Silliman, B. R., Smale, D. A., Starko, S., & Vanderklift, M. A. (2024). Impacts of Climate Change on Marine Foundation Species. *Annual Review of Marine Science*, 16(Volume 16, 2024), 247-282. <https://doi.org/https://doi.org/10.1146/annurev-marine-042023-093037>
- White, C. R., & Kearney, M. R. (2014). Metabolic Scaling in Animals: Methods, Empirical Results, and Theoretical Explanations. In D. M. Pollock (Ed.), *Comprehensive Physiology* (pp. 231-256). <https://doi.org/https://doi.org/10.1002/cphy.c110049>
- White, E. P., Ernest, S. K. M., Kerkhoff, A. J., & Enquist, B. J. (2007). Relationships between body size and abundance in ecology. *Trends in Ecology & Evolution*, 22(6), 323-330. <https://doi.org/10.1016/j.tree.2007.03.007>
- Wicks, L. C., Sampayo, E., Gardner, J. P. A., & Davy, S. K. (2010). Local endemism and high diversity characterise high-latitude coral-Symbiodinium partnerships. *Coral Reefs*, 29(4), 989-1003. <https://doi.org/10.1007/s00338-010-0649-7>
- Williams, G. J., Graham, N. A. J., Jouffray, J.-B., Norström, A. V., Nyström, M., Gove, J. M., Heenan, A., & Wedding, L. M. (2019). Coral reef ecology in the Anthropocene. *Functional Ecology*, 33(6), 1014-1022. <https://doi.org/https://doi.org/10.1111/1365-2435.13290>
- Wogan, G. O. U., & Wang, I. J. (2018). The value of space-for-time substitution for studying fine-scale microevolutionary processes. *Ecography*, 41, 1456-1468. <https://doi.org/10.1111/ecog.03235>
- Wolkovich, E. M., Cook, B. I., Allen, J. M., Crimmins, T. M., Betancourt, J. L., Travers, S. E., Pau, S., Regetz, J., Davies, T. J., Kraft, N. J. B., Ault, T. R., Bolmgren, K., Mazer, S. J., McCabe, G. J., McGill, B. J., Parmesan, C., Salamin, N., Schwartz, M. D., & Cleland, E. E. (2012). Warming experiments underpredict plant phenological responses to climate change. *Nature*, 485(7399), 494-497. <https://doi.org/10.1038/nature11014>
- Yabe, H., & Sugiyama, T. (1935). Geological and Geographical Distribution of Reef-Corals in Japan. *Journal of Paleontology*, 9(3), 183-217. <https://www.jstor.org/stable/1298160>
- Yamano, H., Sugihara, K., & Nomura, K. (2011). Rapid poleward range expansion of tropical reef corals in response to rising sea surface temperatures. *Geophysical Research Letters*, 38(4). <https://doi.org/https://doi.org/10.1029/2010GL046474>

- Yasuda, N., Kitano, Y. F., Taninaka, H., Nagai, S., Mezaki, T., & Yamashita, H. (2021). Genetic Structure of the *Goniopora lobata* and *G. djiboutiensis* Species Complex Is Better Explained by Oceanography Than by Morphological Characteristics [Original Research]. *Frontiers in Marine Science*, 8. <https://doi.org/10.3389/fmars.2021.592608>
- Yen, J. D. L., Thomson, J. R., Paganin, D. M., Keith, J. M., & Mac Nally, R. (2015). Function regression in ecology and evolution: FREE. *Methods in Ecology and Evolution*, 6(1), 17-26. <https://doi.org/https://doi.org/10.1111/2041-210X.12290>
- Yendo, K. (1903). *Seaweed Isoyake Survey Report*. (Fisheries Survey Report, Issue.
- Yoda, K., Kira, T., Ogawa, H., & Hozumi, K. (1963). Self-thinning in overcrowded pure stands under cultivated and natural conditions (Intraspecific competition among higher plants. XI). *Journal of Biology Osaka City University* 14, 107-129.
- Yvon-Durocher, G., & Allen, A. P. (2012). Linking community size structure and ecosystem functioning using metabolic theory. *Philosophical Transactions of the Royal Society B: Biological Sciences*, 367(1605), 2998-3007. <https://doi.org/doi:10.1098/rstb.2012.0246>
- Zaneveld, J. R., Burkepille, D. E., Shantz, A. A., Pritchard, C. E., McMinds, R., Payet, J. P., Welsh, R., Correa, A. M. S., Lemoine, N. P., Rosales, S., Fuchs, C., Maynard, J. A., & Thurber, R. V. (2016). Overfishing and nutrient pollution interact with temperature to disrupt coral reefs down to microbial scales. *Nature Communications*, 7(1), 11833. <https://doi.org/10.1038/ncomms11833>
- Zarco-Perello, S., Bosch, N. E., Bennett, S., Vanderklift, M. A., & Wernberg, T. (2021). Persistence of tropical herbivores in temperate reefs constrains kelp resilience to cryptic habitats. *Journal of Ecology*, 109(5), 2081-2094. <https://doi.org/https://doi.org/10.1111/1365-2745.13621>
- Zarco-Perello, S., Carroll, G., Vanderklift, M., Holmes, T., Langlois, T. J., & Wernberg, T. (2020). Range-extending tropical herbivores increase diversity, intensity and extent of herbivory functions in temperate marine ecosystems. *Functional Ecology*, 34(11), 2411-2421. <https://doi.org/https://doi.org/10.1111/1365-2435.13662>
- Zarzychny, K. M., Rius, M., Williams, S. T., & Fenberg, P. B. (2024). The ecological and evolutionary consequences of tropicalisation. *Trends in Ecology & Evolution*, 39(3), 267-279. <https://doi.org/https://doi.org/10.1016/j.tree.2023.10.006>
- Zarzychny, K. M., Watson, K. M., Verduyn, C. E., Reimer, J. D., Mezaki, T., & Beger, M. (2022). The role of herbivores in shaping subtropical coral communities in warming oceans. *Marine Biology*, 169(5), 62. <https://doi.org/10.1007/s00227-022-04036-9>
- Zvuloni, A., Artzy-Randrup, Y., Stone, L., Van Woesik, R., & Loya, Y. (2008). Ecological size-frequency distributions: how to prevent and correct biases in spatial sampling. *Limnology and Oceanography: Methods*, 6(3), 144-153. <https://doi.org/10.4319/lom.2008.6.144>
- Zweifler, A., O'Leary, M., Morgan, K., & Browne, N. K. (2021). Turbid Coral Reefs: Past, Present and Future—A Review. *Diversity*, 13(6), 251. <https://www.mdpi.com/1424-2818/13/6/251>

Appendices

Appendix A: Supporting information for Chapter 2

S1: Supplemental tables and figures from the main analyses

Table A-1. GPS coordinates and sampling date of the 20 sites, and whether it was sampled before/during (pre-) or after (post-) the 2016 bleaching event. The sites are ordered by decreasing latitude.

	Site name	Latitude (°)	Longitude (°)	Sampling date (dd/mm/yyyy)	Pre- or post-bleaching
1	Black Rock	-30.94837	153.0761	10/09/2018	Post
2	South Solitary Island	-30.20478	153.2652	13/09/2018	Post
3	South West Solitary Island	-30.15921	153.2281	09/09/2018	Post
4	Woolgoolga Reef	-30.09374	153.2056	19/10/2016	Post
5	North West Solitary Island	-30.01897	153.2697	12/09/2018	Post
6	North Rock	-29.97339	153.2572	16/04/2016	Pre
7	North Solitary Island	-29.92772	153.3896	11/09/2018	Post
8	Julian Rock False Trench	-28.61257	153.6286	31/05/2016	Pre
9	Julian Rock Nursery	-28.61087	153.6281	14/09/2018	Post
10	Cook Island	-28.19627	153.5763	07/09/2018	Post
11	Flat Rock	-27.39306	153.5522	15/08/2010	Pre
12	Henderson Rock	-27.13161	153.4781	18/03/2011	Pre

13	Flinders Reef	-26.97765	153.4841	18/09/2018	Post
14	Inner Gneering Shoals	-26.64858	153.1834	29/08/2012	Pre
15	Mudjimba	-26.61614	153.1130	28/08/2012	Pre
16	Wolf Rock	-25.91667	153.2000	09/08/2010	Pre
17	Lady Elliot Island	-24.11500	152.7095	27/09/2018	Post
18	Lady Musgrave Island	-23.90603	152.3870	26/09/2018	Post
19	Libbies Lair	-23.43458	151.9336	23/09/2018	Post
20	Tenements	-23.43274	151.9293	24/09/2018	Post

- 1 Table A-2. Statistical summaries of the size-frequency distribution at the twenty reefs. All areas are in log cm². Numbers are rounded
- 2 to three decimal places where appropriate. Sites are ordered from the lowest to the highest PC1 scores from top to bottom. Increasing
- 3 PC1 scores represent lower sea surface temperature and photosynthetically available radiation (PAR), *i.e.*, colder and darker, and
- 4 high chlorophyll a concentration and turbidity (kd490), *i.e.*, more productive and more turbid.

Site	Number of images sampled	Number of coral colonies	Mean coral area	Median coral area	Standard deviation of coral area	Coefficient of variation (CV)	Skewness	Kurtosis
Lady Elliot Island	63	449	4.374	4.196	1.593	36.42	0.302	2.385
Lady Musgrave Island	78	2101	3.379	3.224	1.441	42.646	0.434	2.776
Libbies Lair	77	1757	3.469	3.335	1.37	39.493	0.421	2.967
Tenements	66	1117	3.814	3.648	1.302	34.137	0.499	3.023
Flat Rock	82	705	3.711	3.659	1.325	35.705	0.171	2.724
Henderson Rock	30	56	4.683	4.489	1.742	37.198	0.243	2.521
Flinders	72	448	3.599	3.592	1.524	42.345	0.076	2.521
Inner Gneering Shoals	90	1310	4.131	4.04	1.301	31.494	0.211	2.729

Wolf Rock	51	224	4.216	4.296	1.147	27.206	-0.016	2.721
Cook Island	69	258	3.794	3.752	1.546	40.749	-0.273	3.094
Mudjimba	90	641	4.008	4.019	1.106	27.595	0.068	3.044
North Solitary Island	88	670	3.988	3.961	1.436	36.008	0.057	2.897
Julian Rock False Trench	49	92	4.624	4.541	1.881	40.679	0.14	2.303
Julian Rock Nursery	55	166	3.588	3.643	1.378	38.406	0.215	3.018
Black Rock	41	59	4.695	4.693	1.398	29.776	0.004	2.481
South Solitary Island	90	757	3.661	3.658	1.511	41.273	0.15	2.696
North West Solitary Island	88	602	4.475	4.343	1.41	31.508	0.102	2.647
Woolgoolga Reef	21	38	4.949	5.02	1.654	33.421	-0.281	2.361
North Rock	33	76	4.857	4.793	1.597	32.88	0.096	2.308

South West Solitary Island	88	698	4.294	4.233	1.48	34.467	0.127	2.496
-------------------------------	----	-----	-------	-------	------	--------	-------	-------

5

6 Table A-3. Linear regressions showing the relationship between number of coral
7 colonies and the PC1 and PC2 scores. The best model (lowest AIC) is in bold. PC1
8 captures the differences in sea surface temperature, photosynthetically available
9 radiation, high chlorophyll a concentration and turbidity (kd490). More positive PC2
10 scores mean higher minima of chlorophyll a concentration and kd490, but lower
11 standard deviations of PAR. Values unless stated otherwise are corrected to three
12 significant figures.

Model formula	Predictor	Estimate	Std. Error	t value	P value	Adjusted R ²	AIC (2 d.p.)
Coral count ~ PC1	Intercept	611	116	5.24	< 0.001	0.185	252.16
	PC1	-86.9	37.7	-2.31	0.0333		
Coral count ~ PC2	Intercept	611	118	5.20	< 0.001	0.173	252.46
	PC2	162	72.8	2.23	0.0388		
Coral count ~ PC1 + PC2	Intercept	611	102	6.00	< 0.001	0.379	247.59
	PC1	-87.0	32.9	-2.64	0.0171		
	PC2	162	63.1	2.57	0.0198		
Coral count ~ PC1 * PC2	Intercept	611	101	6.05	< 0.001	0.388	248.07
	PC1	-61.4	39.8	-1.54	0.142		
	PC2	151	63.4	2.39	0.0298		
	PC1:PC2	-27.8	24.8	-1.12	0.278		

13

14

15 Table A-4. Linear regressions showing the relationship between the median coral
 16 colony size and the PC1 and PC2 scores. The best model (lowest AIC) is in bold. PC1
 17 captures the differences in sea surface temperature, photosynthetically available
 18 radiation, high chlorophyll a concentration and turbidity (kd490). More positive PC2
 19 scores mean higher minima of chlorophyll a concentration and kd490, but lower
 20 standard deviations of PAR. Values are corrected to three significant figures.

Model formula	Predictor	Estimate	Std. Error	t value	P value	Adjusted R ²	AIC
Median size ~ PC1	Intercept	4.06	0.0902	45.0	< 0.001	0.338	-34.4
	PC1	0.0954	0.0292	3.27	0.00422		
Median size ~ PC2	Intercept	4.06	0.113	35.9	< 0.001	-0.0366	-25.4
	PC2	-0.0402	0.0700	-0.574	0.573		
Median size ~ PC1 + PC2	Intercept	4.06	0.0915	44.3	< 0.001	0.319	-33.0
	PC1	0.0955	0.0296	3.23	0.00494		
	PC2	-0.0402	0.0567	-0.708	0.488		
Median size ~ PC1 * PC2	Intercept	4.06	0.0902	45.0	< 0.001	0.339	-32.8
	PC1	0.0706	0.0355	1.99	0.064		
	PC2	-0.0293	0.0566	-0.518	0.611		
	PC1:PC2	0.0272	0.0221	1.23	0.237		

21

22

23 Table A-5. Linear regressions showing the relationship between skewness and the
 24 PC1 and PC2 scores. The best model (lowest AIC) is in bold. PC1 captures the
 25 differences in sea surface temperature, photosynthetically available radiation, high
 26 chlorophyll a concentration and turbidity (kd490). More positive PC2 scores mean
 27 higher minima of chlorophyll a concentration and kd490, but lower standard
 28 deviations of PAR. Values are corrected to three significant figures.

Model formula	Predictor	Estimate	Std. Error	t value	P value	Adjusted R ²	AIC
Skewness ~ PC1	Intercept	0.137	0.0371	3.70	0.00163	0.306	-70.0
	PC1	-0.0367	0.0120	-3.06	0.00675		
Skewness ~ PC2	Intercept	0.137	0.0430	3.21	0.00486	0.0763	-64.3
	PC2	0.0425	0.0265	1.60	0.126		
Skewness ~ PC1 + PC2	Intercept	0.137	0.0344	4.00	< 0.001	0.404	-72.2
	PC1	-0.0367	0.0111	-3.30	0.00420		
	PC2	0.0425	0.0213	2.00	0.0622		
Skewness ~ PC1 * PC2	Intercept	0.137	0.0354	3.87	0.00134	0.367	-70.1
	PC1	-0.0369	0.0139	-2.65	0.0176		
	PC2	0.0426	0.0222	1.92	0.0733		
	PC1:PC ²	0.000230	0.00869	0.0260	0.979		

29

30

31

32

33 Table A-6. Linear regressions showing the relationship between the coefficient of
 34 variation and the PC1 and PC2 scores. The best model (lowest AIC) is in bold. PC1
 35 captures the differences in sea surface temperature, photosynthetically available
 36 radiation, high chlorophyll a concentration and turbidity (kd490). More positive PC2
 37 scores mean higher minima of chlorophyll a concentration and kd490, but lower
 38 standard deviations of PAR. Values are corrected to three significant figures.

Model formula	Predictor	Estimate	Std. Error	t value	P value	Adjusted R ²	AIC
CV ~ PC1	Intercept	35.7	1.02	35.0	< 0.001	0.0660	62.6
	PC1	-0.505	0.330	-1.53	0.143		
CV ~ PC2	Intercept	35.7	1.06	33.5	< 0.001	-0.0155	64.3
	PC2	-0.555	0.660	-0.842	0.411		
CV ~ PC1 + PC2	Intercept	35.7	1.03	34.7	< 0.001	0.0535	63.7
	PC1	-0.505	0.332	-1.52	0.147		
	PC2	-0.555	0.637	-0.872	0.395		
CV ~ PC1 * PC2	Intercept	35.7	1.05	33.9	< 0.001	0.00795	65.5
	PC1	-0.428	0.414	-1.03	0.317		
	PC2	-0.598	0.660	-0.906	0.378		
	PC1:PC2	-0.0942	0.258	-0.365	0.720		

39

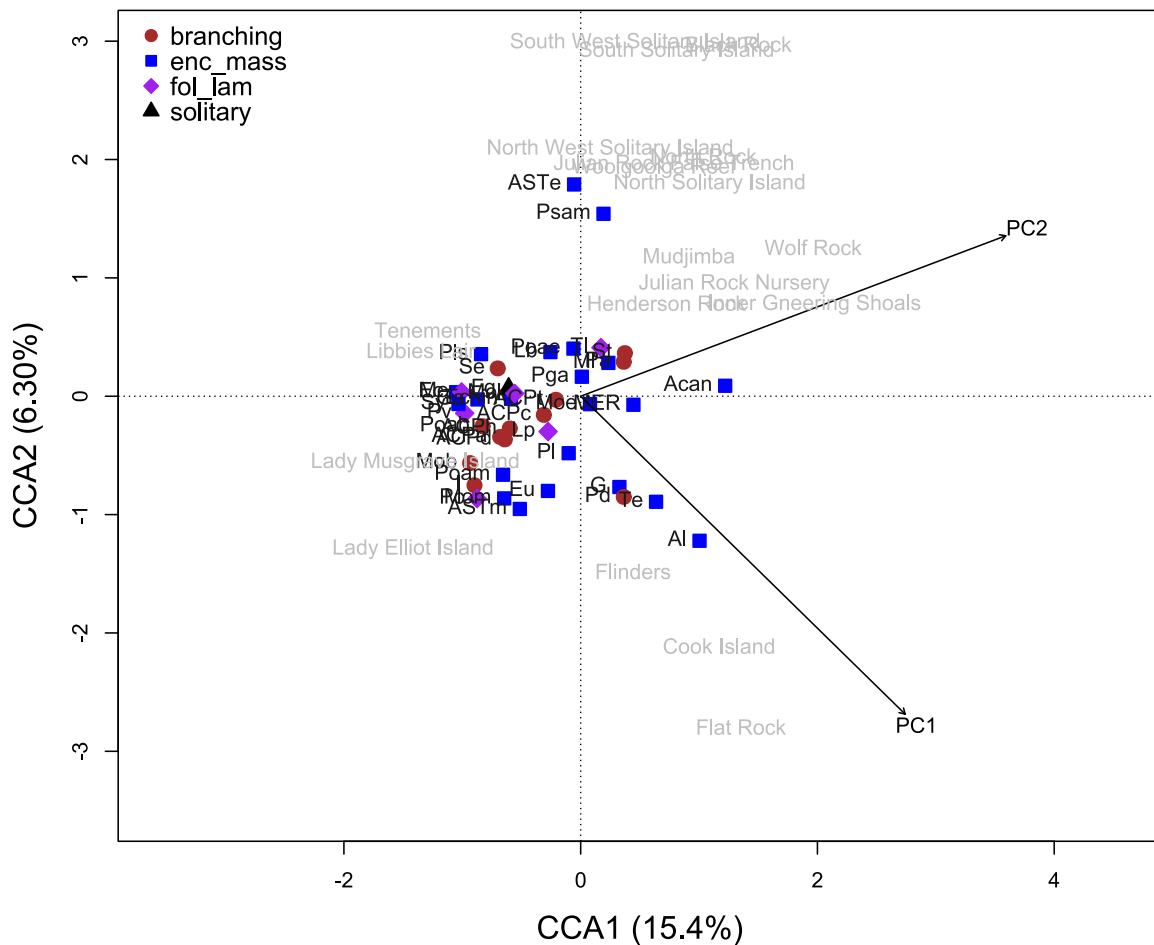
40

41 Table A-7. Linear regressions showing the relationship between kurtosis and the PC1
 42 and PC2 scores. The best model (lowest AIC) is in bold. PC1 captures the differences
 43 in sea surface temperature, photosynthetically available radiation, high chlorophyll a
 44 concentration and turbidity (kd490). More positive PC2 scores mean higher minima of
 45 chlorophyll a concentration and kd490, but lower standard deviations of PAR. Values
 46 are corrected to three significant figures.

Model formula	Predictor	Estimate	Std. Error	t value	P value	Adjusted R ²	AIC
Kurtosis ~ PC1	Intercept	2.69	0.0557	48.2	< 0.001	0.0749	-53.7
	PC1	-0.0287	0.0180	-1.59	0.129		
Kurtosis ~ PC2	Intercept	2.69	0.0594	45.2	< 0.001	-0.0527	-51.1
	PC2	0.00820	0.0368	0.223	0.826		
Kurtosis ~ PC1 + PC2	Intercept	2.69	0.0572	46.9	< 0.001	0.0236	-51.8
	PC1	-0.0287	0.0185	-1.55	0.139		
	PC2	0.00820	0.0355	0.231	0.820		
Kurtosis ~ PC1 * PC2	Intercept	2.69	0.0536	50.1	< 0.001	0.143	-53.6
	PC1	-0.00656	0.0211	-0.311	0.760		
	PC2	-0.00146	0.0336	-0.043	0.966		
	PC1:PC2	-0.0242	0.0132	-1.84	0.848		

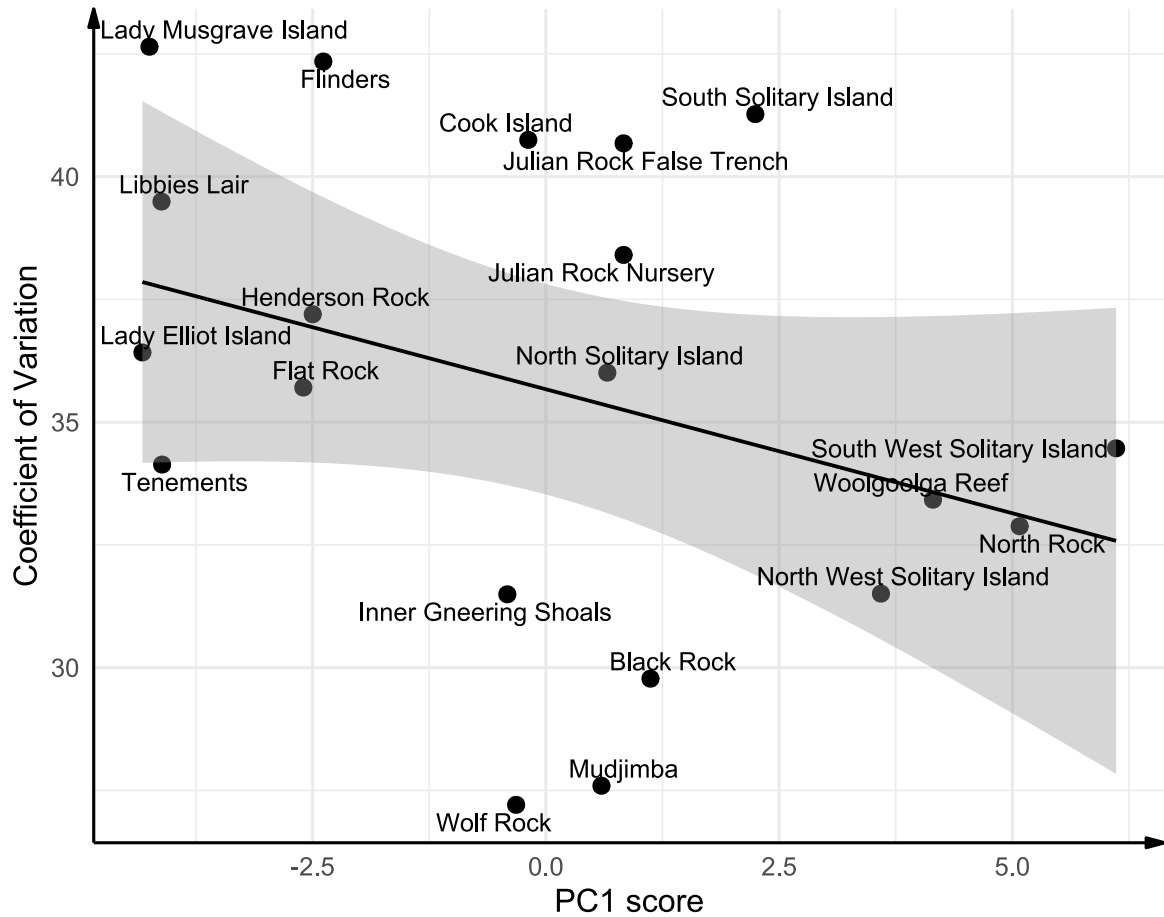
47

48



49

50 Figure A-1. Canonical Correspondence Analysis (CCA) biplot of the 41 coral taxa,
 51 sites and PC1 and PC2 scores. The two CCA axes jointly explain 21.7% of the
 52 variation. Coral taxa are coloured based on four broad morphological groups:
 53 'branching' (brown circles), 'enc_mass' (encrusting/massive; blue squares), 'fol_lam'
 54 (foliose/laminar; violet diamonds) and 'solitary' (black triangle). High PC1 scores
 55 represent lower sea surface temperature and photosynthetically available radiation
 56 (PAR), *i.e.*, colder and darker, and high chlorophyll a concentration and turbidity
 57 (kd490), *i.e.*, more productive and more turbid. High PC2 scores represent higher
 58 minima of chlorophyll a concentration and kd490, but lower standard deviations of
 59 PAR. The overall permutation test was significant $F_{2,17} = 2.36$, $P = 0.009$. For more
 60 detail on the methods and interpretation, see section S2: Coral taxonomic identity
 61 along the environmental gradient.



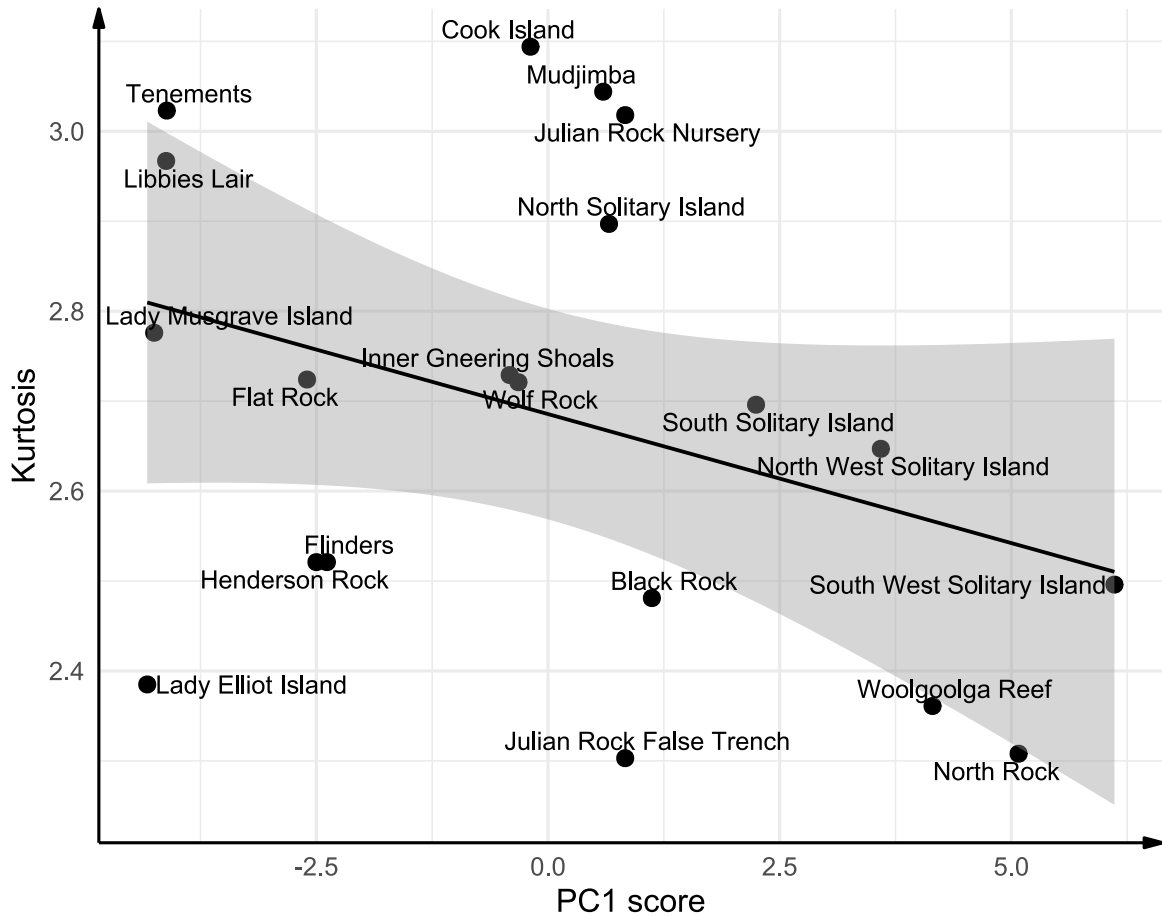
62

63 Figure A-2. The colony size coefficient of variation (CV) decreases with PC1. PC1 is
 64 fitted as the explanatory variable here because of model selection (Table A-6). Black
 65 line is the line of best fit, and the grey region is the 95% confidence band. More positive
 66 PC1 scores represent lower sea surface temperature and photosynthetically available
 67 radiation (PAR), *i.e.*, colder and darker, and high chlorophyll *a* concentration and
 68 turbidity (kd490), *i.e.*, more productive and more turbid.

69

70

71



72

73 Figure A-3. Kurtosis of the coral size-frequency distribution decreases with PC1. PC1
 74 is fitted as the explanatory variable here because of model selection (Table A-7). Black
 75 line is the line of best fit, and the grey region is the 95% confidence band. More positive
 76 PC1 scores represent lower sea surface temperature and photosynthetically available
 77 radiation (PAR), *i.e.*, colder and darker, and high chlorophyll a concentration and
 78 turbidity (kd490), *i.e.*, more productive and more turbid.

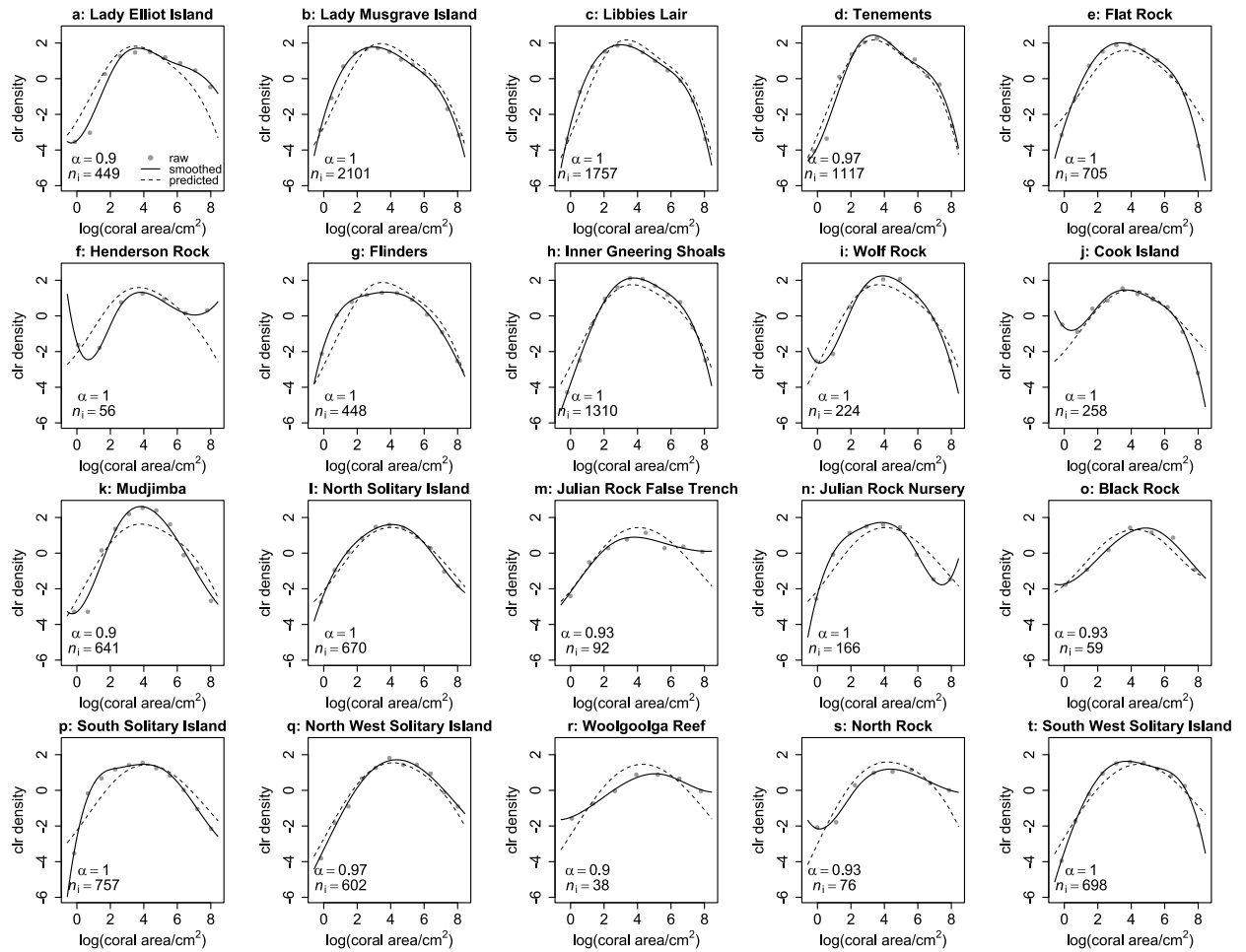


Figure A-4. Centred log-ratio (clr) transformed densities of log coral area for the 20 reefs, ordered from low to high PC1 scores (left to right; top to bottom). Grey dots are binned raw data points, black solid lines are smoothed densities and dotted lines are predicted clr densities from a compositional functional regression. For each site, α is the value of the smoothing parameter and n_i is the number of corals at the site.

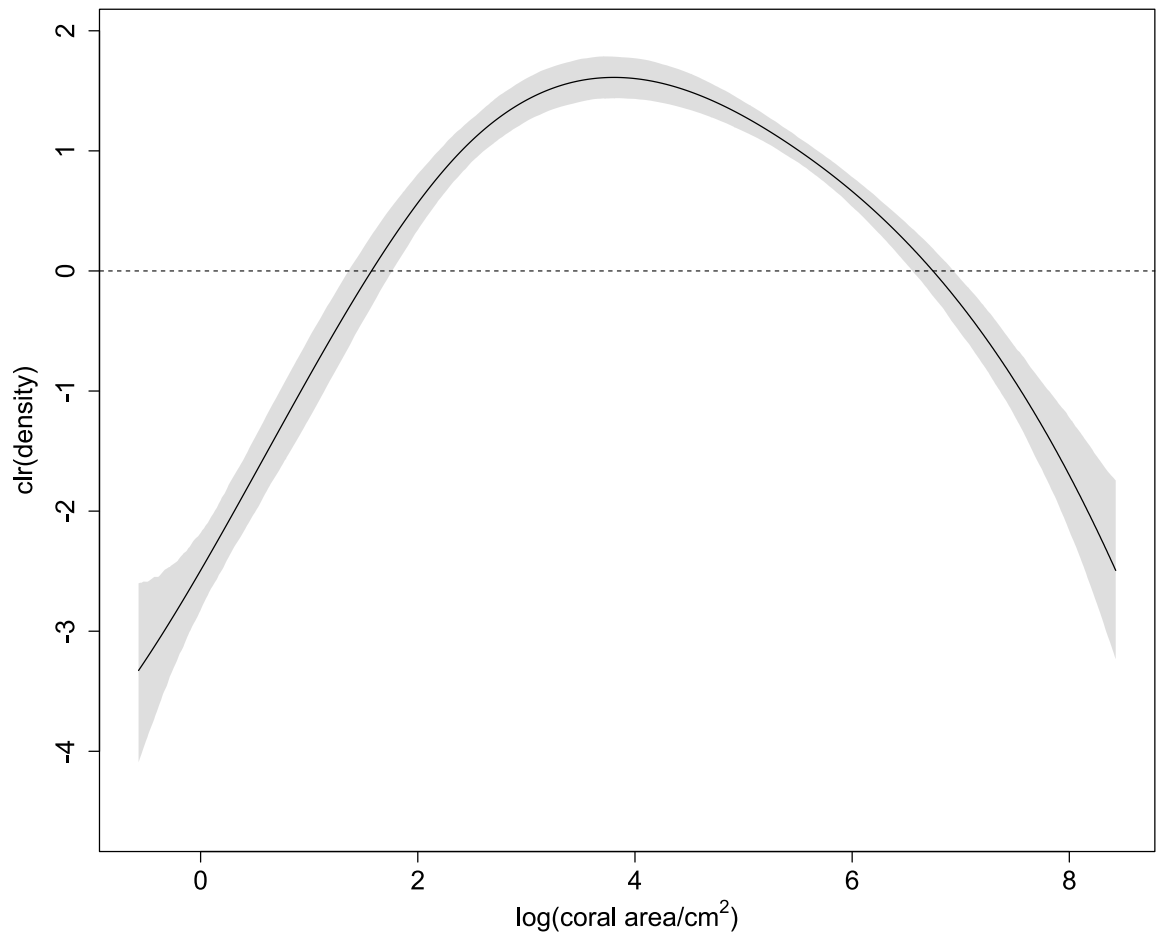


Figure A-5. When the mean values of PC1 and PC2 are both zero, the coral size-frequency distribution is symmetrical. The black line is the estimated centred log-ratio (clr) transformation of the coefficient function β_0 (the intercept), which is the prediction when PC1 and PC2 are both equal to zero. The grey shaded region is the bootstrap 95% confidence band.

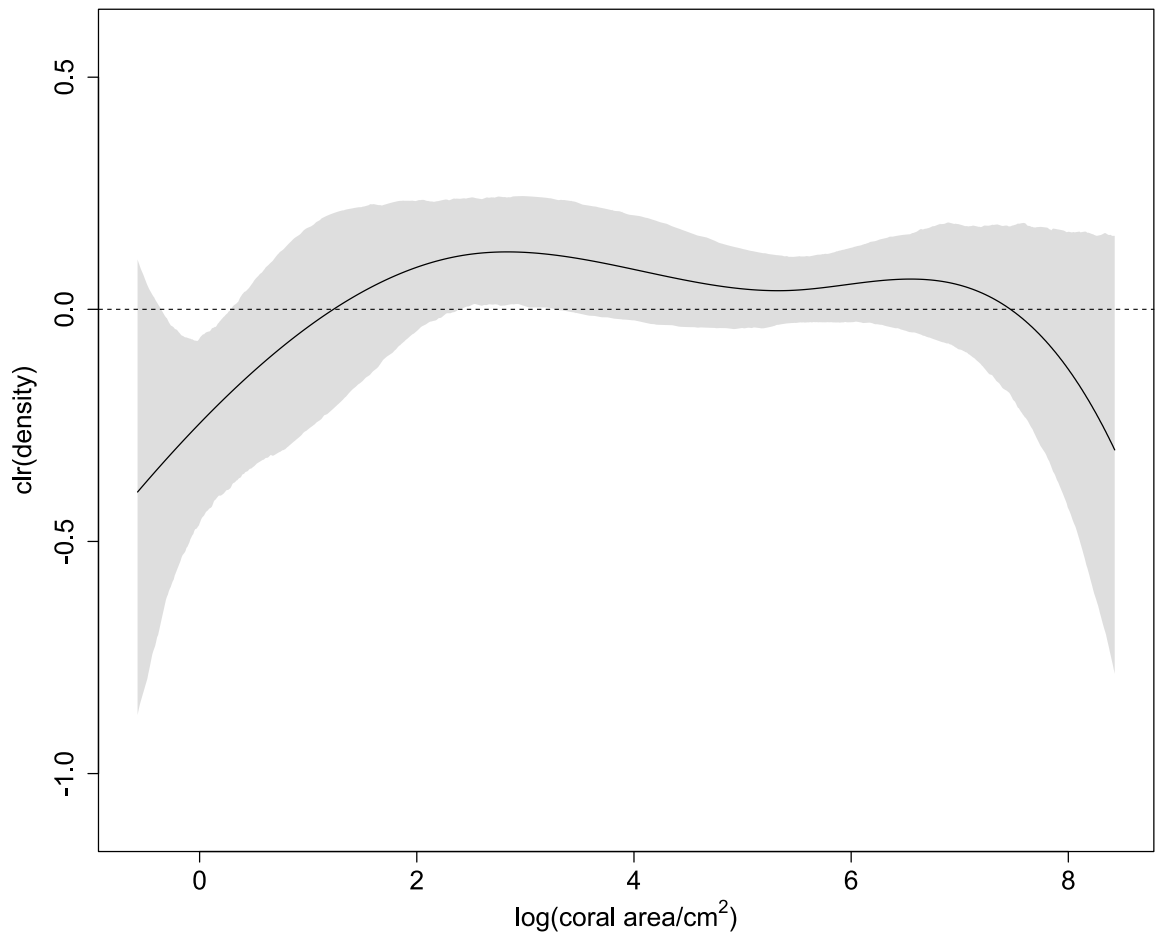


Figure A-6. Increases in second axis (PC2) scores might mean lower densities of corals at the extreme sizes but a higher density of corals $\sim 1-7 \log \text{ cm}^2$, however no effect is plausible as the grey shaded region (bootstrap 95% confidence band) almost always crossed the dashed line (no effect on the probability densities), except for $\sim 3 \log \text{ cm}^2$. Increases in PC2 represent higher minimum chl_a and kd₄₉₀ and lower standard deviation of PAR. The black line is the estimated centred log-ratio (clr) transformation of the coefficient function β_2 , which measures the effect of a unit increase in PC2 on the probability density of a given log coral area. Positive values on the y-axis mean that the corresponding log coral area on the x-axis becomes more likely as PC2 increases, and negative values mean that the corresponding log coral area becomes less likely.

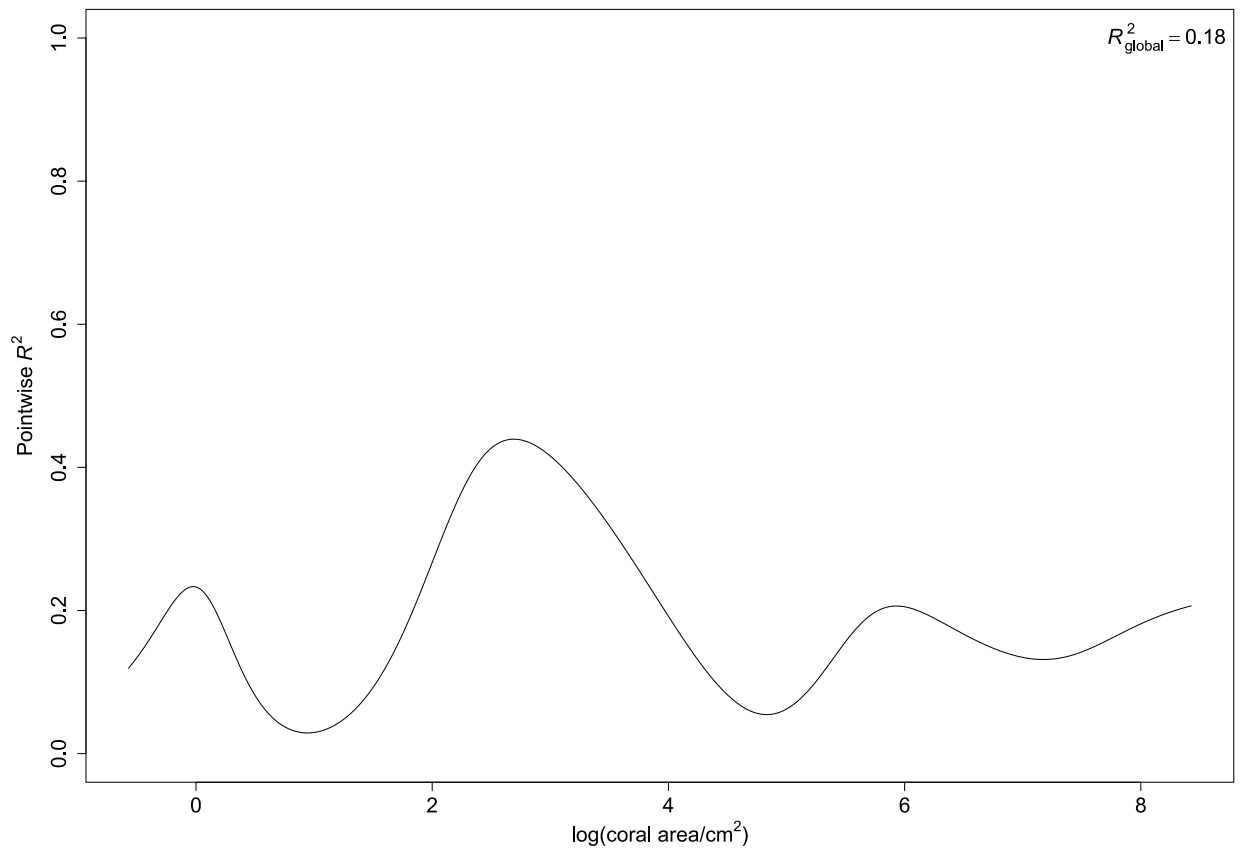


Figure A-7. The proportion of variation in probability density explained by the model (pointwise R^2) at each log coral area, with most explanatory power at approx. 3 log cm². Global R^2 (the total proportion of variation explained by the model) is 0.18.

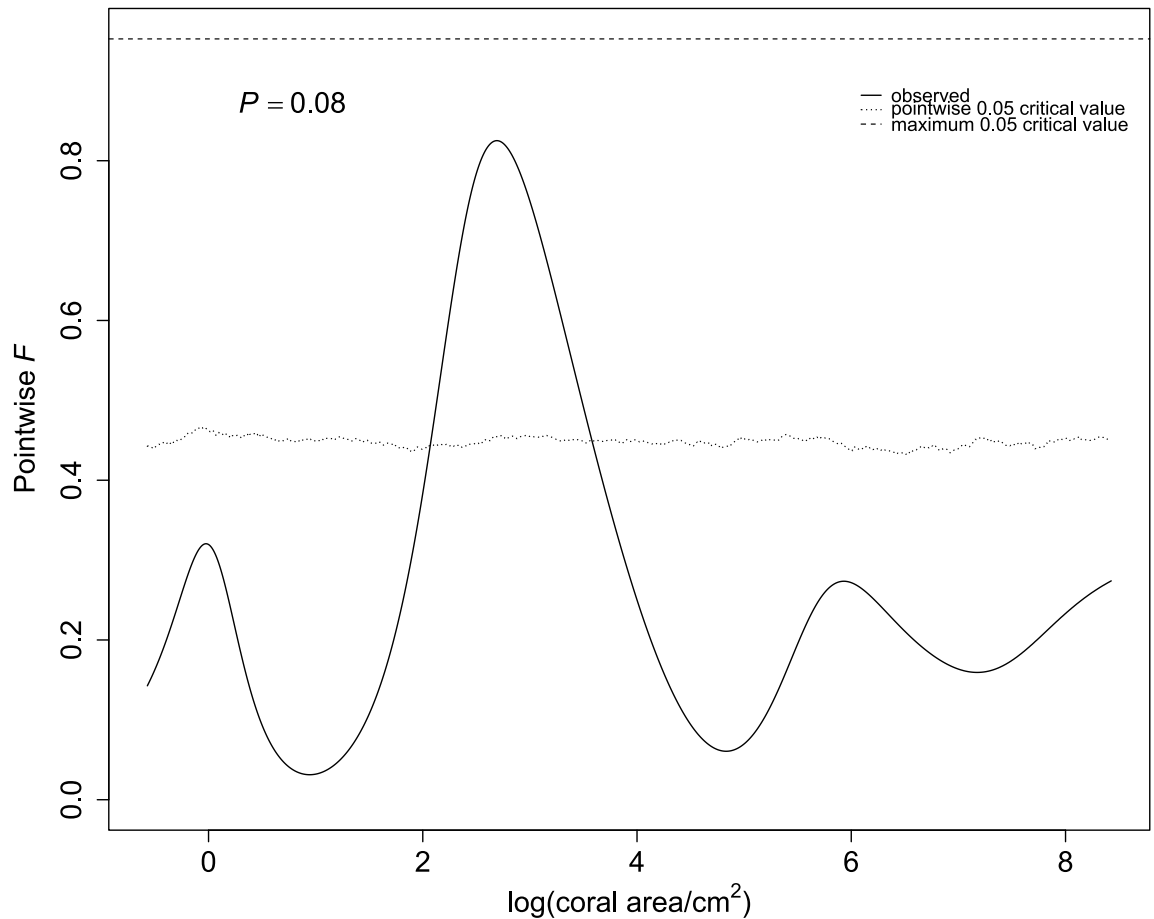


Figure A-8. Permutation F test for the predictive relationship between log coral area and the PC scores (PC1 and PC2). The observed F statistic (solid line) is highest at 3 log cm², suggesting that the explanatory variables PC1 and PC2 had the most effect there; however, because the observed F statistic did not cross the maximum critical value (dashed line) anywhere in the distribution, it was plausible that neither of the explanatory variables affected coral size-frequency distributions. Dotted line: pointwise 0.05 critical values such that only one permuted F statistic in 20 exceeds this value at a given log coral area. Dashed line: maximum 0.05 critical value such that only one permuted F statistic in 20 exceeds this value at any log coral area. Functional F -test, maximum $F =$ observed maximum $F = 0.83$, $P = 0.08$ from 9,999 permutations.

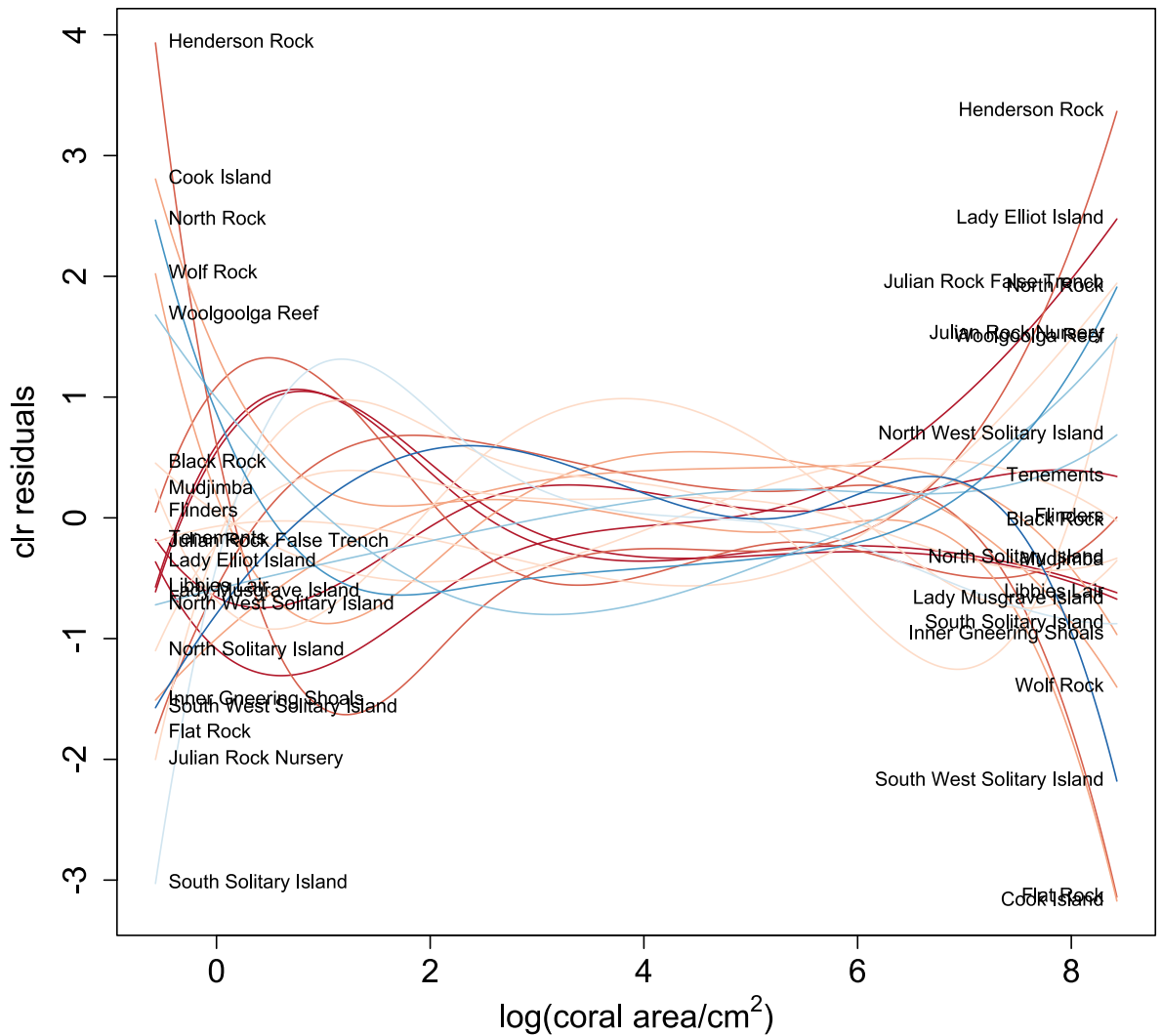


Figure A-9. Centred log-ratio (clr) residuals for the predictive relationship between log coral area and the PC scores (PC1 and PC2). Little systematic pattern in the residual functions can be seen, except that they tended to be further from zero at the extreme coral sizes. Line colours go from blue to red in eight steps, where the darkest blue indicates the site with the highest PC1 scores (more turbidity and chlorophyll *a*) and the darkest red are sites with the lowest PC1 scores (high PAR and SST).

S2: Coral taxonomic identity along the environmental gradient

We examined the potential shifts in community composition along the gradient using Canonical Correspondence Analysis (CCA) using R package 'vegan' (Oksanen *et al.*, 2020). For easier comparison, the 41 taxa were placed into four morphological groups: branching, encrusting/massive (enc_mass), foliose/laminar (fol_lam) and solitary. Most corals (22) were encrusting/massive, twelve were branching, six were foliose/laminar and one was solitary. For the full list of taxa names, see the supplementary data file 'ROI type classification.xlsx'. The two CCA axes together explain 21.7% of the variation. The overall permutation test was significant ($F_{2,17} = 2.36$, $P = 0.009$; 999 permutations). The CCA biplot (Figure A-1) show that the taxa cloud cluster in the middle, suggesting that some taxa were shared among sites. Encrusting/massive corals were found throughout the entire gradient. However, sites that have more negative PC1 scores (more 'tropical' sites, *e.g.* Tenements, Libbies Lair, Lady Musgrave and Lady Elliot Islands) are likely characterised by different branching and foliose/laminar corals compared to marginal reefs. For example, Acroporids are the common branching corals in the tropical sites, while Pocilloporids (*Stylophora*, *Pocillpora aliciae*, *P. damicornis*) are more common in marginal reefs. For laminar/foliose corals, *Mycedium*, *Pavona*, and laminar *Montipora* were found in the tropical reefs, while laminar *Turbinaria* was more common in marginal reefs.

S3: Bayes Space

A vector space is an algebraic structure with an addition operation defined for the elements of the space (known as vectors), and a scalar multiplication operation defined for a scalar (such as a real number) and a vector, where the operations must satisfy familiar axioms such as commutativity of addition and distributivity of scalar multiplication (Judson, 2019, pp. 310-311). The most familiar example of a vector space is n -dimensional Euclidean space, in which the vectors are the n -tuples of real numbers, vector addition of two vectors $\mathbf{v} = (v_1, v_2, \dots, v_n)$ and $\mathbf{w} = (w_1, w_2, \dots, w_n)$ is defined by $\mathbf{v} + \mathbf{w} = (v_1 + w_1, v_2 + w_2, \dots, v_n + w_n)$, the scalars are real numbers, and the scalar product of a scalar r and a vector \mathbf{v} is defined by $r\mathbf{v} = (rv_1, rv_2, \dots, rv_n)$. However, there are many other vector spaces satisfying the same axioms. In Bayes space, the vectors are probability density functions whose support is a closed interval, the addition operation is perturbation, and the scalar multiplication operation is powering (Egozcue *et al.*, 2006). Let f_1, f_2 be continuous probability density functions whose support is a closed interval $I = [a, b] \subset \mathbb{R}$, and let $x \in \mathbb{R}$. Then the addition operation in Bayes space is perturbation $f_1 \oplus f_2$, defined by

$$(f_1 \oplus f_2)(t) = \frac{f_1(t)f_2(t)}{\int_a^b f_1(s)f_2(s)ds},$$

for $t \in I$, The addition operation is Bayes' Theorem (Egozcue *et al.*, 2013), hence the name "Bayes space", but this does not imply the use of Bayesian statistics. The scalar multiplication operation is powering $x \odot f_1$, defined by

$$(x \odot f_1)(t) = \frac{f_1^x(t)}{\int_a^b f_1^x(s)ds}$$

for $t \in I$ (Talská *et al.*, 2018). These operations can be thought of as infinite-dimensional versions of the perturbation and powering operations for compositional data, which have been used previously in analyses of the effects of environmental disturbances on coral reef composition and stability (e.g., Gross & Edmunds, 2015; Vercelloni *et al.*, 2020).

S4: Size-biased sampling

We assume that sampling probability is a function of size alone. This is the case for minus sampling provided that colony shape does not vary systematically with the values of explanatory variables (Baddeley, 1998b, p. 50). Let $g(s)$ be the probability density for sampling colonies of size s . Then the size-frequency distribution of sampled colonies, when the true size-frequency distribution has density function $y(s)$, is

$$\frac{y(s)g(s)}{\int_a^b y(t)g(t)dt} = \mathbf{y} \oplus \mathbf{g},$$

(Baddeley, 1998a, p. 20). We can show using the change-of-variables formula that the same result holds when the size measure of interest (e.g., log colony area) is a strictly monotone transformation of the size measure that determines sampling bias. Thus, with size-biased sampling, Equation 1 becomes

$$\begin{aligned} \mathbf{y}_i \oplus \mathbf{g} &= (\boldsymbol{\beta}_0 \oplus (x_{1,i} \odot \boldsymbol{\beta}_1) \oplus (x_{2,i} \odot \boldsymbol{\beta}_2) \oplus \boldsymbol{\varepsilon}_i) \oplus \mathbf{g} \\ &= (\boldsymbol{\beta}_0 \oplus \mathbf{g}) \oplus (x_{1,i} \odot \boldsymbol{\beta}_1) \oplus (x_{2,i} \odot \boldsymbol{\beta}_2) \oplus \boldsymbol{\varepsilon}_i, \end{aligned}$$

by associativity and commutativity of perturbation. Thus, instead of the true intercept function $\boldsymbol{\beta}_0$, we will estimate the perturbed intercept $\boldsymbol{\beta}_0 \oplus \mathbf{g}$, and the overall shape of the estimated response distribution will be biased. However, the estimates of $\boldsymbol{\beta}_1$ and $\boldsymbol{\beta}_2$, which are of primary interest, will not be affected.

S5: Further compositional functional regression results and model diagnostics

It was plausible that PC2 had little effect on coral sizes except for corals at ~ 3 log cm², as the 95% confidence band included zero almost everywhere (Figure A-6). The predicted distribution of log area at the mean values of PC1 and PC2 (given by the intercept function β_0) was symmetrical, with a mode of approximately 4 log cm², corresponding to 54.6 cm² (Figure A-5).

The smoothed centred log-ratio (clr) densities (Figure A-4; analogous to Figure 4) were generally a good representation of our data, except for some sites (*e.g.*, Henderson Rock, North Rock and Wolf Rock), where estimated densities were artificially high at the lowest log areas. This could be due to those sites supporting small numbers of colonies.

Residual plots showed little systematic pattern in the residual functions, except that they tended to be further from zero at the smallest or largest coral areas (Figure A-9). This might be associated with smoothing artefacts (Machalová *et al.*, 2021), where there are lower numbers of colonies at the extreme sizes.

S6: Testing compositional functional regression model robustness

The effect of varying bin numbers

In our original analysis, we used Sturges' Rule to select the number of histogram bins at each site. This rule gave between seven and thirteen bins. To check whether the results were sensitive to the number of bins, we refitted the models using either seven bins at all sites or thirteen bins at all sites. The resulting coefficient functions (Figure A-10; Figure A-15) were similar to our original estimates. Previous simulation studies on the methods we used (Talská *et al.*, 2018, section 7; Machalová *et al.*, 2021, section 6) also suggest that these methods are not very sensitive to the number of bins used in histogram smoothing.

The effect of removing sites with the fewest coral colonies

We tested the effect of removing sites with the fewest number of coral colonies to determine the potential effect of a higher sampling variability in histogram fitting at these sites. Through the inspection of Figure A-4, it seems that sites with more than 400 corals fitted well, and did not appear to have artefacts where the density functions are increasing at the extreme values, which seems biologically unlikely (e.g., Cook Island and Wolf Rock, with 258 and 224 colonies respectively (Figure A-4i-j)). Removing sites with fewer than 400 corals resulted in twelve sites, with at least 448 colonies each. We refitted the model including only those sites. The shapes of the estimated coefficient functions (Figure A-16; Figure A-18) are similar to the results of when all 20 sites were included. Furthermore, although the pointwise R^2 is higher at some points, the global R^2 is now a bit lower (0.13; Figure A-19). This suggests that the low proportion of variation explained was not because of sampling variability in histogram fitting.

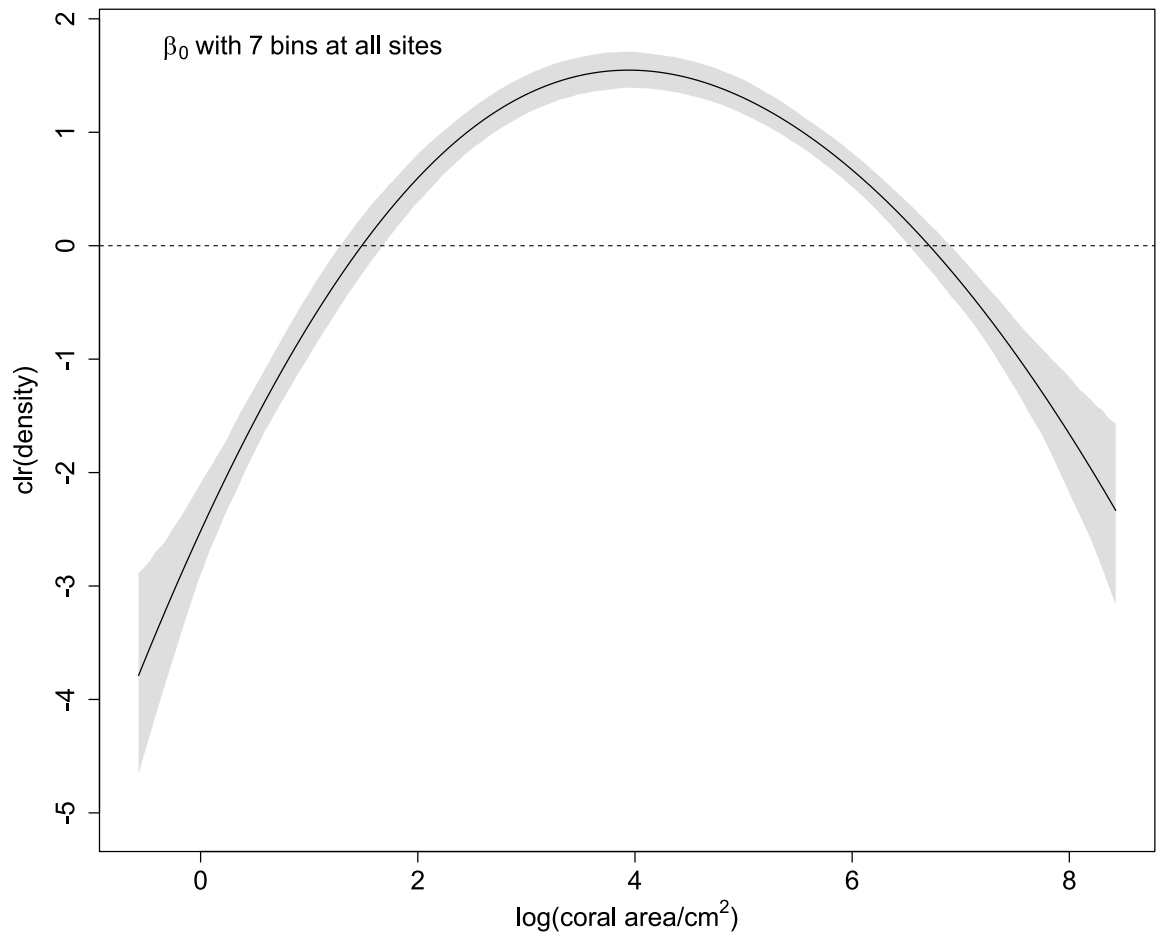


Figure A-10. When the mean values of PC1 and PC2 are both zero, the coral size-frequency distribution is symmetrical. The black line is the estimated centred log-ratio (clr) transformation of the coefficient function β_0 (the intercept), which is the prediction when PC1 and PC2 are both equal to zero. The grey shaded region is the bootstrap 95% confidence band. Seven bins were used at all sites for histogram smoothing.

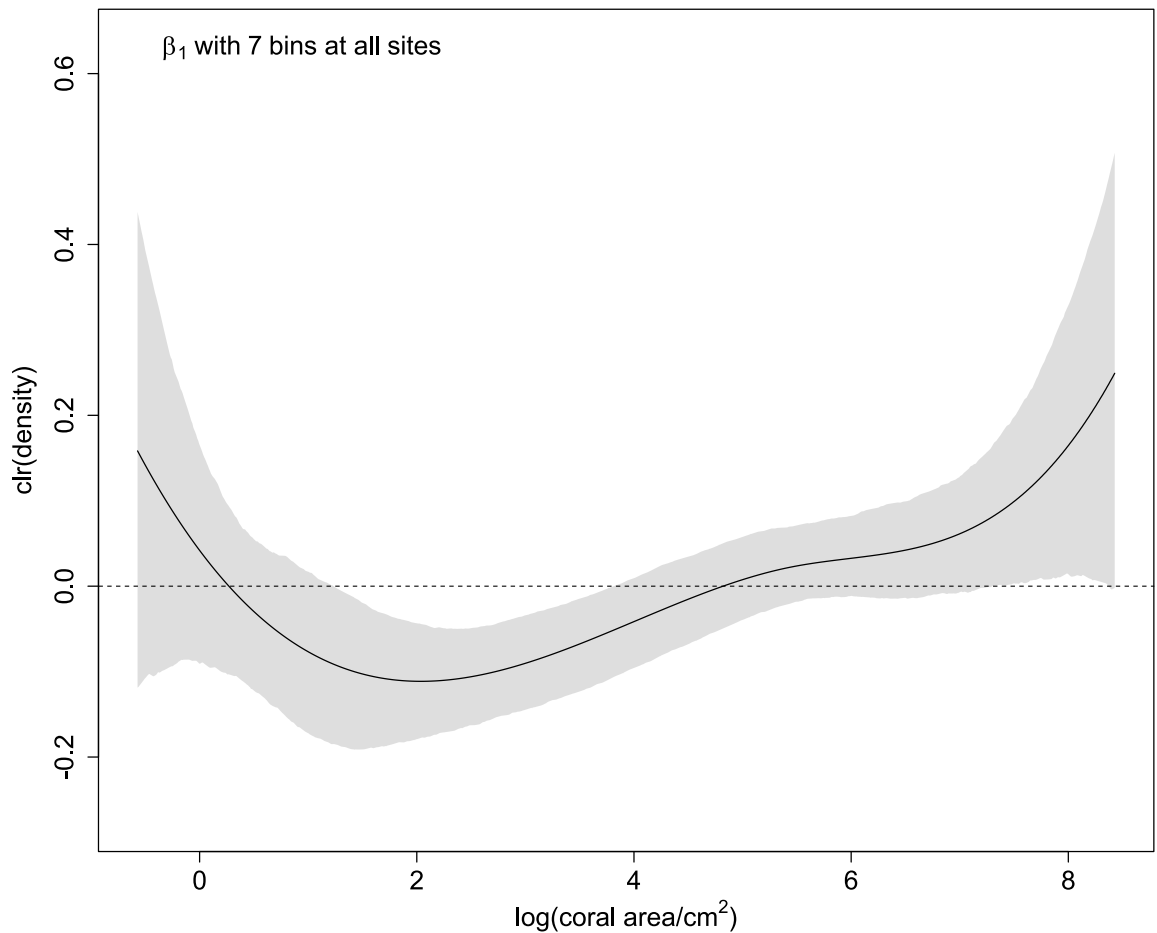


Figure A-11. Increases in first axis (PC1) scores mean lower densities of corals at $\sim 1-4 \log \text{ cm}^2$. Increases in PC1 represents increasingly marginal conditions (colder, darker, more turbid and productive waters). The black line is the estimated centred log-ratio (clr) transformation of the coefficient function β_1 , which measures the effect of a unit increase in PC1 on the probability density of a given log coral area. Positive values on the y-axis suggest that the corresponding log coral area on the x-axis becomes more likely as PC1 increases, and negative values suggest that the corresponding log coral area becomes less likely. The shaded region is the bootstrap 95% confidence band. The horizontal dashed line represents no effect of PC1 on the probability density of log coral area. Seven bins were used at all sites for histogram smoothing.

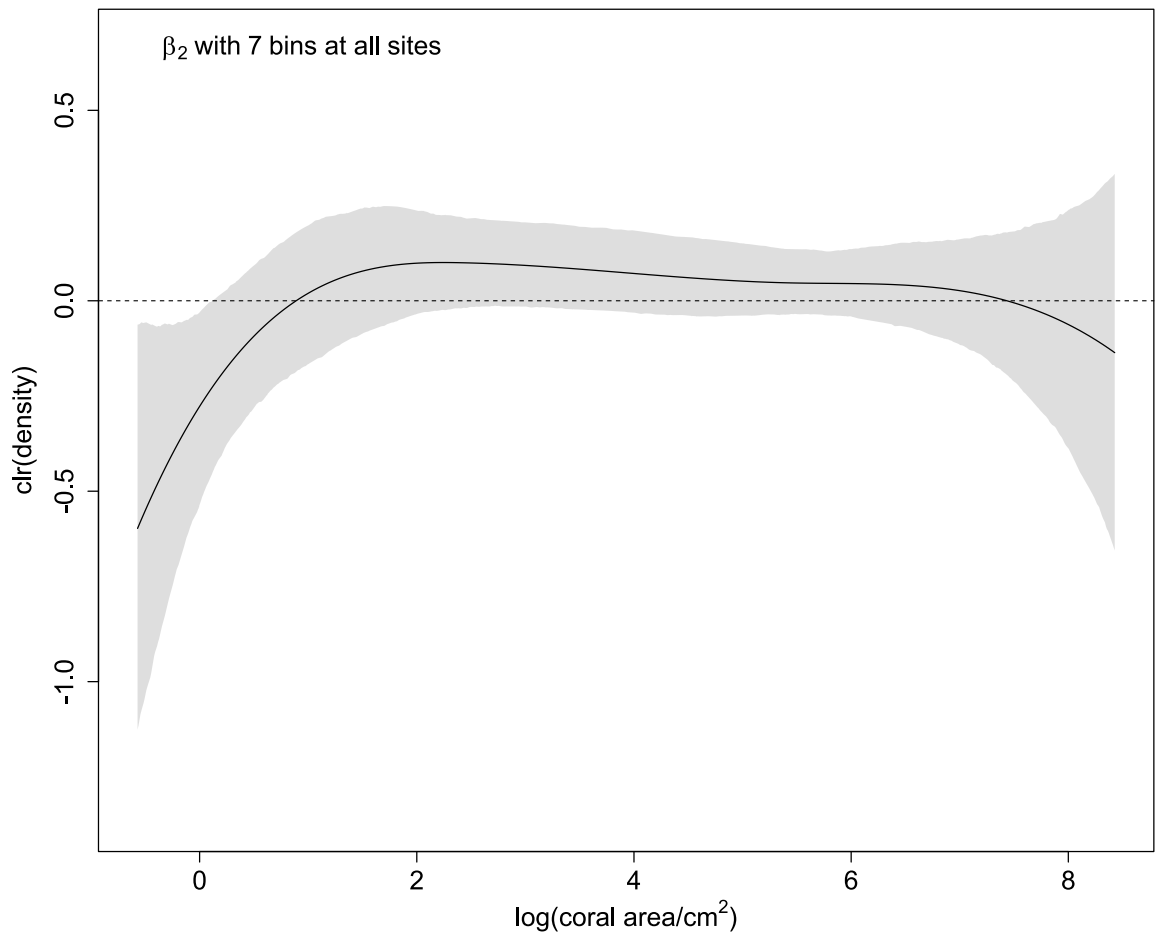


Figure A-12. Increases in second axis (PC2) scores might mean lower densities of corals at the extreme sizes but a higher density of corals $\sim 1\text{-}7 \log \text{cm}^2$, however no effect is plausible as the grey shaded region (bootstrap 95% confidence band) always crossed the dashed line (no effect on the probability densities). Increases in PC2 represent higher minimum chl_a and kd₄₉₀ and lower standard deviation of PAR. The black line is the estimated centred log-ratio (clr) transformation of the coefficient function β_2 , which measures the effect of a unit increase in PC2 on the probability density of a given log coral area. Positive values on the y-axis mean that the corresponding log coral area on the x-axis becomes more likely as PC2 increases, and negative values mean that the corresponding log coral area becomes less likely. Seven bins were used at all sites for histogram smoothing.

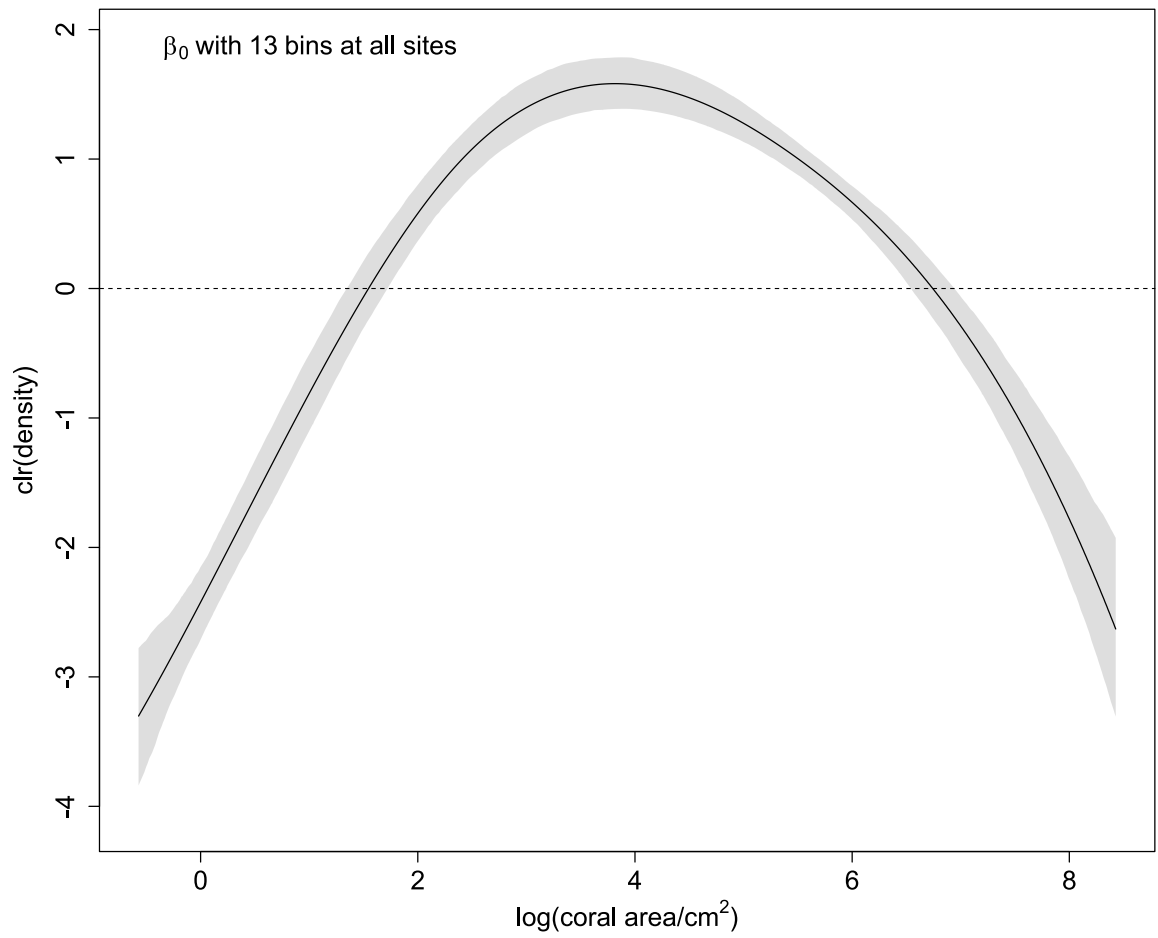


Figure A-13. When the mean values of PC1 and PC2 are both zero, the coral size-frequency distribution is symmetrical. The black line is the estimated centred log-ratio (clr) transformation of the coefficient function β_0 (the intercept), which is the prediction when PC1 and PC2 are both equal to zero. The grey shaded region is the bootstrap 95% confidence band. Thirteen bins were used at all sites for histogram smoothing.

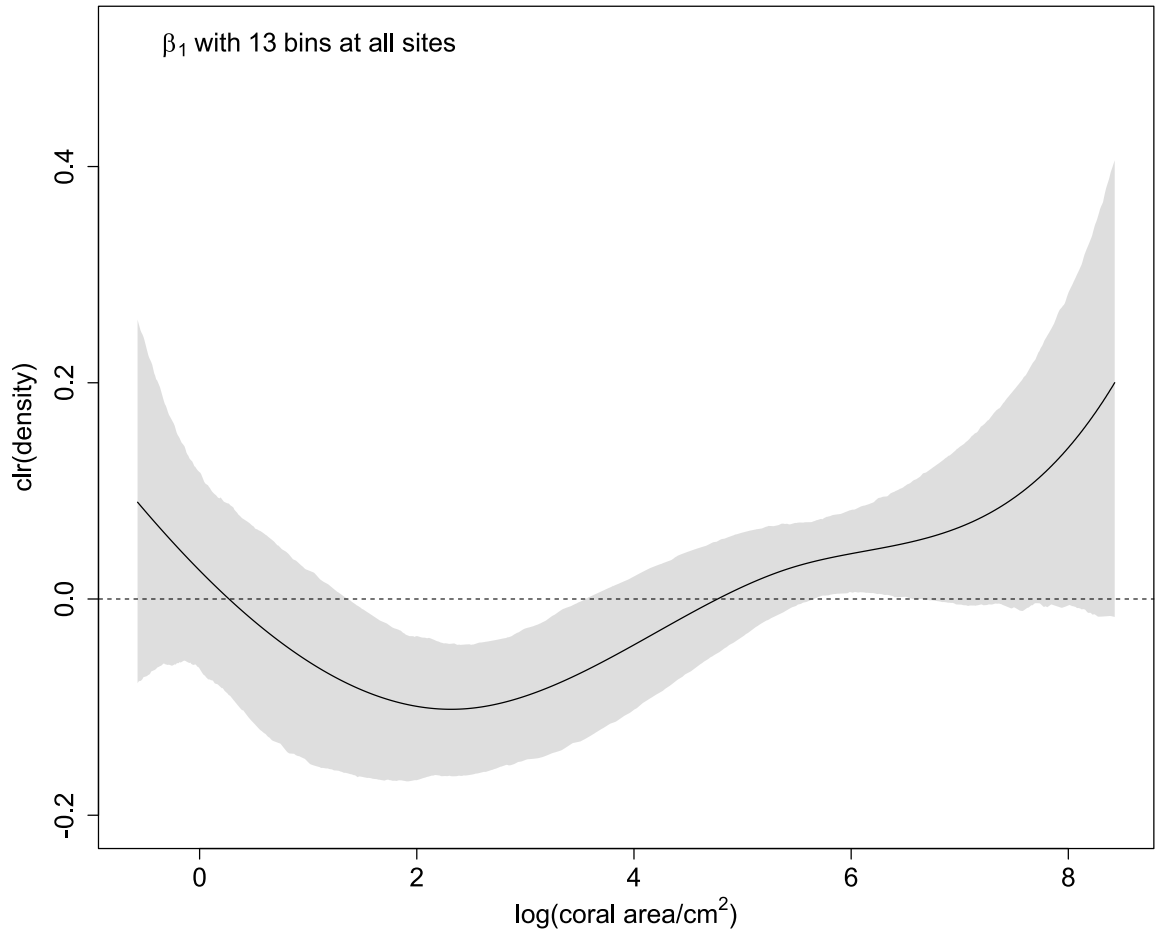


Figure A-14. Increases in first axis (PC1) scores mean lower densities of corals at $\sim 1-4 \log \text{cm}^2$. Increases in PC1 represents increasingly marginal conditions (colder, darker, more turbid and productive waters). The black line is the estimated centred log-ratio (clr) transformation of the coefficient function β_1 , which measures the effect of a unit increase in PC1 on the probability density of a given log coral area. Positive values on the y-axis suggest that the corresponding log coral area on the x-axis becomes more likely as PC1 increases, and negative values suggest that the corresponding log coral area becomes less likely. The shaded region is the bootstrap 95% confidence band. The horizontal dashed line represents no effect of PC1 on the probability density of log coral area. Thirteen bins were used at all sites for histogram smoothing.

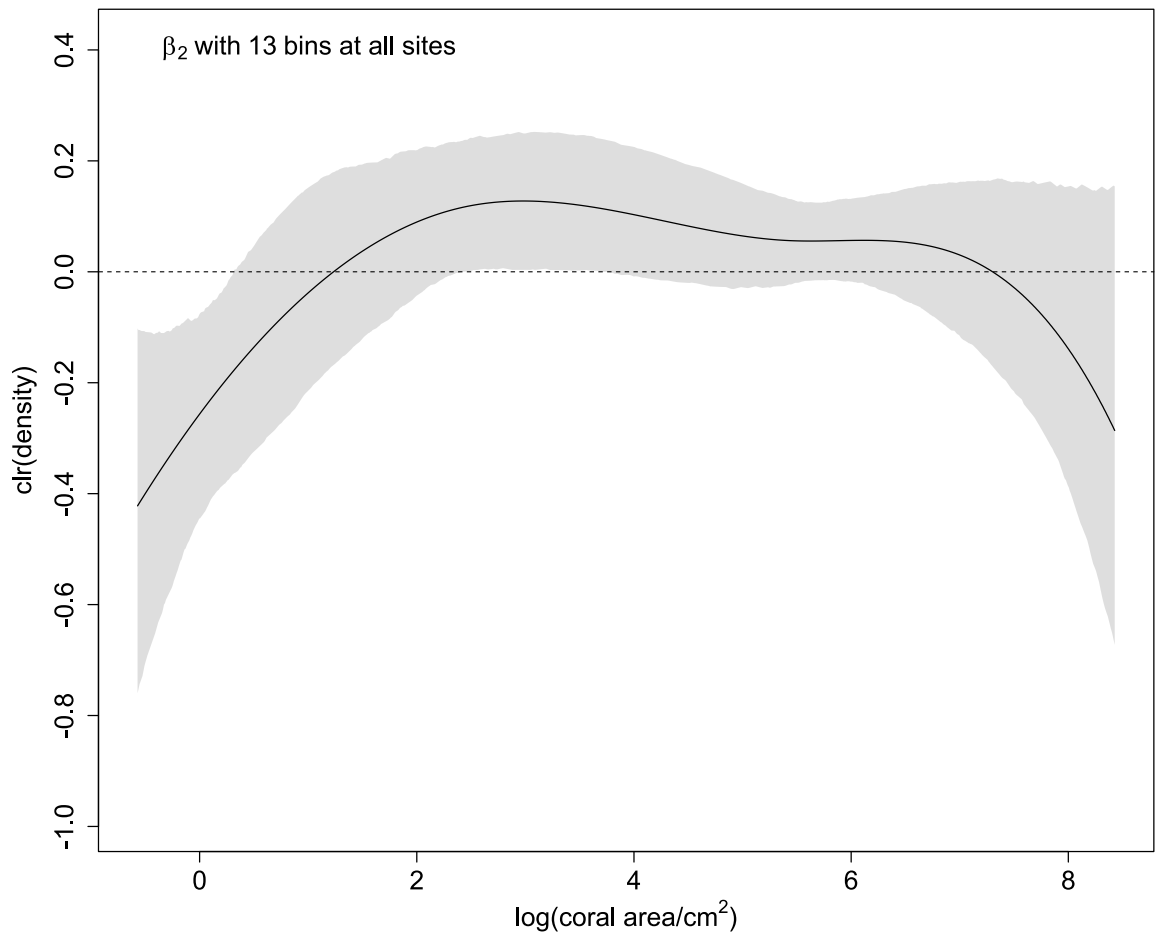


Figure A-15. Increases in second axis (PC2) scores might mean lower densities of corals at the extreme sizes but a higher density of corals $\sim 1-7 \log \text{ cm}^2$, however no effect is plausible as the grey shaded region (bootstrap 95% confidence band) almost always crossed the dashed line (no effect on the probability densities), except for $\sim 3 \log \text{ cm}^2$. Increases in PC2 represent higher minimum chl_a and kd₄₉₀ and lower standard deviation of PAR. The black line is the estimated centred log-ratio (clr) transformation of the coefficient function β_2 , which measures the effect of a unit increase in PC2 on the probability density of a given log coral area. Positive values on the y-axis mean that the corresponding log coral area on the x-axis becomes more likely as PC2 increases, and negative values mean that the corresponding log coral area becomes less likely. Thirteen bins were used at all sites for histogram smoothing.

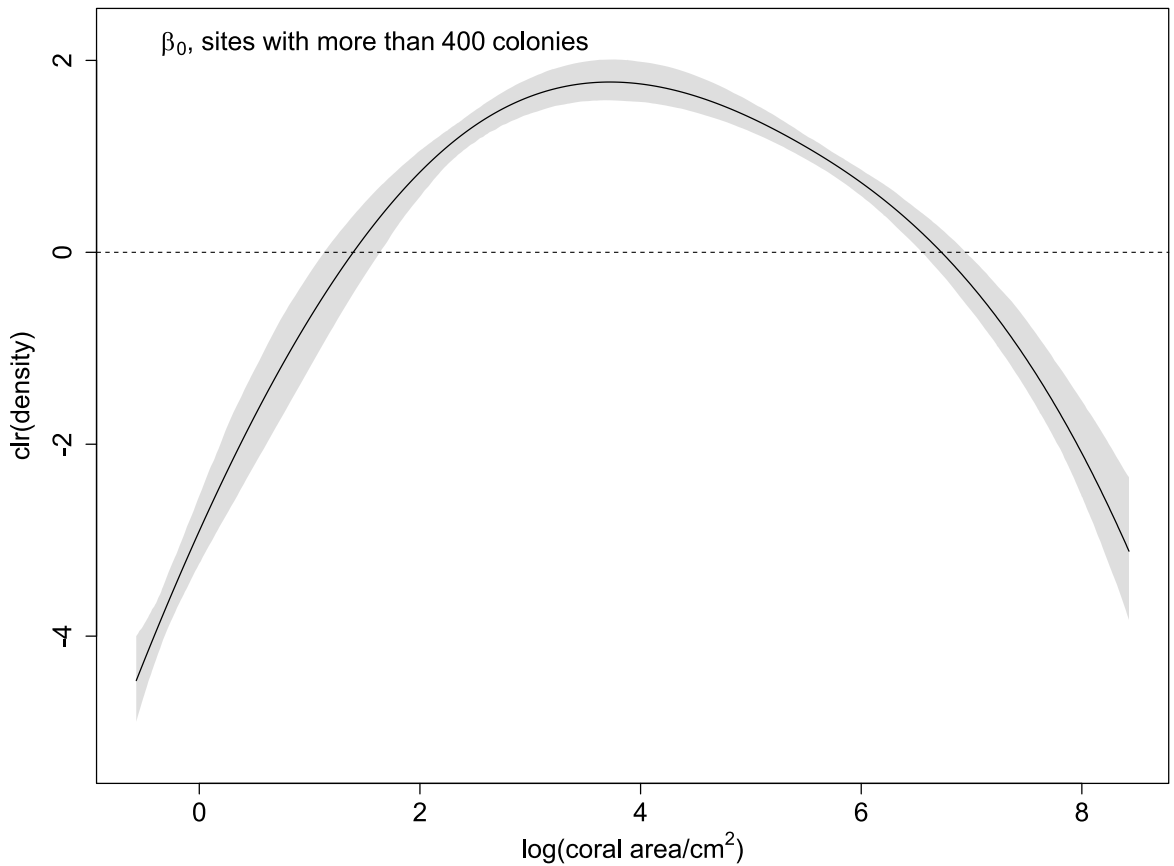


Figure A-16. When the mean values of PC1 and PC2 are both zero, the coral size-frequency distribution is symmetrical. The black line is the estimated centred log-ratio (clr) transformation of the coefficient function β_0 (the intercept), which is the prediction when PC1 and PC2 are both equal to zero. The grey shaded region is the bootstrap 95% confidence band. Fitted to the twelve sites that had more than 400 coral colonies.

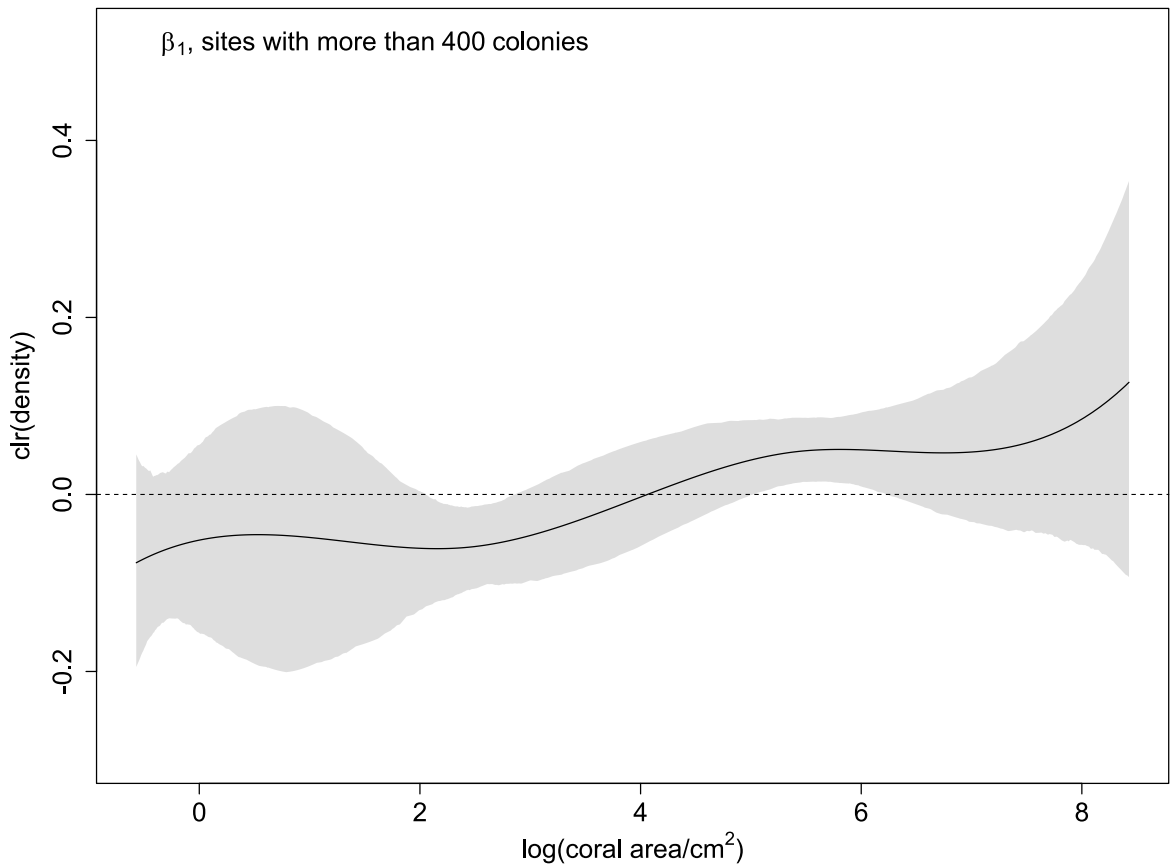


Figure A-17. Increases in first axis (PC1) scores mean lower densities of corals at ~ 2 - $3 \log \text{ cm}^2$ and a high density of corals 5 - $6 \log \text{ cm}^2$. Increases in PC1 represents increasingly marginal conditions (colder, darker, more turbid and productive waters). The black line is the estimated centred log-ratio (clr) transformation of the coefficient function β_1 , which measures the effect of a unit increase in PC1 on the probability density of a given log coral area. Positive values on the y-axis suggest that the corresponding log coral area on the x-axis becomes more likely as PC1 increases, and negative values suggest that the corresponding log coral area becomes less likely. The shaded region is the bootstrap 95% confidence band. The horizontal dashed line represents no effect of PC1 on the probability density of log coral area. Fitted to the twelve sites that had more than 400 coral colonies.

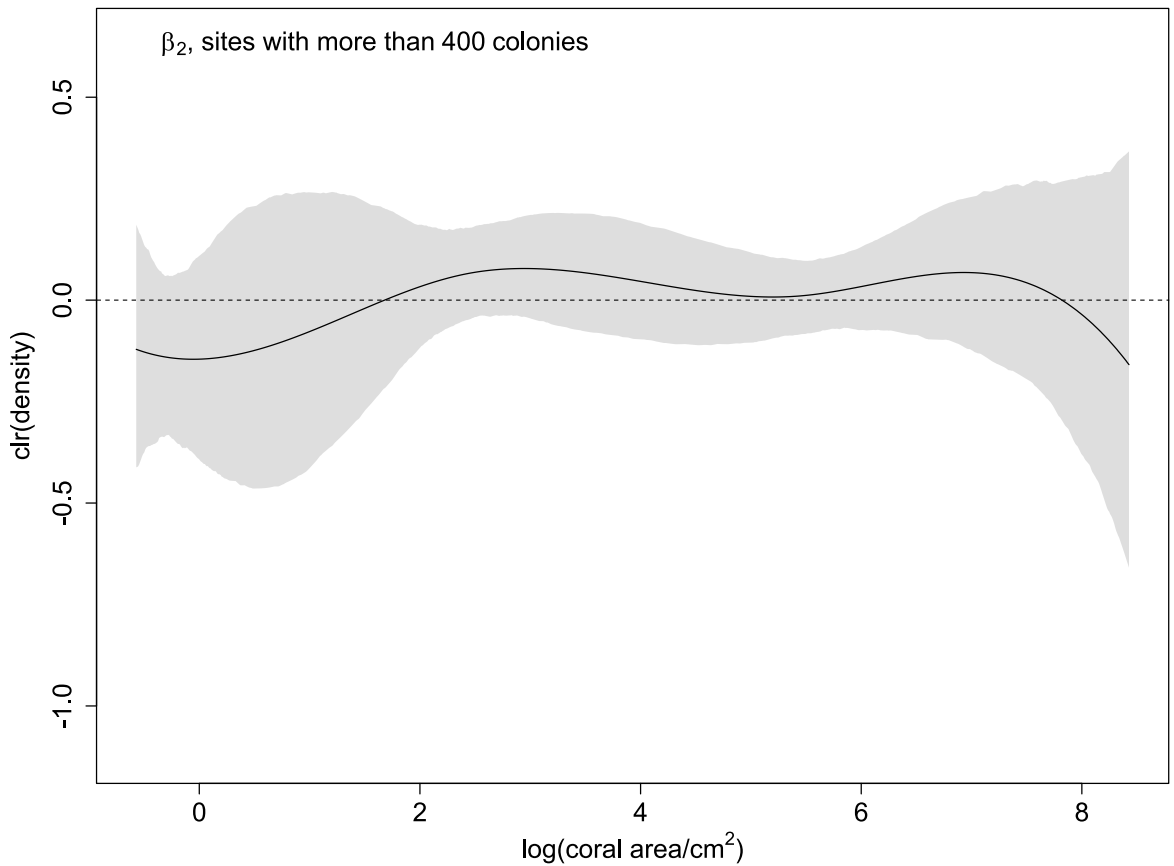


Figure A-18. Increases in second axis (PC2) scores might mean lower densities of corals at the extreme sizes but a higher density of corals $\sim 2-7 \log \text{cm}^2$, however no effect is plausible as the grey shaded region (bootstrap 95% confidence band) always crossed the dashed line (no effect on the probability densities). Increases in PC2 represent higher minimum chl_a and kd₄₉₀ and lower standard deviation of PAR. The black line is the estimated centred log-ratio (clr) transformation of the coefficient function β_2 , which measures the effect of a unit increase in PC2 on the probability density of a given log coral area. Positive values on the y-axis mean that the corresponding log coral area on the x-axis becomes more likely as PC2 increases, and negative values mean that the corresponding log coral area becomes less likely. Fitted to the twelve sites that had more than 400 coral colonies.

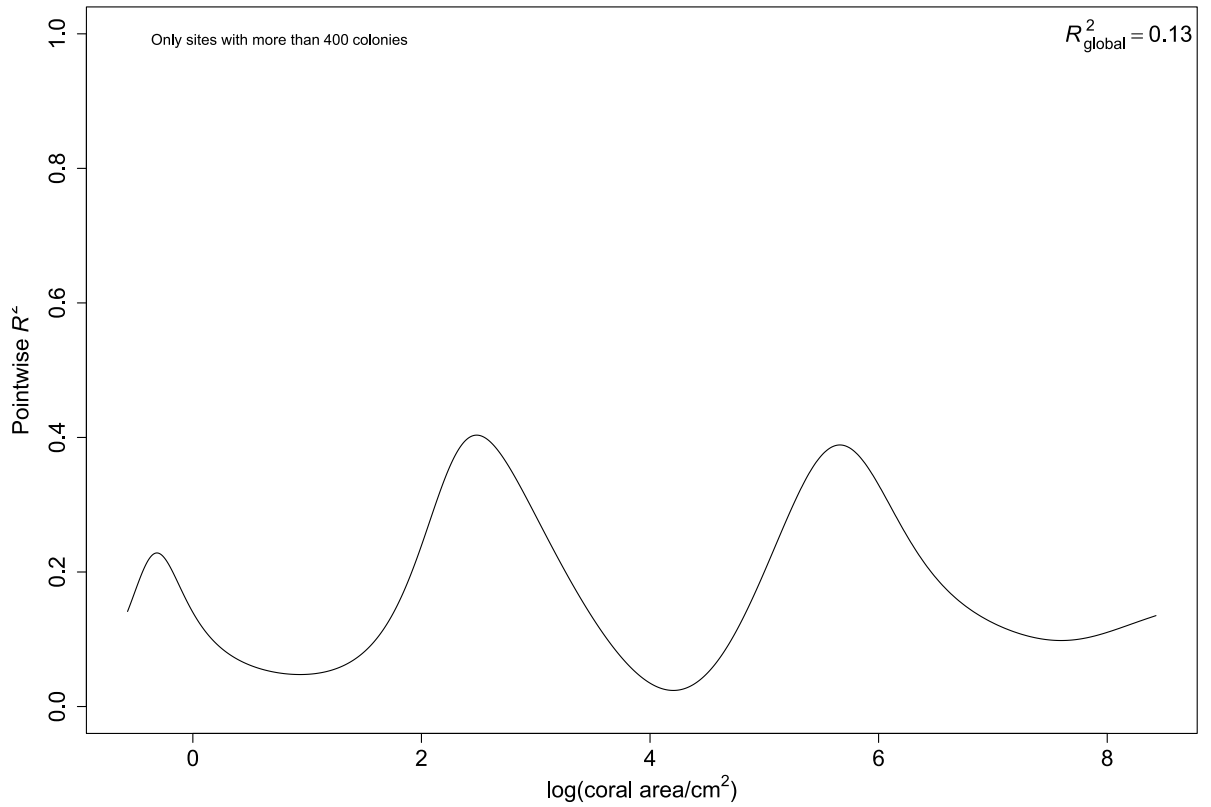


Figure A-19. The proportion of variation in probability density explained by the model (pointwise R^2) at each log coral area, with most explanatory power at approx. 3 and 6 log cm². Global R^2 (the total proportion of variation explained by the model) is 0.13.

S7: Model sensitivity to the 2016 bleaching event

To check whether the bleaching event of 2016 in Eastern Australia affected size distributions of our sites, we added a categorical explanatory variable, distinguishing sites visited before the 2016 bleaching event, and after it. North Rock and Julian Rock False Trench were visited in April and May 2016, during the period of peak heat stress in the region (Kim *et al.*, 2019). Since the effect of bleaching (if any) does not immediately reflect in population size structure changes, we have classified the data from these two sites as ‘pre’ bleaching (Table A-1).

In linear regression, adding the categorical bleaching variable (Table A-8) to the best model for each summary statistic improved the model fit (lowered AIC) and explained more variation (higher adjusted R^2) for median colony size (Table A-4) and coefficient of variation (Table A-6). Sites surveyed post 2016 bleaching had smaller median coral sizes ($F_{2,17} = 7.31$; $P = 0.005$, $R^2 = 0.399$; Figure A-20), and a higher CV ($F_{2,17} = 2.96$; $P = 0.0790$, $R^2 = 0.171$; Figure A-21). For number of coral colonies, the model not considering bleaching remained a better fit (Table A-3), but more of the variation was explained with the bleaching model (Table A-8). Adding bleaching did not improve the model fit nor variation explanation for skewness or kurtosis (Table A-5; Table A-7). Nonetheless, the bleaching variable was not a significant explanatory variable in any of the additional linear regressions (Table A-8).

In compositional functional regression, the coefficient function for the effect of being post-bleaching suggested that post-bleaching sites may have relatively more small corals (Figure A-25), while the other coefficient functions were fairly similar to the original versions (Figure A-22; Figure A-24) and the global R^2 increases to 0.23 (Figure A-26). However, the observed maximum pointwise F was almost unchanged, while the maximum 0.05-critical value was substantially higher, so that the permutation P -value increases from 0.08 to 0.20 (Figure A-27). This suggests that the increase in global R^2 was simply because of the presence of another explanatory variable, rather than because of any clear association between that variable and size distributions.

Table A-8. Linear regression with the bleaching explanatory variable added to the best models of the five summary statistics: 1) number of coral colonies, 2) median coral size, 3) skewness, 4) coefficient of variation (CV) and 5) kurtosis (Figure A-3Figure A-7). Median coral size and CV (bolded) have a lower AIC with the bleaching variable included. PC1 captures the differences in sea surface temperature, photosynthetically available radiation, high chlorophyll a concentration and turbidity (kd490). More positive PC2 scores mean higher minima of chlorophyll a concentration and kd490, but lower standard deviations of PAR. Values are corrected to three significant figures.

Model formula	Predictor	Estimate	Std. Error	t value	P value	Adjusted R ²	AIC (2 d.p.)
Coral count ~ PC1 + PC2 + bleaching	Intercept	445	170	2.62	0.0185	0.396	247.83
	PC1	-86.0	32.4	-2.65	0.0175		
	PC2	163	62.3	2.63	0.0182		
	Bleaching	256	210	1.21	0.243		
Median size ~ PC1 + bleaching	Intercept	4.25	0.145	29.3	< 0.001	0.399	-35.47
	PC1	0.0944	0.0278	3.40	0.00344		
	Bleaching	-0.302	0.180	-1.68	0.112		
Skewness ~ PC1 + PC2 + bleaching	Intercept	0.132	0.0599	2.21	0.0421	0.368	-70.19
	PC1	-0.0367	0.0114	-3.20	0.00554		
	PC2	0.0426	0.0219	1.94	0.0704		

	Bleachin g	0.00781	0.074 3	0.10 5	0.918		
CV ~ PC1 + bleachin g	Intercept	33.3	1.63	20.5	< 0.001	0.171	61.09
	PC1	-0.492	0.310	-1.58	0.132		
	Bleachin g	3.649	2.02	1.81	0.0880		
Kurtosis ~ PC1 + bleaching	Intercept	2.62	0.095 1	27.6	< 0.001	0.0561	-52.44
	PC1	-0.0284	0.018 2	-1.56	0.138		
	Bleachin g	0.0945	0.118	0.80 1	0.434		

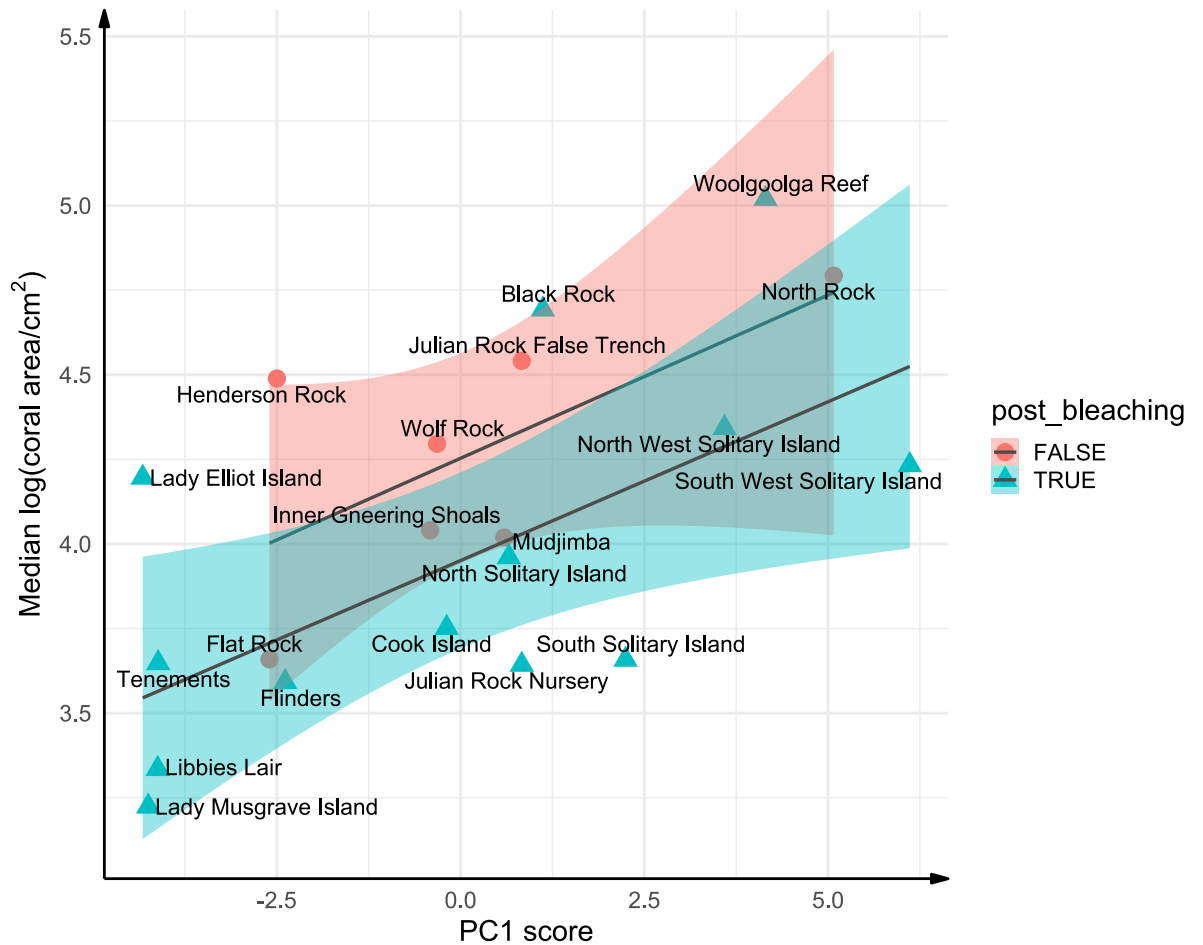


Figure A-20. Median coral colony size increases with PC1 and sites surveyed after the 2016 bleaching event tend to have smaller median sizes. PC1 is fitted as the explanatory variable here because of model selection (Table A-6). The sites were coloured based on whether it was surveyed after the 2016 bleaching event, light blue triangles for post-bleaching ('TRUE') and pink circles for pre-bleaching ('FALSE'). Black lines are the respectively lines of best fit, and the shaded regions are the 95% confidence bands. More positive PC1 scores represent lower sea surface temperature and photosynthetically available radiation (PAR), i.e., colder and darker, and high chlorophyll a concentration and turbidity (kd490), i.e., more productive and more turbid.

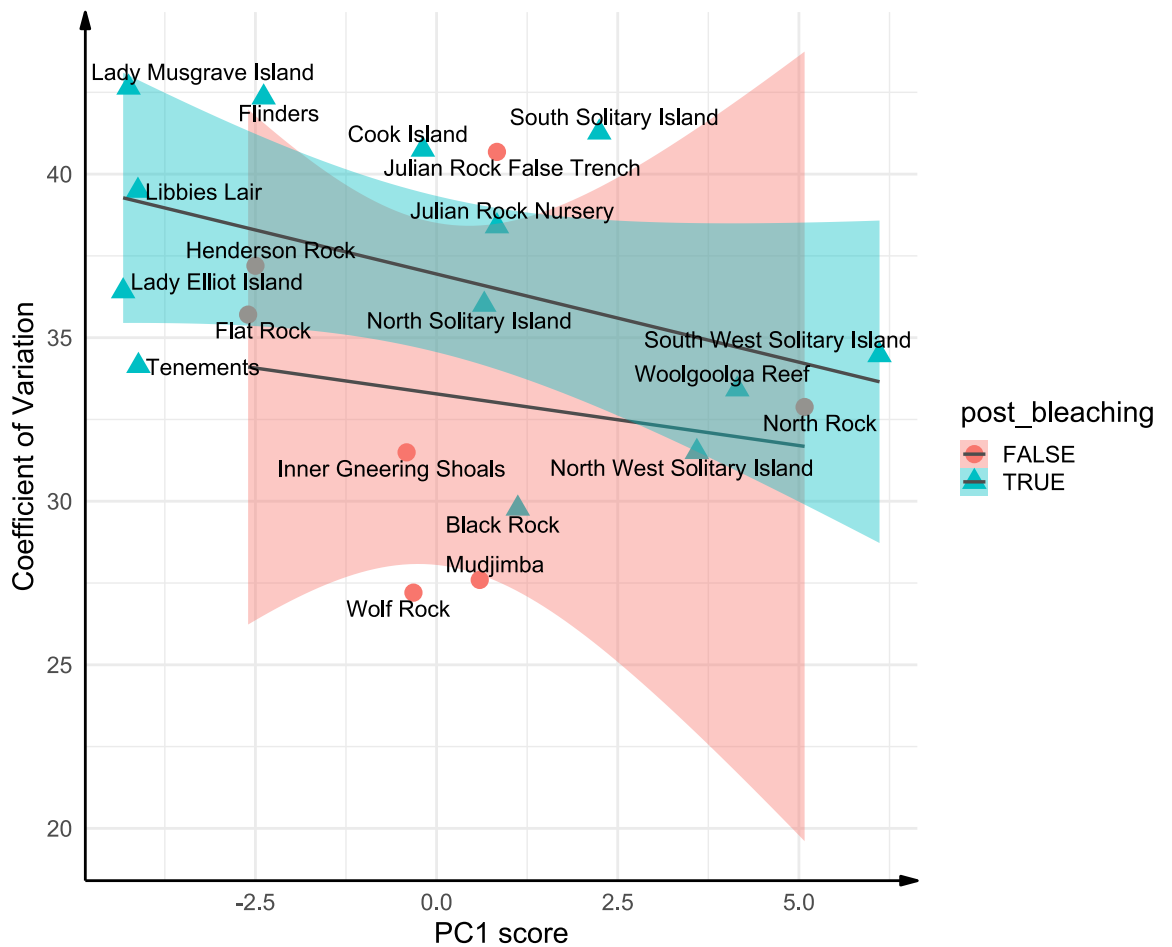


Figure A-21. The colony size coefficient of variation (CV) decreases with PC1. PC1 is fitted as the explanatory variable here because of model selection (Table A-6). The sites were coloured based on whether it was surveyed after the 2016 bleaching event, light blue triangles for post-bleaching ('TRUE') and pink circles for pre-bleaching ('FALSE'). Black lines are the respective line of best fit, and the shaded regions are the 95% confidence bands. More positive PC1 scores represent lower sea surface temperature and photosynthetically available radiation (PAR), i.e., colder and darker, and high chlorophyll a concentration and turbidity (kd490), i.e., more productive and more turbid.

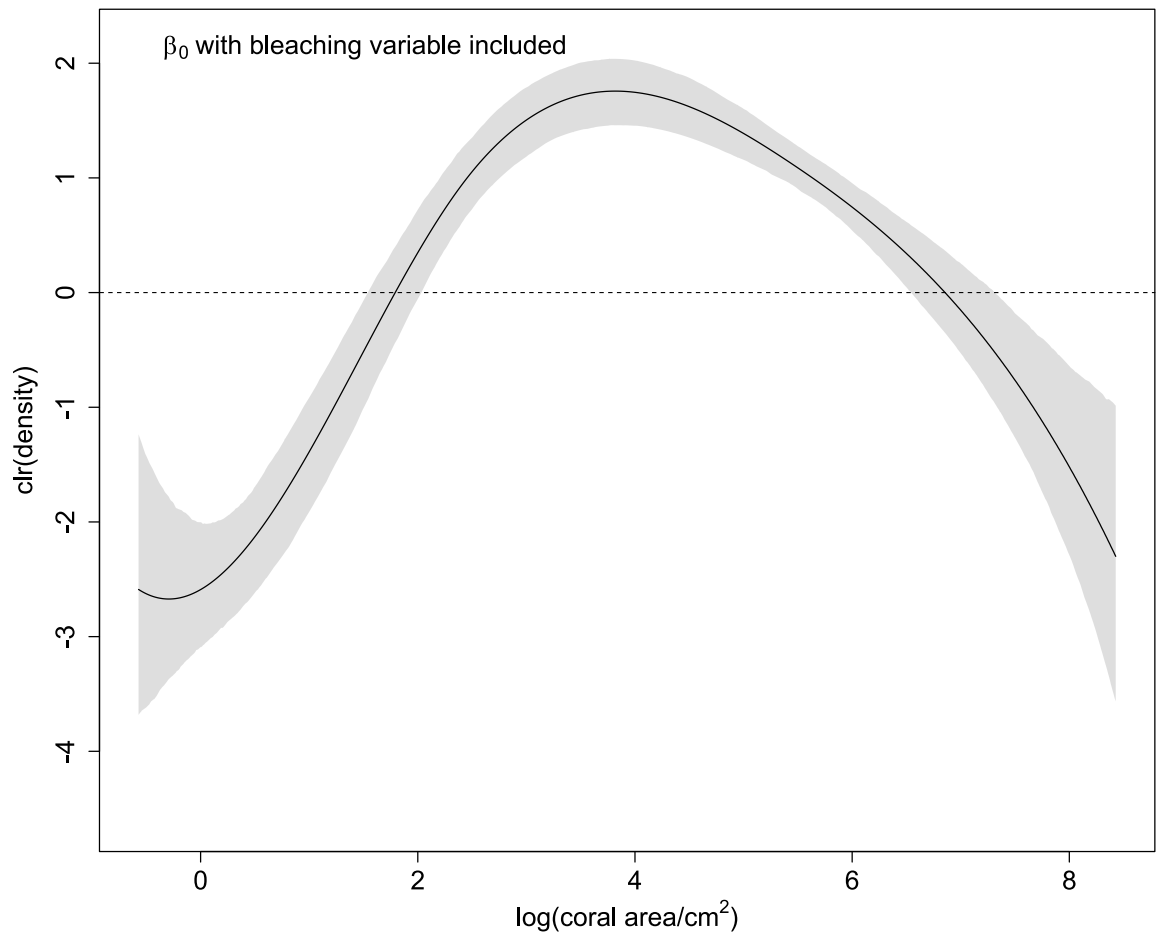


Figure A-22. When the mean values of PC1 and PC2 are both zero, the coral size-frequency distribution is symmetrical. The black line is the estimated centred log-ratio (clr) transformation of the coefficient function β_0 (the intercept), which is the prediction when PC1 and PC2 are both equal to zero. The grey shaded region is the bootstrap 95% confidence band. The horizontal dashed line represents no effect of the intercept on the probability density of log coral area.

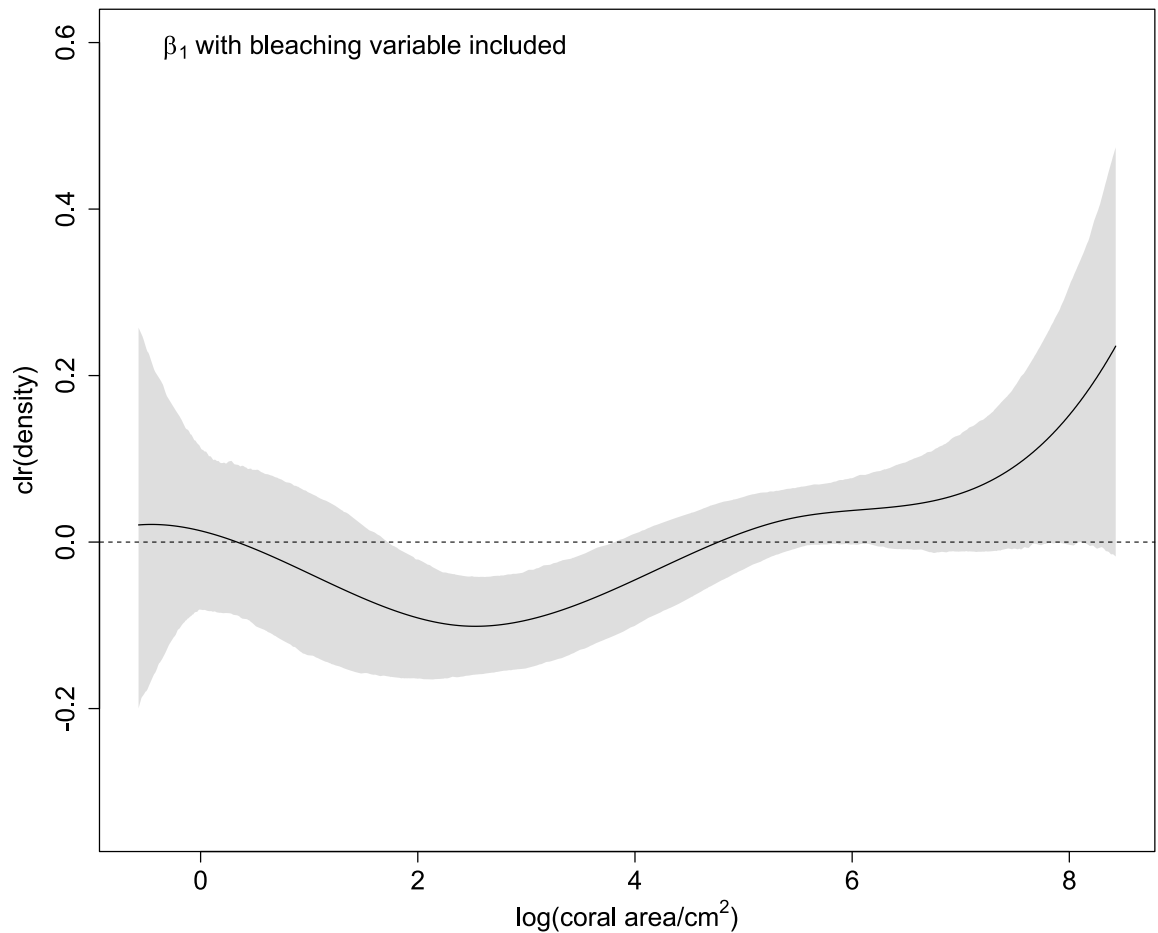


Figure A-23. Increases in first axis (PC1) scores mean lower densities of corals at $\sim 2-4 \log \text{cm}^2$. Increases in PC1 represents increasingly marginal conditions (colder, darker, more turbid and productive waters). The black line is the estimated centred log-ratio (clr) transformation of the coefficient function β_1 , which measures the effect of a unit increase in PC1 on the probability density of a given log coral area. Positive values on the y-axis suggest that the corresponding log coral area on the x-axis becomes more likely as PC1 increases, and negative values suggest that the corresponding log coral area becomes less likely. The shaded region is the bootstrap 95% confidence band. The horizontal dashed line represents no effect of PC1 on the probability density of log coral area.

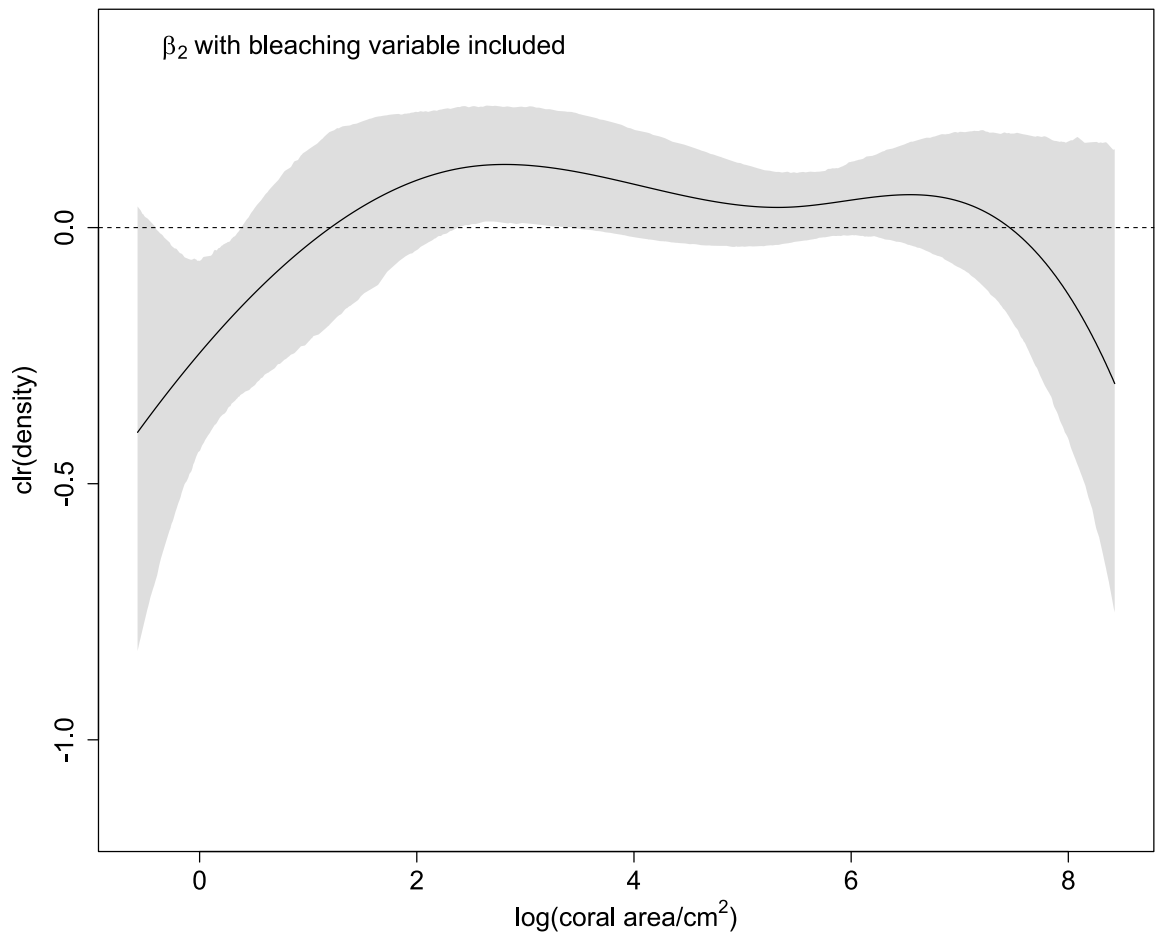


Figure A-24. Increases in second axis (PC2) scores might mean lower densities of corals at the extreme sizes but a higher density of corals $\sim 1-7 \log \text{cm}^2$, however no effect is plausible as the grey shaded region (bootstrap 95% confidence band) almost always crossed the dashed line (no effect on the probability densities), except for $\sim 3 \log \text{cm}^2$. Increases in PC2 represent higher minimum chl_a and kd₄₉₀ and lower standard deviation of PAR. The black line is the estimated centred log-ratio (clr) transformation of the coefficient function β_2 , which measures the effect of a unit increase in PC2 on the probability density of a given log coral area. Positive values on the y-axis mean that the corresponding log coral area on the x-axis becomes more likely as PC2 increases, and negative values mean that the corresponding log coral area becomes less likely.

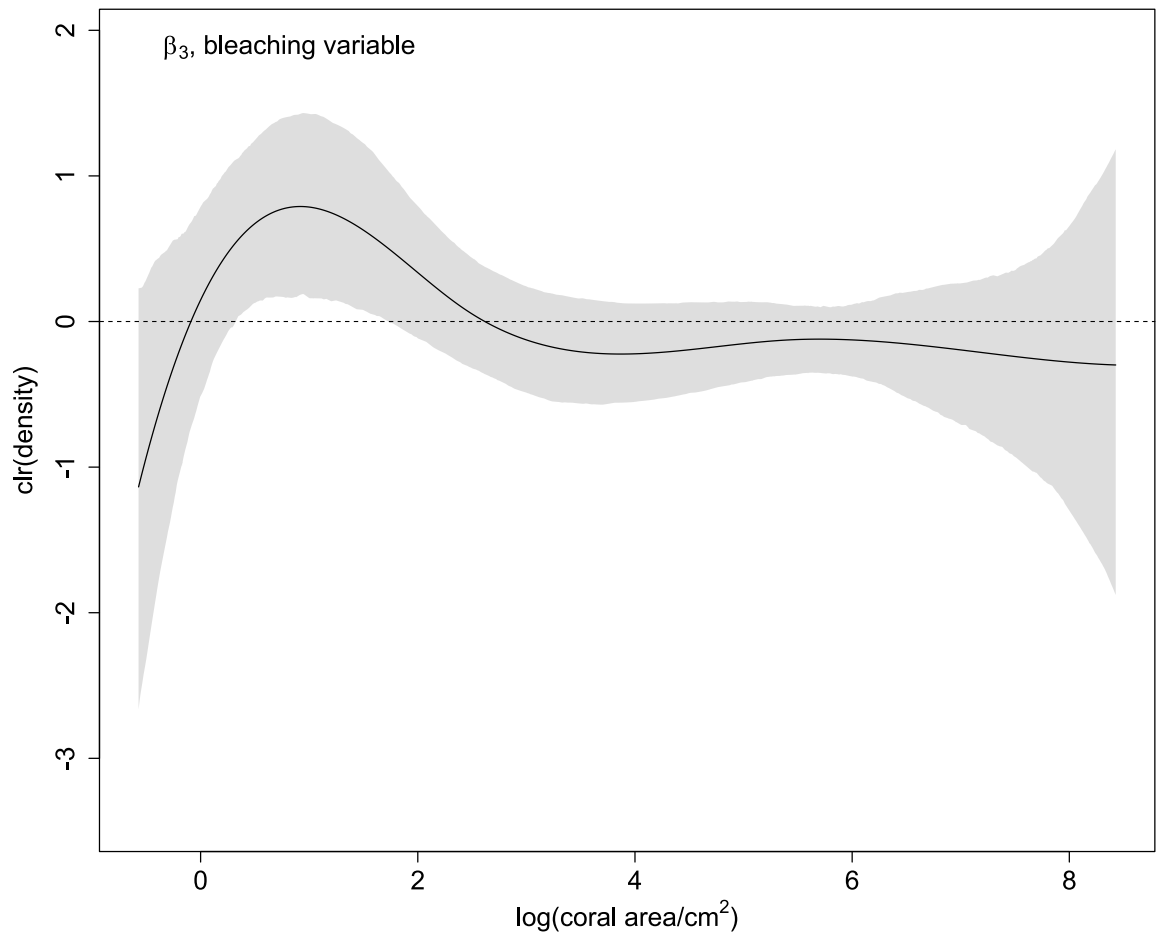


Figure A-25. Bleaching might lead to higher densities of smaller corals at ~ 0-2 cm². The black line is the estimated centre log-ratio (clr) transformation of the bleaching coefficient function β_3 , which measures the effect of pre or post bleaching on the probability density of a given log area. Positive values on the y-axis mean that the corresponding log coral area on the x-axis becomes more likely because of bleaching, and negative values mean that the corresponding log coral area becomes less likely.

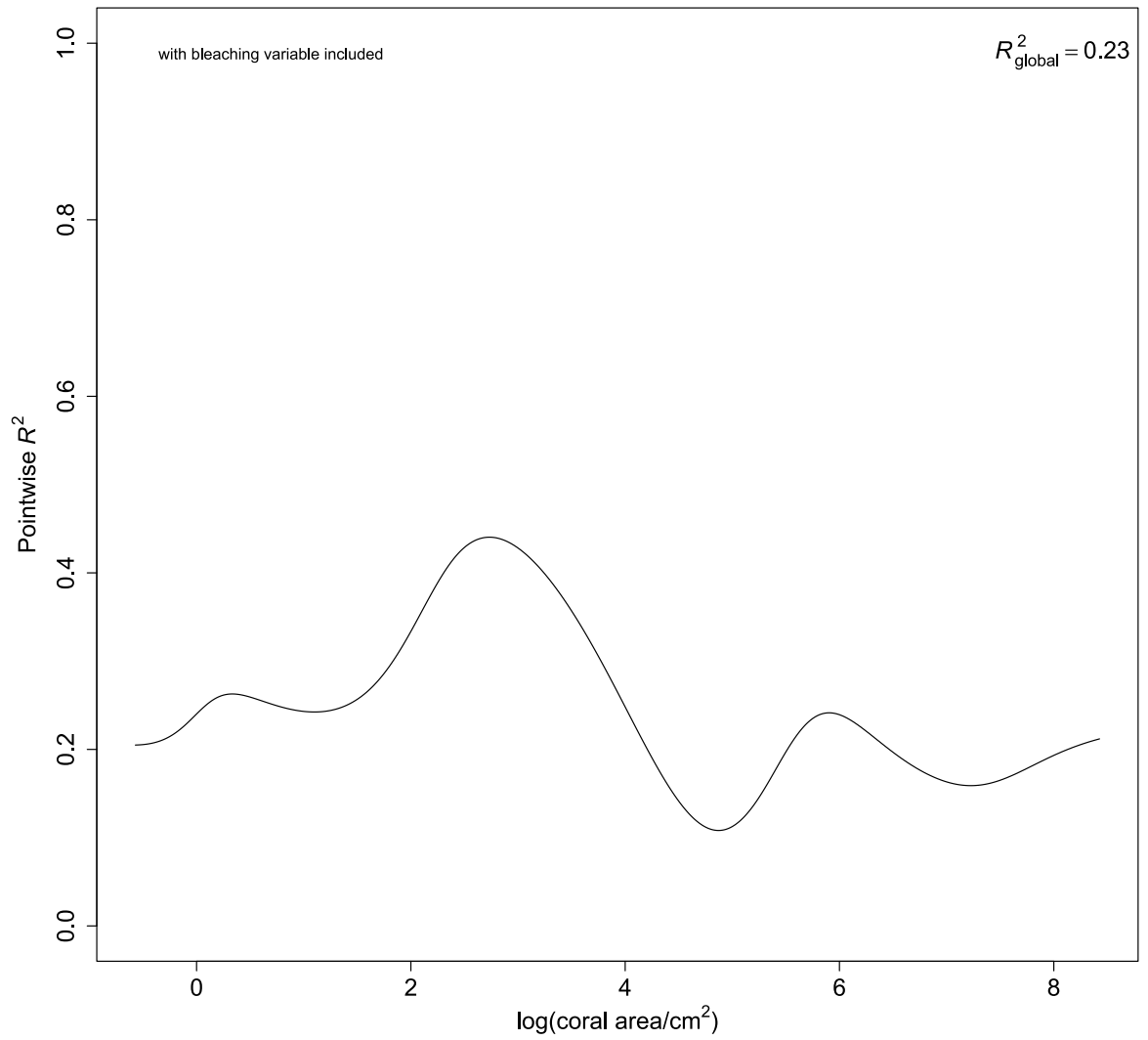


Figure A-26. The proportion of variation in probability density explained by the bleaching model (pointwise R^2) at each log coral area, with most explanatory power at approx. 3 log cm². Global R^2 (the total proportion of variation explained by the model) is 0.23.

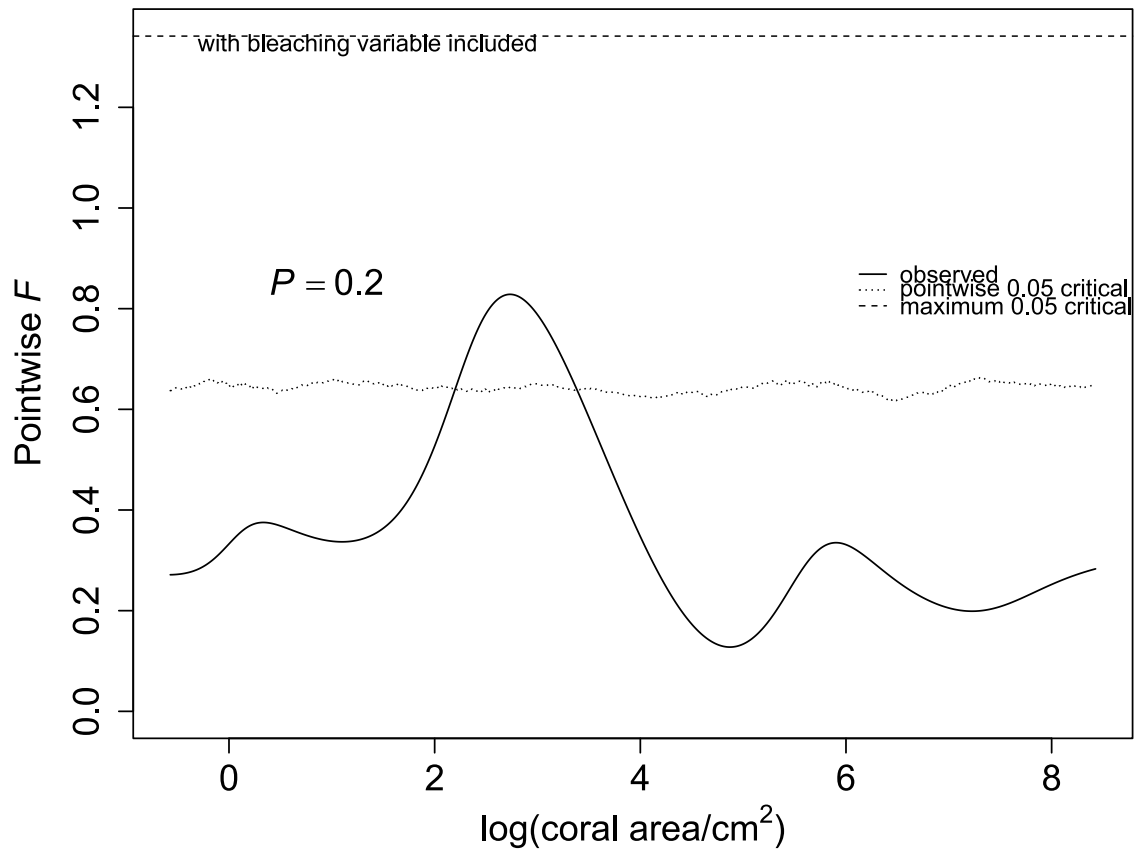


Figure A-27. Permutation F test for the predictive relationship between log coral area and the PC scores (PC1 and PC2) and the bleaching explanatory variable. The observed F statistic (solid line) is highest at 3 log cm², suggesting that PC1, PC2 and the bleaching variable had the most effect there. However, because the observed F statistic did not cross the maxima (dashed line) anywhere in the distribution, it was plausible that neither of the explanatory variables affected coral size-frequency distributions. Dotted line: pointwise 0.05 critical values such that only one permuted F statistic in 20 exceeds this value at a given log coral area. Dashed line: maximum 0.05 critical value such that only one permuted F statistic in 20 exceeds this value at any log coral area. Functional F-test, maximum F = observed maximum F = 0.83, P = 0.2 from 9,999 permutations.

References

- Baddeley, A. J. (1998a). A crash course in stochastic geometry. In O. E. Barndorff-Nielsen, W. S. Kendall, & M. N. M. van Lieshout (Eds.), *Stochastic Geometry: Likelihood and Computation* (1st ed.). Routledge. <https://doi.org/https://doi.org/10.1201/9780203738276>
- Baddeley, A. J. (1998b). Spatial sampling and censoring. In O. E. Barndorff-Nielsen, W. S. Kendall, & M. N. M. van Lieshout (Eds.), *Stochastic Geometry: Likelihood and Computation* (1st ed.). Routledge. <https://doi.org/https://doi.org/10.1201/9780203738276>
- Egozcue, J. J., Díaz-Barrero, J. L., & Pawlowsky-Glahn, V. (2006). Hilbert Space of Probability Density Functions Based on Aitchison Geometry. *Acta Mathematica Sinica, English Series*, 22(4), 1175-1182. <https://doi.org/10.1007/s10114-005-0678-2>
- Egozcue, J. J., Pawlowsky-Glahn, V., Tolosana-Delgado, R., Ortego, M. I., & Van Den Boogaart, K. G. (2013). Bayes spaces: use of improper distributions and exponential families. *Revista de la Real Academia de Ciencias Exactas, Físicas y Naturales. Serie A. Matemáticas*, 107(2), 475-486. <https://doi.org/10.1007/s13398-012-0082-6>
- Gross, K., & Edmunds, P. J. (2015). Stability of Caribbean coral communities quantified by long-term monitoring and autoregression models. *Ecology*, 96(7), 1812-1822. <https://doi.org/10.1890/14-0941.1>
- Judson, T. W. (2019). *Abstract algebra: theory and applications* (2019 ed.). Orthogonal Publishing Inc.
- Kim, S. W., Sampayo, E. M., Sommer, B., Sims, C. A., Gómez-Cabrera, M. d. C., Dalton, S. J., Beger, M., Malcolm, H. A., Ferrari, R., Fraser, N., Figueira, W. F., Smith, S. D. A., Heron, S. F., Baird, A. H., Byrne, M., Eakin, C. M., Edgar, R., Hughes, T. P., Kyriacou, N., Liu, G., Matis, P. A., Skirving, W. J., & Pandolfi, J. M. (2019). Refugia under threat: Mass bleaching of coral assemblages in high-latitude eastern Australia. *Global Change Biology*, 25(11), 3918-3931. <https://doi.org/https://doi.org/10.1111/gcb.14772>
- Machalová, J., Talská, R., Hron, K., & Gába, A. (2021). Compositional splines for representation of density functions. *Computational Statistics*, 36(2), 1031-1064. <https://doi.org/10.1007/s00180-020-01042-7>
- Oksanen, J., Blanchet, F. G., Friendly, M., Kindt, R., Legendre, P., McGlinn, D., Minchin, P. R., O'Hara, R. B., Simpson, G. L., Sólymos, P., Stevens, M. H. H., Szoecs, E., & Wagner, H. (2020). *vegan: Community Ecology Package*. In (Version 2.5-7) <https://CRAN.R-project.org/package=vegan>
- Talská, R., Menafoglio, A., Machalová, J., Hron, K., & Fišerová, E. (2018). Compositional regression with functional response. *Computational Statistics & Data Analysis*, 123, 66-85. <https://doi.org/https://doi.org/10.1016/j.csda.2018.01.018>
- Vercelloni, J., Lique, B., Kennedy, E. V., González-Rivero, M., Caley, M. J., Peterson, E. E., Puotinen, M., Hoegh-Guldberg, O., & Mengersen, K. (2020). Forecasting intensifying disturbance effects on coral reefs. *Global Change Biology*, 26(5), 2785-2797. <https://doi.org/10.1111/gcb.15059>

Appendix B: Supporting information for Chapter 3

S1: Supplementary information

Table B-1. GPS coordinates and survey dates of the 20 sites. Sites are ordered from the lowest to the highest first principal component (PC1) scores of the PCA of means, maxima, minima and standard deviations of sea surface temperature (SST), photosynthetically available radiation (PAR), chlorophyll a concentration and kd490 (diffuse attenuation coefficient at 490 nm, a proxy for turbidity) (Chong et al., 2023). Increasing PC1 scores represent lower SST and PAR, i.e., colder and darker, and high chlorophyll a concentration and kd490, i.e., more productive and more turbid waters.

	Site	Latitude (°)	Longitude (°)	Sampling date (dd/mm/yyyy)	PC1 scores
1	Lady Elliot Island	- 24.11500	152.7095	27/09/2018	-4.325
2	Lady Musgrave Island	- 23.90603	152.3870	26/09/2018	-4.250
3	Libbies Lair	- 23.43458	151.9336	23/09/2018	-4.121
4	Tenements	- 23.43274	151.9293	24/09/2018	-4.114
5	Flat Rock	- 27.39306	153.5522	15/08/2010	-2.600
6	Henderson Rock	- 27.13161	153.4781	18/03/2011	-2.499
7	Flinders Reef	- 26.97765	153.4841	18/09/2018	-2.386
8	Inner Gneering Shoals	- 26.64858	153.1834	29/08/2012	-0.413

9	Wolf Rock	- 25.91667	153.2000	09/08/2010	-0.319
10	Cook Island	- 28.19627	153.5763	07/09/2018	-0.189
11	Mudjimba	- 26.61614	153.1130	28/08/2012	0.595
12	North Solitary Island	- 29.92772	153.3896	11/09/2018	0.658
13	Julian Rock False Trench	- 28.61257	153.6286	31/05/2016	0.833
14	Julian Rock Nursery	- 28.61087	153.6281	14/09/2018	0.833
15	Black Rock	- 30.94837	153.0761	10/09/2018	1.121
16	South Solitary Island	- 30.20478	153.2652	13/09/2018	2.245
17	North West Solitary Island	- 30.01897	153.2697	12/09/2018	3.592
18	Woolgoolga Reef	- 30.09374	153.2056	19/10/2016	4.150
19	North Rock	- 29.97339	153.2572	16/04/2016	5.078
20	South West Solitary Island	- 30.15921	153.2281	09/09/2018	6.112

Table B-2. Statistical summaries of coral size-frequency distribution at the twenty reefs. All areas are in log cm². Numbers are rounded to three decimal places where appropriate. Sites are ordered from the lowest to the highest first principal component (PC1) scores (Chong *et al.*, 2023) of the PCA of means, maxima, minima and standard deviations of sea surface temperature (SST), photosynthetically available radiation (PAR), chlorophyll a concentration and kd490 (diffuse attenuation coefficient at 490 nm, a proxy for turbidity). Increasing PC1 scores represent lower SST and PAR, *i.e.*, colder and darker, and high chlorophyll a concentration and kd490, *i.e.*, more productive and more turbid.

Site	Number of images sampled	Number of coral colonies	Mean coral area	Median coral area	Standard deviation of coral area	Coefficient of variation (CV)	Skewness	Kurtosis	PC1 scores
Lady Elliot Island	63	449	4.374	4.196	1.593	36.42	0.302	2.385	-4.325
Lady Musgrave Island	78	2101	3.379	3.224	1.441	42.646	0.434	2.776	-4.250
Libbies Lair	77	1757	3.469	3.335	1.37	39.493	0.421	2.967	-4.121
Tenements	66	1117	3.814	3.648	1.302	34.137	0.499	3.023	-4.114
Flat Rock	82	705	3.711	3.659	1.325	35.705	0.171	2.724	-2.600
Henderson Rock	30	56	4.683	4.489	1.742	37.198	0.243	2.521	-2.499

Flinders	72	448	3.599	3.592	1.524	42.345	0.076	2.521	-2.386
Inner Gneering Shoals	90	1310	4.131	4.04	1.301	31.494	0.211	2.729	-0.413
Wolf Rock	51	224	4.216	4.296	1.147	27.206	-0.016	2.721	-0.319
Cook Island	69	258	3.794	3.752	1.546	40.749	-0.273	3.094	-0.189
Mudjimba	90	641	4.008	4.019	1.106	27.595	0.068	3.044	0.595
North Solitary Island	88	670	3.988	3.961	1.436	36.008	0.057	2.897	0.658
Julian Rock False Trench	49	92	4.624	4.541	1.881	40.679	0.14	2.303	0.833
Julian Rock Nursery	55	166	3.588	3.643	1.378	38.406	0.215	3.018	0.833
Black Rock	41	59	4.695	4.693	1.398	29.776	0.004	2.481	1.121
South Solitary Island	90	757	3.661	3.658	1.511	41.273	0.15	2.696	2.245
North West Solitary Island	88	602	4.475	4.343	1.41	31.508	0.102	2.647	3.592
Woolgoolga Reef	21	38	4.949	5.02	1.654	33.421	-0.281	2.361	4.150

North Rock	33	76	4.857	4.793	1.597	32.88	0.096	2.308	5.078
South West Solitary Island	88	698	4.294	4.233	1.48	34.467	0.127	2.496	6.112

Table B-3. Statistical summaries of fish abundances and sizes at the twenty reefs. Standard deviation, skewness and kurtosis of fish data were calculated from the log-transformed biomass (kg). Numbers are rounded to three decimal places where appropriate. Sites are ordered from the lowest to the highest PC1 scores as in Table B-1 and Table B-2.

Site	Number of fishes	Mean fish length (cm)	Mean fish biomass (kg)	Median fish biomass (kg)	Mean log fish biomass (kg)	Median log fish biomass (kg)	Standard deviation of log fish biomass (kg)	Skewness	Kurtosis
Lady Elliot Island	2941	9.57	0.115	0.006	-4.753	-5.063	2.192	-0.084	4.31
Lady Musgrave Island	1605	11.297	0.067	0.028	-4.309	-3.568	2.169	-0.387	2.12
Libbies Lair	1299	9.176	0.132	0.006	-4.797	-5.063	1.842	0.916	4.092
Tenements	2416	12.301	0.21	0.004	-4.486	-5.427	2.434	0.837	2.605

Flat Rock	1057	16.497	0.217	0.06	-3.1	-2.806	2.079	-0.353	2.506
Henderson Rock	912	19.09	1.058	0.083	-3.157	-2.486	2.992	-0.377	2.293
Flinders	2151	14.79	0.182	0.026	-3.302	-3.666	1.914	-0.099	2.882
Inner Gneering Shoals	2481	12.922	0.114	0.028	-3.35	-3.581	1.377	0.398	3.344
Wolf Rock	720	18.865	0.32	0.06	-2.927	-2.81	2.36	-0.249	1.892
Cook Island	1362	9.82	0.074	0.003	-4.976	-5.744	2.3	0.457	1.887
Mudjimba	623	15.345	0.138	0.047	-3.06	-3.053	1.672	-0.601	4.015
North Solitary Island	1293	18.428	0.365	0.073	-2.541	-2.622	1.836	-0.934	4.34
Julian Rock False Trench	790	24.737	1.007	0.32	-1.717	-1.139	2.09	-0.851	3.291
Julian Rock Nursery	1240	14.838	0.247	0.035	-3.57	-3.362	1.963	-0.807	4.637
Black Rock	1264	9.348	0.127	0	-7.229	-10.82	4.338	0.505	1.45
South Solitary Island	767	10.4	0.067	0.021	-4.367	-3.864	2.138	-0.208	1.888

North West Solitary Island	2343	11.82	0.234	0.004	-4.601	-5.488	2.386	0.851	2.712
Woolgoolga Reef	222	15.216	0.176	0.073	-3.397	-2.624	2.185	-0.487	2.165
North Rock	585	12.487	0.079	0.027	-3.937	-3.599	1.829	-0.092	2.353
South West Solitary Island	1842	15.163	0.161	0.048	-3.353	-3.031	2.119	-0.219	1.893

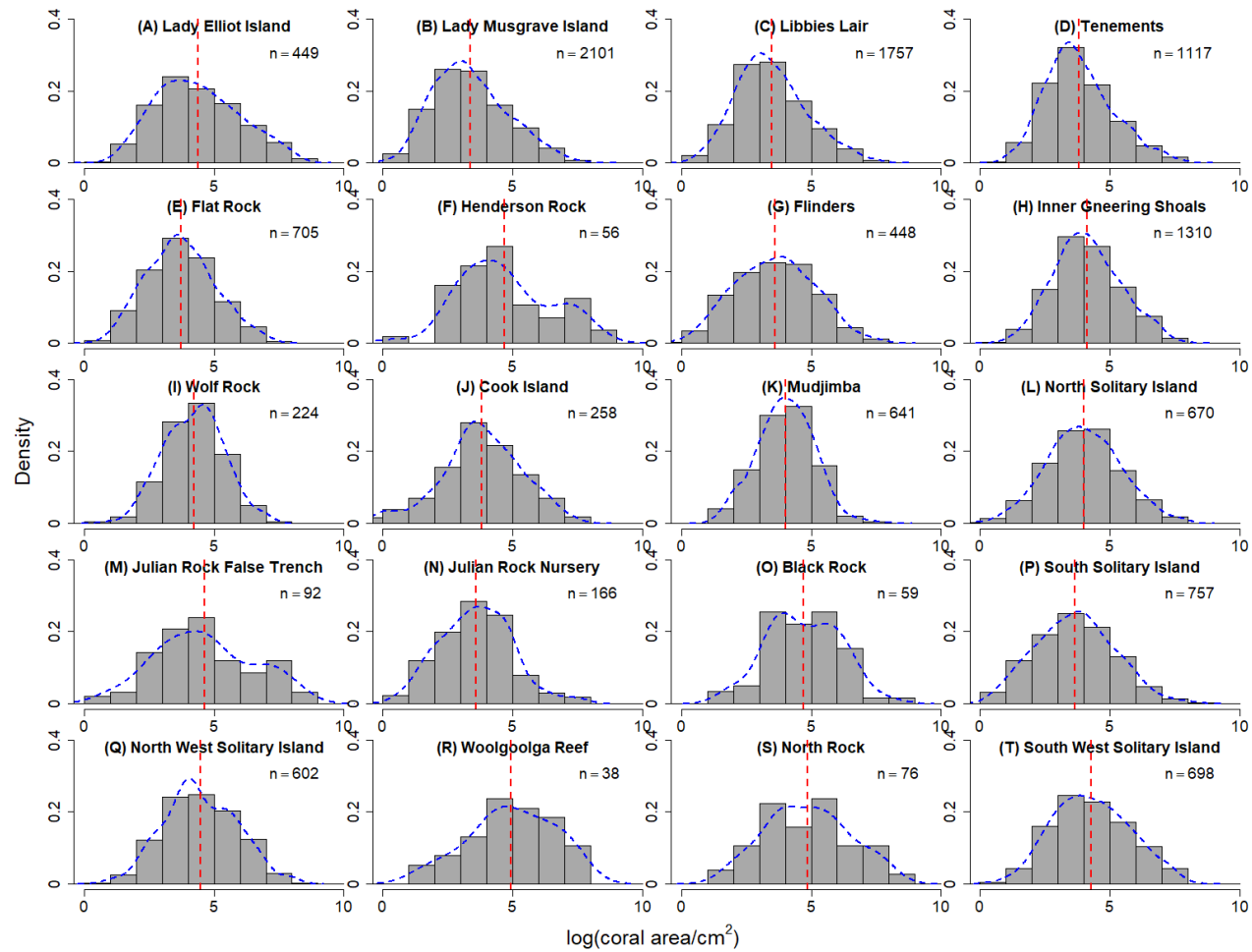


Figure B-1. Histograms showing the size frequency distribution of log-transformed coral area. Blue dashed lines are kernel density estimates, red dashed lines are site-wise mean log coral area. The number of corals sampled from each site is indicated by “n”. Sites are ordered by PC1 scores as on Table B-1.

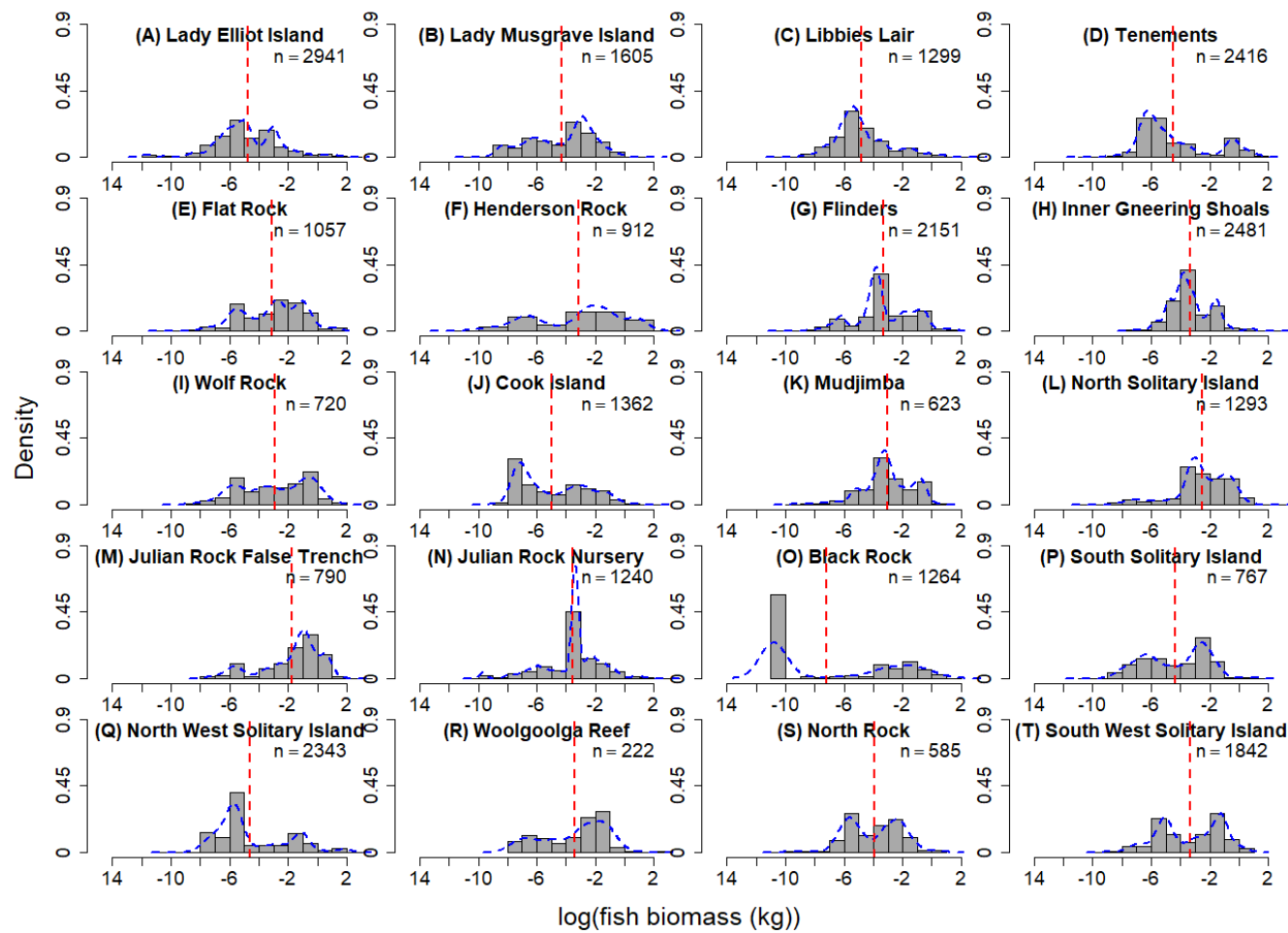


Figure B-2. Histograms showing the size frequency distribution of log-transformed fish biomass (kg). Blue dashed lines are kernel density estimates, red dashed lines are site-wise mean fish biomass (kg). The total number of fish counted from each site are indicated by “n=”. Sites are ordered by PC1 scores as on Table B-1.

The largest coral (assumed to be circular, indicated by the blue circle in Figure B-3) that can fit entirely in the frame of width w and height v , has a radius of $\frac{v}{2}$, and an area of $\pi \left(\frac{v}{2}\right)^2 = \frac{\pi}{4}v^2$. Let the area of a coral with radius r (indicated by the red circle in Figure B-3) be x . Then

$$\pi r^2 = x$$

$$r = \sqrt{\frac{x}{\pi}}$$

$$2r = 2\sqrt{\frac{x}{\pi}}$$

The diameter ($2r$) of the coral, $2\sqrt{\frac{x}{\pi}}$, is also the side length of the smallest square (blue outlines) that contains the entire coral.

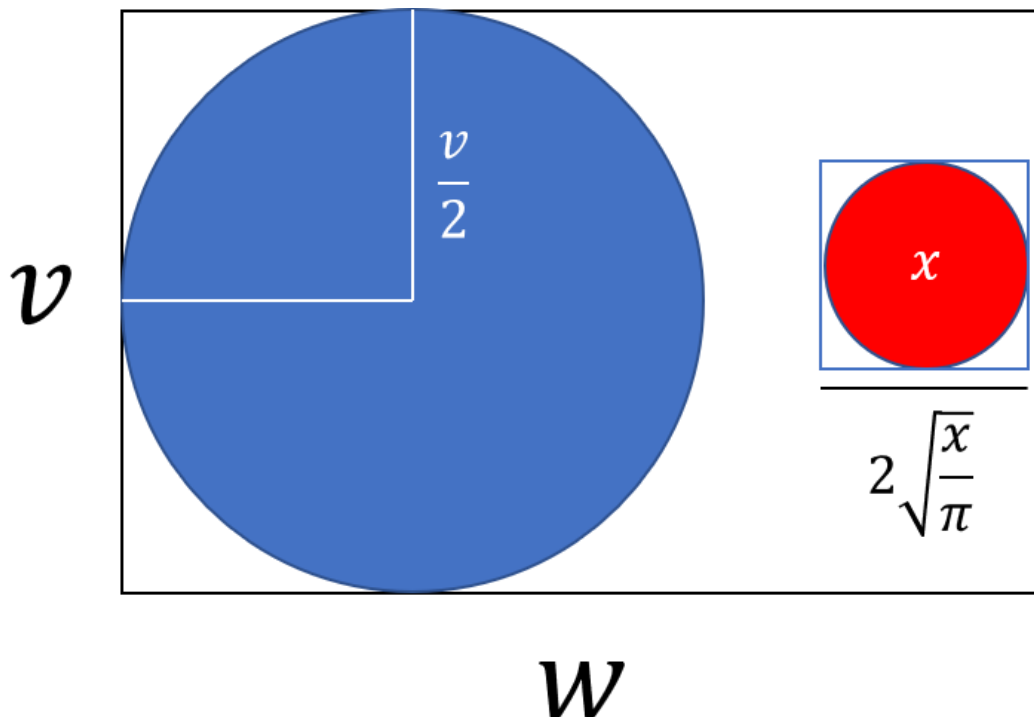


Figure B-3. Schematic showing the largest circular coral (blue circle) that could fit entirely within a rectangular frame of area $v \times w$. The red circle demonstrates how for

a given circular coral with area x , its diameter is $2\sqrt{\frac{x}{\pi}}$ and can be used to calculate the probability of the coral fitting entirely within the frame (Equation 6 in the main text).

Table B-4. Maximum likelihood estimates of the log-normal and minus-sampled log normal coral size standard deviation $\hat{\sigma}$. Sites are ordered from the lowest to the highest PC1 scores as in Table B-1.

Site	Log-normal $\hat{\sigma}$	Minus-sampled log-normal $\hat{\sigma}$
Lady Elliot Island	1.59	1.92
Lady Musgrave Island	1.44	1.54
Libbies Lair	1.37	1.45
Tenements	1.30	1.39
Flat Rock	1.32	1.41
Henderson Rock	1.73	2.39
Flinders	1.52	1.67
Inner Gneering Shoals	1.30	1.41
Wolf Rock	1.14	1.22
Cook Island	1.54	1.72
Mudjimba	1.11	1.16
North Solitary Island	1.43	1.59
Julian Rock False Trench	1.87	2.79
Julian Rock Nursery	1.37	1.47
Black Rock	1.39	1.63
South Solitary Island	1.51	1.66
North West Solitary Island	1.41	1.62
Woolgoolga Reef	1.63	2.31
North Rock	1.59	2.12
South West Solitary Island	1.48	1.70

S2: Probability density function for the minus-sampled bounded power law

From Equation 8 in the main text, the conditional density in the minus-sampled bounded power law for $x_{min} \leq x < x_{mw}$, where $x_{mw} = \frac{\pi}{4}v^2$, is given by

$$f(x|\theta) = \frac{\mathbb{P}(\theta|x)f(x)}{\int \mathbb{P}(\theta|x)f(x)dx}$$

$$\begin{aligned}
&= \frac{\left(w - 2\sqrt{\frac{x}{\pi}}\right)\left(v - 2\sqrt{\frac{x}{\pi}}\right)}{wv} Cx^b && \text{(from Equations 1 and 6)} \\
&= \frac{\int_{x_{min}}^{x_{mw}} \left(w - 2\sqrt{\frac{x}{\pi}}\right)\left(v - 2\sqrt{\frac{x}{\pi}}\right) Cx^b dx}{wv} \\
&= \frac{\int_{x_{min}}^{x_{mw}} \left(w - 2\sqrt{\frac{x}{\pi}}\right)\left(v - 2\sqrt{\frac{x}{\pi}}\right) x^b dx}{wv} \\
&= \frac{\frac{4}{\pi}x^{b+1} - \frac{2(w+v)}{\sqrt{\pi}}x^{b+1/2} + wvx^b}{d^+ - d^-},
\end{aligned}$$

where

$$d^+ = \begin{cases} \frac{wv}{b+1}x_{mw}^{b+1} - \frac{2(w+v)}{\sqrt{\pi}(b+\frac{3}{2})}x_{mw}^{b+\frac{3}{2}} + \frac{4}{\pi}\log(x_{mw}), & \text{if } b = -2, \\ \frac{wv}{b+1}x_{mw}^{b+1} - \frac{2(w+v)}{\sqrt{\pi}}\log x_{mw} + \frac{4}{\pi(b+2)}x_{mw}^{b+2}, & \text{if } b = -\frac{3}{2}, \\ wv\log x_{mw} - \frac{2(w+v)}{\sqrt{\pi}(b+\frac{3}{2})}x_{mw}^{b+\frac{3}{2}} + \frac{4}{\pi(b+2)}x_{mw}^{b+2}, & \text{if } b = -1, \\ \frac{wv}{b+1}x^{b+1} - \frac{2(w+v)}{\sqrt{\pi}(b+\frac{3}{2})}x^{b+\frac{3}{2}} + \frac{4}{\pi(b+2)}x^{b+2}, & \text{otherwise,} \end{cases}$$

and

$$d^- = \begin{cases} \frac{wv}{b+1}x_{min}^{b+1} - \frac{2(w+v)}{\sqrt{\pi}(b+\frac{3}{2})}x_{min}^{b+\frac{3}{2}} + \frac{4}{\pi}\log x_{min}, & \text{if } b = -2, \\ \frac{wv}{b+1}x_{min}^{b+1} - \frac{2(w+v)}{\sqrt{\pi}}\log x_{min} + \frac{4}{\pi(b+2)}x_{min}^{b+2}, & \text{if } b = -\frac{3}{2}, \\ wv\log x_{min} - \frac{2(w+v)}{\sqrt{\pi}(b+\frac{3}{2})}x_{min}^{b+\frac{3}{2}} + \frac{4}{\pi(b+2)}x_{min}^{b+2}, & \text{if } b = -1, \\ \frac{wv}{b+1}x_{min}^{b+1} - \frac{2(w+v)}{\sqrt{\pi}(b+\frac{3}{2})}x_{min}^{b+\frac{3}{2}} + \frac{4}{\pi(b+2)}x_{min}^{b+2}, & \text{otherwise.} \end{cases}$$

S3: Quantile-quantile plots of coral data for all sites

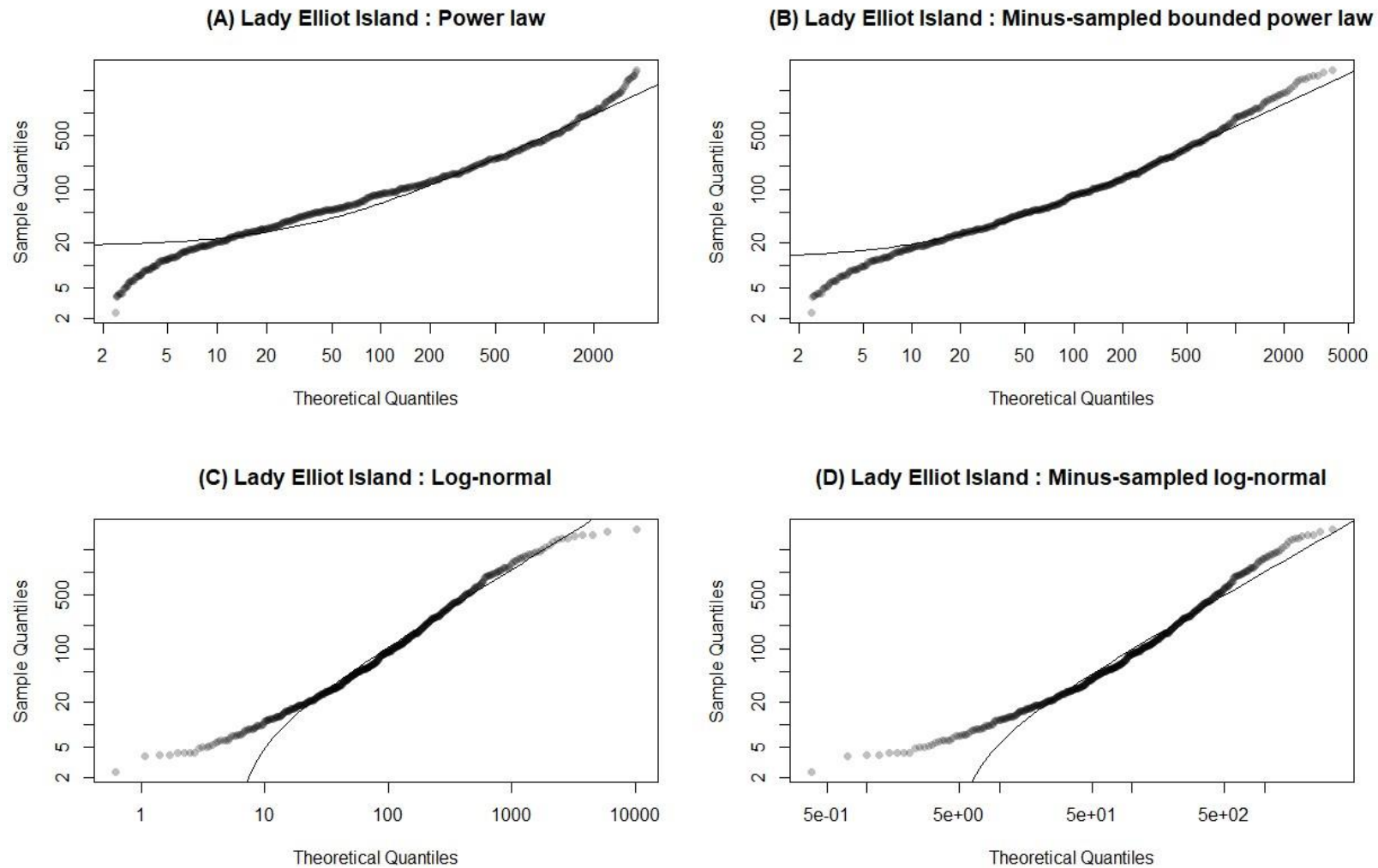


Figure B-4. Lady Elliot Island coral quantile-quantile (Q-Q) plots with the four distributions: (A) bounded power law (B) minus-sampled bounded power law; (C) log-normal; (D) minus-sampled log-normal. The axes of the Q-Q plots are in log scale.

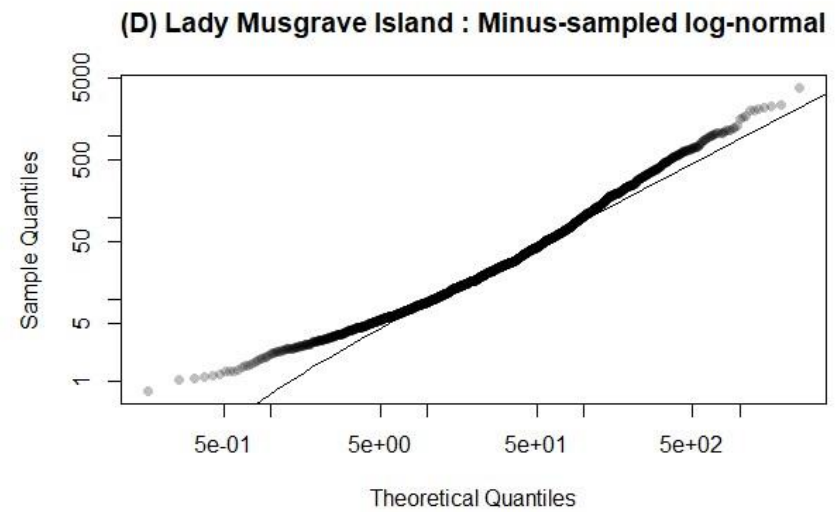
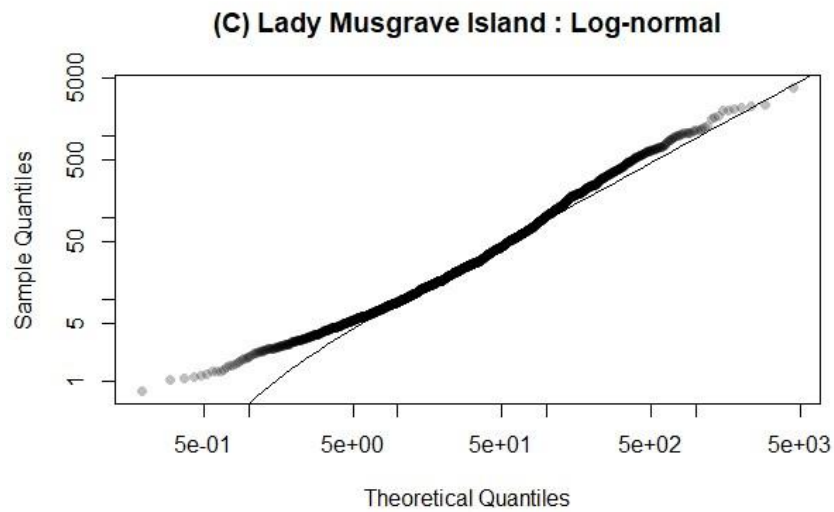
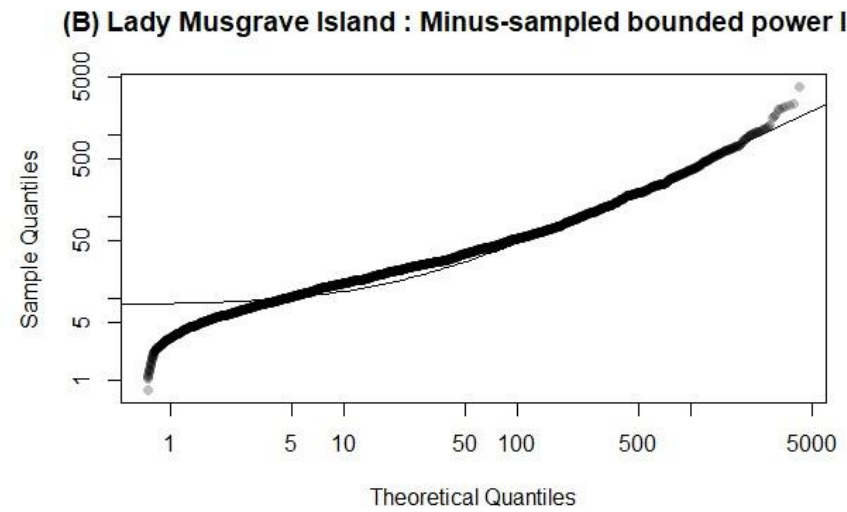
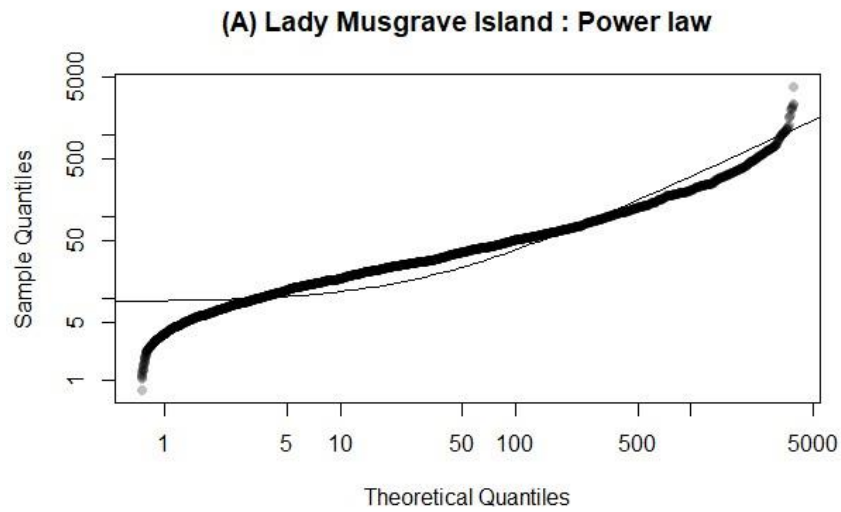


Figure B-5. Lady Musgrave Island coral quantile-quantile (Q-Q) plots with the four distributions: (A) bounded power law (B) minus-sampled bounded power law; (C) log-normal; (D) minus-sampled log-normal. The axes of the Q-Q plots are in log scale.

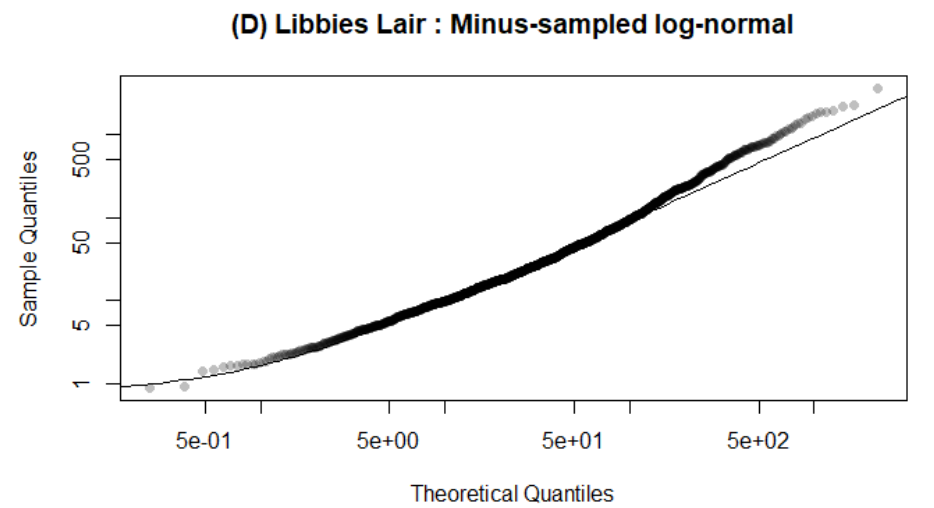
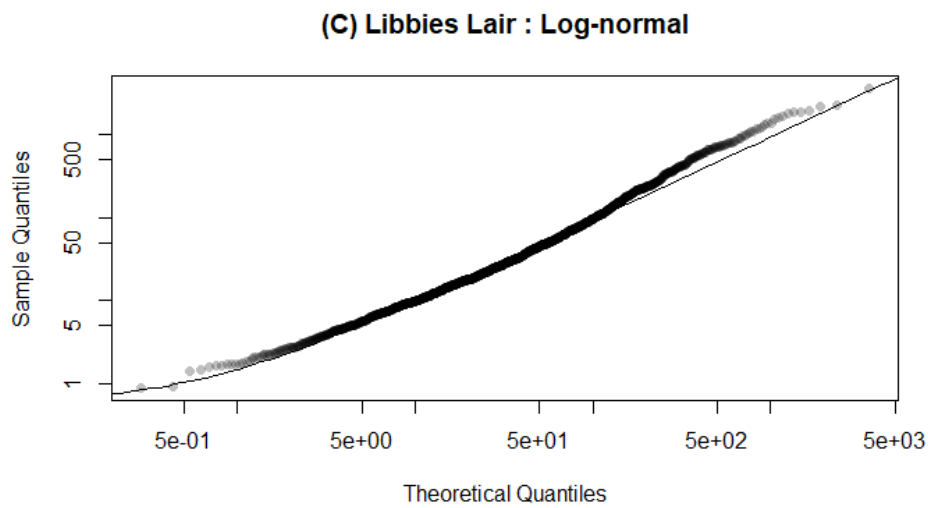
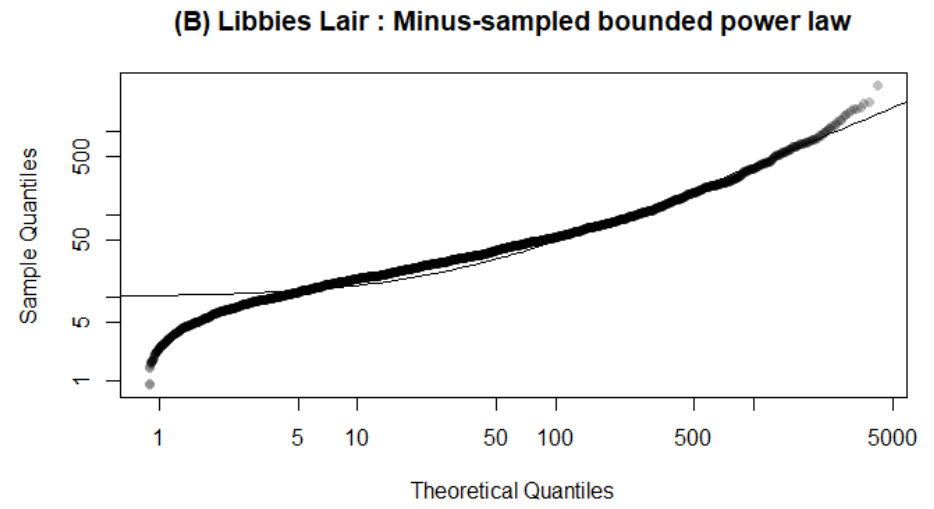
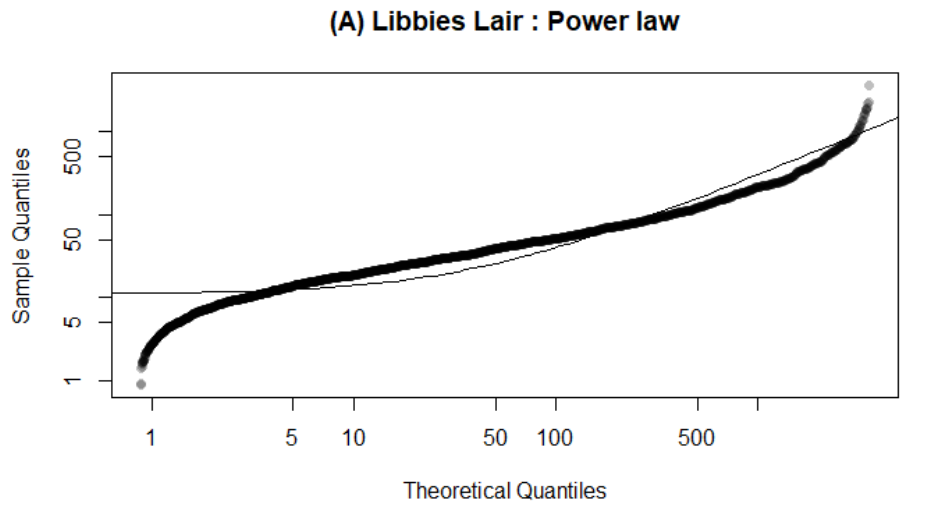


Figure B-6. Libbies Lair coral quantile-quantile (Q-Q) plots with the four distributions: (A) bounded power law (B) minus-sampled bounded power law; (C) log-normal; (D) minus-sampled log-normal. The axes of the Q-Q plots are in log scale.

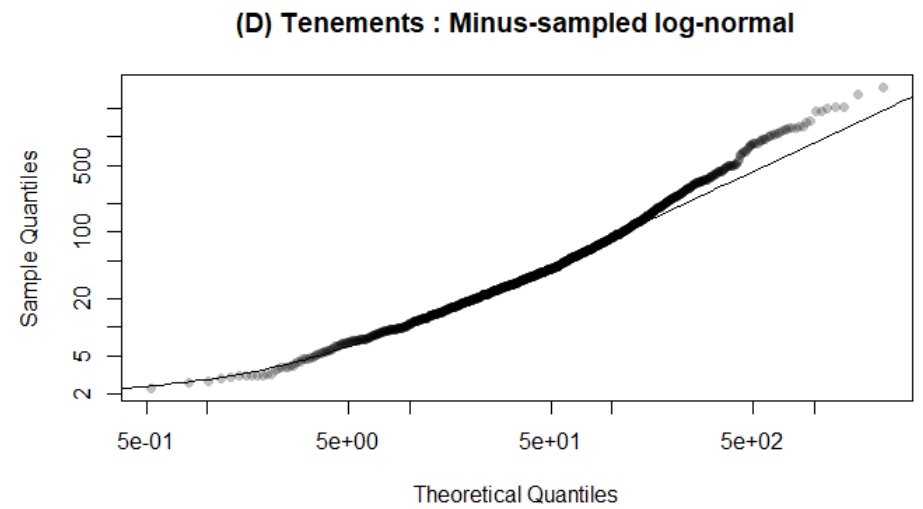
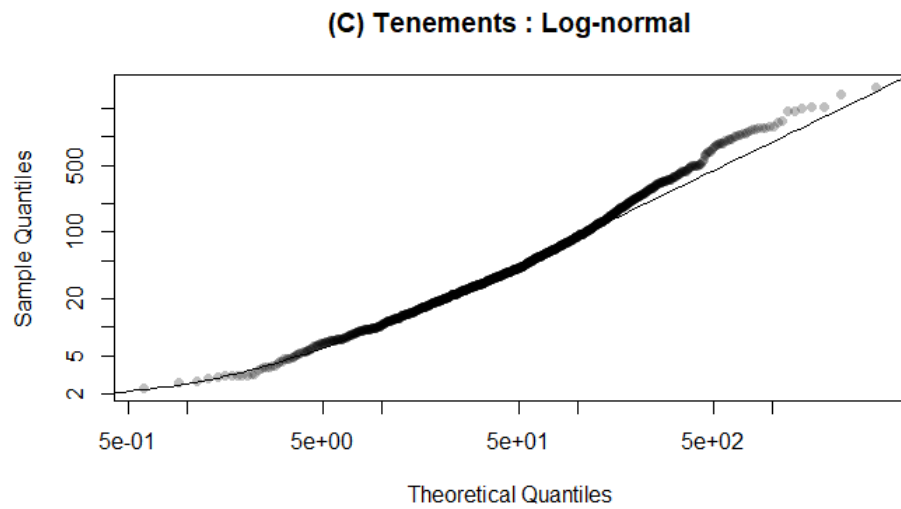
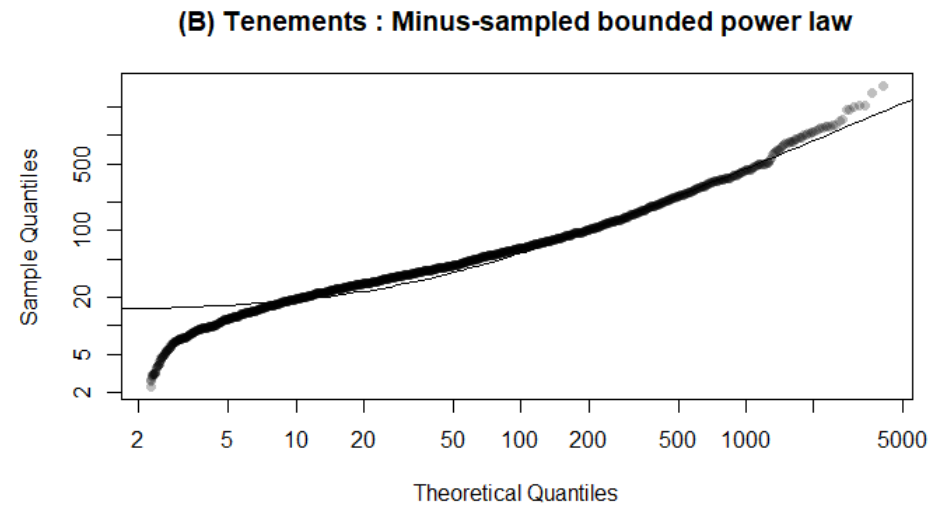
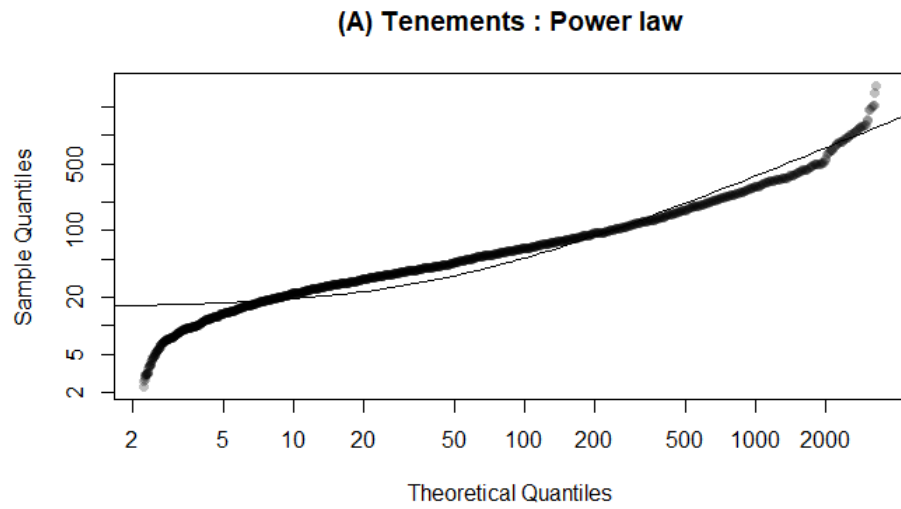


Figure B-7. Tenements coral quantile-quantile (Q-Q) plots with the four distributions: (A) bounded power law (B) minus-sampled bounded power law; (C) log-normal; (D) minus-sampled log-normal. The axes of the Q-Q plots are in log scale.

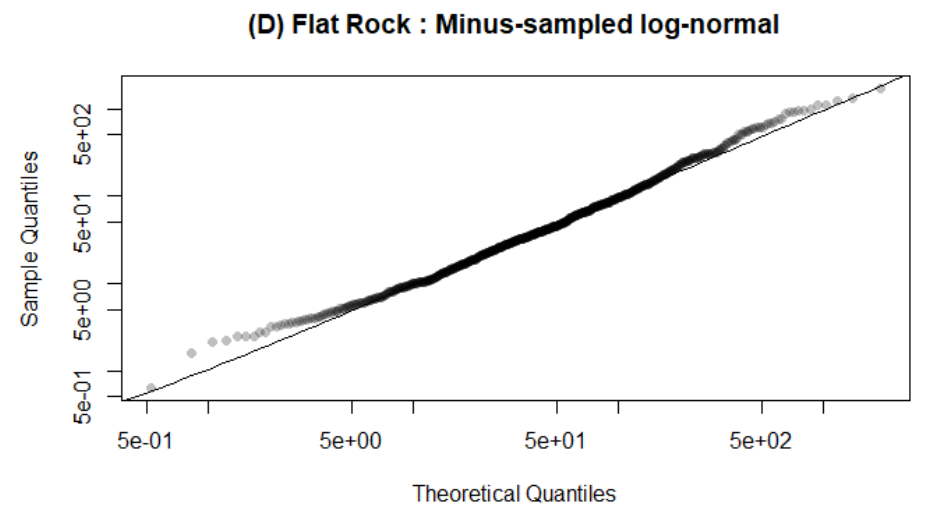
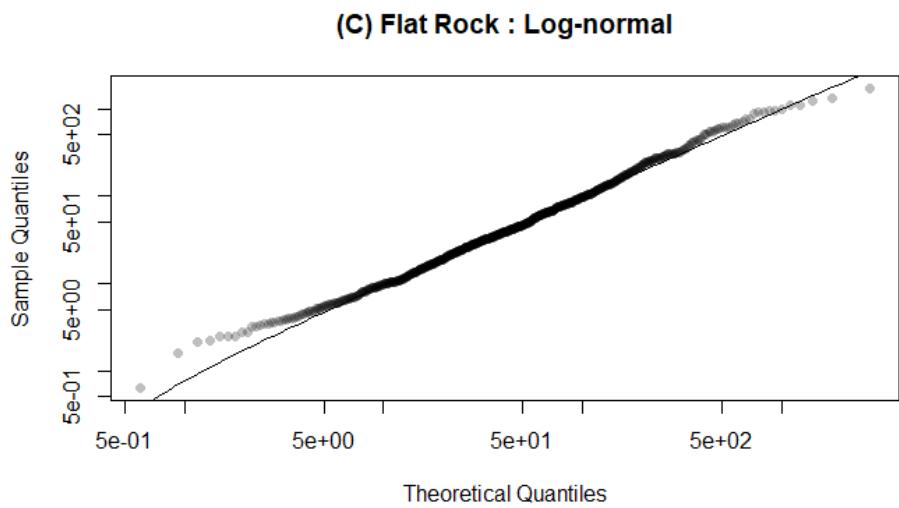
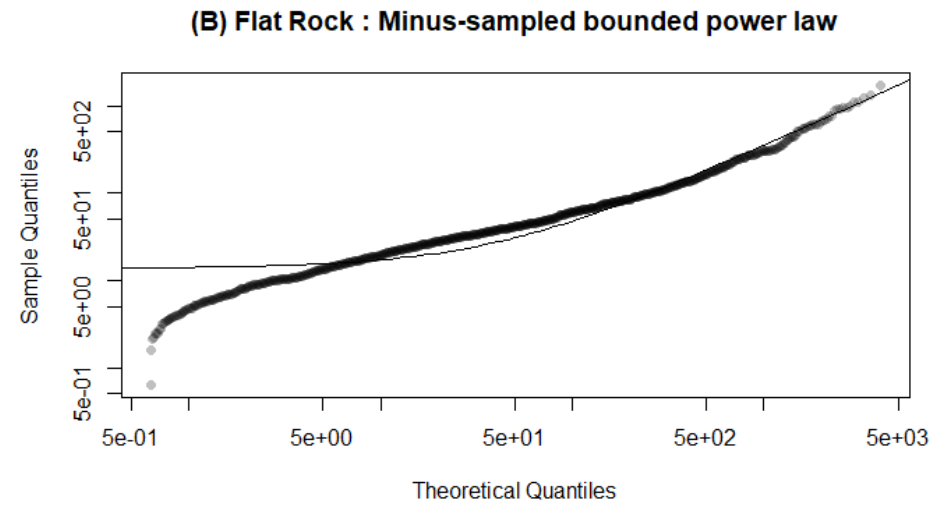
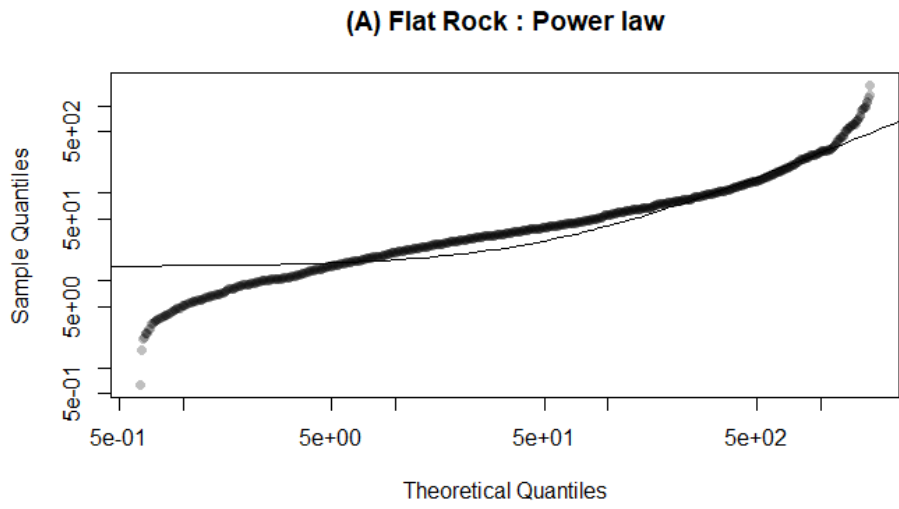


Figure B-8. Flat Rock coral quantile-quantile (Q-Q) plots with the four distributions: (A) bounded power law (B) minus-sampled bounded power law; (C) log-normal; (D) minus-sampled log-normal. The axes of the Q-Q plots are in log scale.

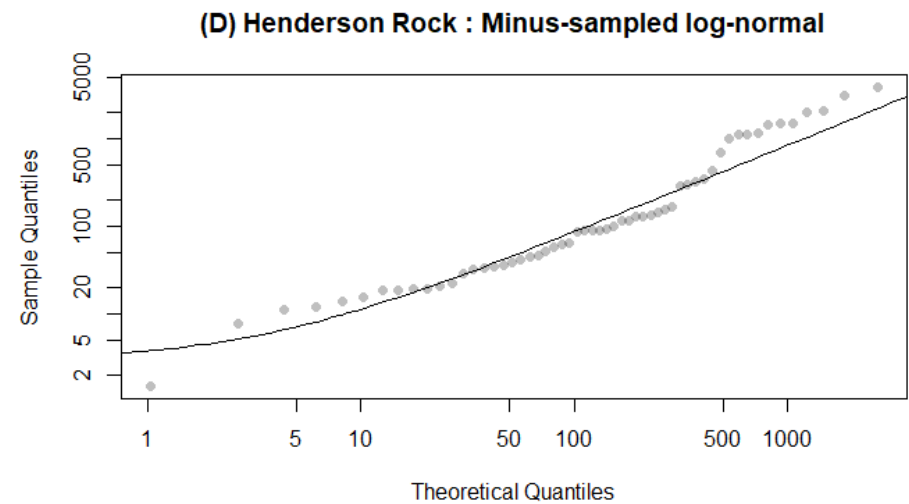
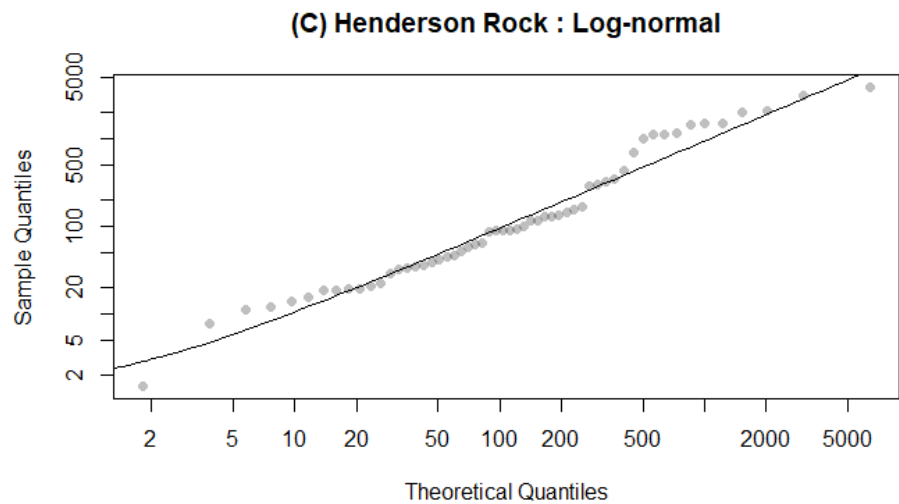
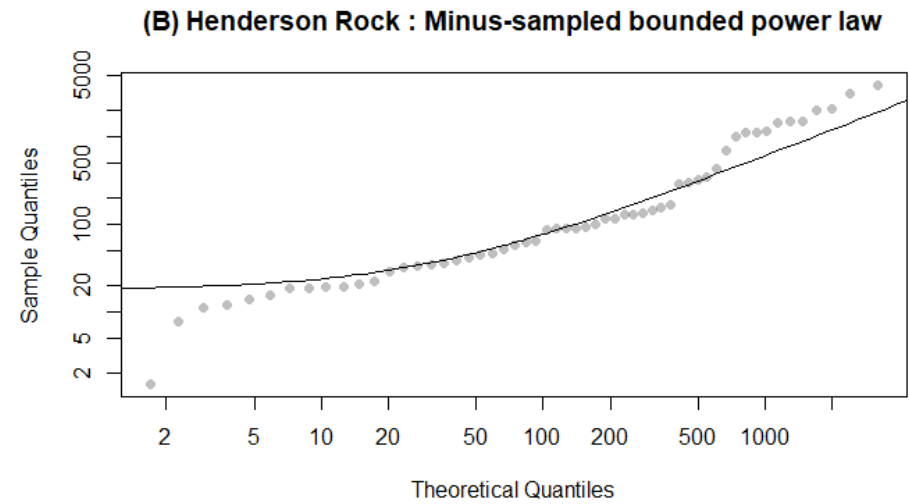
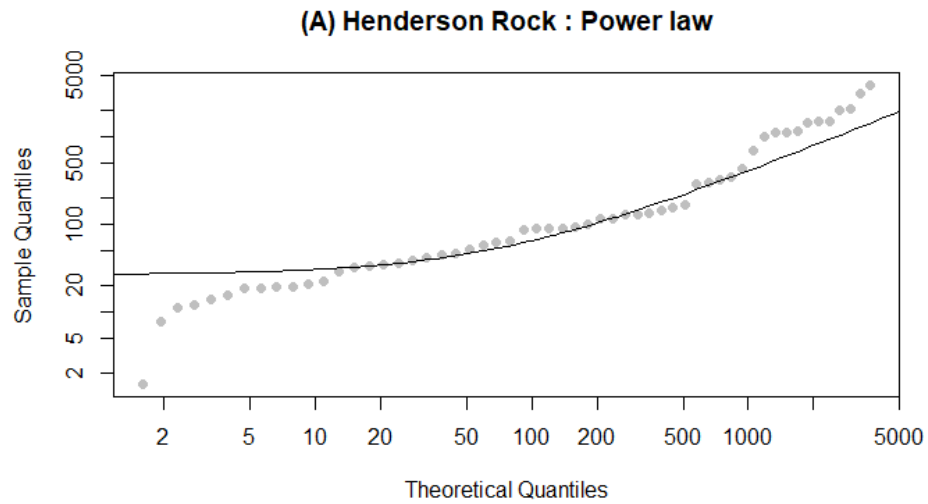


Figure B-9. Henderson Rock coral quantile-quantile (Q-Q) plots with the four distributions: (A) bounded power law (B) minus-sampled bounded power law; (C) log-normal; (D) minus-sampled log-normal. The axes of the Q-Q plots are in log scale.

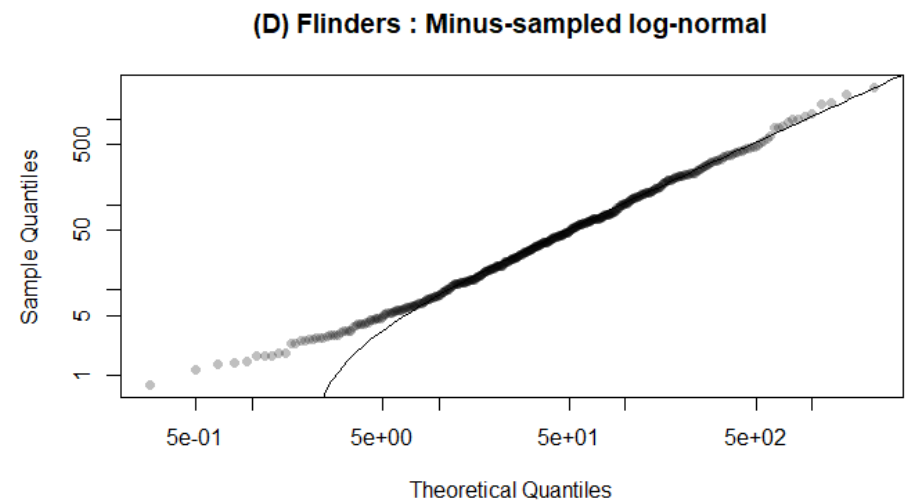
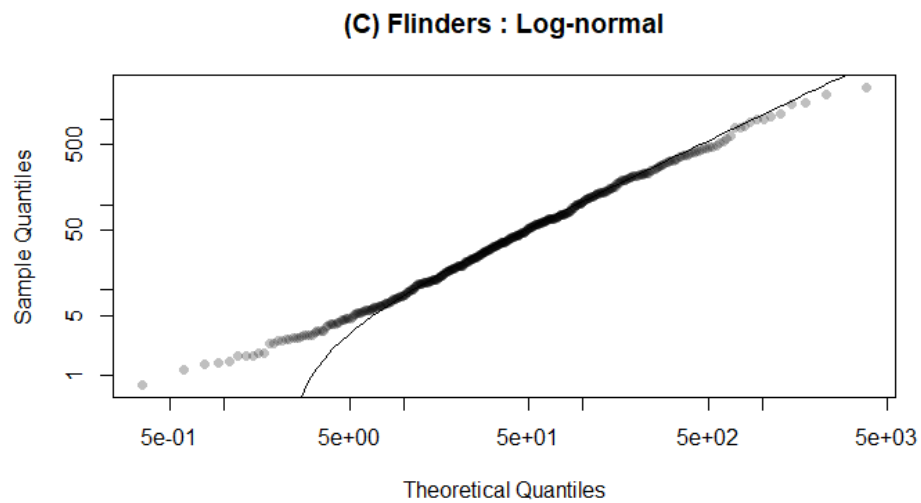
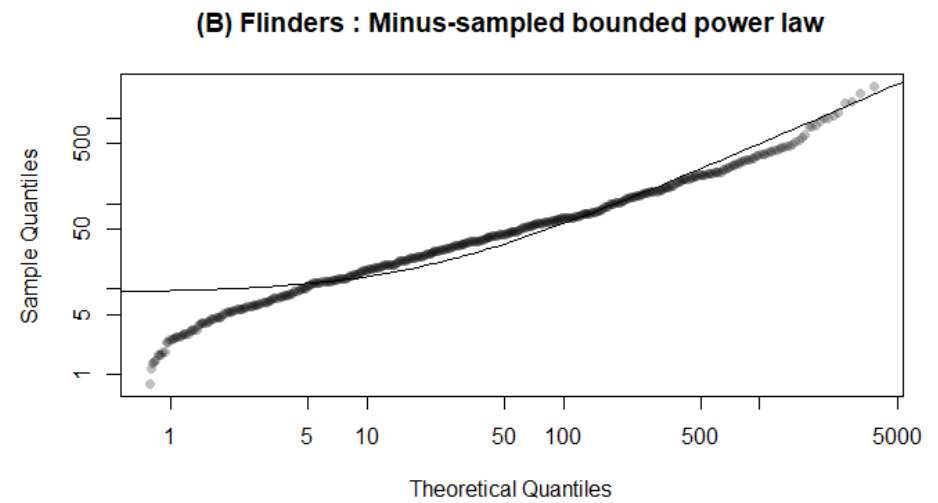
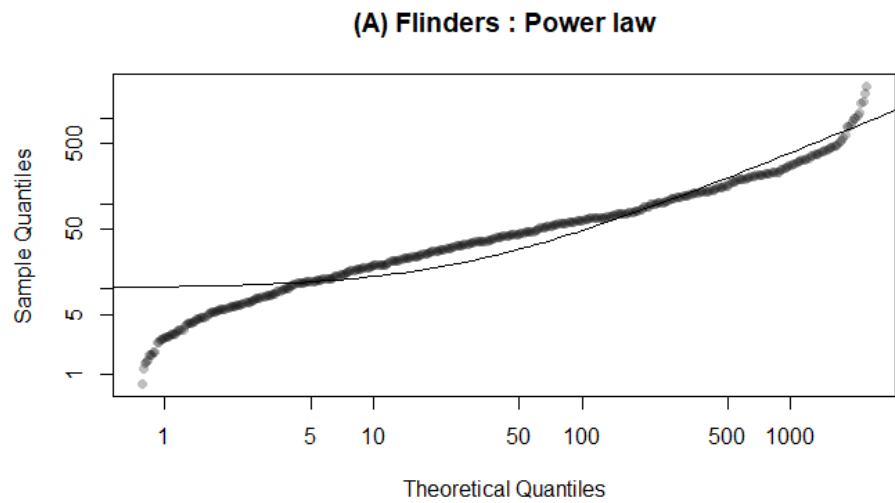


Figure B-10. Flinders coral quantile-quantile (Q-Q) plots with the four distributions: (A) bounded power law (B) minus-sampled bounded power law; (C) log-normal; (D) minus-sampled log-normal. The axes of the Q-Q plots are in log scale.

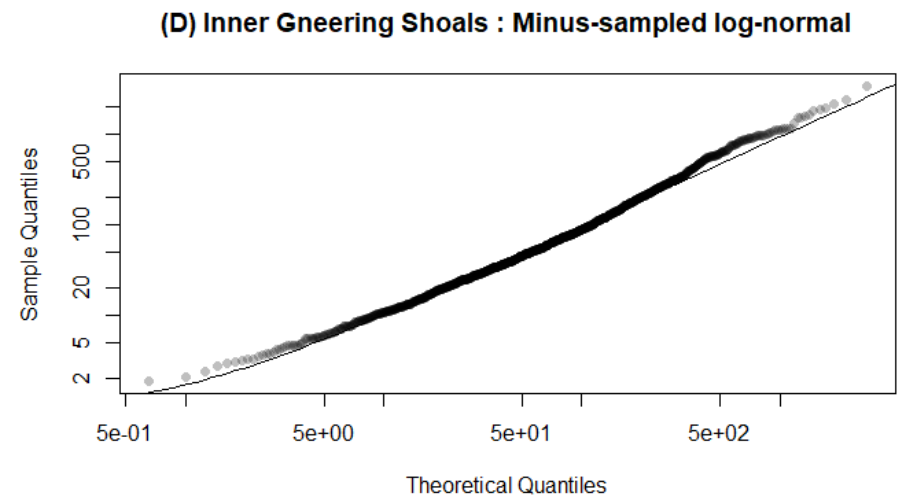
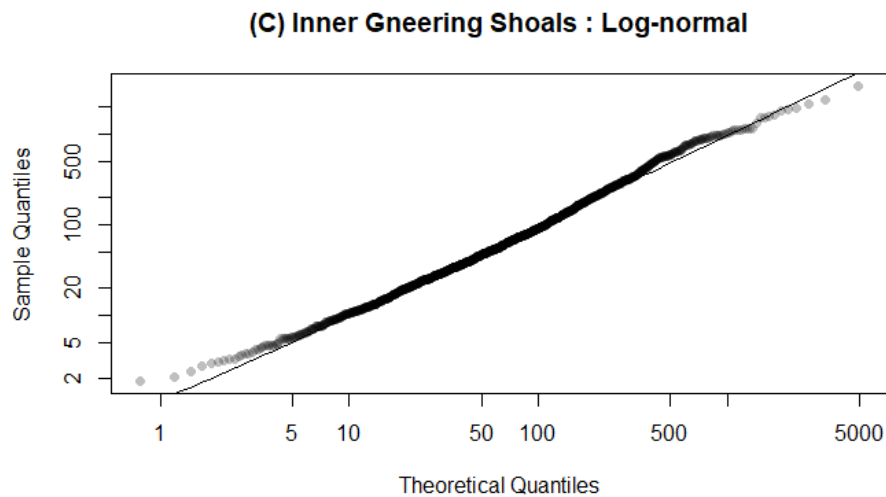
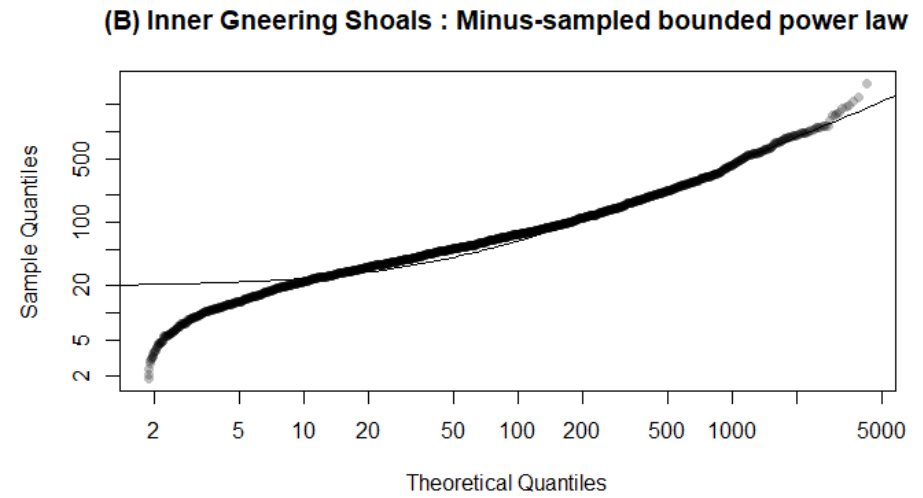
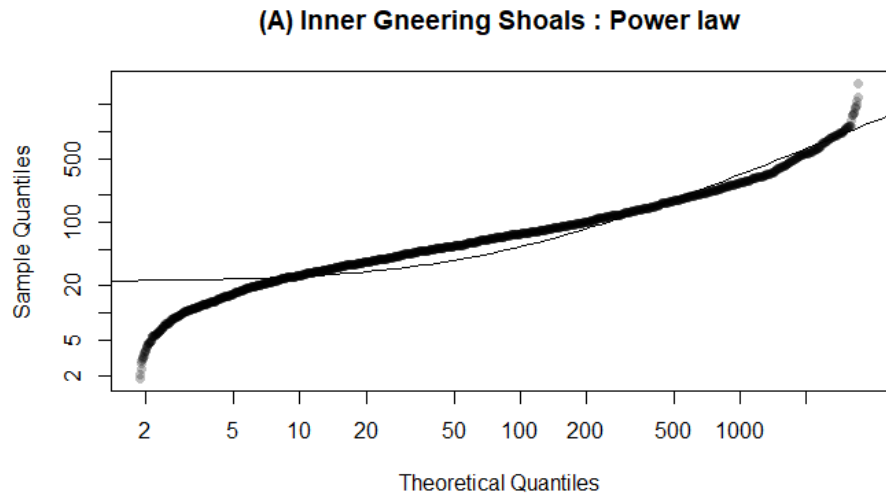


Figure B-11. Inner Gneering Shoals coral quantile-quantile (Q-Q) plots with the four distributions: (A) bounded power law (B) minus-sampled bounded power law; (C) log-normal; (D) minus-sampled log-normal. The axes of the Q-Q plots are in log scale.

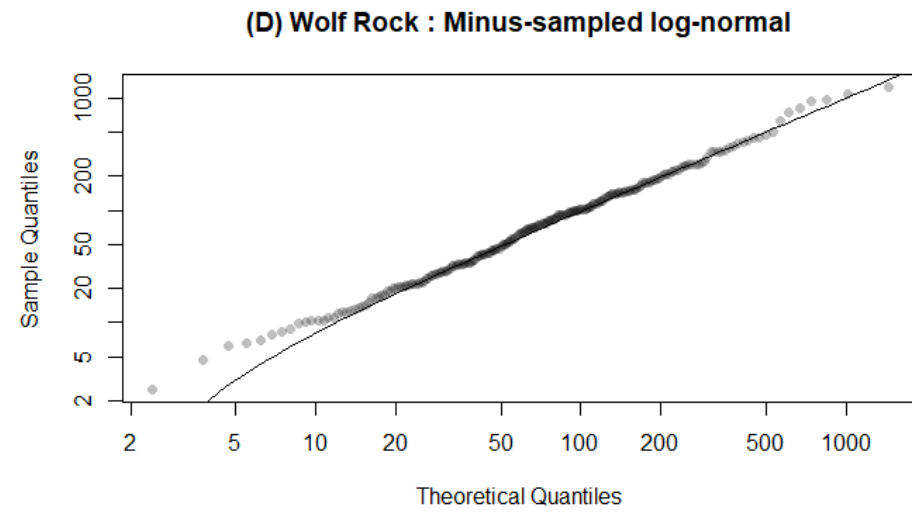
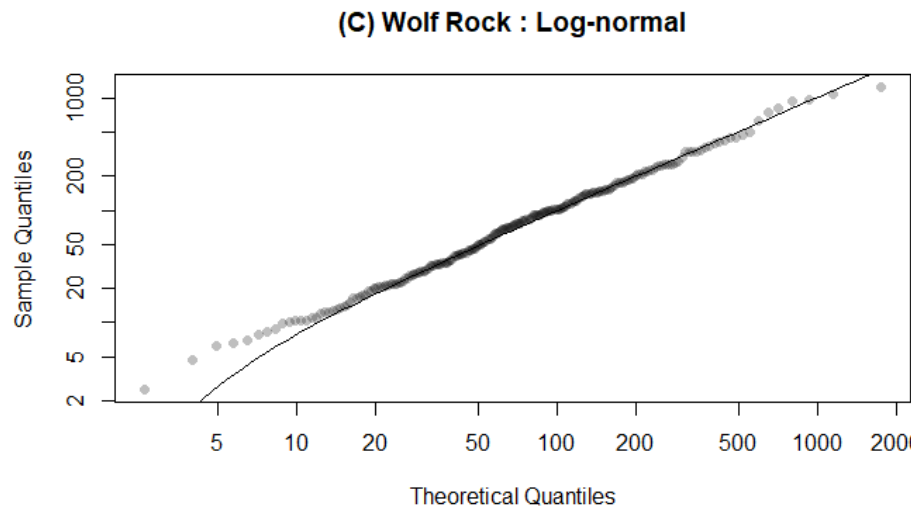
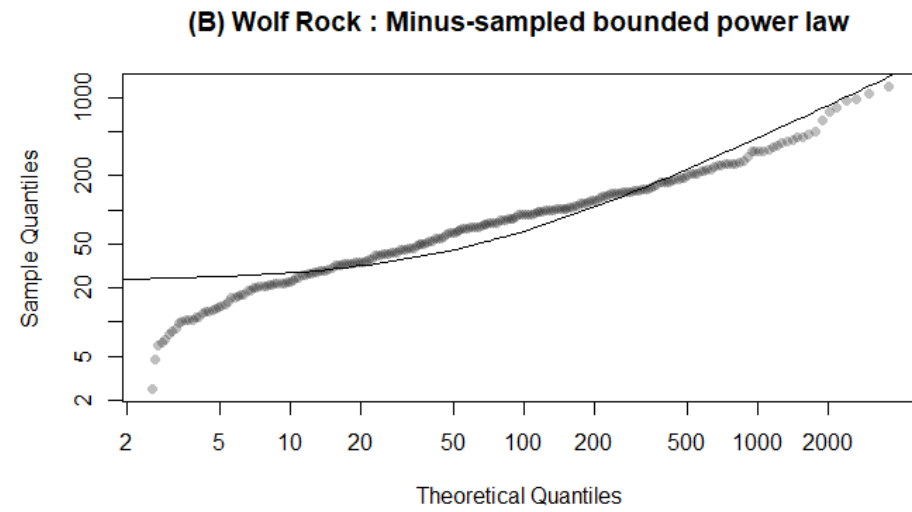
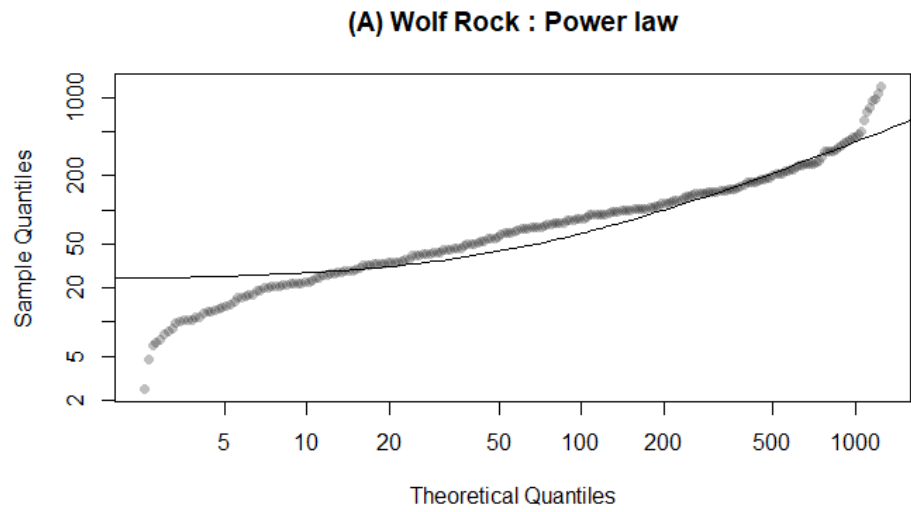


Figure B-12. Wolf Rock coral quantile-quantile (Q-Q) plots with the four distributions: (A) bounded power law (B) minus-sampled bounded power law; (C) log-normal; (D) minus-sampled log-normal. The axes of the Q-Q plots are in log scale.

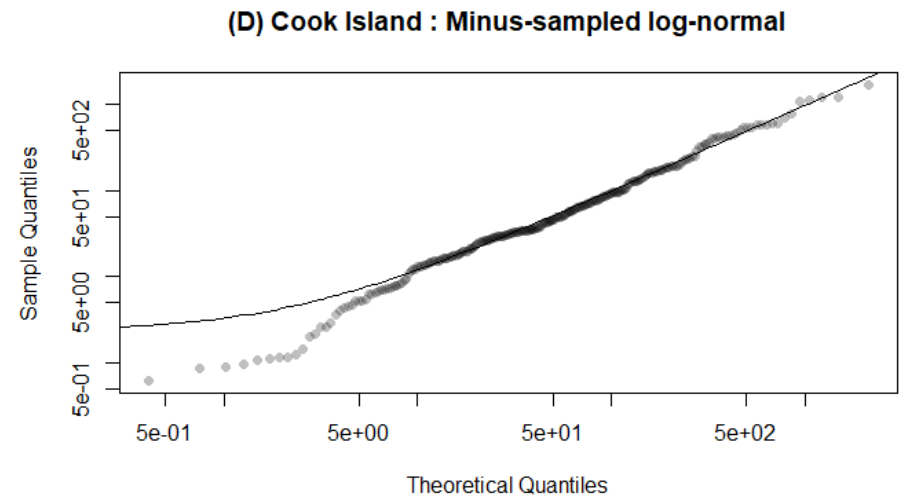
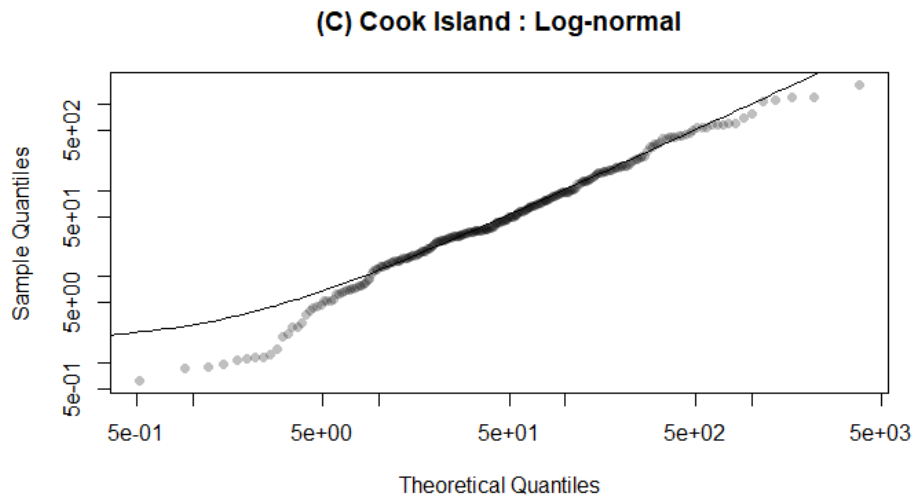
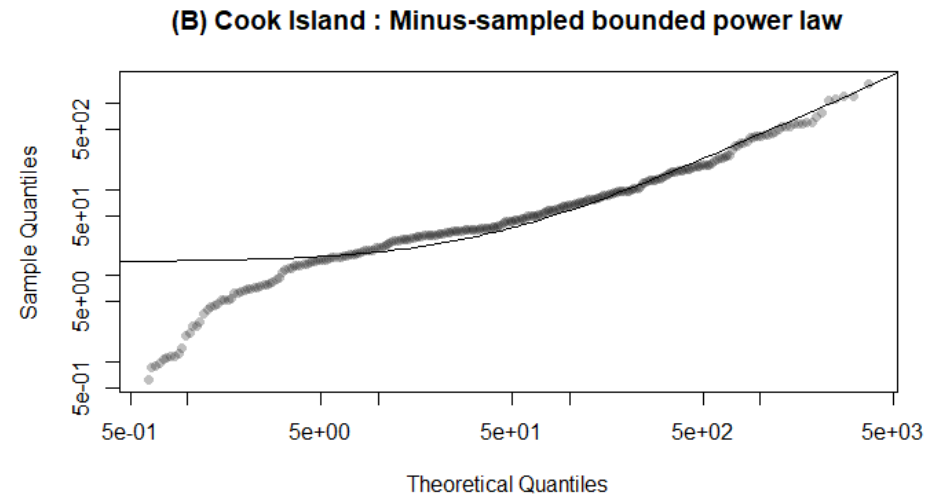
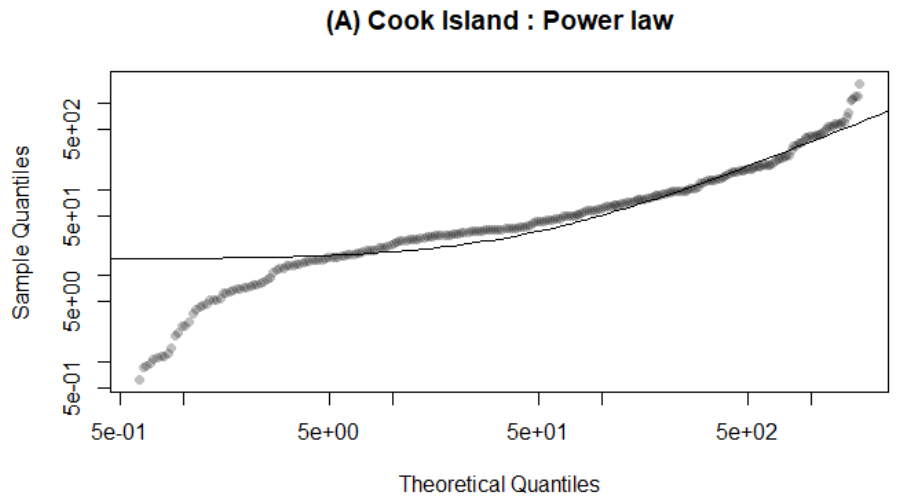


Figure B-13. Cook Island coral quantile-quantile (Q-Q) plots with the four distributions: (A) bounded power law (B) minus-sampled bounded power law; (C) log-normal; (D) minus-sampled log-normal. The axes of the Q-Q plots are in log scale.

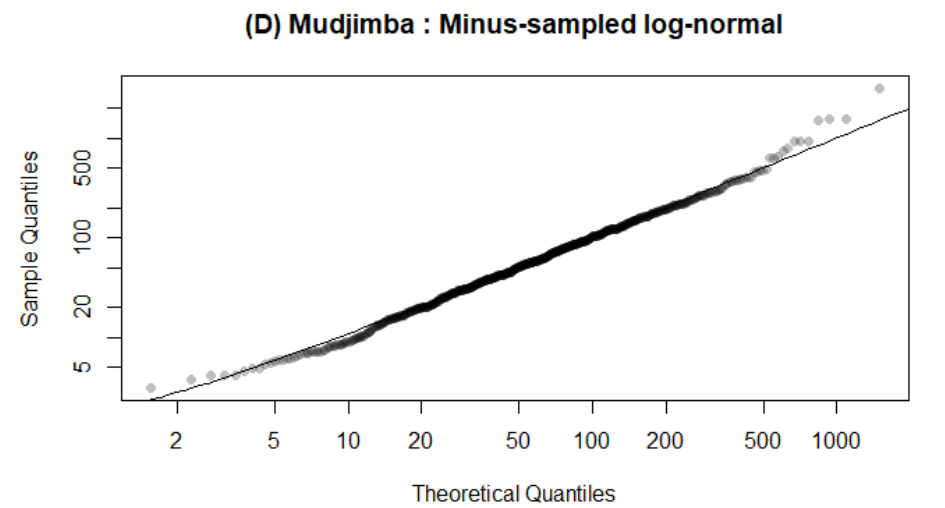
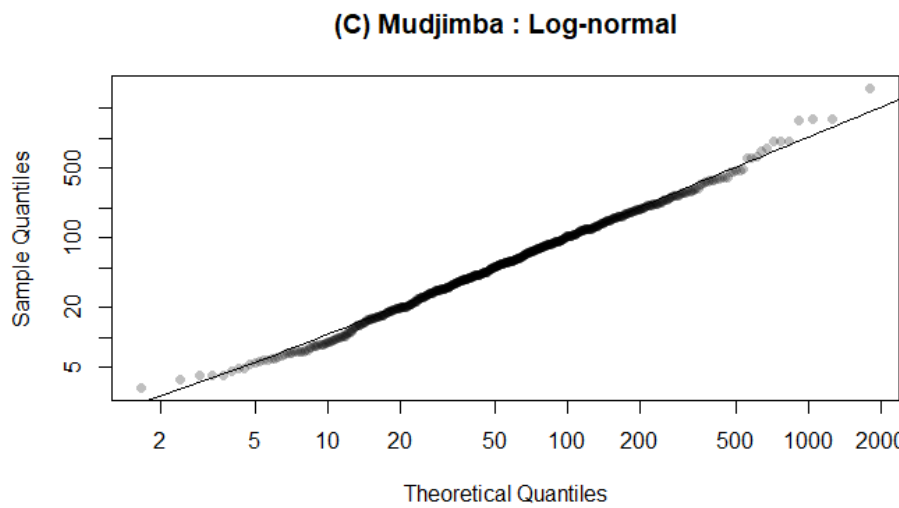
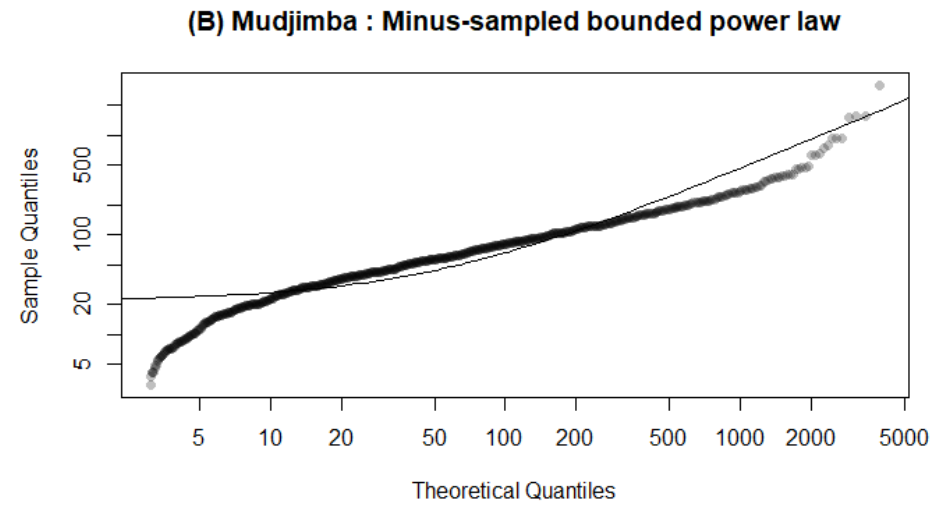
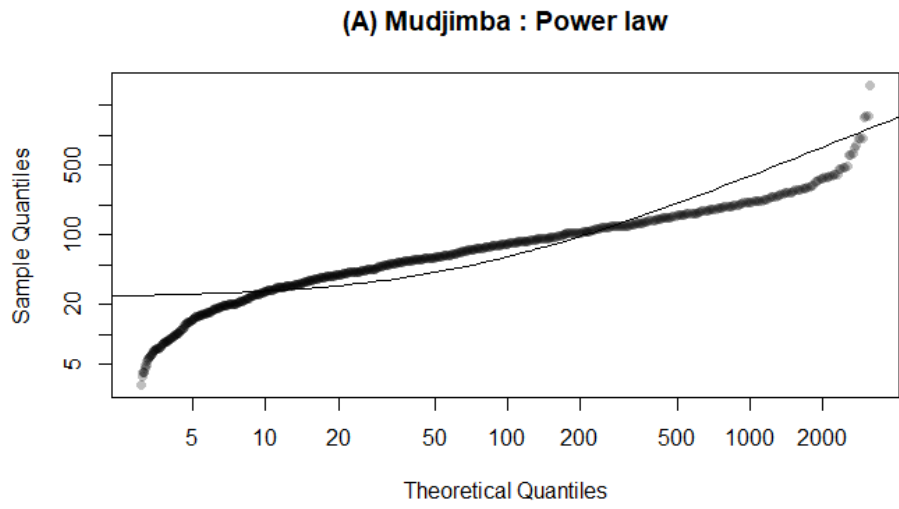


Figure B-14. Mudjimba coral quantile-quantile (Q-Q) plots with the four distributions: (A) bounded power law (B) minus-sampled bounded power law; (C) log-normal; (D) minus-sampled log-normal. The axes of the Q-Q plots are in log scale.

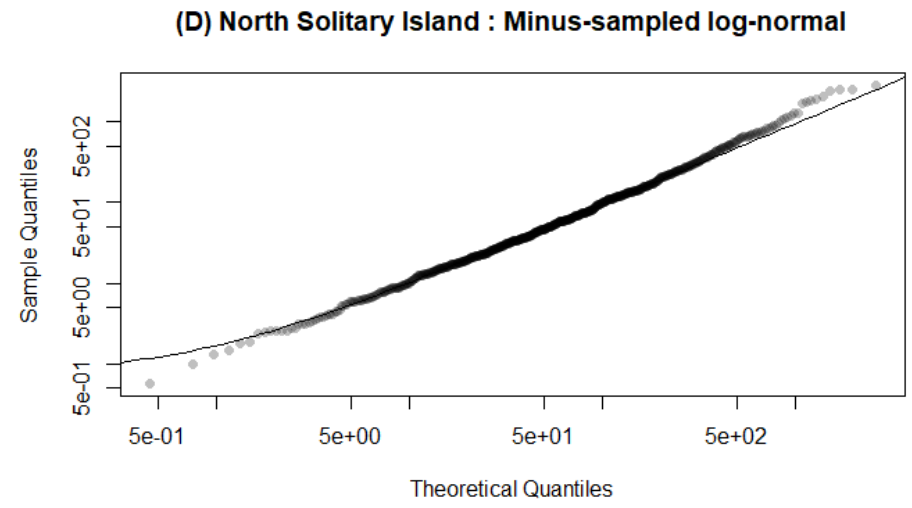
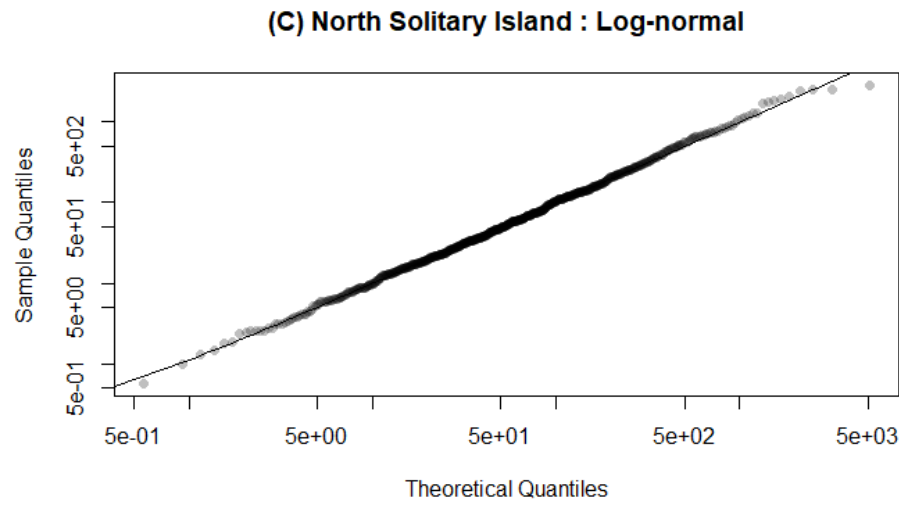
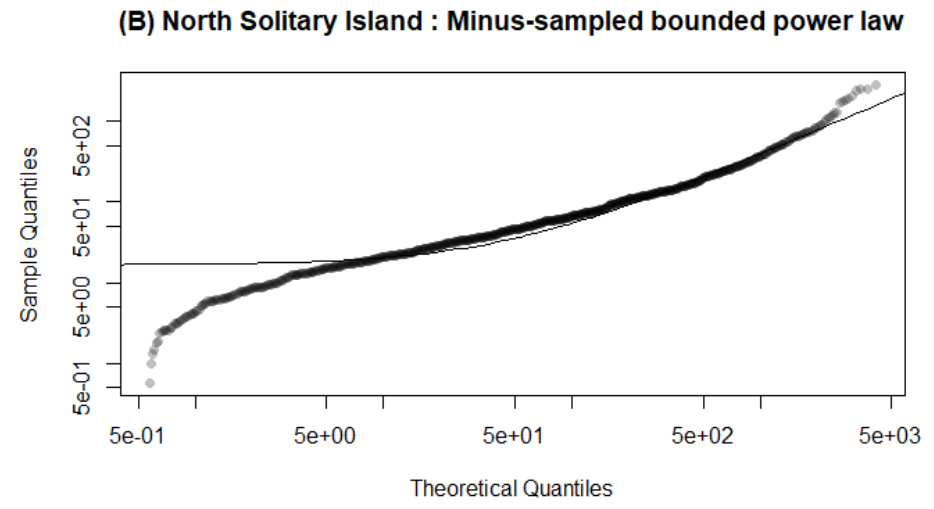
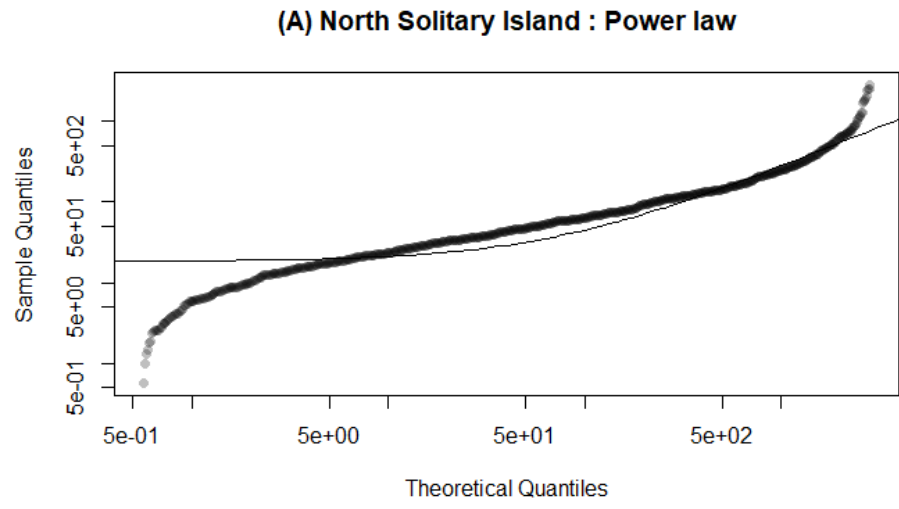


Figure B-15. North Solitary Island coral quantile-quantile (Q-Q) plots with the four distributions: (A) bounded power law (B) minus-sampled bounded power law; (C) log-normal; (D) minus-sampled log-normal. The axes of the Q-Q plots are in log scale.

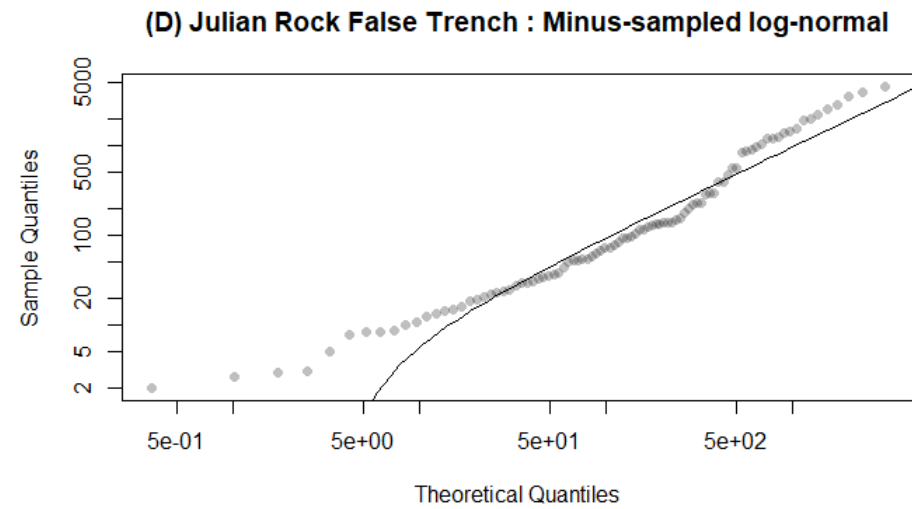
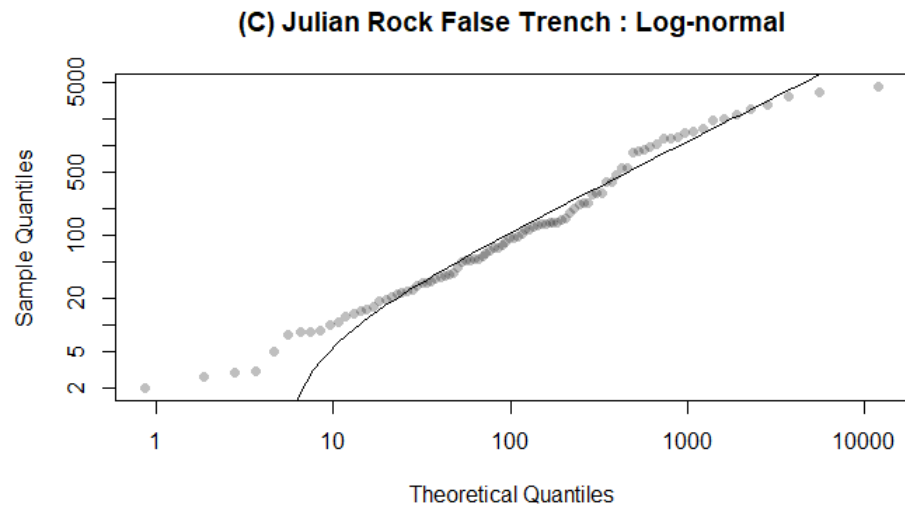
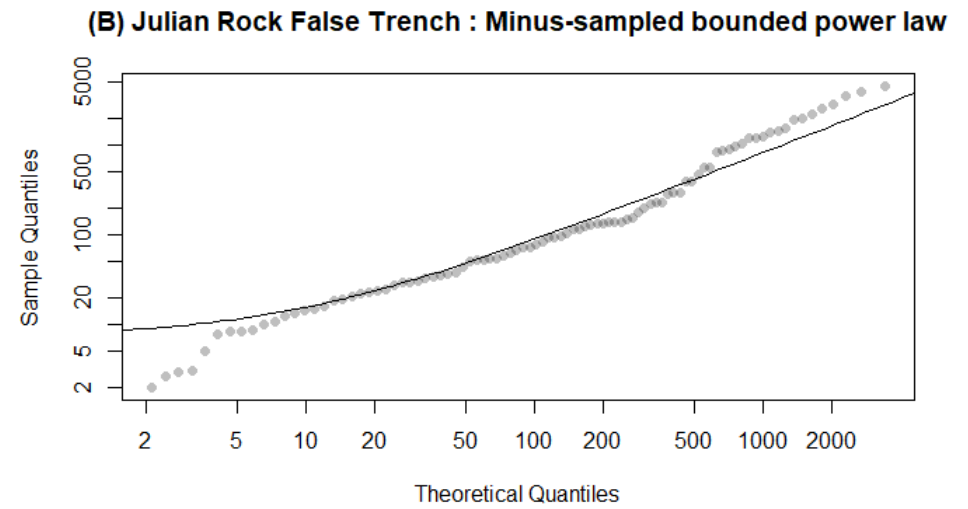
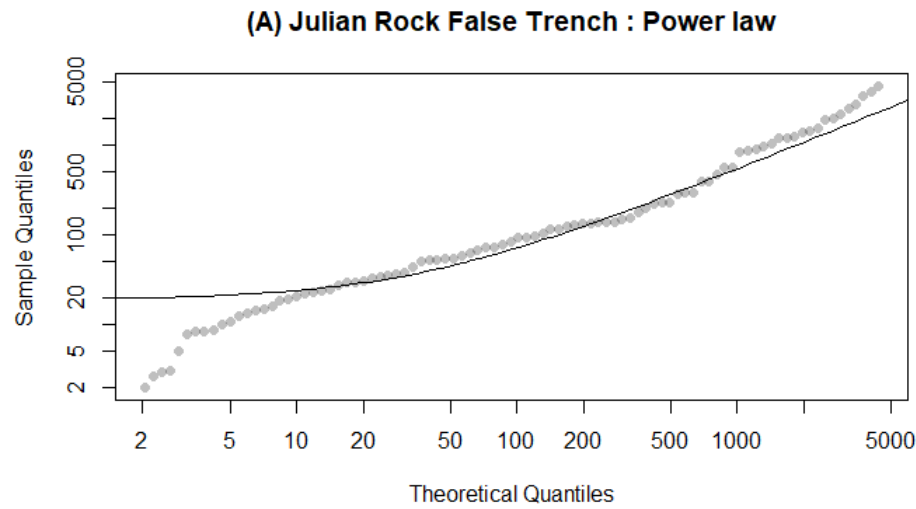


Figure B-16. Julian Rock False Trench coral quantile-quantile (Q-Q) plots with the four distributions: (A) bounded power law (B) minus-sampled bounded power law; (C) log-normal; (D) minus-sampled log-normal. The axes of the Q-Q plots are in log scale.

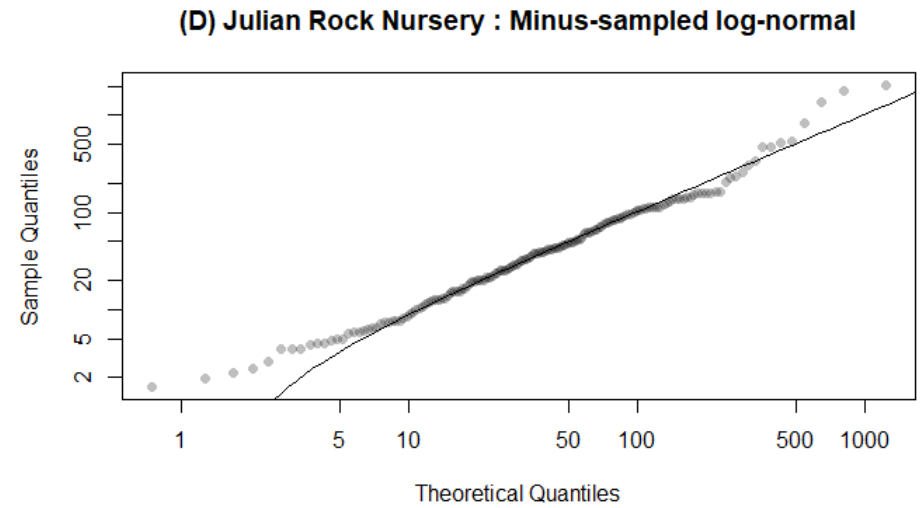
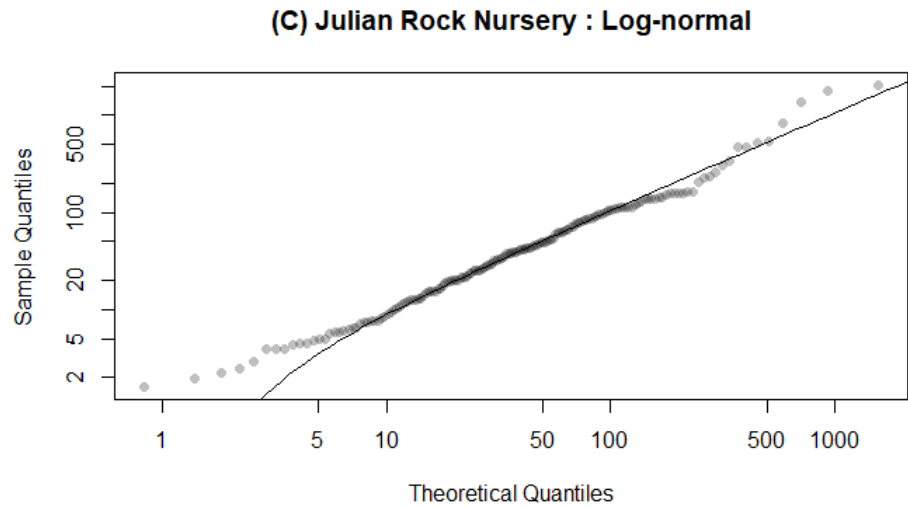
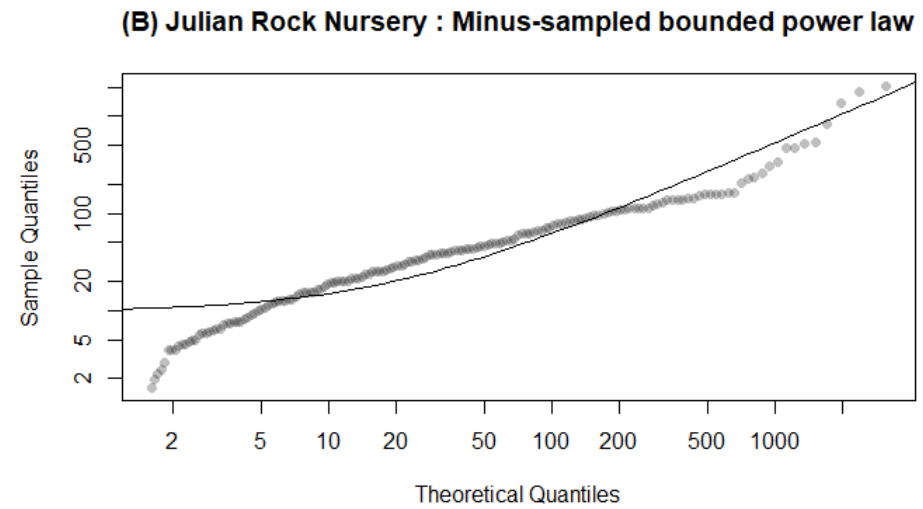
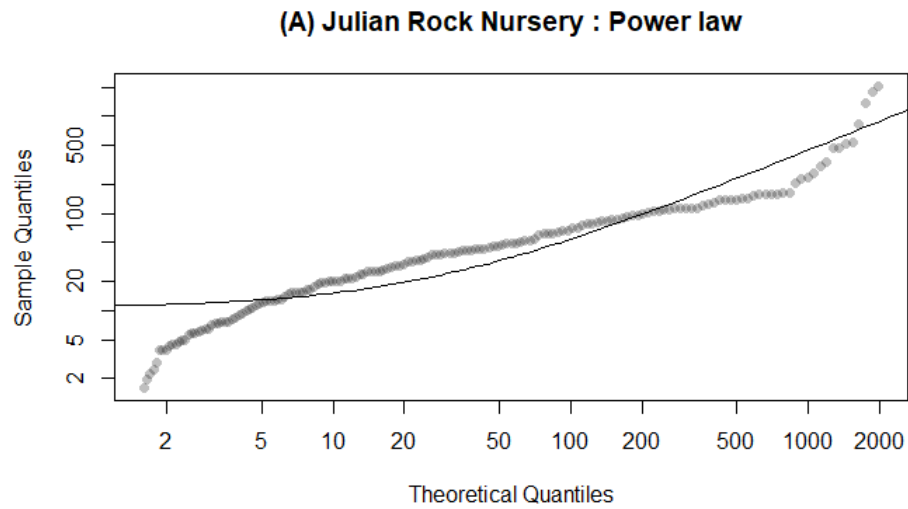


Figure B-17. Julian Rock Nursery coral quantile-quantile (Q-Q) plots with the four distributions: (A) bounded power law (B) minus-sampled bounded power law; (C) log-normal; (D) minus-sampled log-normal. The axes of the Q-Q plots are in log scale.

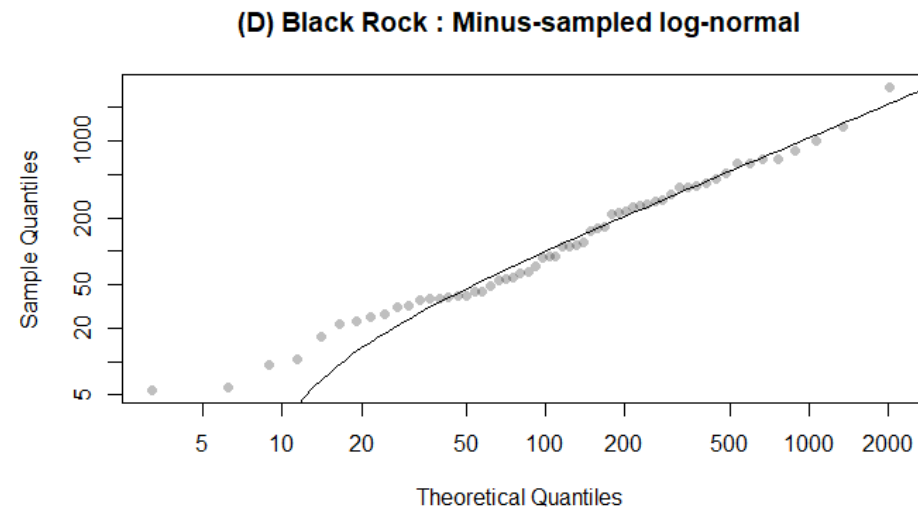
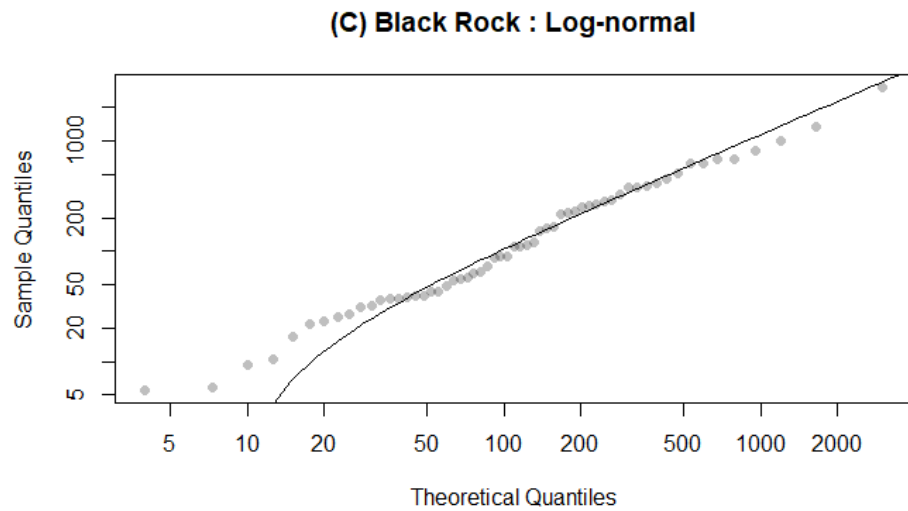
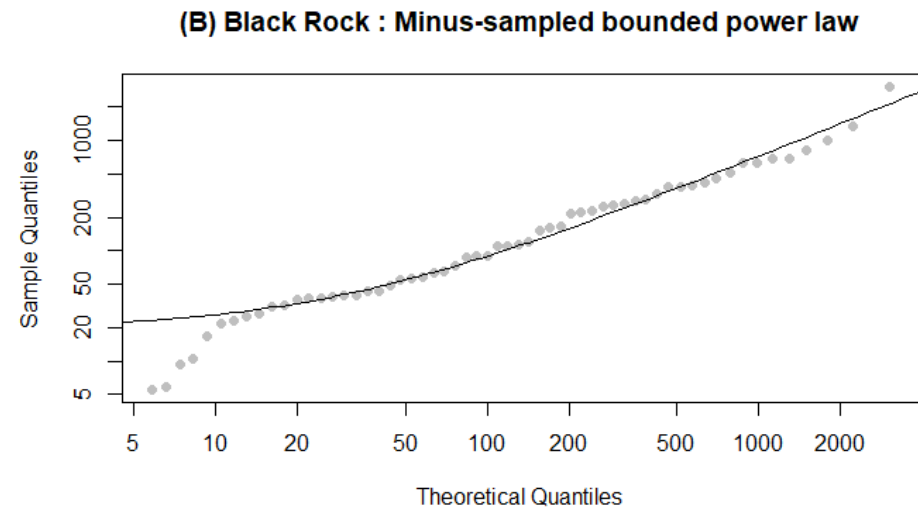
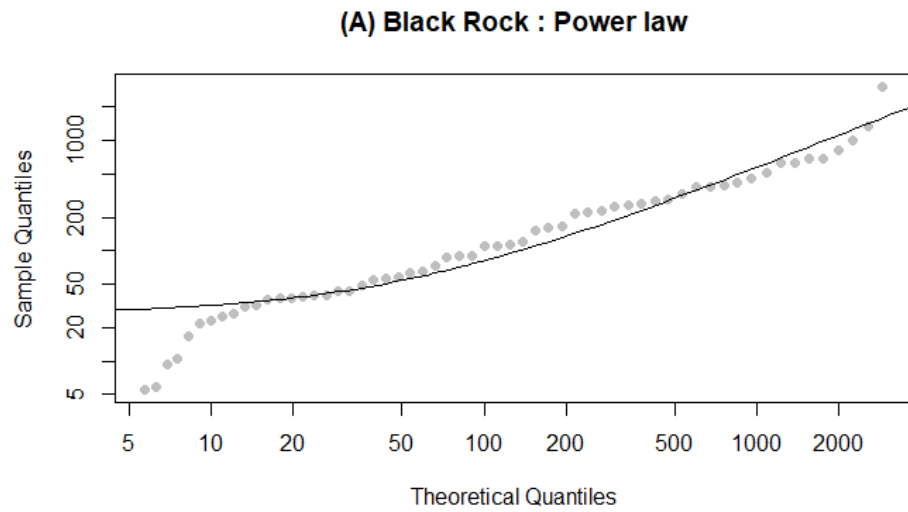


Figure B-18. Black Rock coral quantile-quantile (Q-Q) plots with the four distributions: (A) bounded power law (B) minus-sampled bounded power law; (C) log-normal; (D) minus-sampled log-normal. The axes of the Q-Q plots are in log scale.

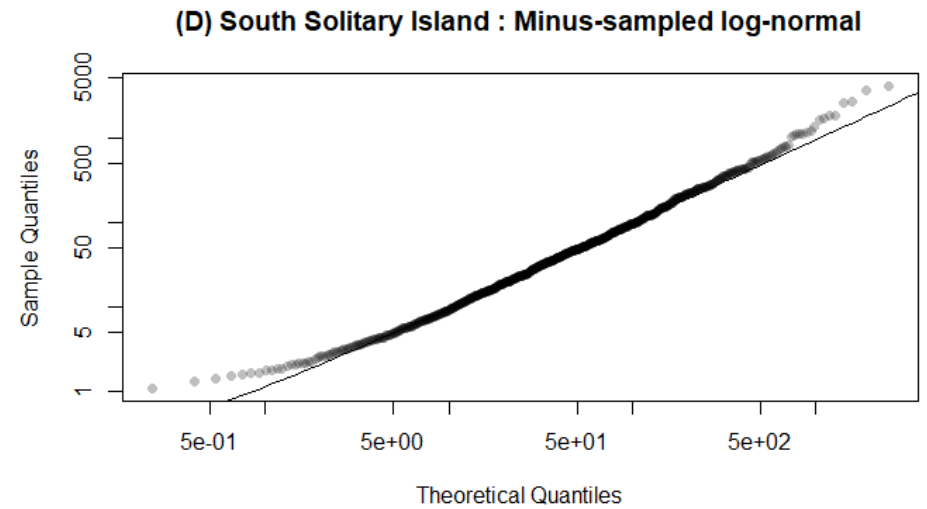
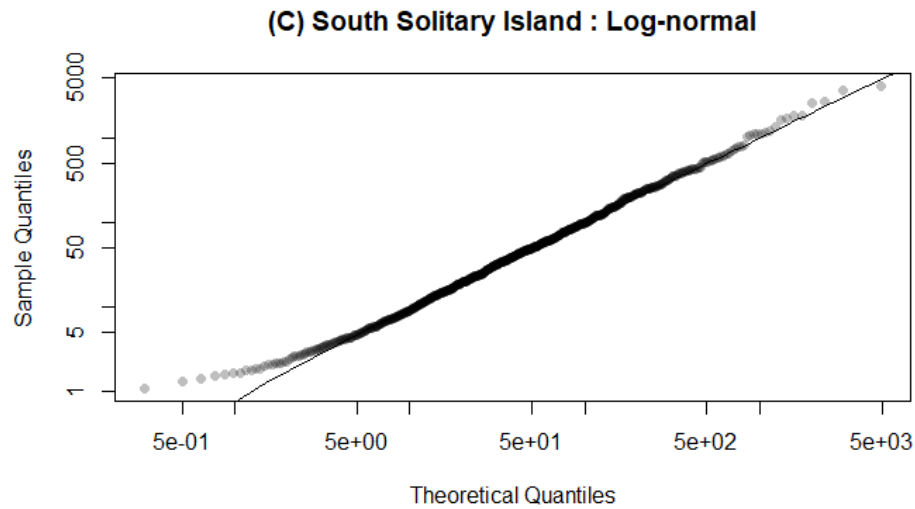
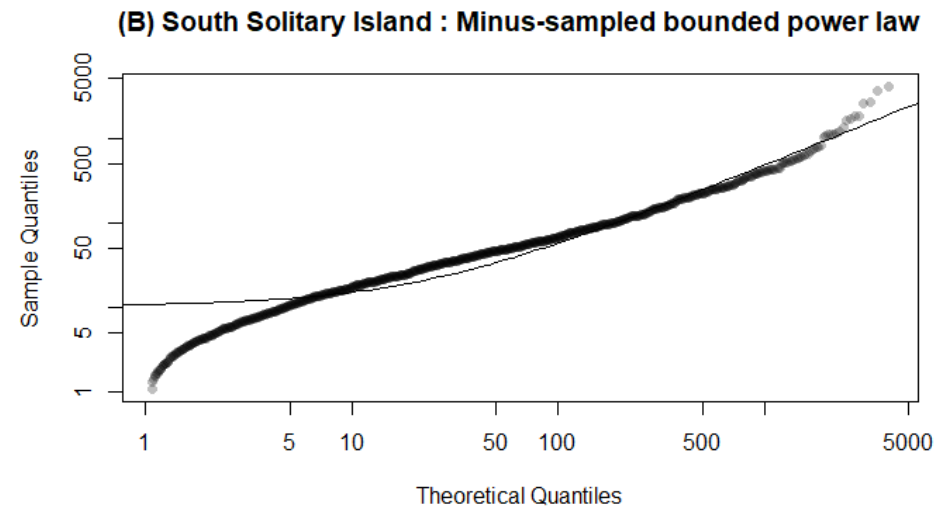
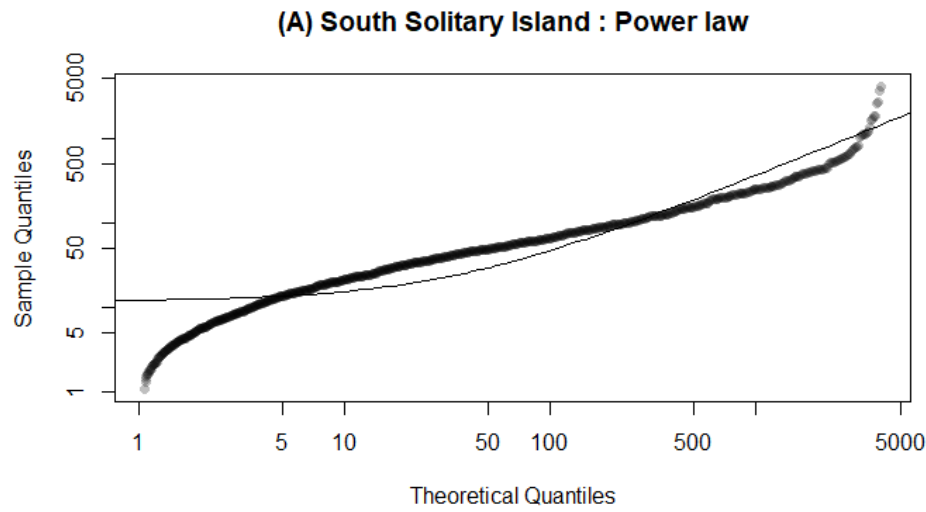


Figure B-19. South Solitary Island coral quantile-quantile (Q-Q) plots with the four distributions: (A) bounded power law (B) minus-sampled bounded power law; (C) log-normal; (D) minus-sampled log-normal. The axes of the Q-Q plots are in log scale.

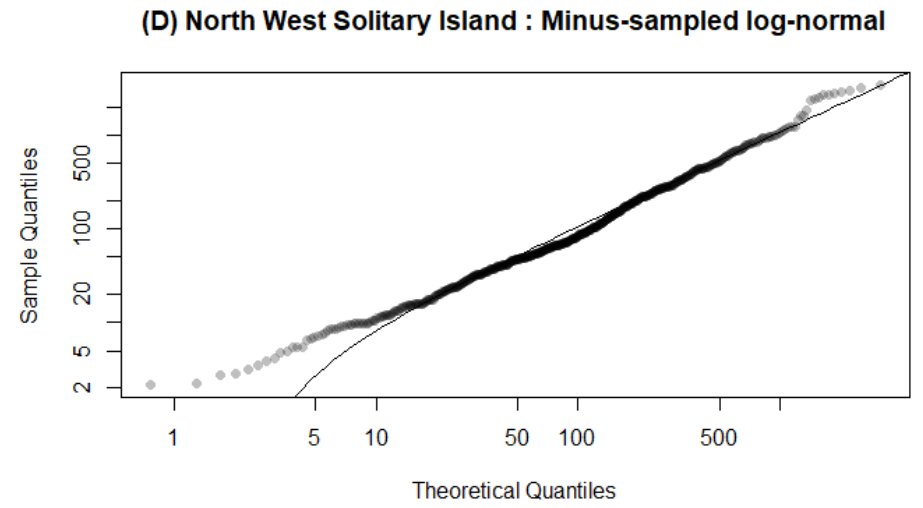
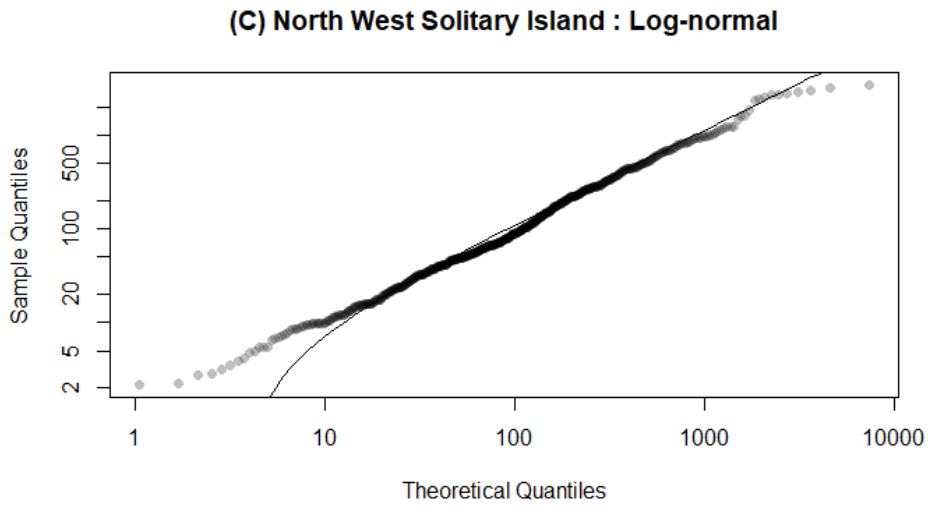
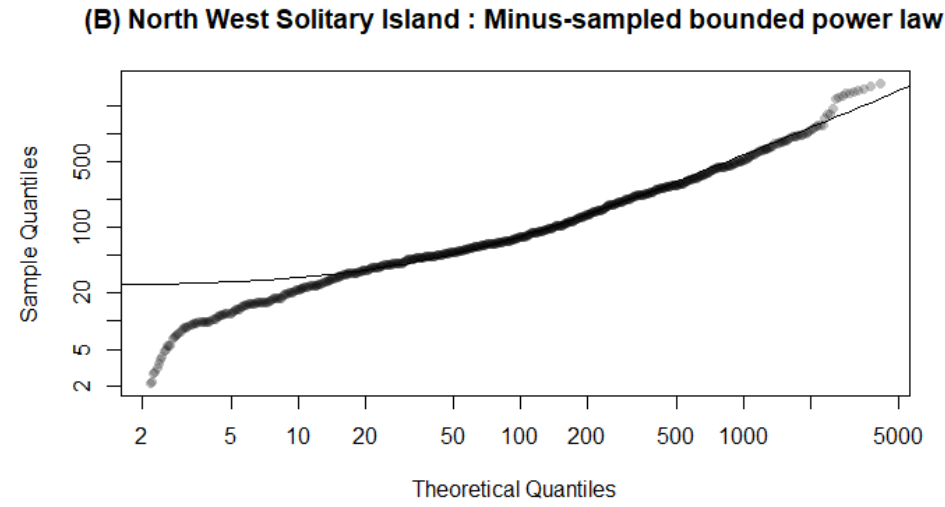
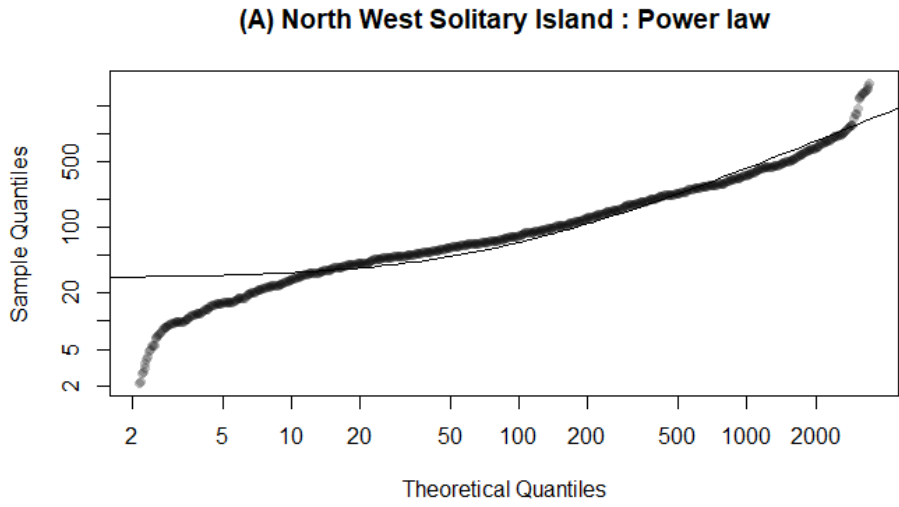


Figure B-20. North West Solitary Island coral quantile-quantile (Q-Q) plots with the four distributions: (A) bounded power law (B) minus-sampled bounded power law; (C) log-normal; (D) minus-sampled log-normal. The axes of the Q-Q plots are in log scale.

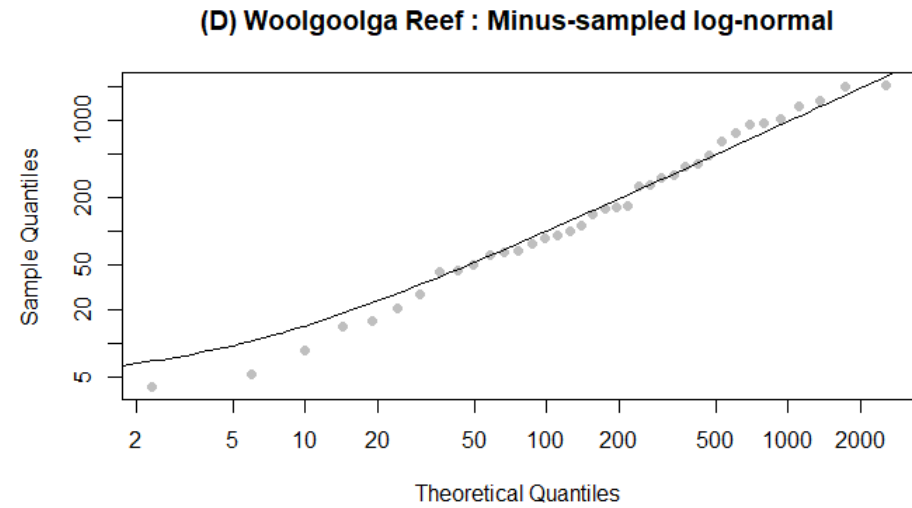
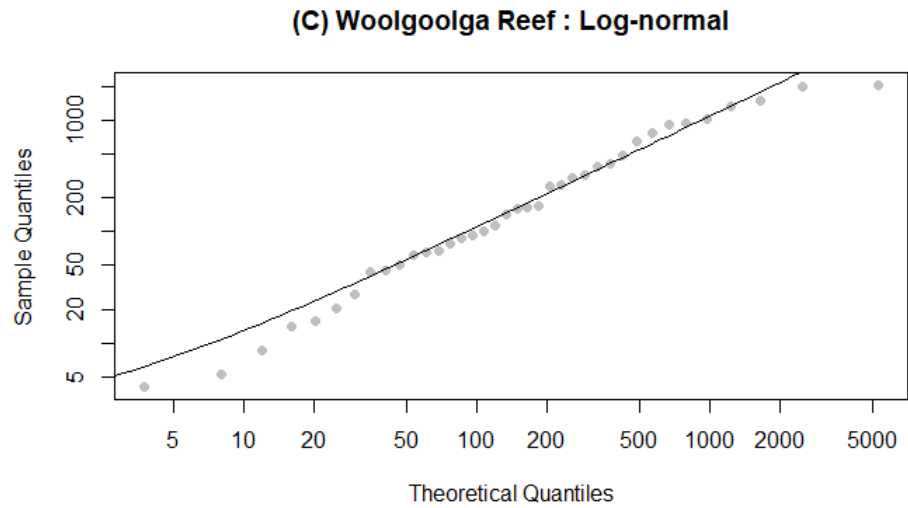
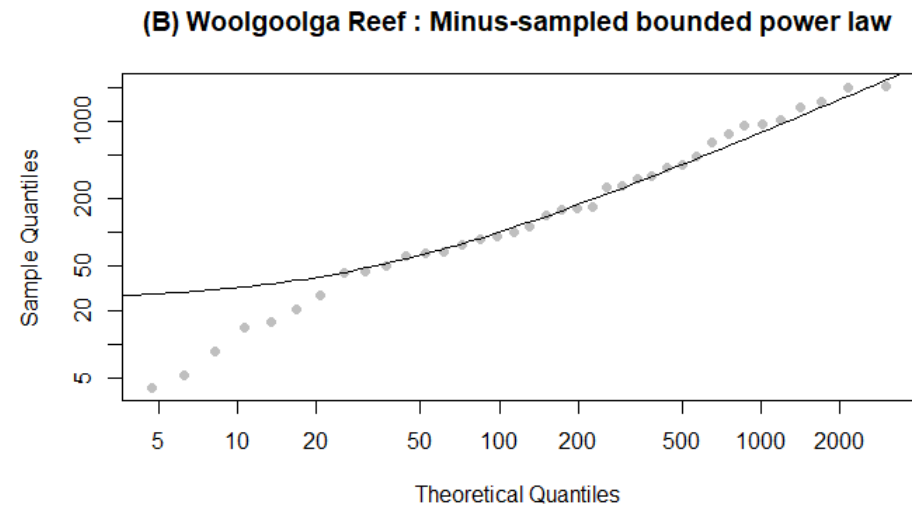
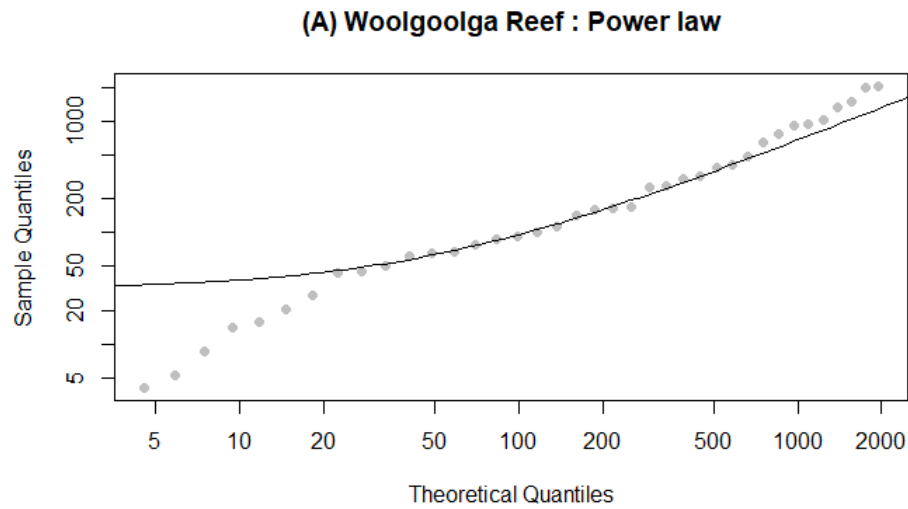


Figure B-21. Woolgoolga Reef coral quantile-quantile (Q-Q) plots with the four distributions: (A) bounded power law (B) minus-sampled bounded power law; (C) log-normal; (D) minus-sampled log-normal. The axes of the Q-Q plots are in log scale.

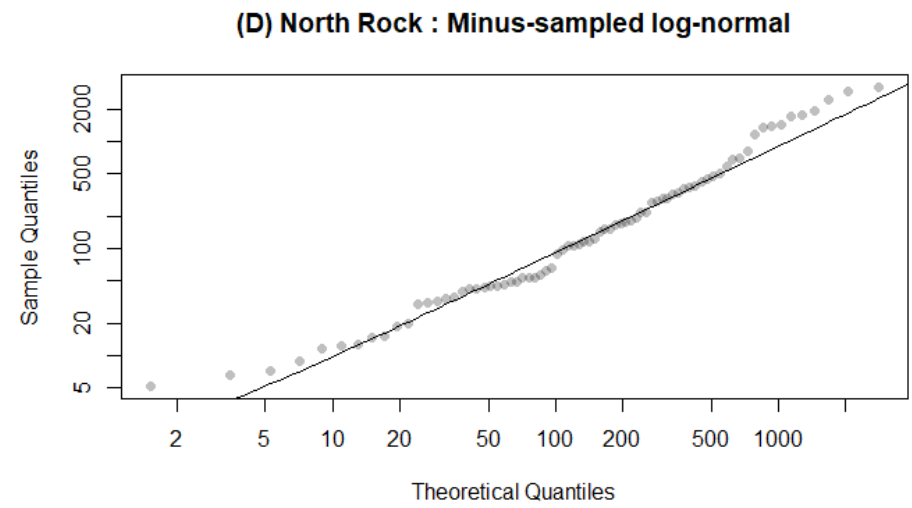
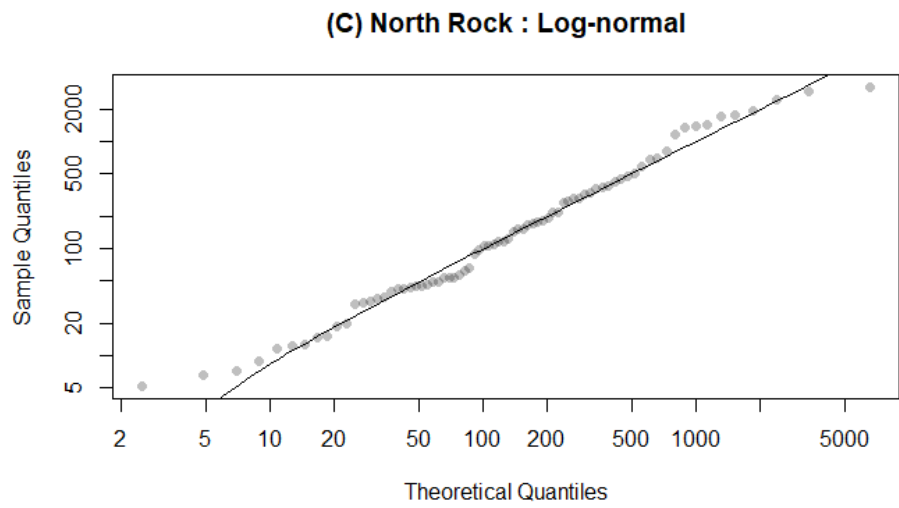
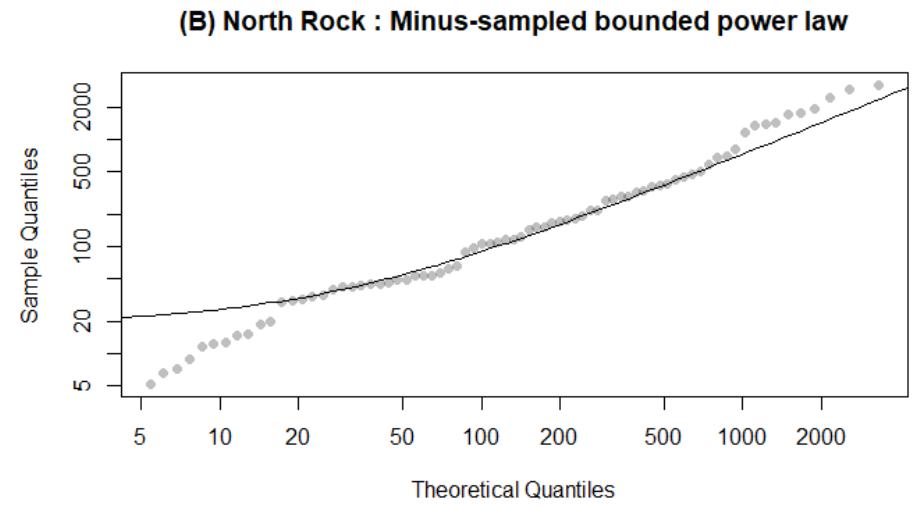
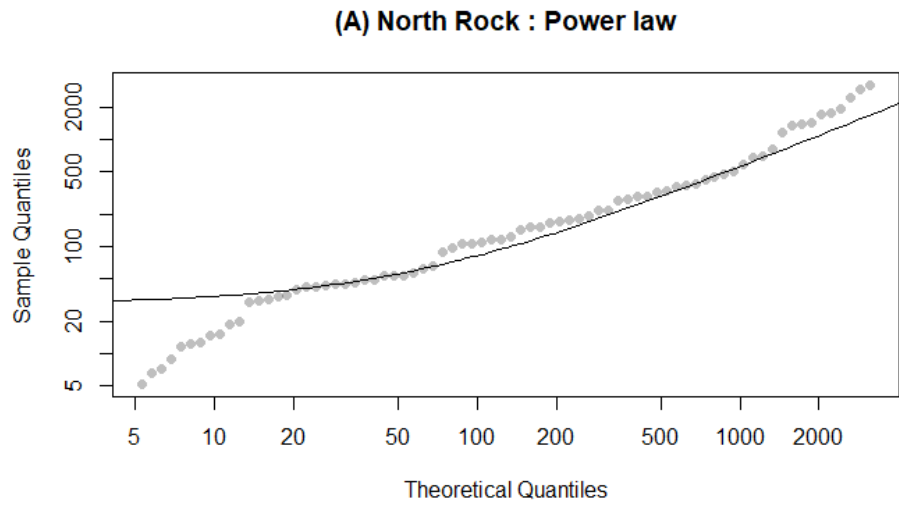


Figure B-22. North Rock coral quantile-quantile (Q-Q) plots with the four distributions: (A) bounded power law (B) minus-sampled bounded power law; (C) log-normal; (D) minus-sampled log-normal. The axes of the Q-Q plots are in log scale.

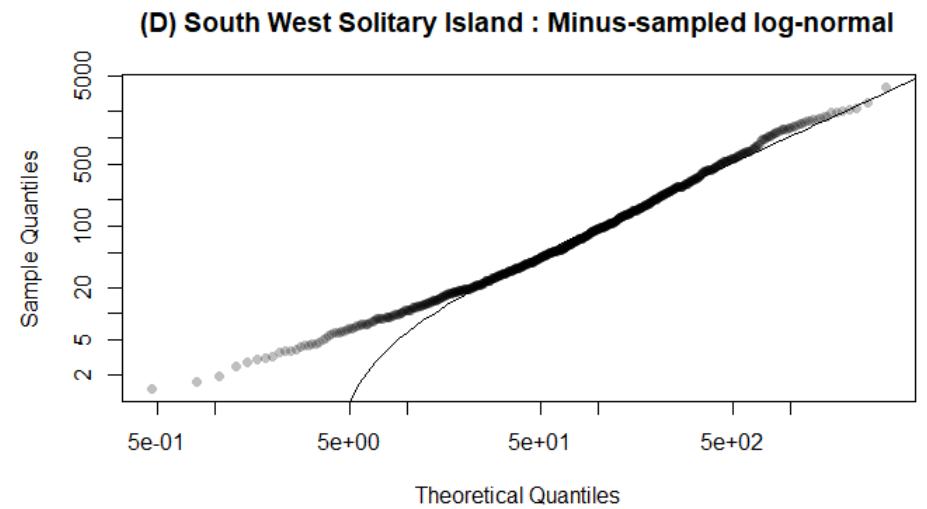
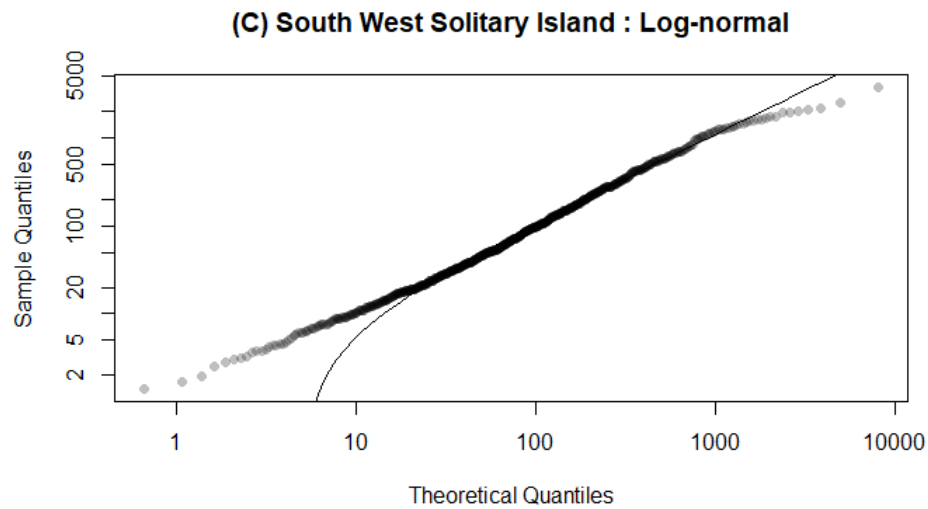
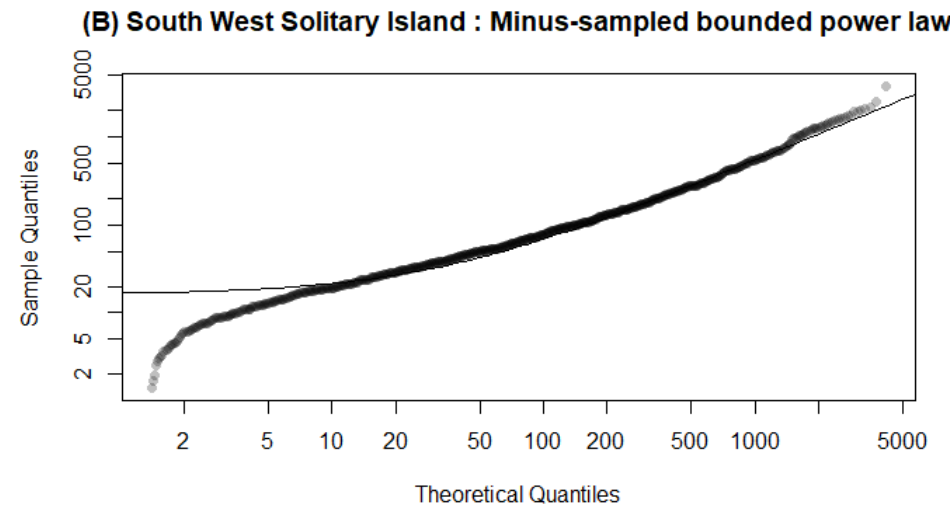
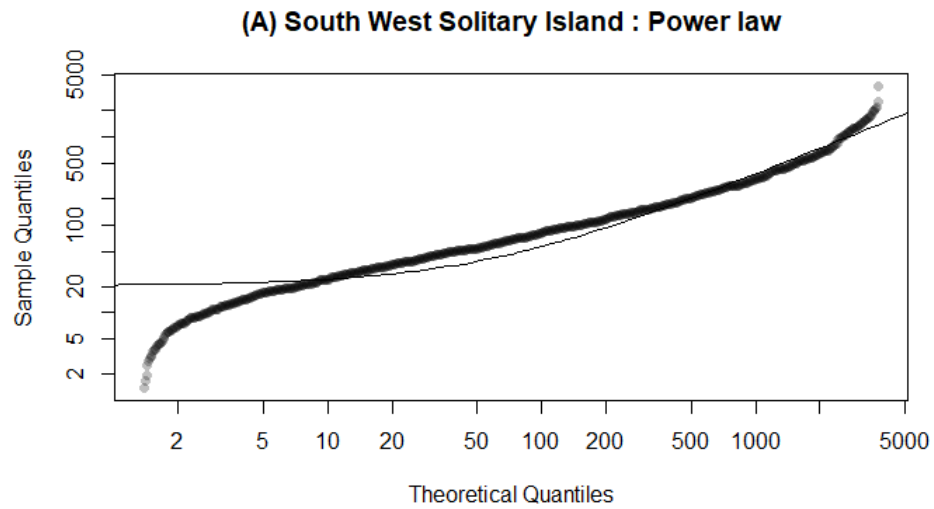
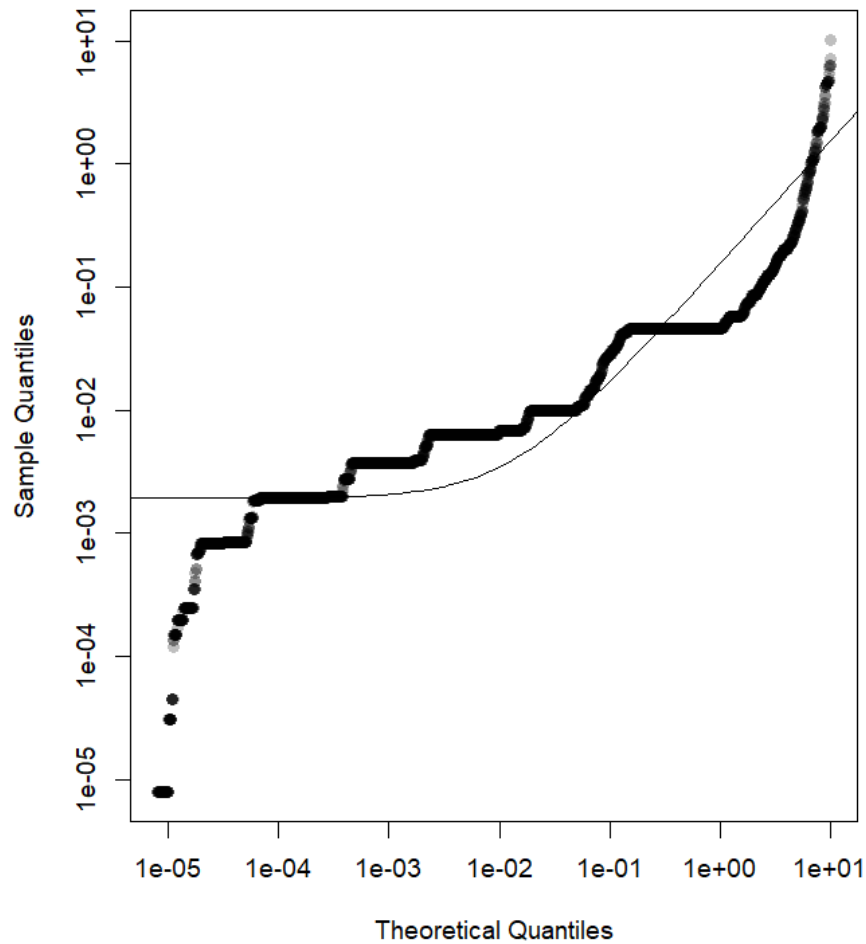


Figure B-23. South West Solitary Island coral quantile-quantile (Q-Q) plots with the four distributions: (A) bounded power law (B) minus-sampled bounded power law; (C) log-normal; (D) minus-sampled log-normal. The axes of the Q-Q plots are in log scale.

S4: Quantile-quantile plots of fish data for all sites

(A) Lady Elliot Island : Power law Q-Q plot



(B) Lady Elliot Island : Log-normal Q-Q plot

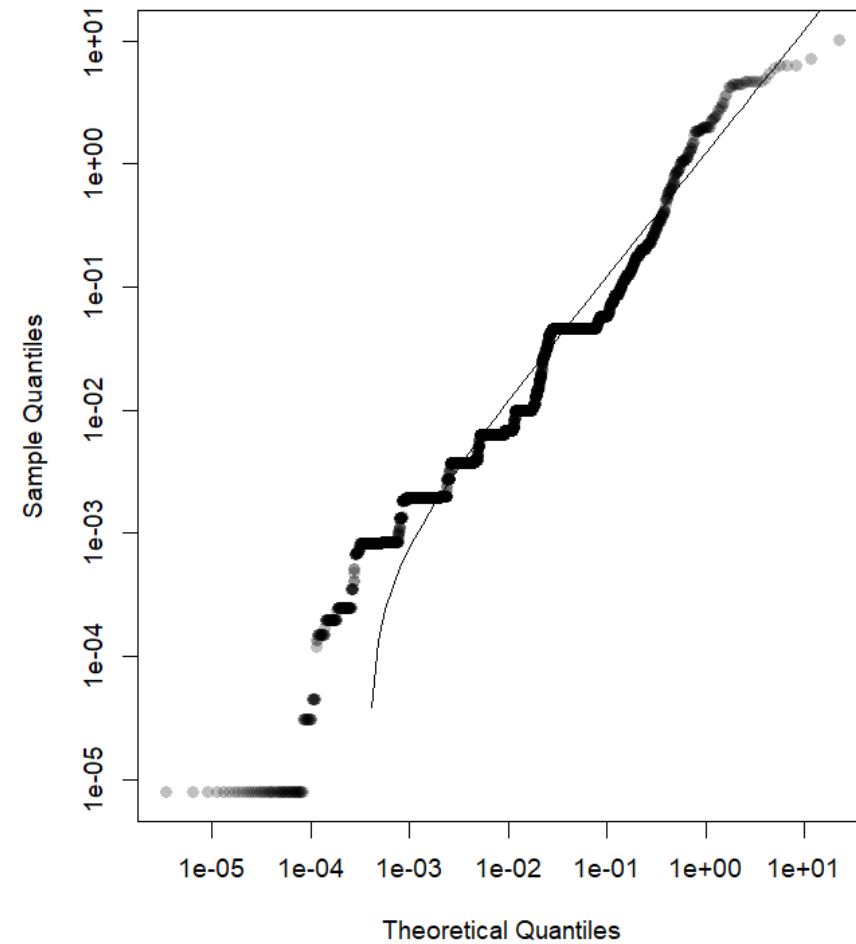
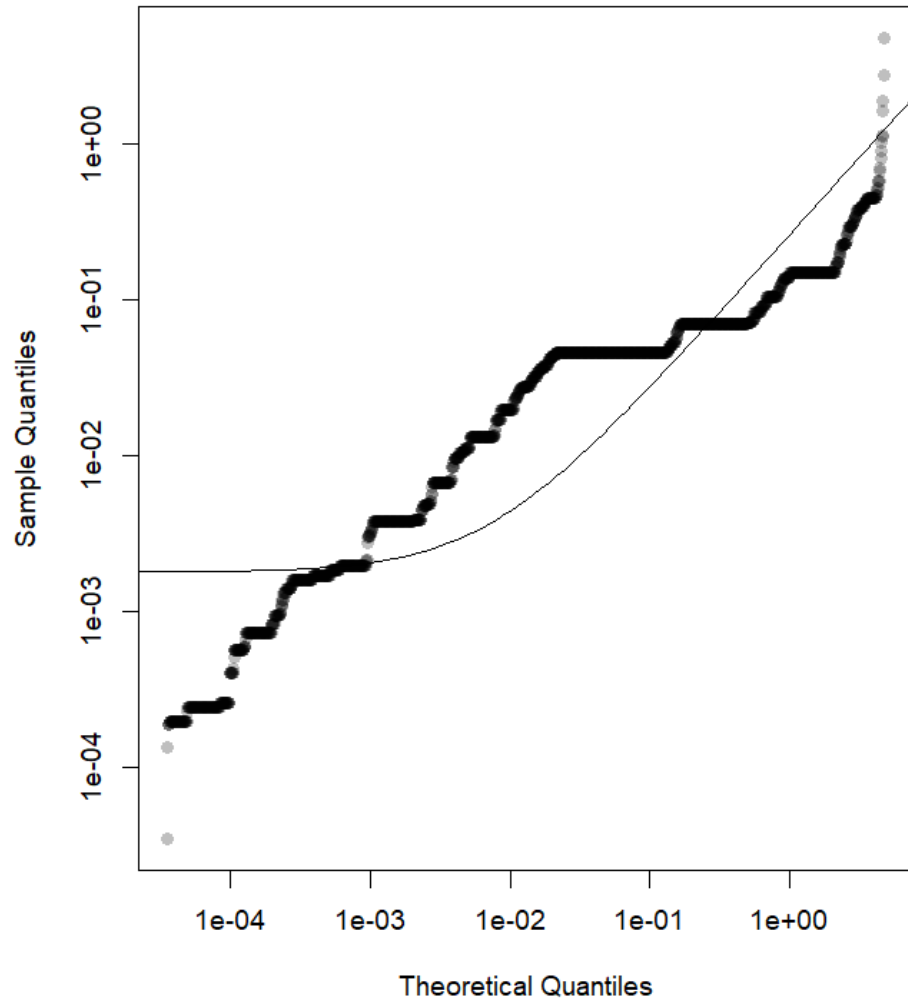


Figure B-24. Lady Elliot Island fish quantile-quantile (Q-Q) plots with (A) bounded power law and (B) log-normal distributions. The axes of the Q-Q plots are in log scale.

(A) Lady Musgrave Island : Power law Q-Q plot



(B) Lady Musgrave Island : Log-normal Q-Q plot

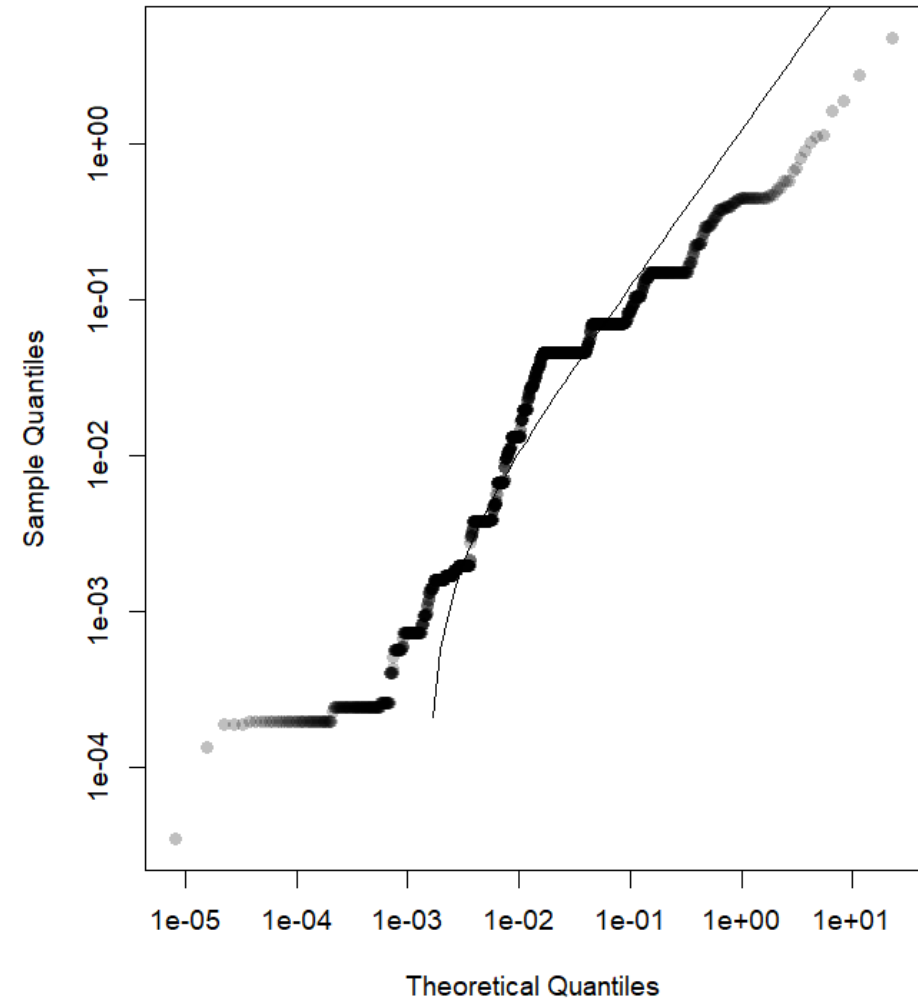


Figure B-25. Lady Musgrave Island fish quantile-quantile (Q-Q) plots with (A) bounded power law and (B) log-normal distributions. The axes of the Q-Q plots are in log scale.

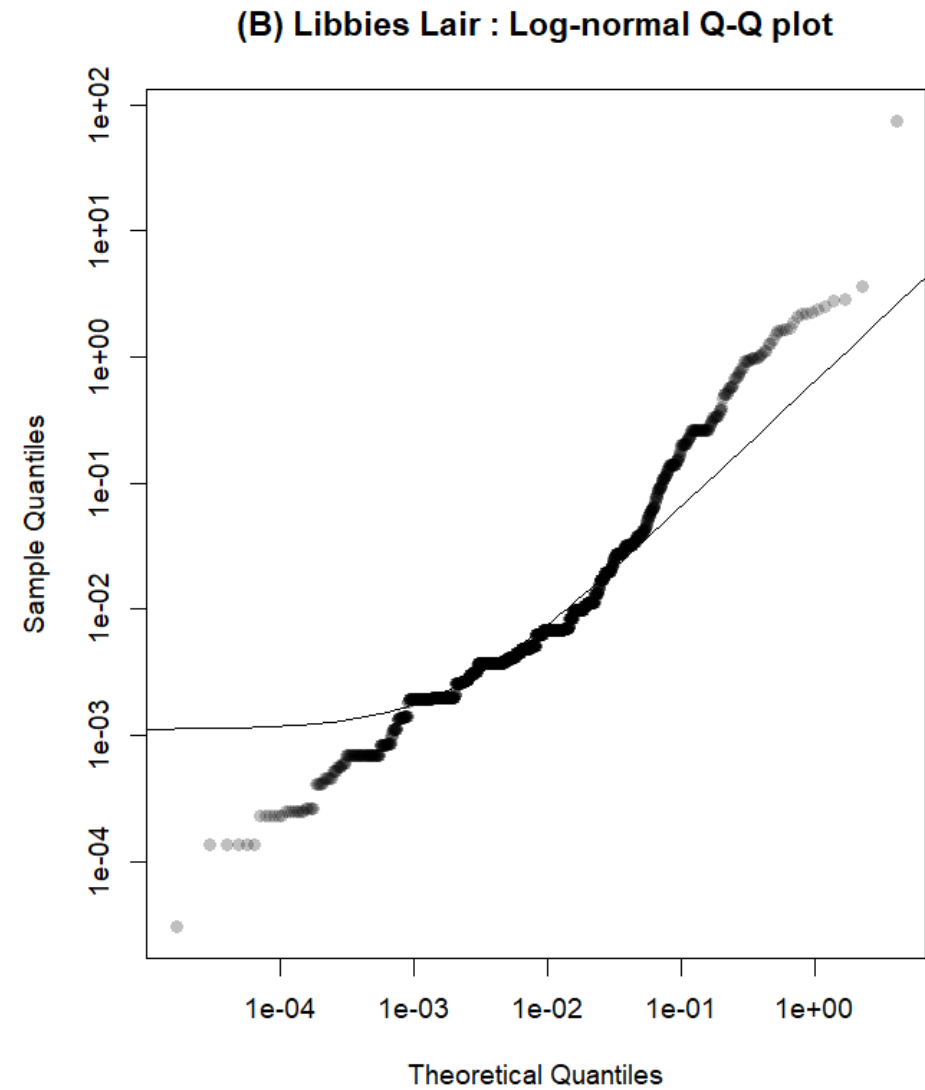
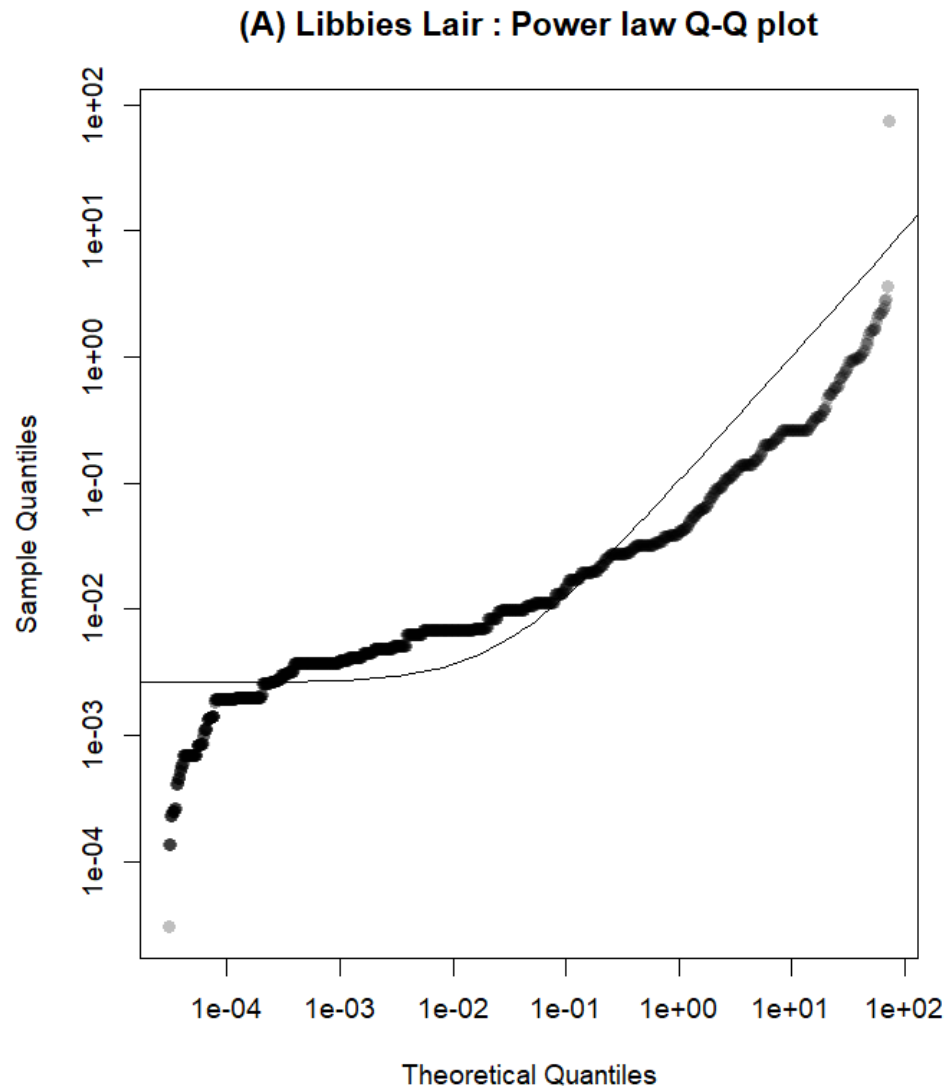
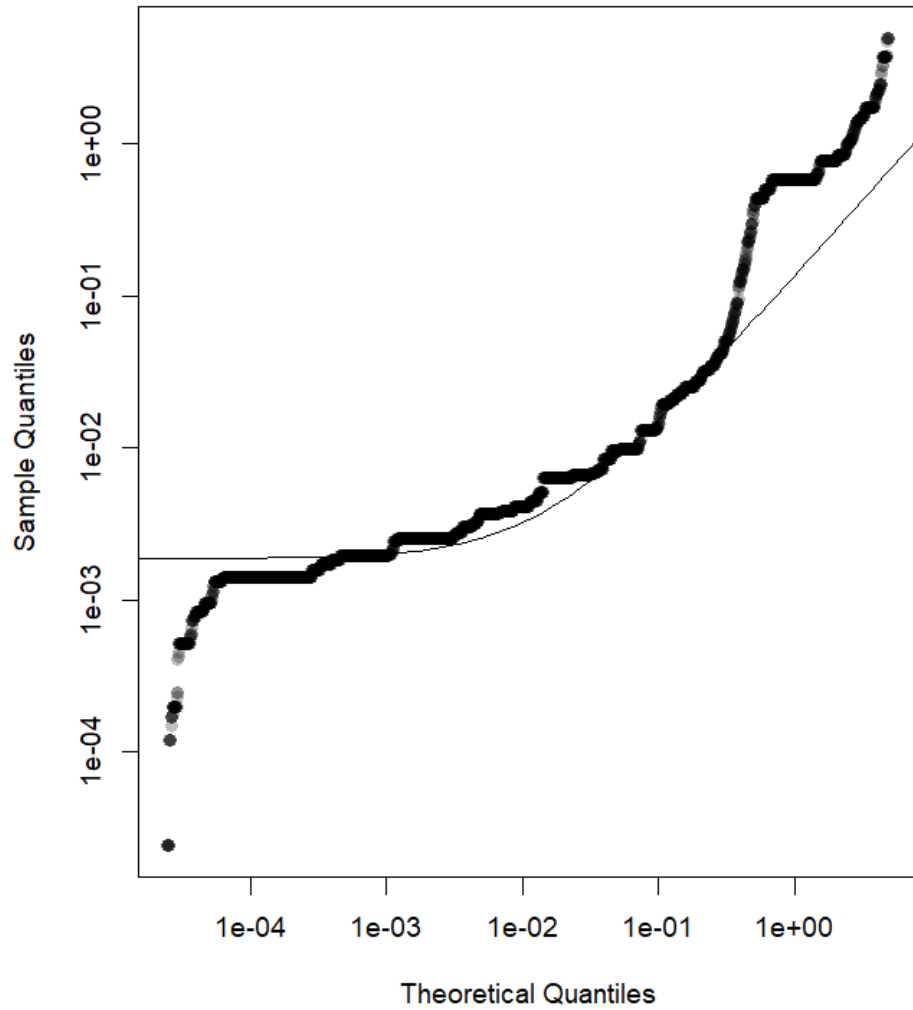


Figure B-26. Libbies Lair fish quantile-quantile (Q-Q) plots with (A) bounded power law and (B) log-normal distributions. The axes of the Q-Q plots are in log scale.

(A) Tenements : Power law Q-Q plot



(B) Tenements : Log-normal Q-Q plot

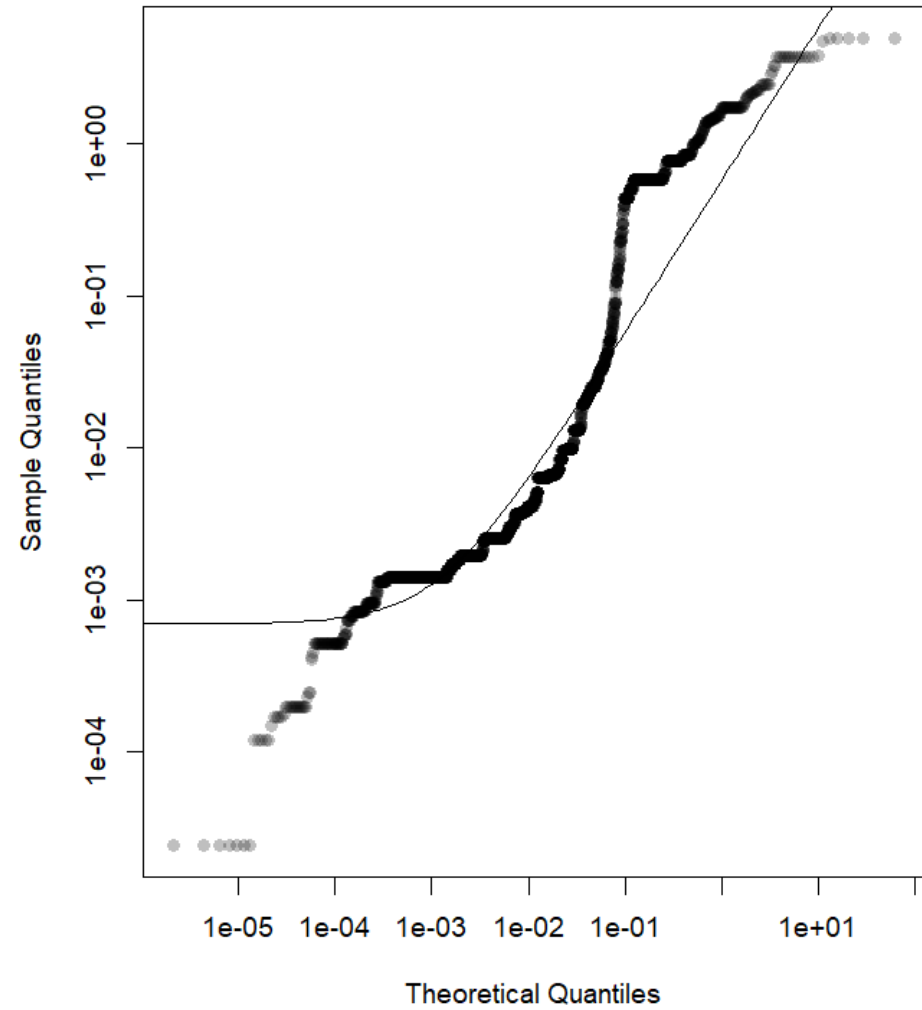
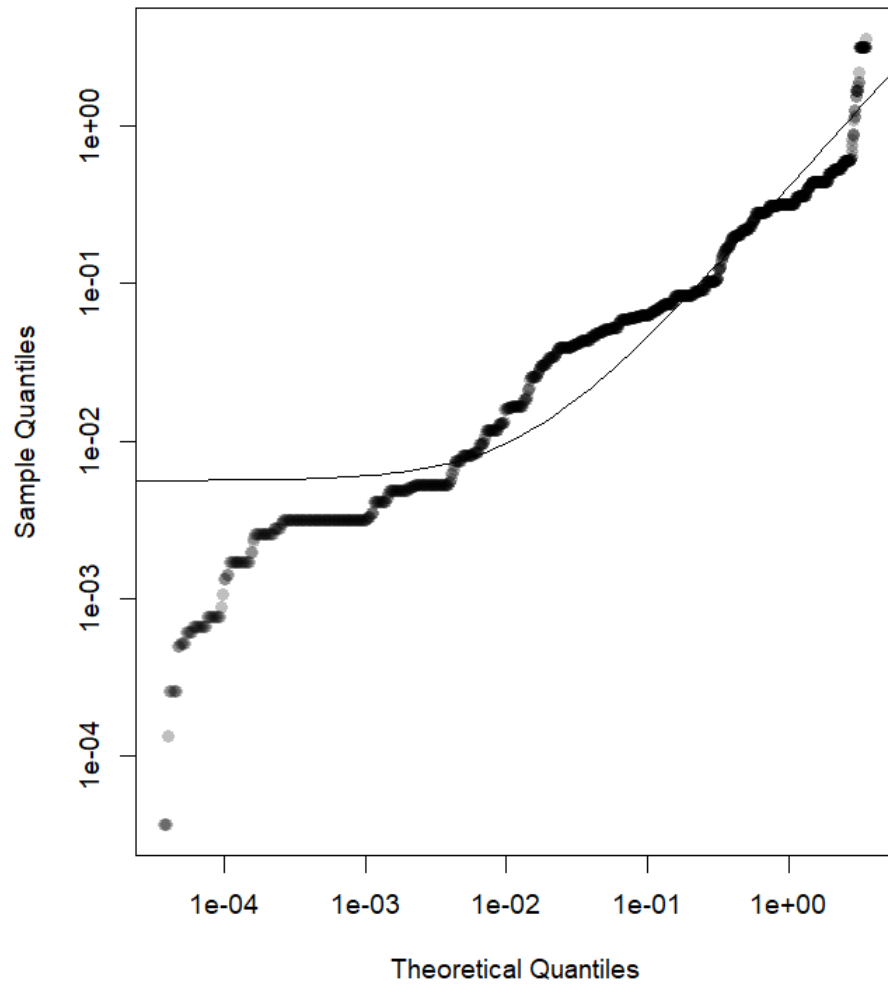


Figure B-27. Tenements fish quantile-quantile (Q-Q) plots with (A) bounded power law and (B) log-normal distributions. The axes of the Q-Q plots are in log scale.

(A) Flat Rock : Power law Q-Q plot



(B) Flat Rock : Log-normal Q-Q plot

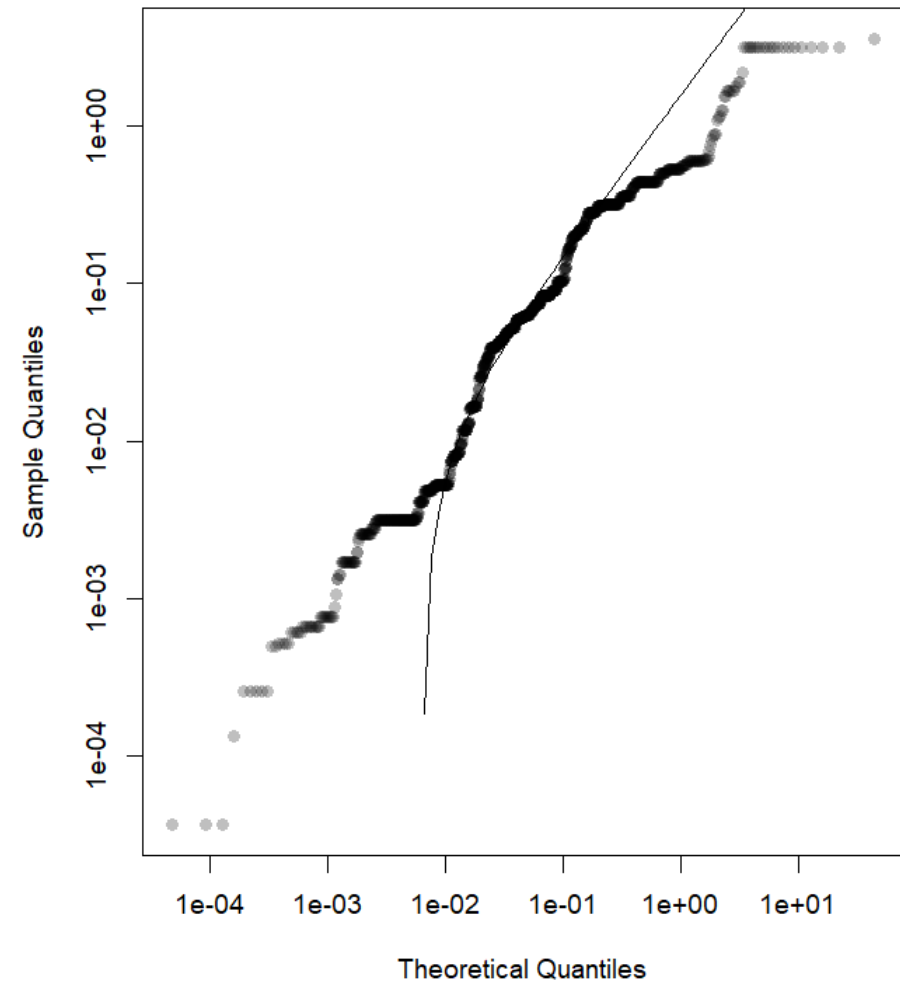
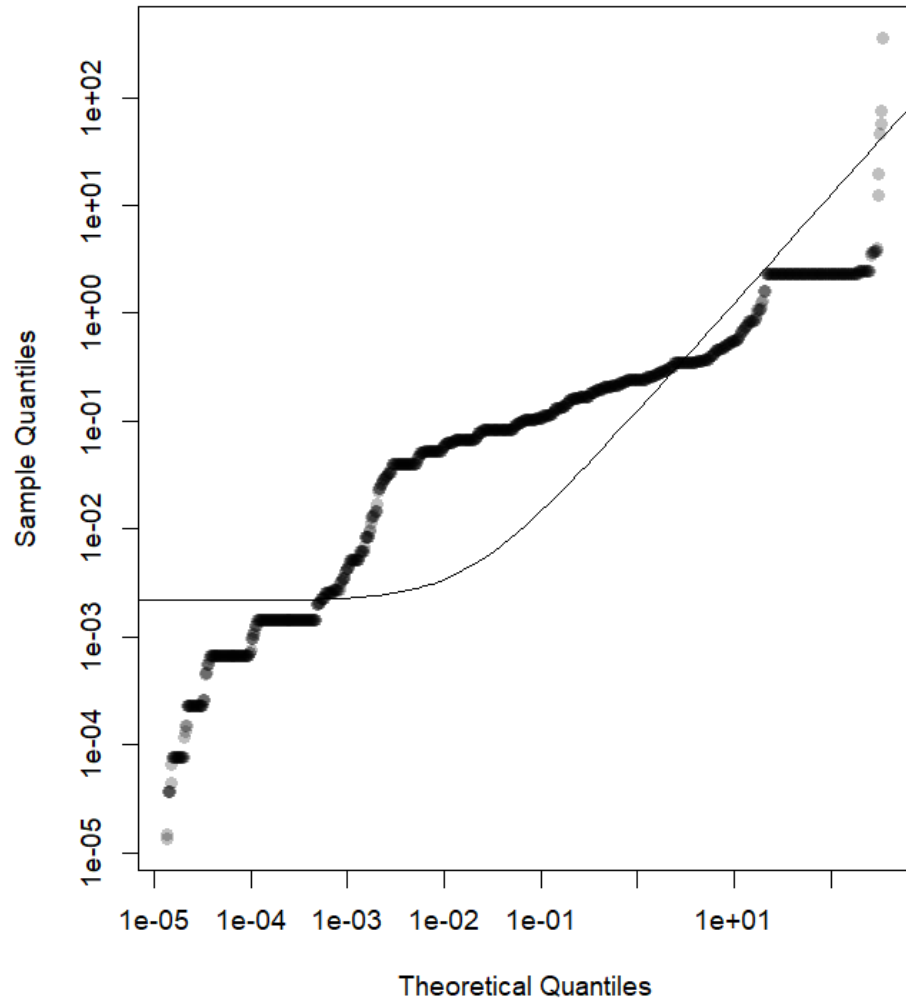


Figure B-28. Flat Rock fish quantile-quantile (Q-Q) plots with (A) bounded power law and (B) log-normal distributions. The axes of the Q-Q plots are in log scale.

(A) Henderson Rock : Power law Q-Q plot



(B) Henderson Rock : Log-normal Q-Q plot

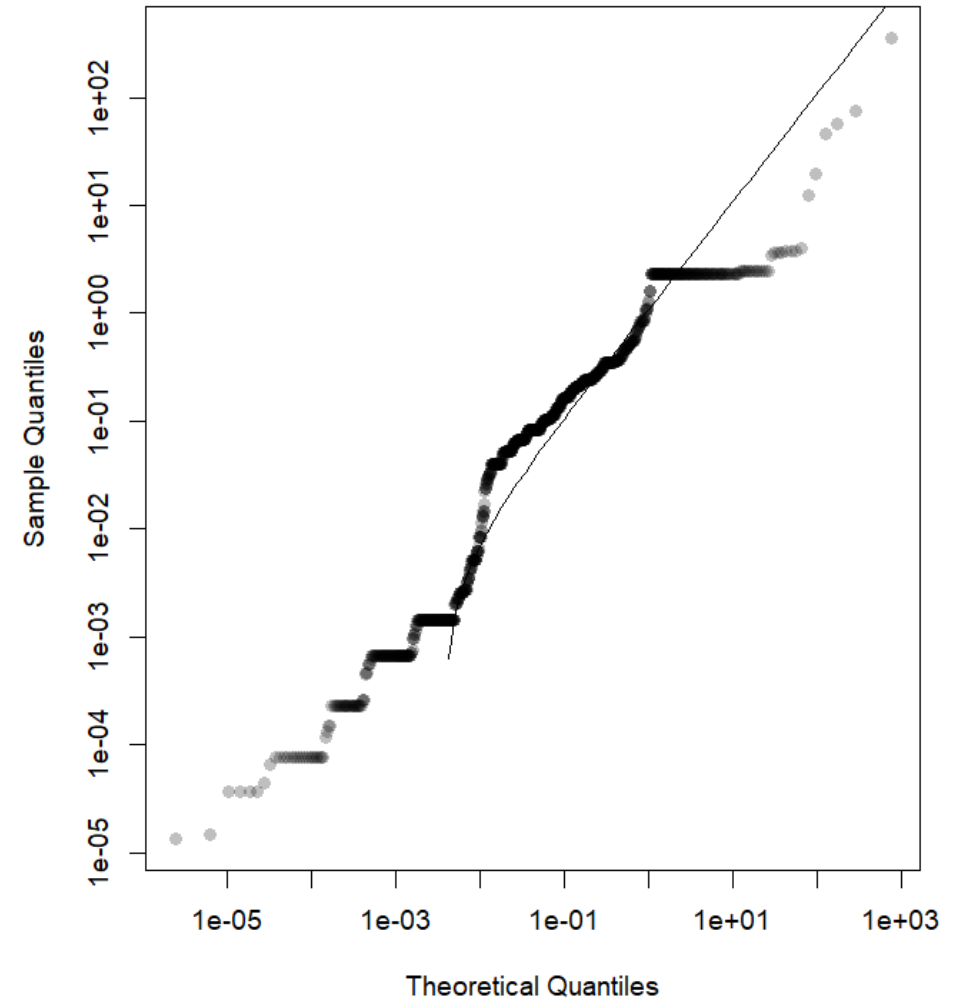
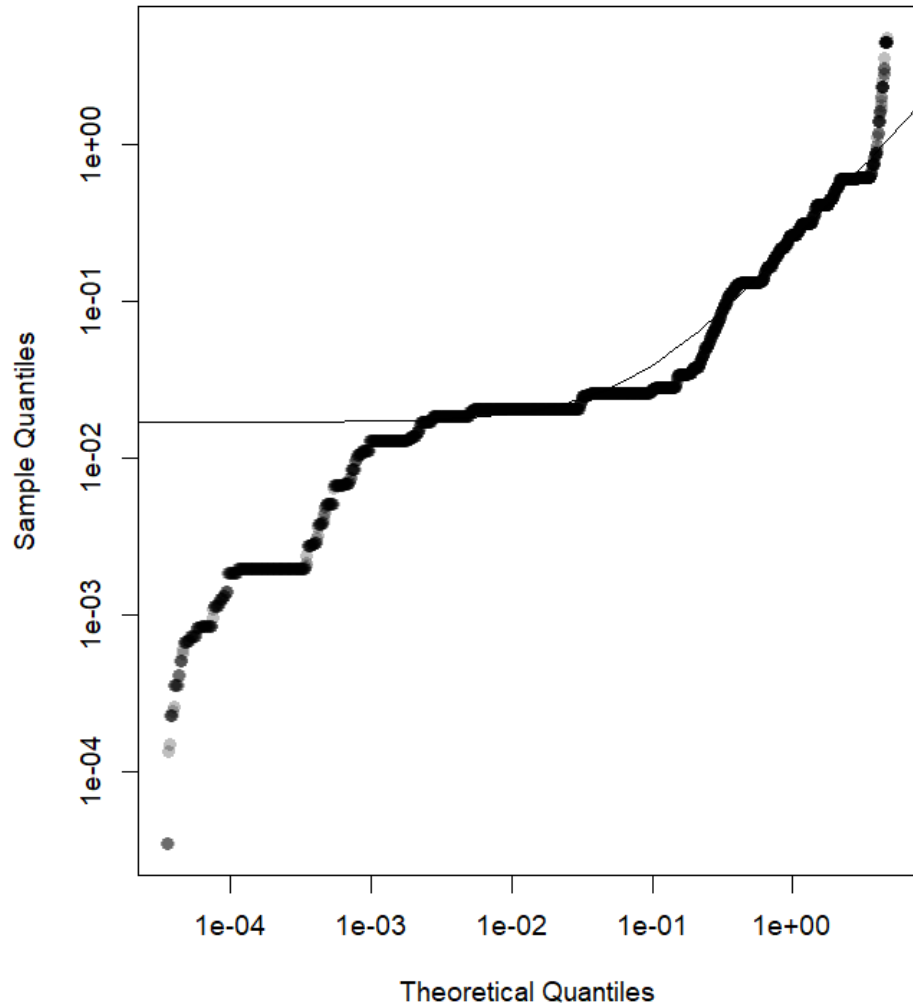


Figure B-29. Henderson Rock fish quantile-quantile (Q-Q) plots with (A) bounded power law and (B) log-normal distributions. The axes of the Q-Q plots are in log scale.

(A) Flinders : Power law Q-Q plot



(B) Flinders : Log-normal Q-Q plot

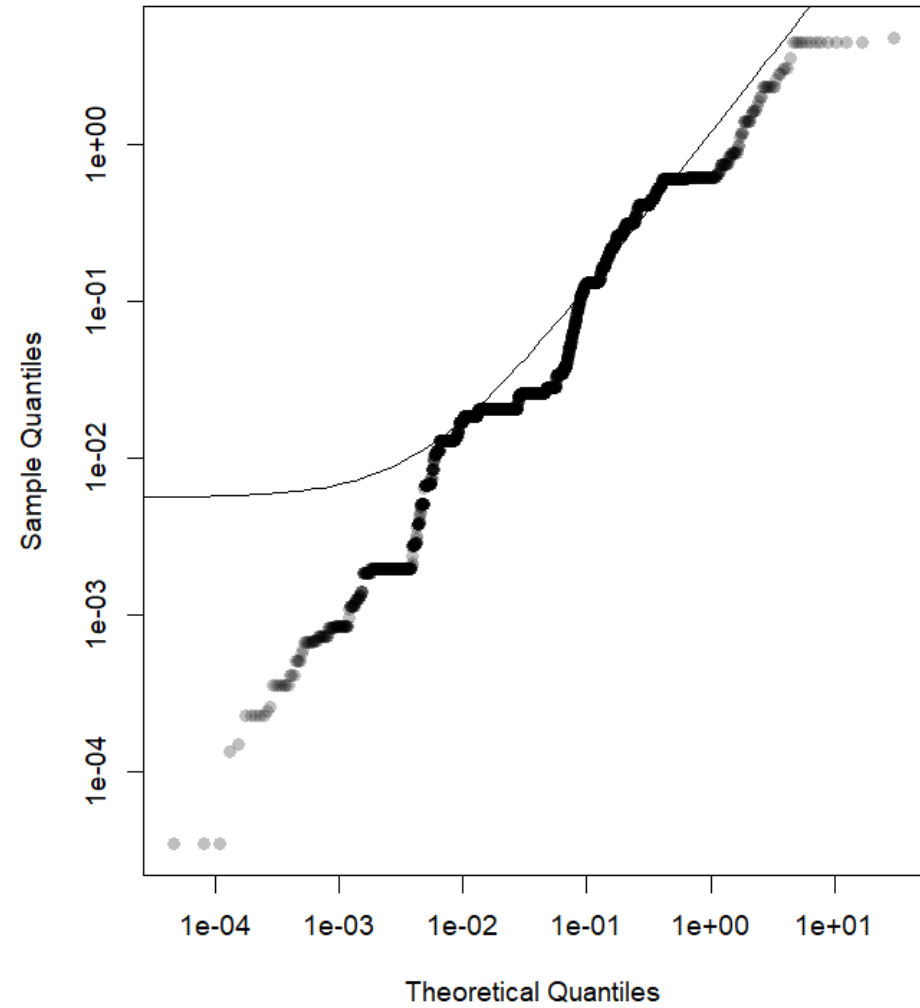
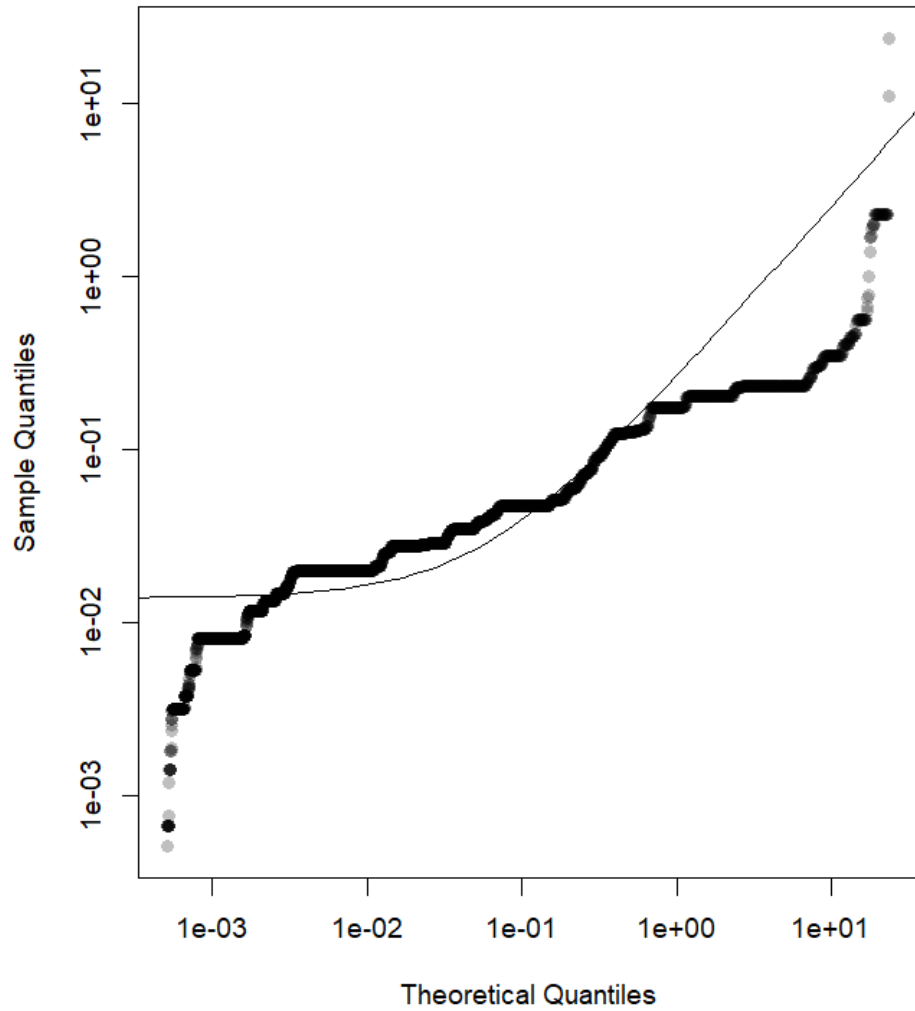


Figure B-30. Flinders fish quantile-quantile (Q-Q) plots with (A) bounded power law and (B) log-normal distributions. The axes of the Q-Q plots are in log scale.

(A) Inner Gneering Shoals : Power law Q-Q plot



(B) Inner Gneering Shoals : Log-normal Q-Q plot

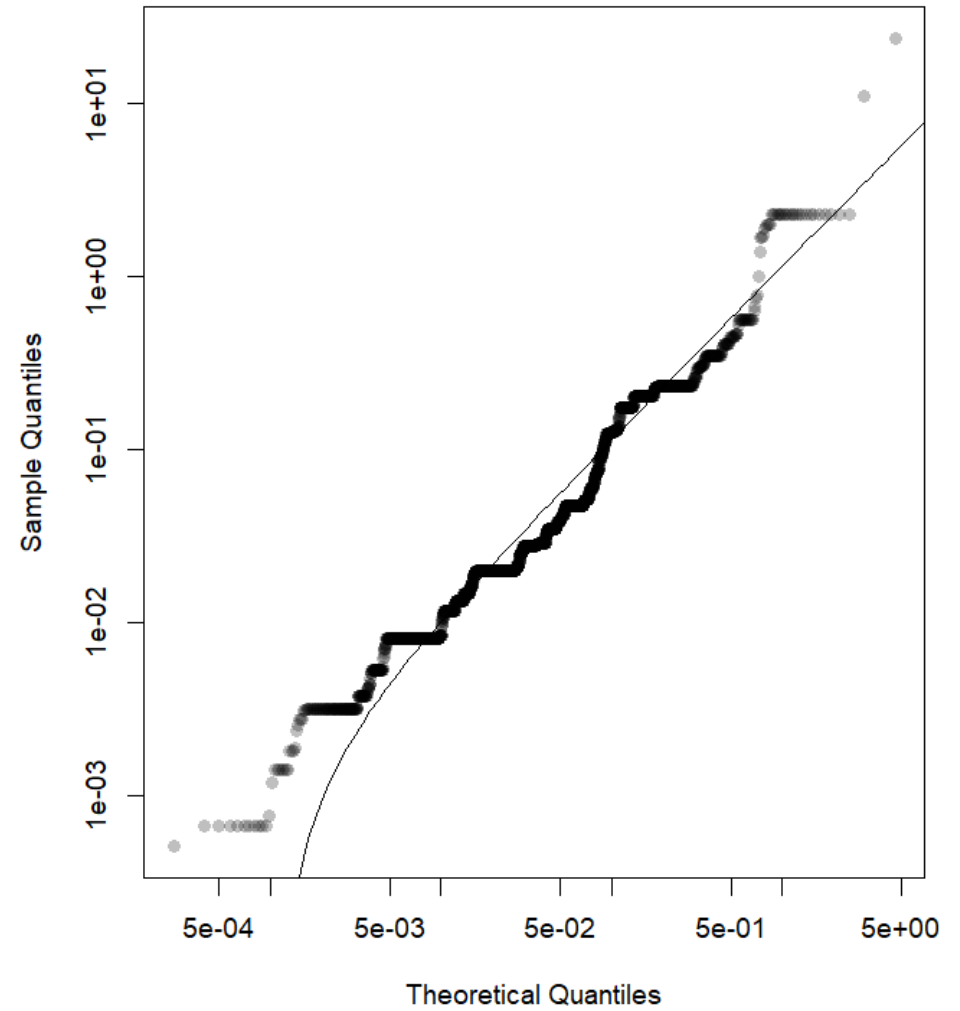


Figure B-31. Inner Gneering Shoals fish quantile-quantile (Q-Q) plots with (A) bounded power law and (B) log-normal distributions. The axes of the Q-Q plots are in log scale.

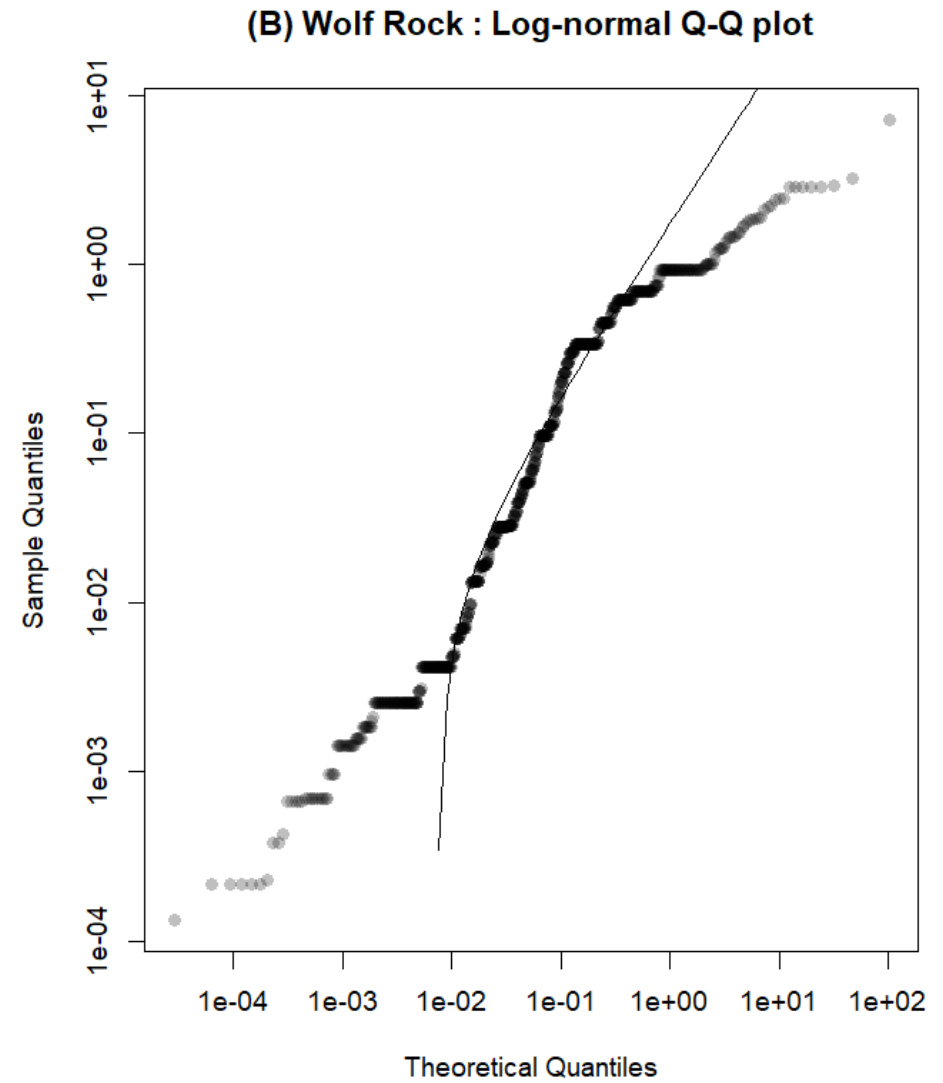
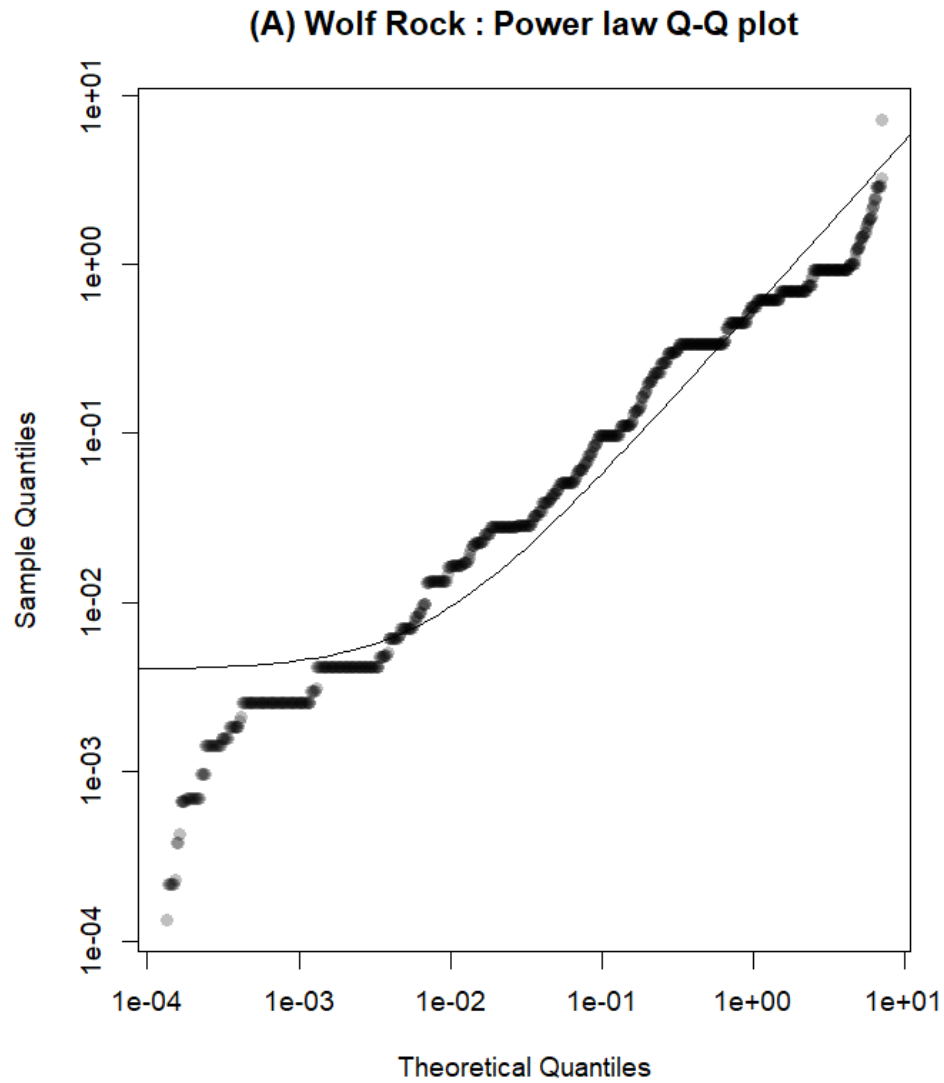


Figure B-32. Wolf Rock fish quantile-quantile (Q-Q) plots with (A) bounded power law and (B) log-normal distributions. The axes of the Q-Q plots are in log scale.

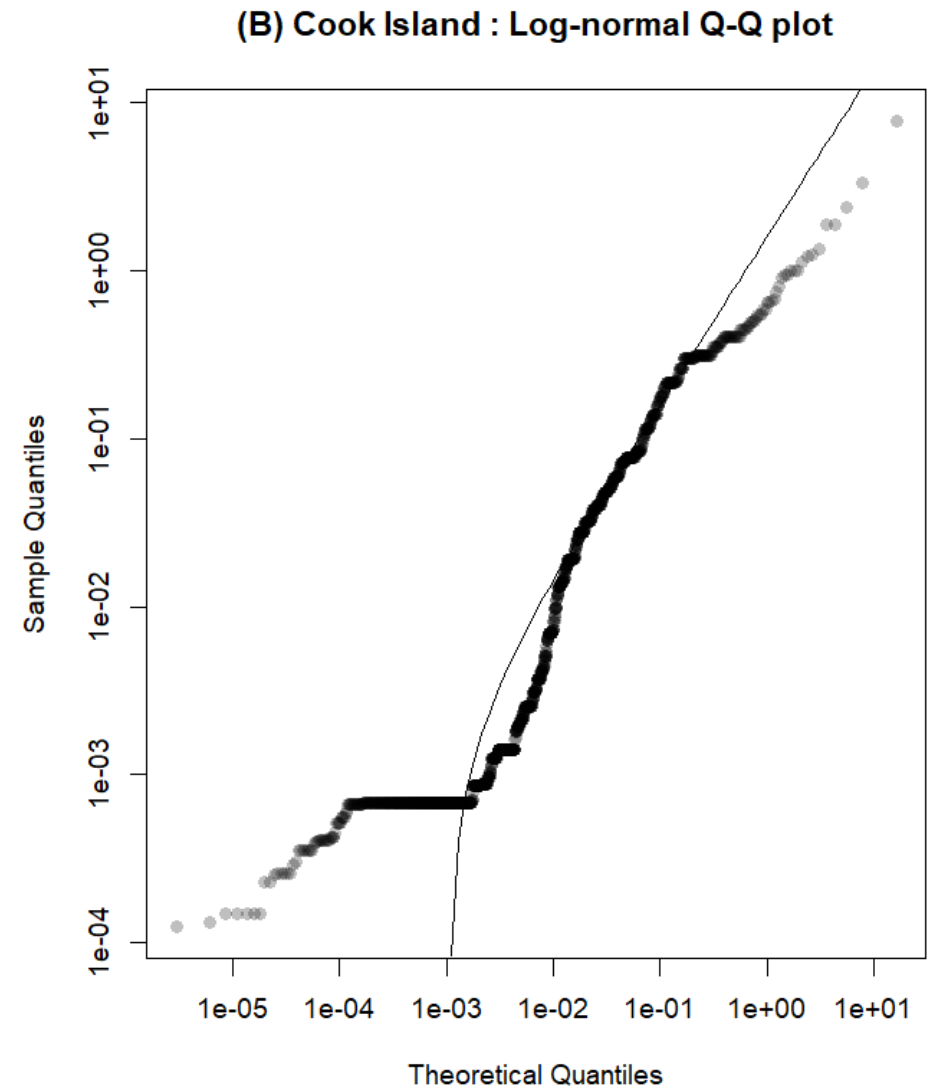
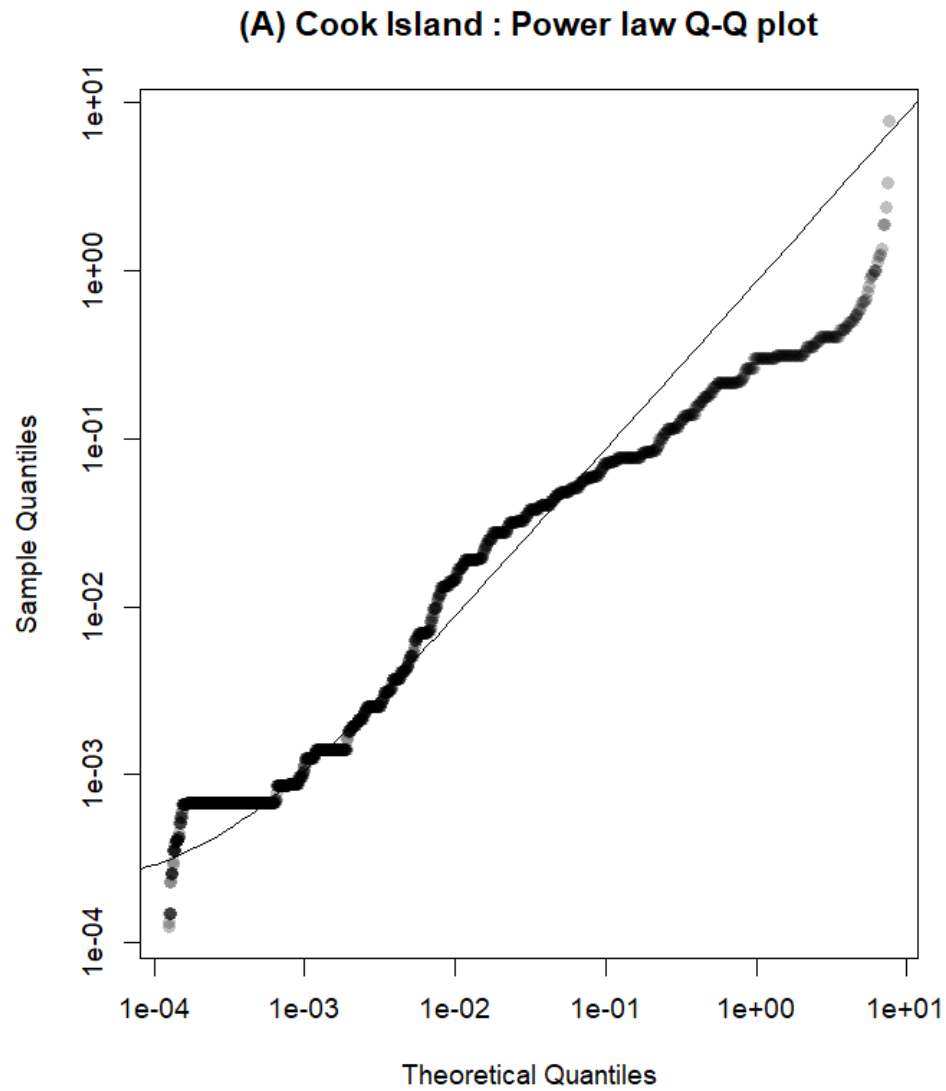
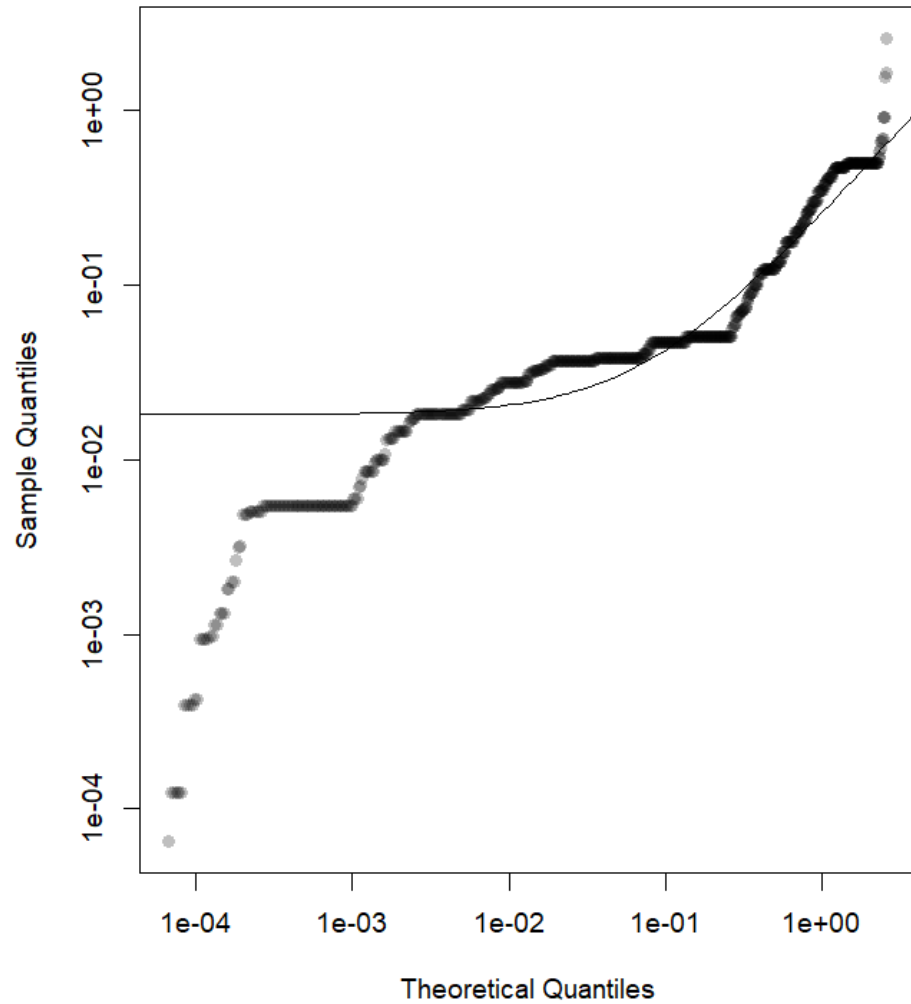


Figure B-33. Cook Island fish quantile-quantile (Q-Q) plots with (A) bounded power law and (B) log-normal distributions. The axes of the Q-Q plots are in log scale.

(A) Mudjimba : Power law Q-Q plot



(B) Mudjimba : Log-normal Q-Q plot

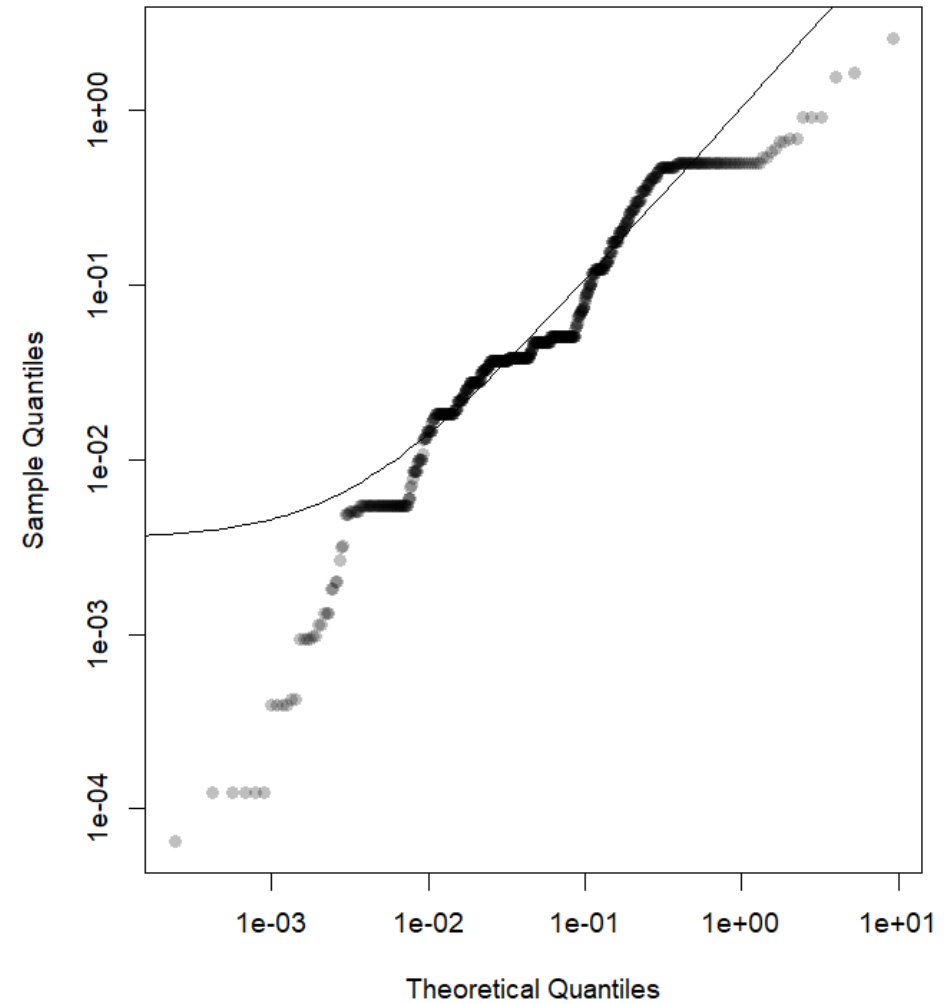
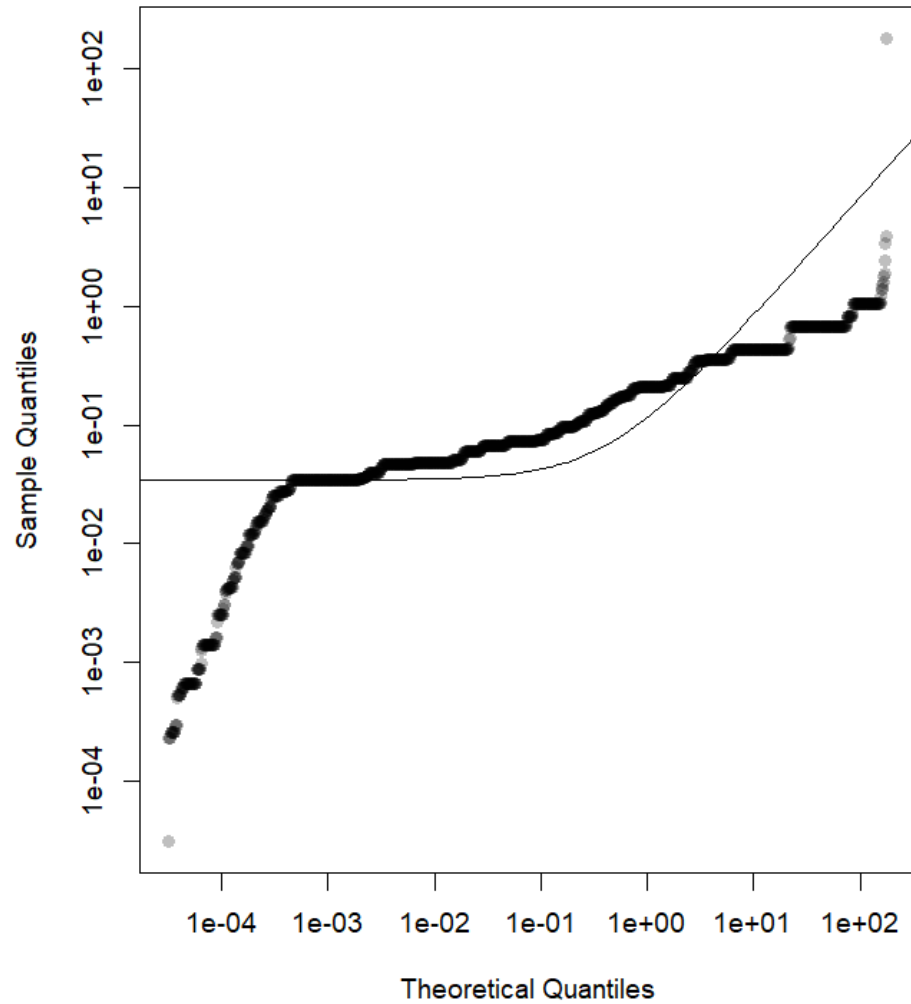


Figure B-34. Mudjimba fish quantile-quantile (Q-Q) plots with (A) bounded power law and (B) log-normal distributions. The axes of the Q-Q plots are in log scale.

(A) North Solitary Island : Power law Q-Q plot



(B) North Solitary Island : Log-normal Q-Q plot

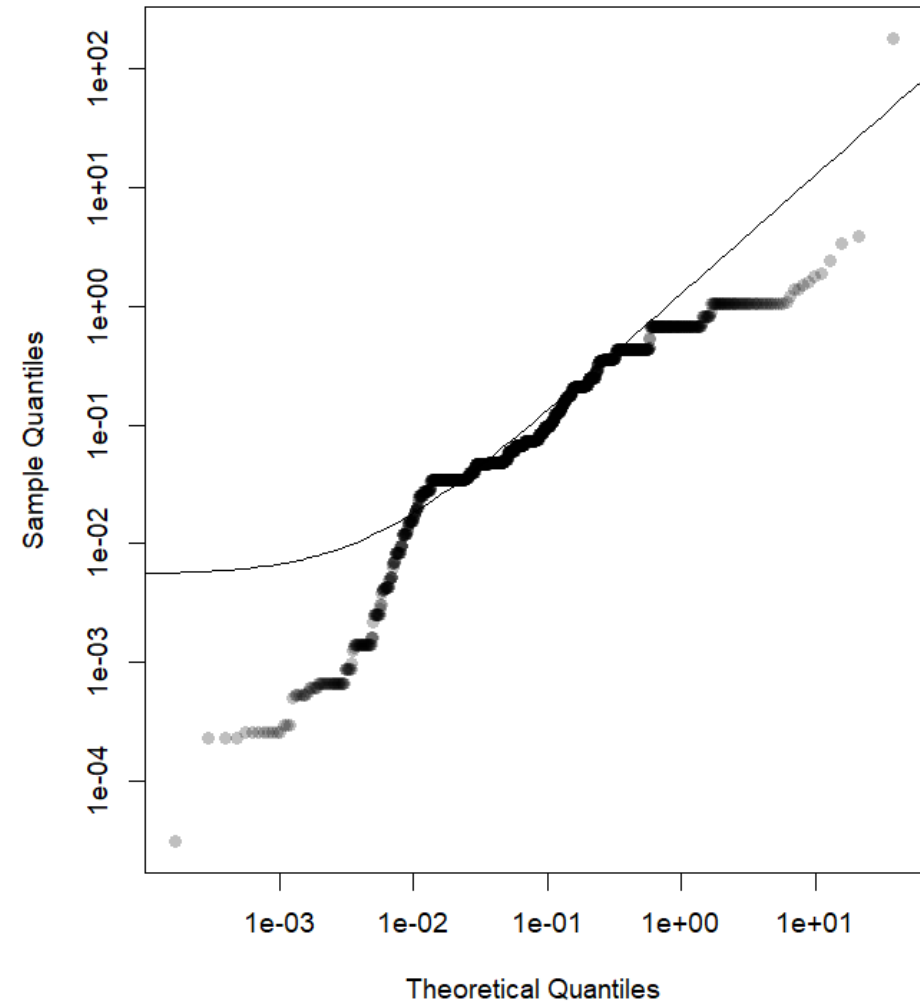
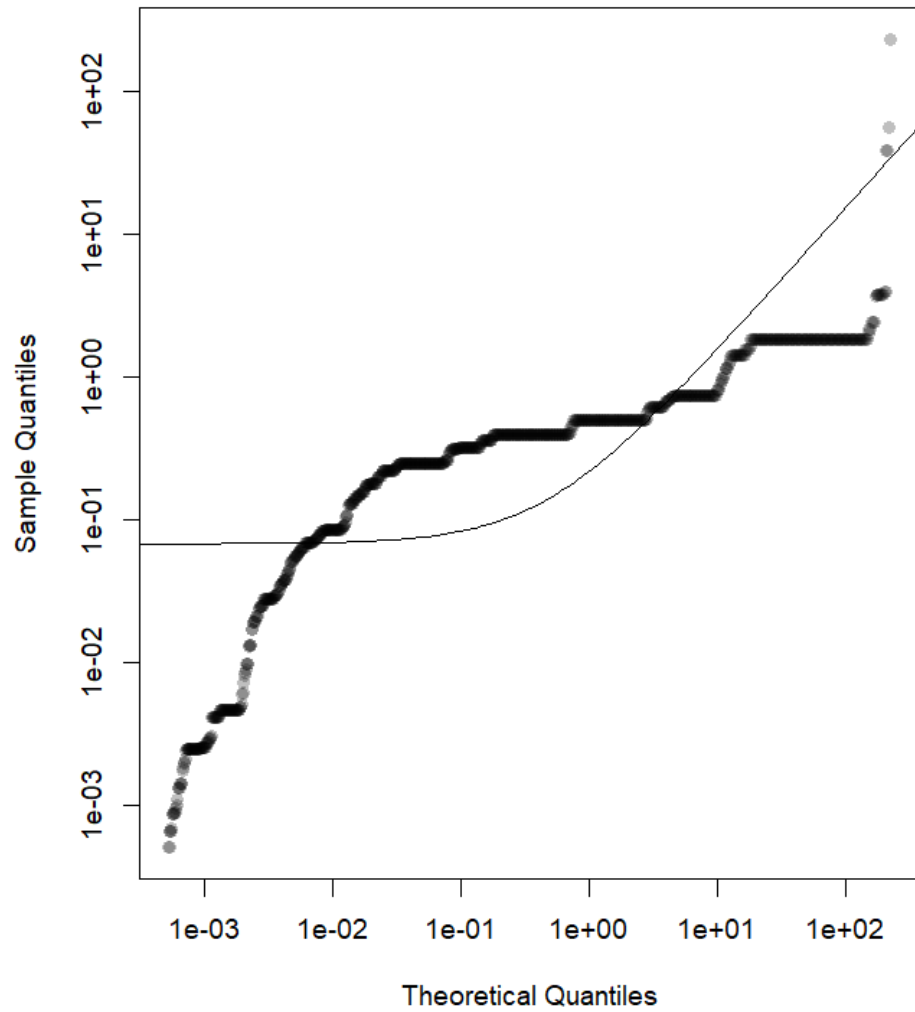


Figure B-35. North Solitary Island fish quantile-quantile (Q-Q) plots with (A) bounded power law and (B) log-normal distributions. The axes of the Q-Q plots are in log scale.

(A) Julian Rock False Trench : Power law Q-Q plot



(B) Julian Rock False Trench : Log-normal Q-Q plot

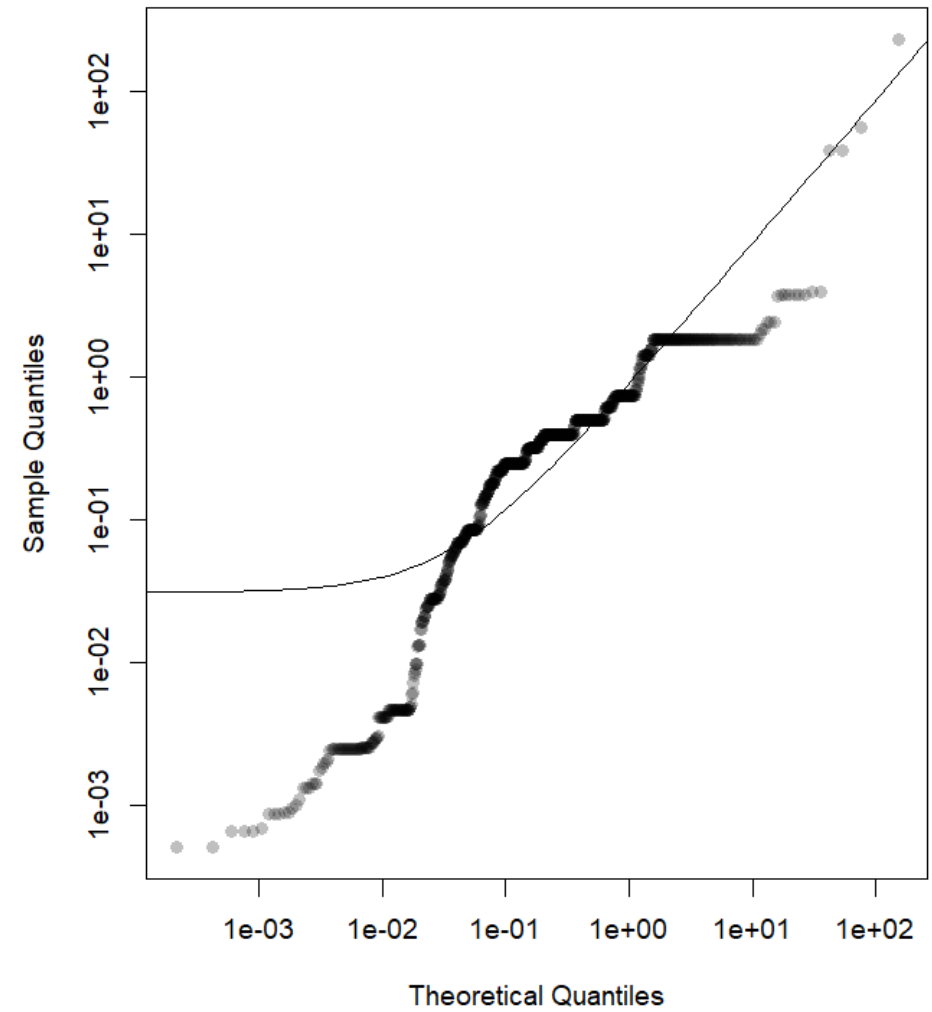
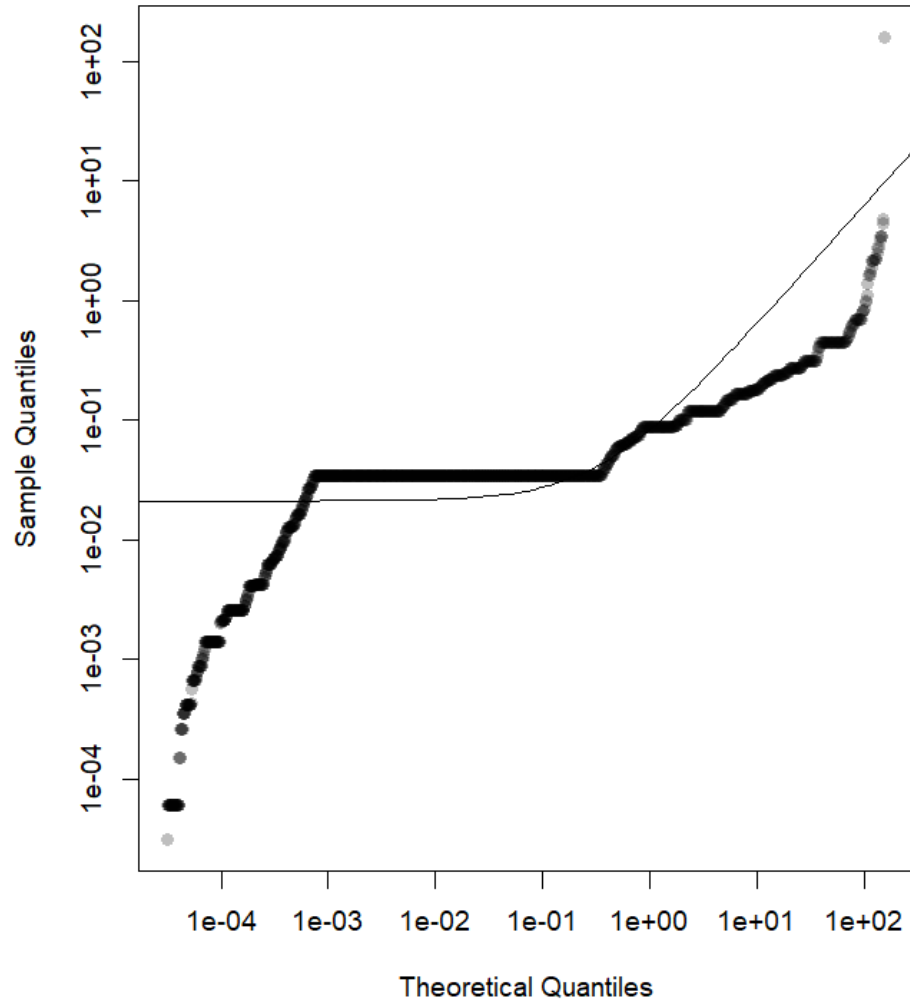


Figure B-36. Julian Rock False Trench fish quantile-quantile (Q-Q) plots with (A) bounded power law and (B) log-normal distributions. The axes of the Q-Q plots are in log scale

(A) Julian Rock Nursery : Power law Q-Q plot



(B) Julian Rock Nursery : Log-normal Q-Q plot

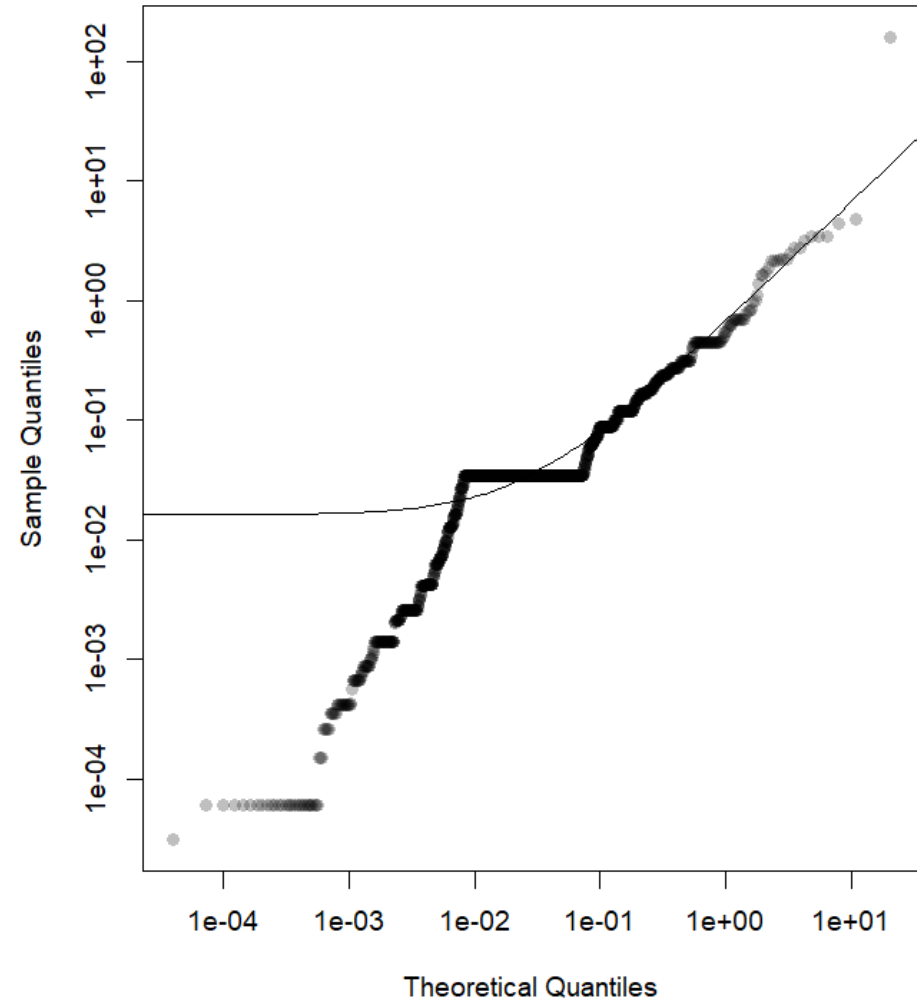
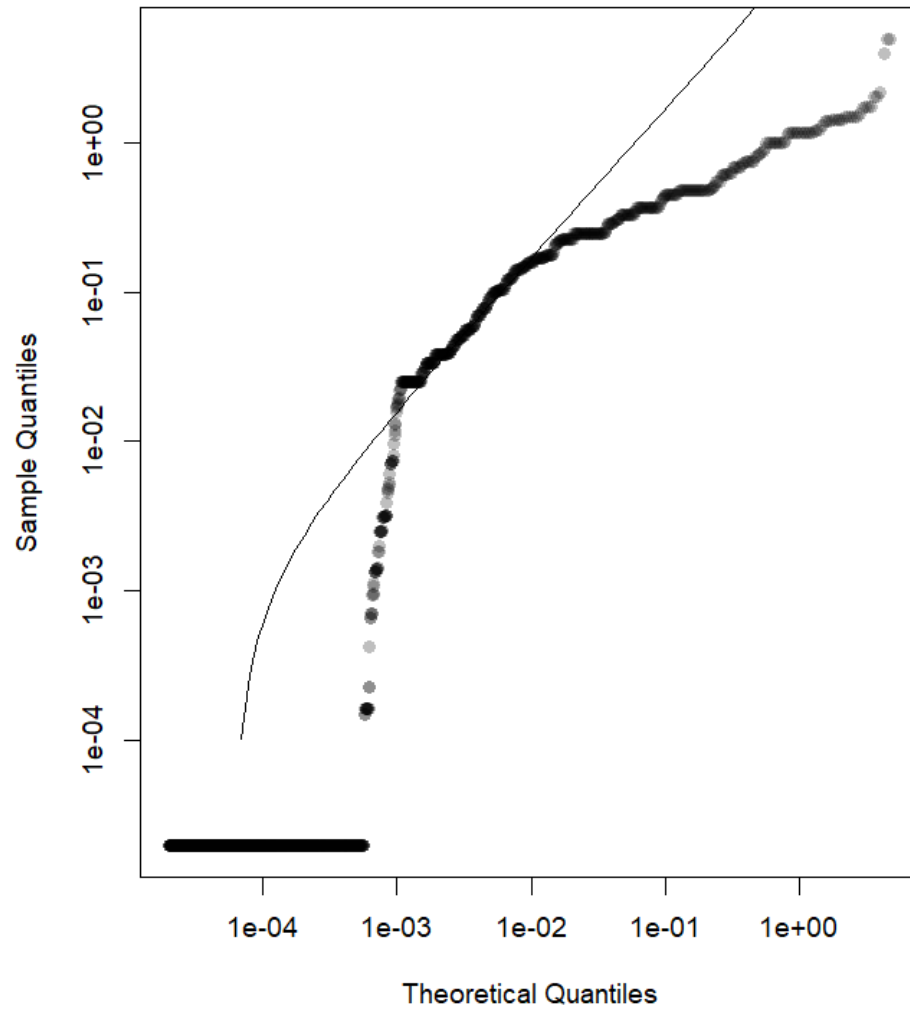


Figure B-37. Julian Rock Nursery fish quantile-quantile (Q-Q) plots with (A) bounded power law and (B) log-normal distributions. The axes of the Q-Q plots are in log scale.

(A) Black Rock : Power law Q-Q plot



(B) Black Rock : Log-normal Q-Q plot

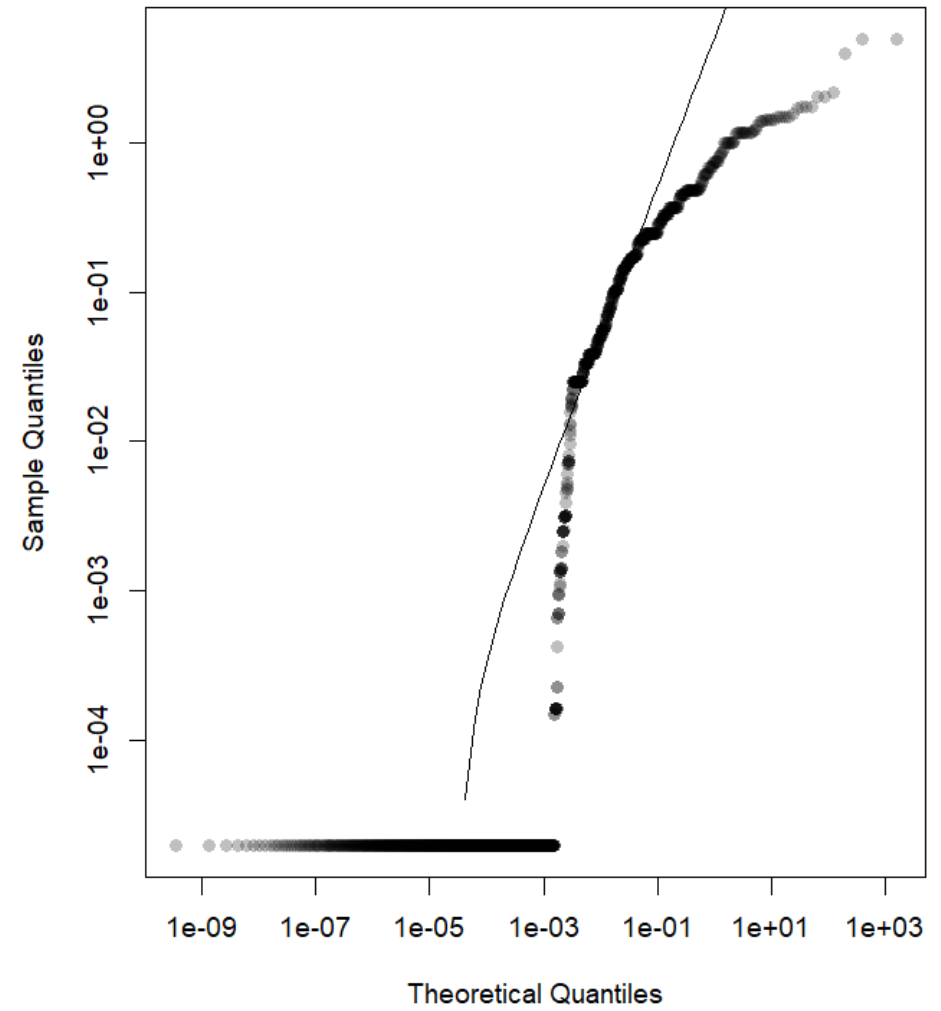
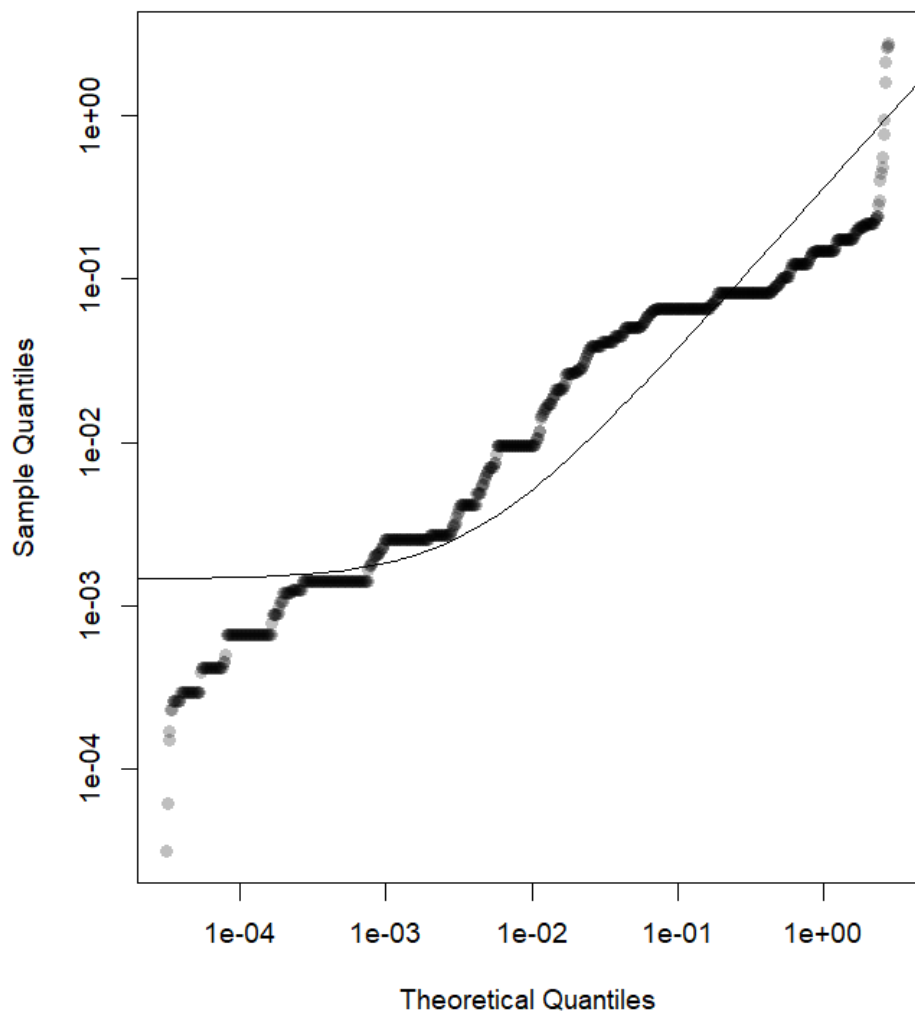


Figure B-38. Black Rock fish quantile-quantile (Q-Q) plots with (A) bounded power law and (B) log-normal distributions. The axes of the Q-Q plots are in log scale.

(A) South Solitary Island : Power law Q-Q plot



(B) South Solitary Island : Log-normal Q-Q plot

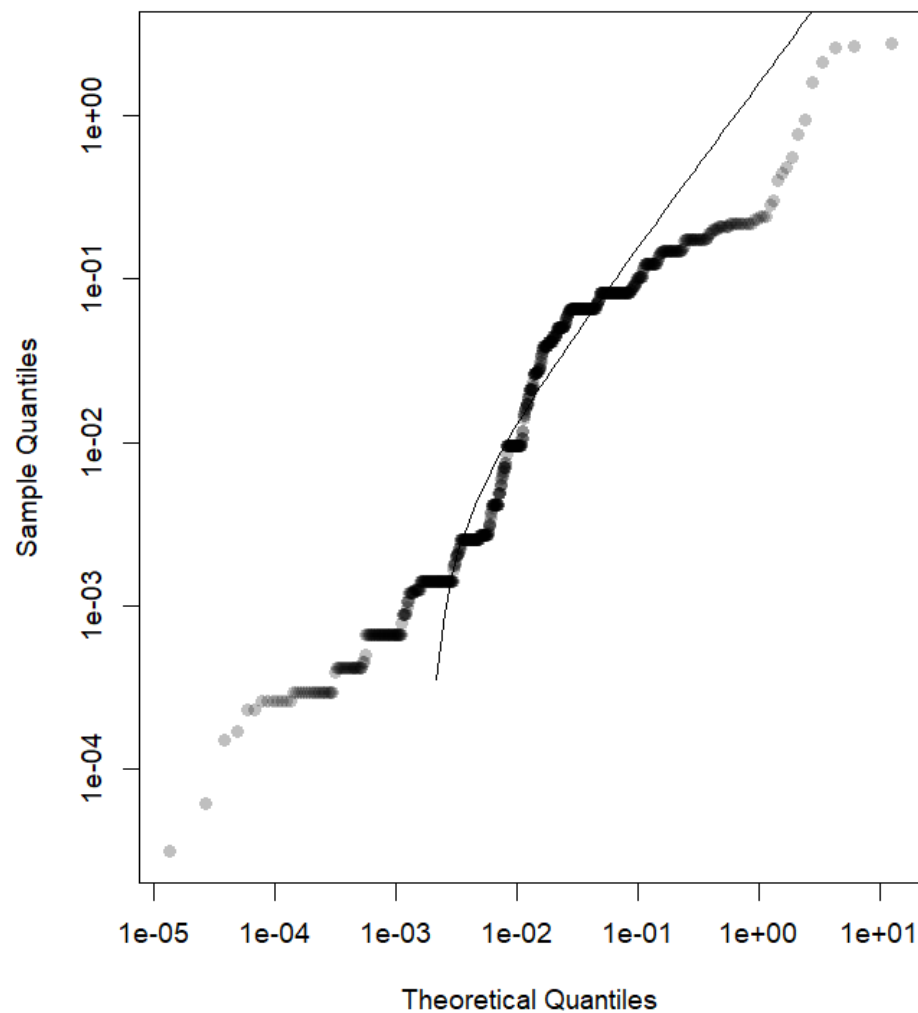
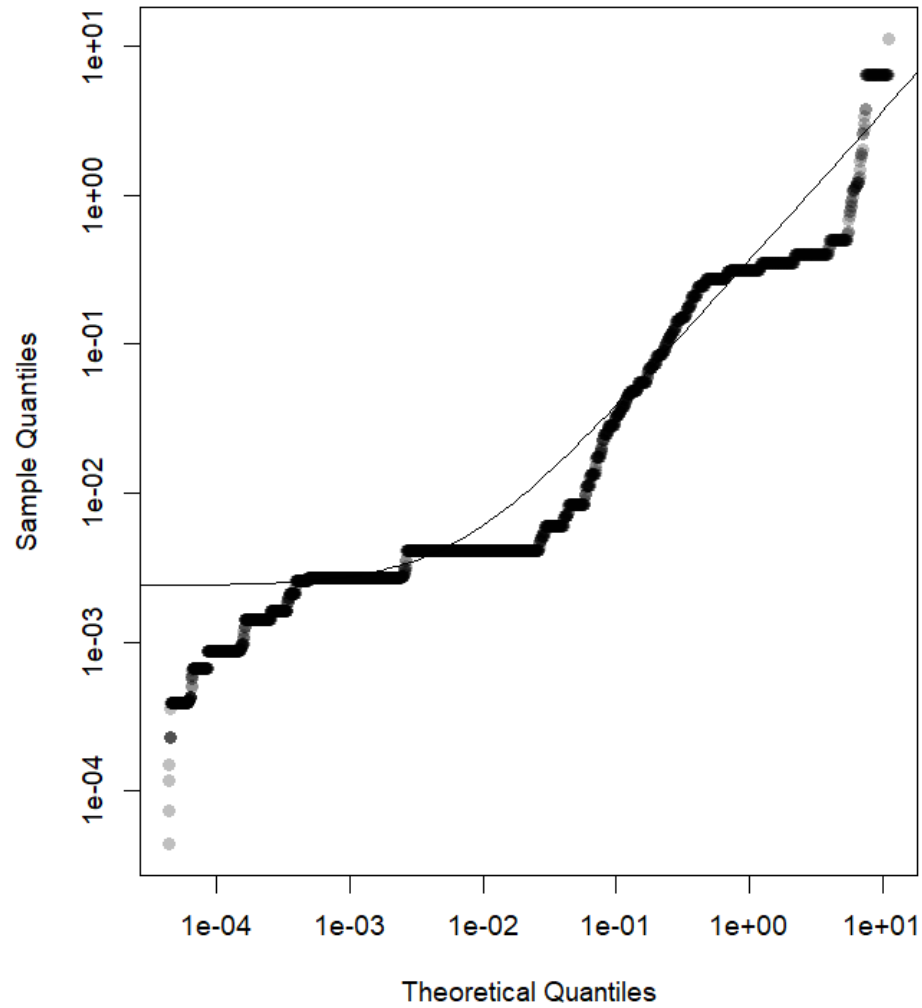


Figure B-39. South Solitary Island fish quantile-quantile (Q-Q) plots with (A) bounded power law and (B) log-normal distributions. The axes of the Q-Q plots are in log scale.

(A) North West Solitary Island : Power law Q-Q plot



(B) North West Solitary Island : Log-normal Q-Q plot

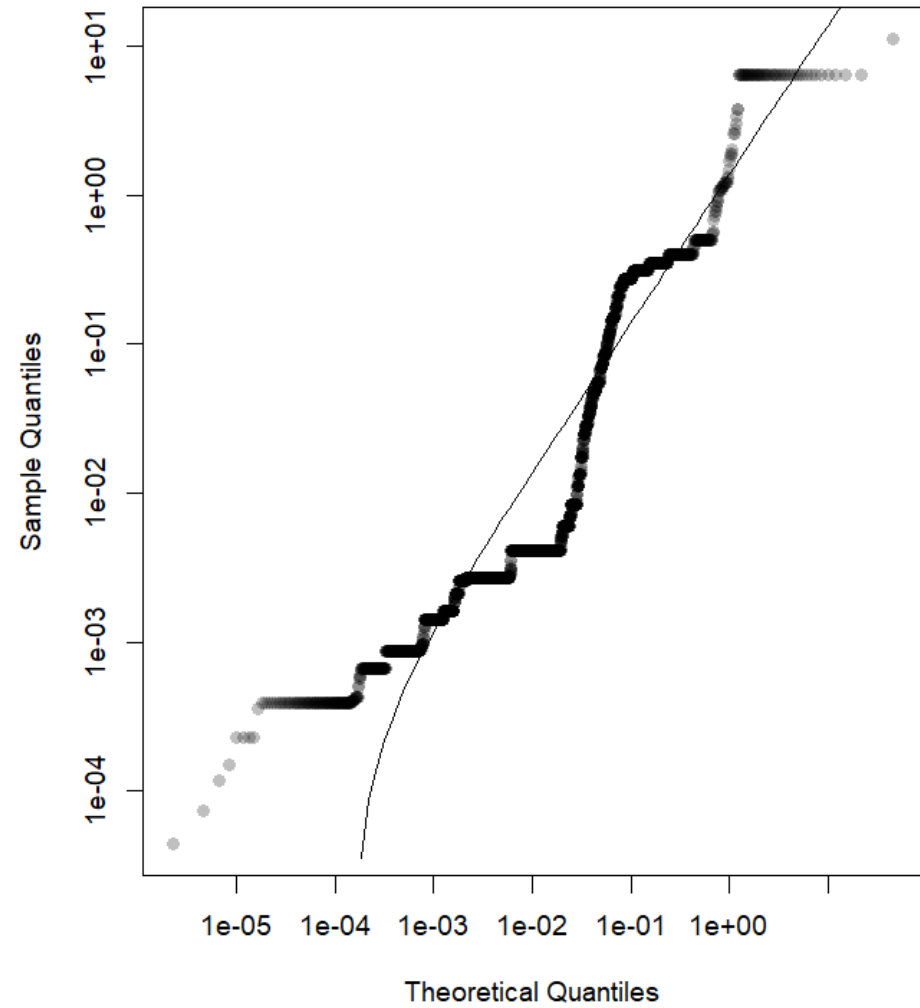
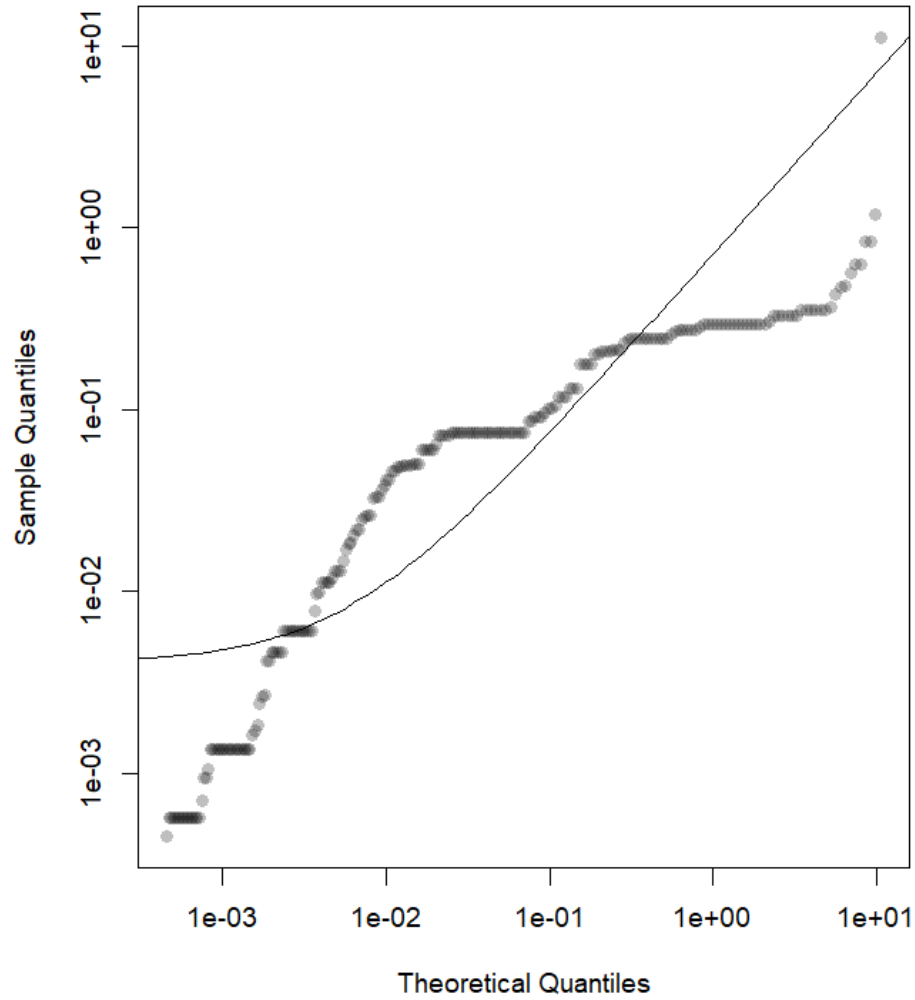


Figure B-40. North West Solitary Island fish quantile-quantile (Q-Q) plots with (A) bounded power law and (B) log-normal distributions. The axes of the Q-Q plots are in log scale.

(A) Woolgoolga Reef : Power law Q-Q plot



(B) Woolgoolga Reef : Log-normal Q-Q plot

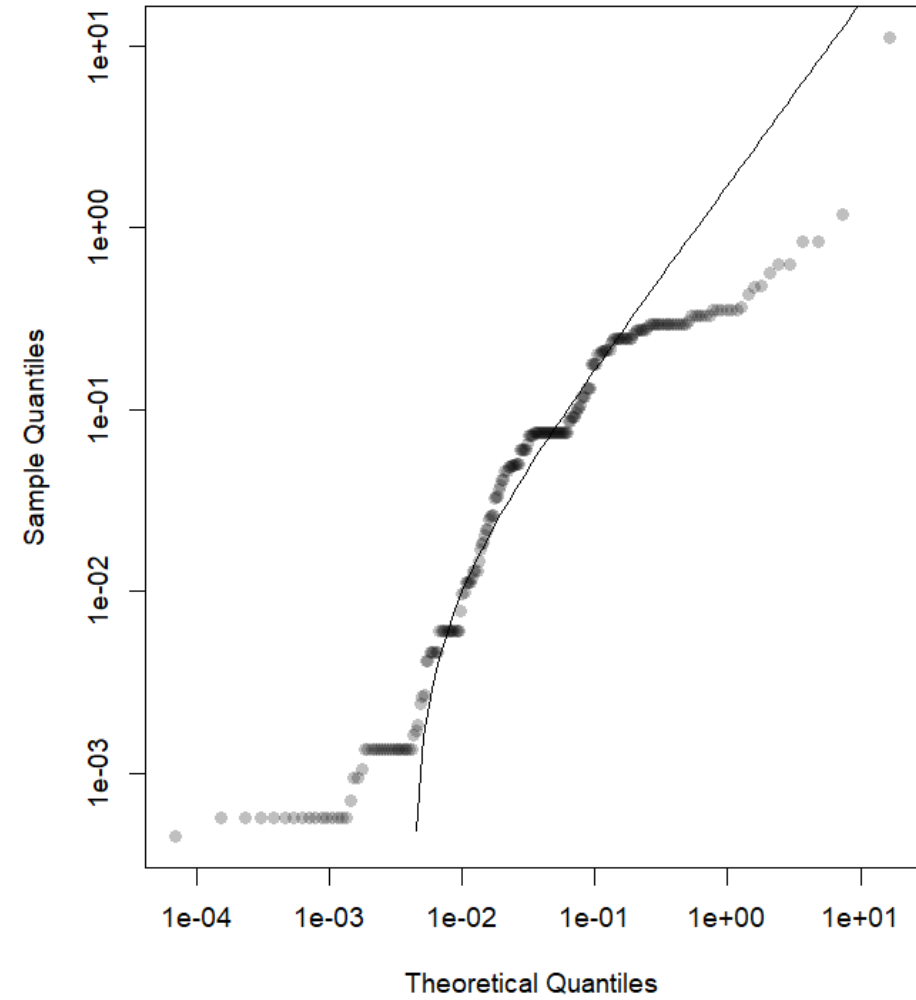
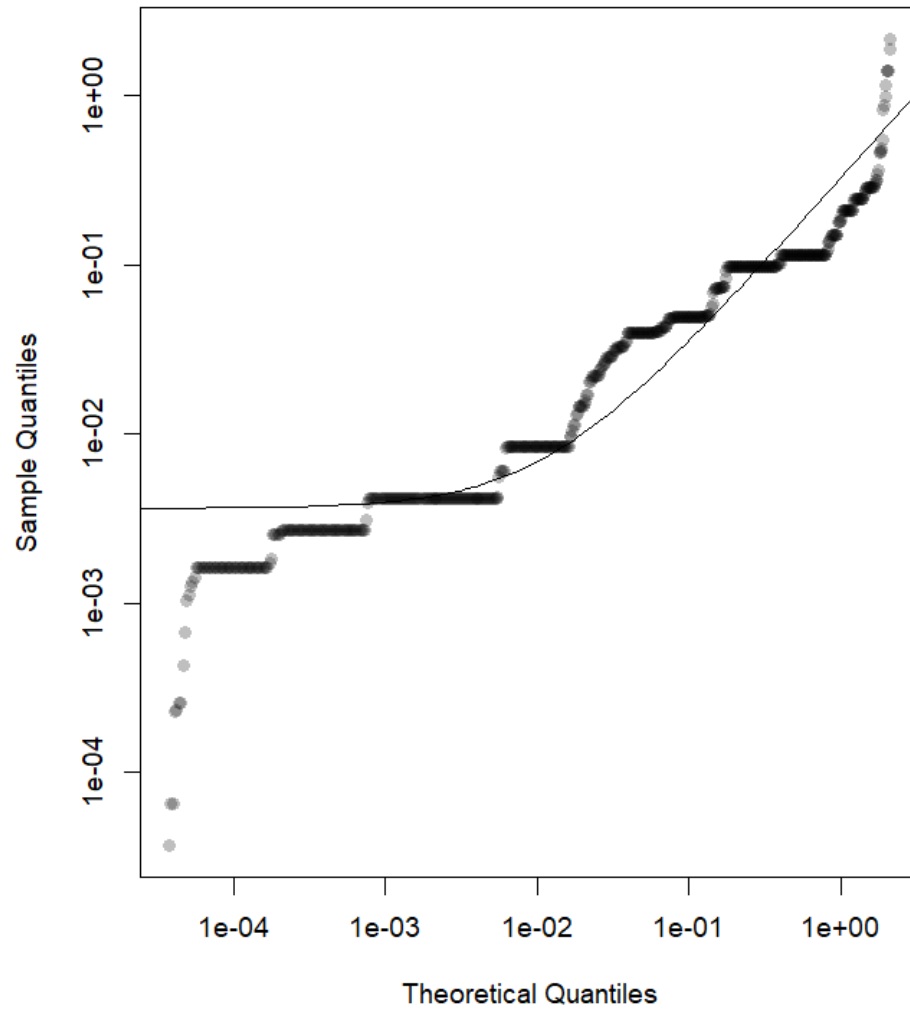


Figure B-41. Woolgoolga Reef fish quantile-quantile (Q-Q) plots with (A) bounded power law and (B) log-normal distributions. The axes of the Q-Q plots are in log scale.

(A) North Rock : Power law Q-Q plot



(B) North Rock : Log-normal Q-Q plot

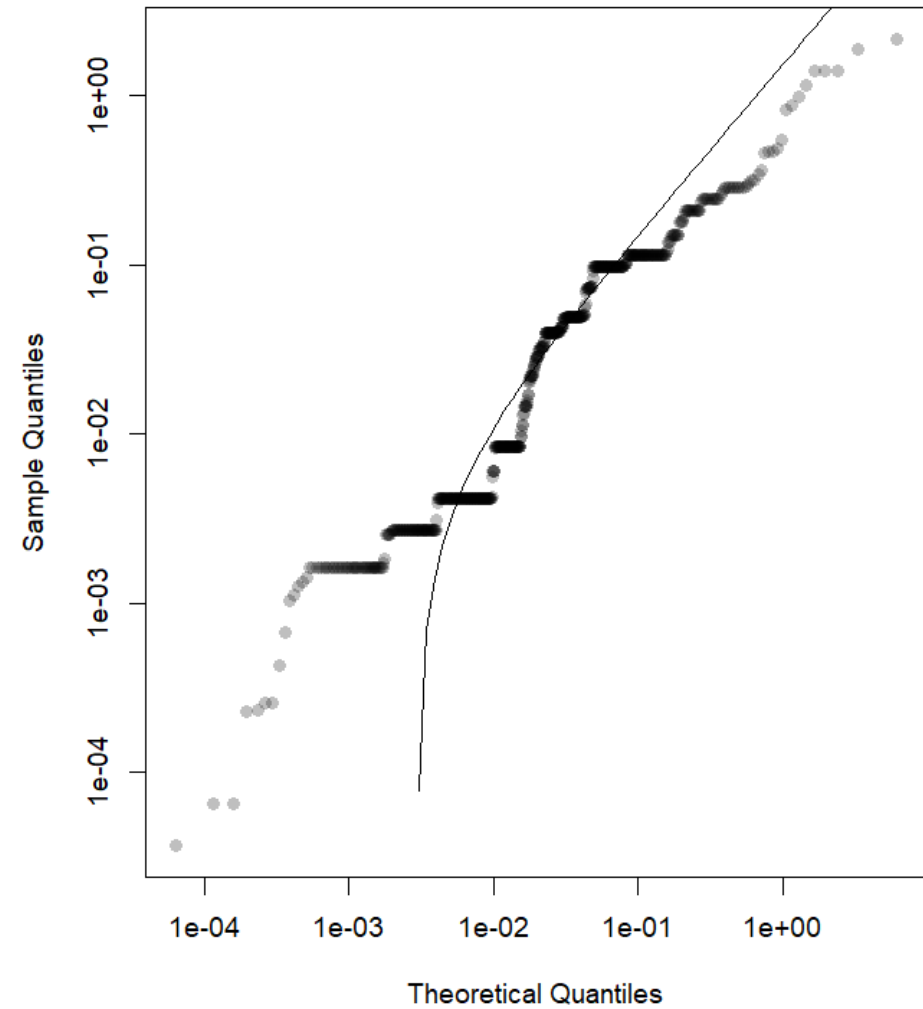
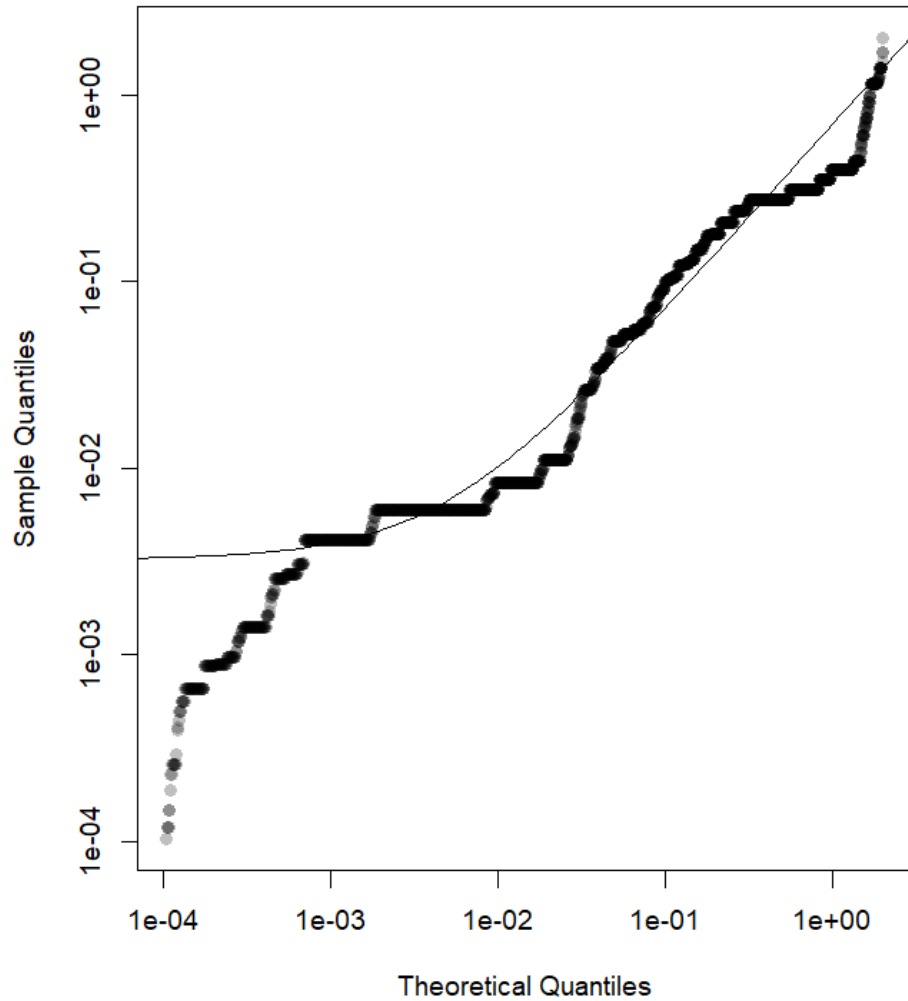


Figure B-42. North Rock fish quantile-quantile (Q-Q) plots with (A) bounded power law and (B) log-normal distributions. The axes of the Q-Q plots are in log scale.

(A) South West Solitary Island : Power law Q-Q plot



(B) South West Solitary Island : Log-normal Q-Q plot

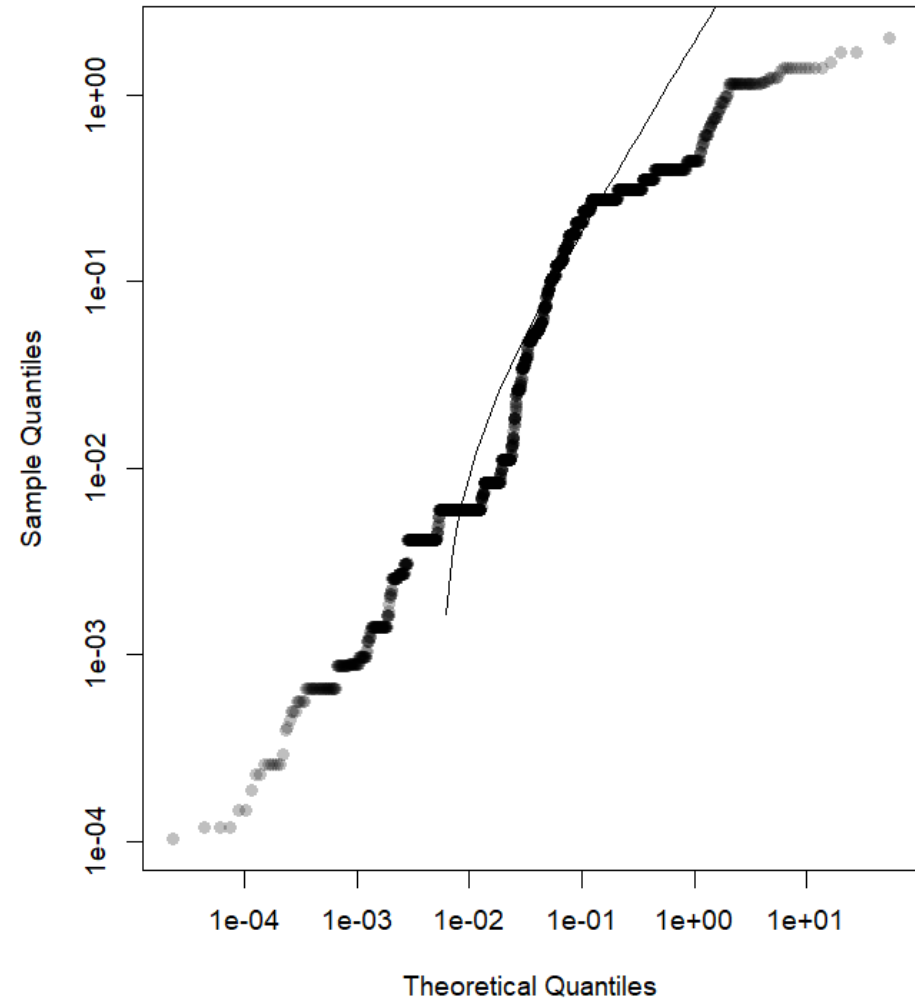


Figure B-43. South West Solitary Island fish quantile-quantile (Q-Q) plots with (A) bounded power law and (B) log-normal distributions. The axes of the Q-Q plots are in log scale.

S5: Indonesian fish data from Carvalho *et al.* (2021)

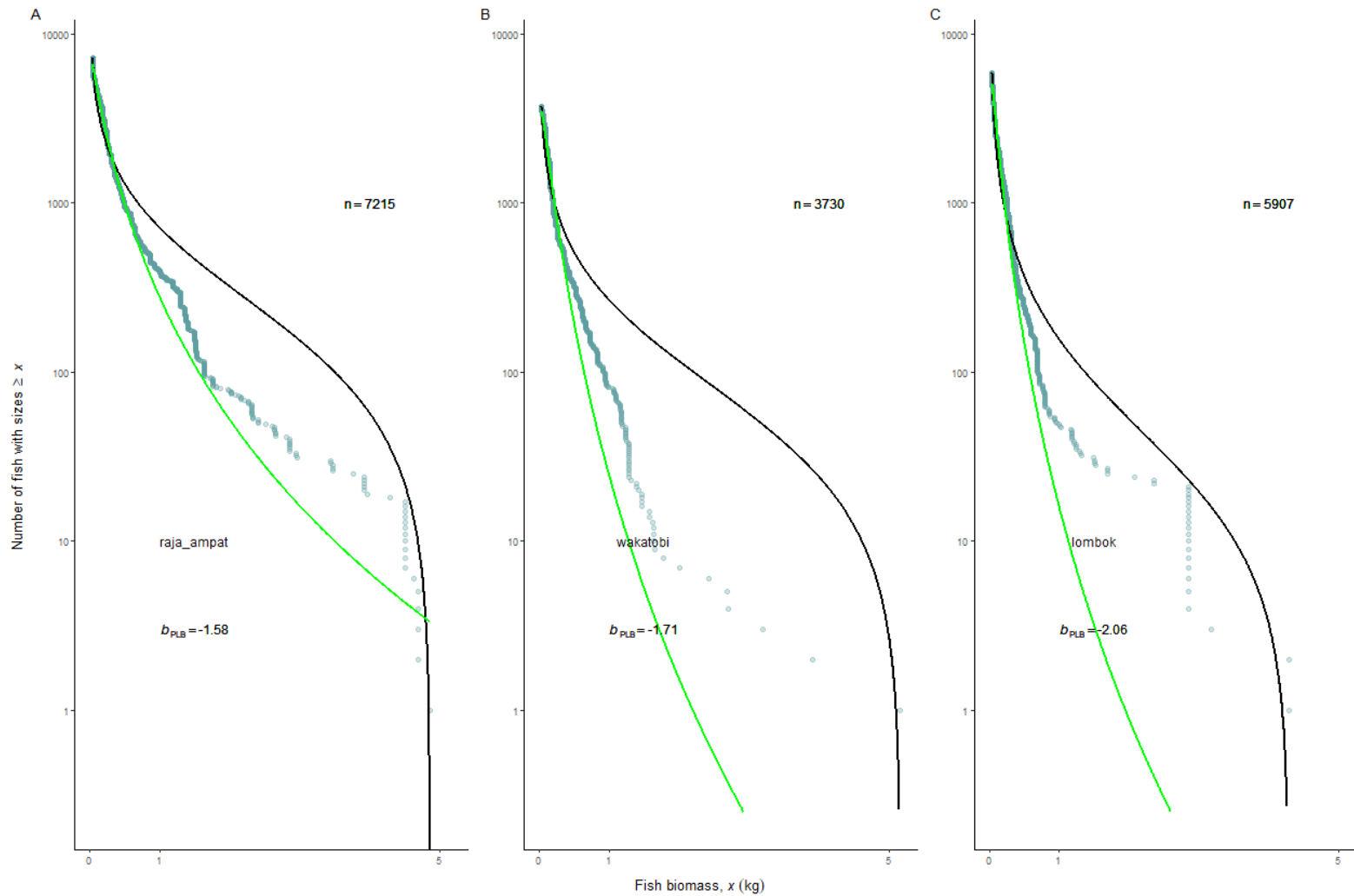
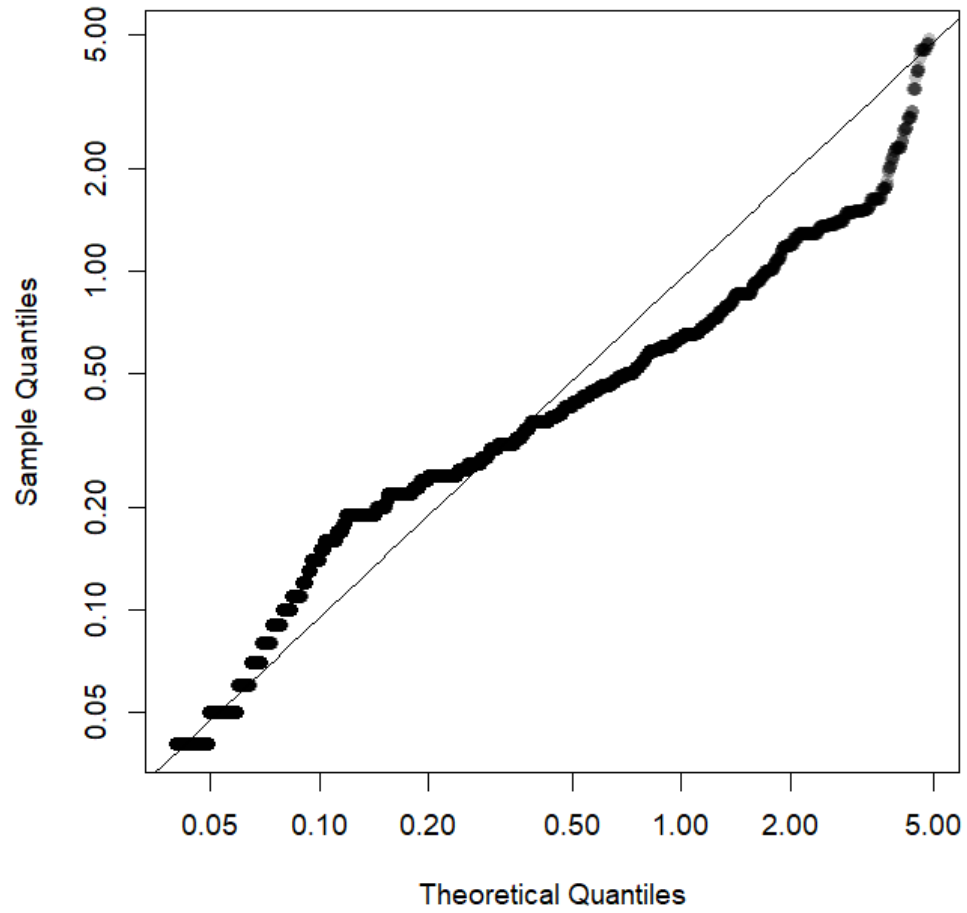


Figure B-44. The number of fishes with biomass $\geq x$ plotted against biomass x in kg on logarithmic scales at (A) Raja Ampat, (B) Wakatobi and (C) Lombok. The number of fishes sampled from each site are indicated by “ n ”. Dark green circles are data points. Black lines: bounded power law; green lines: log-normal distribution. All lines are fitted by maximum likelihood estimation. The exponent b for bounded power law is displayed.

(A) raja_ampat : Power law



(B) raja_ampat : Log-normal

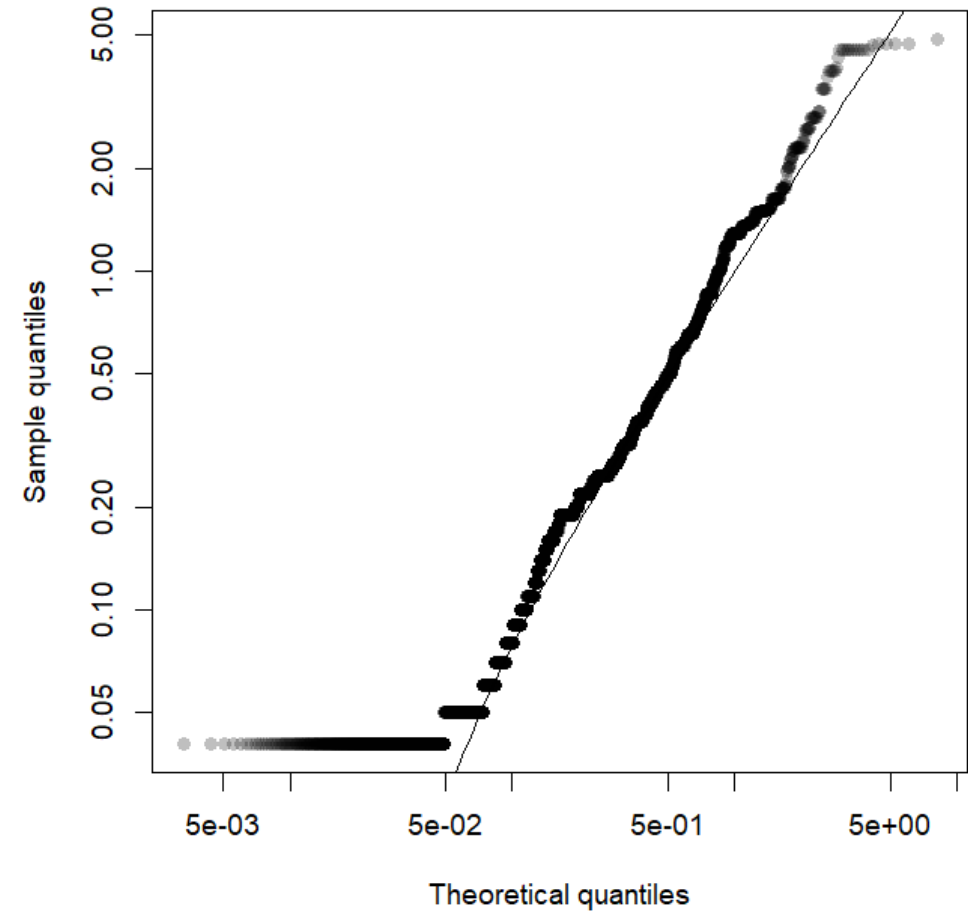
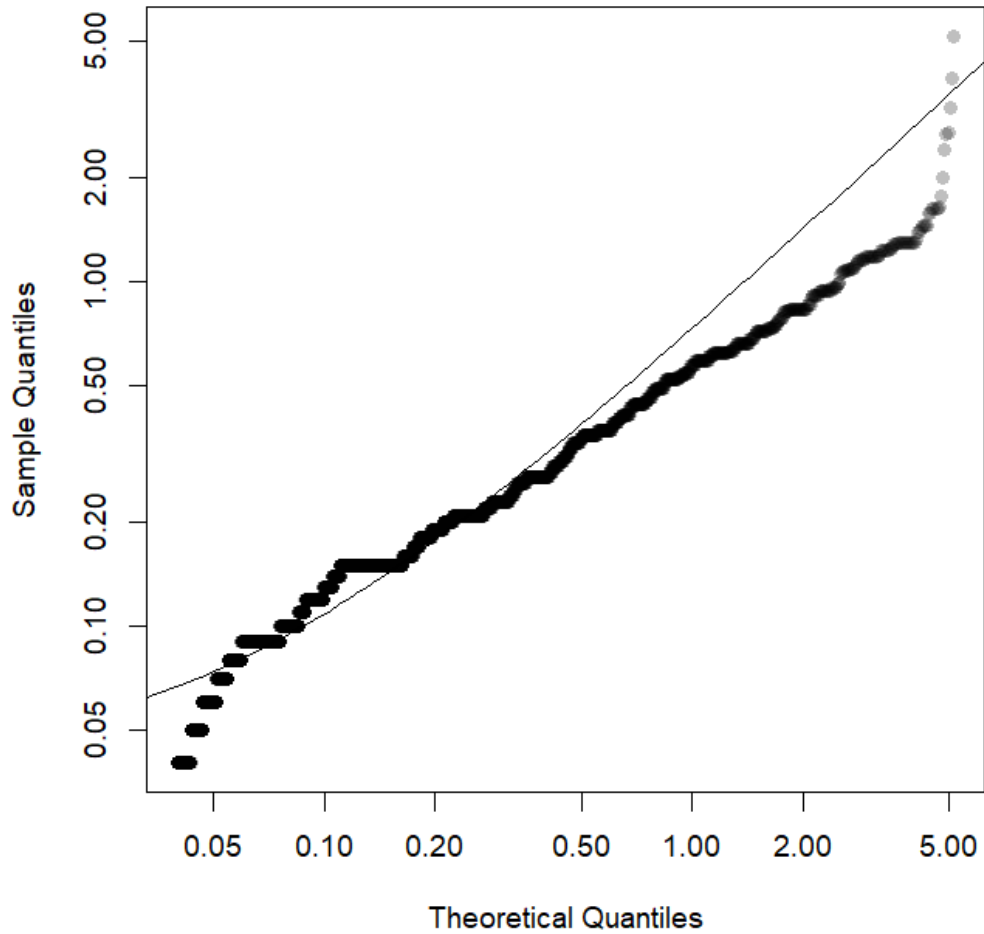


Figure B-45. Raja Ampat fish quantile-quantile (Q-Q) plots with (A) bounded power law and (B) log-normal distributions. The axes of the Q-Q plots are in log scale.

(A) wakatobi : Power law



(B) wakatobi : Log-normal

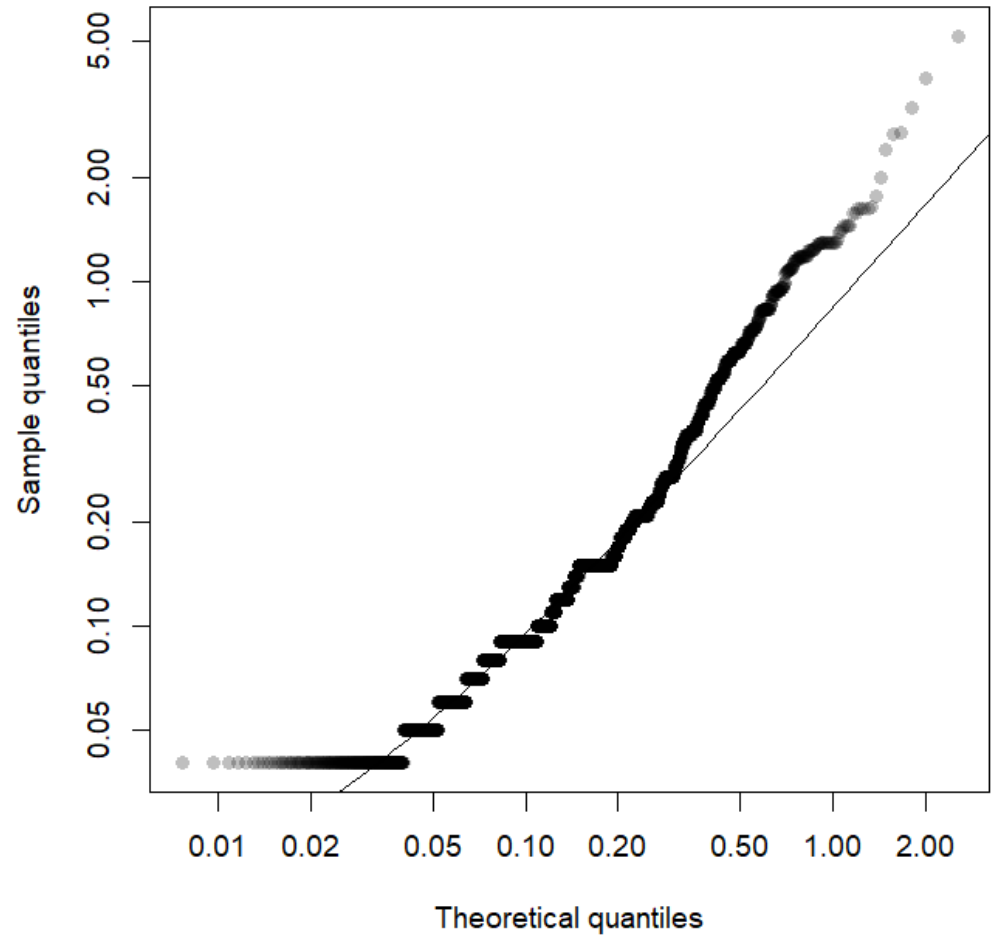
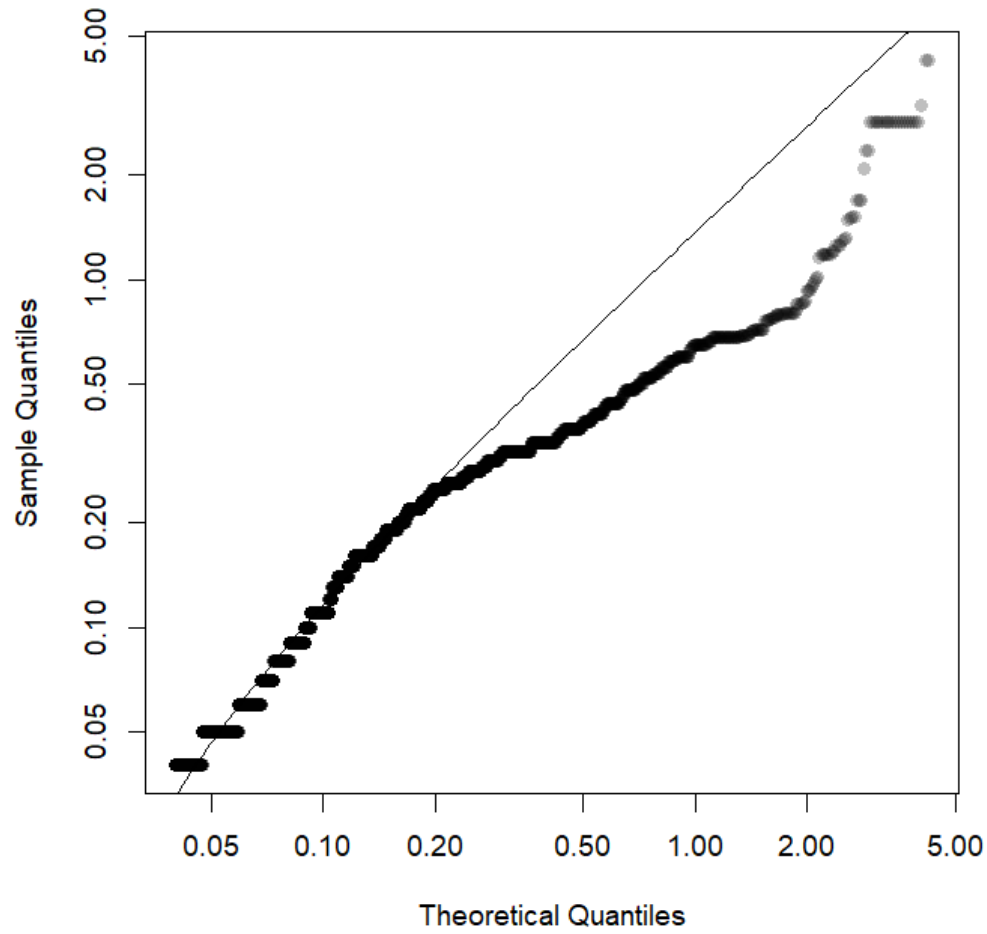


Figure B-46. Wakatobi fish quantile-quantile (Q-Q) plots with (A) bounded power law and (B) log-normal distributions. The axes of the Q-Q plots are in log scale.

(A) lombok : Power law



(B) lombok : Log-normal

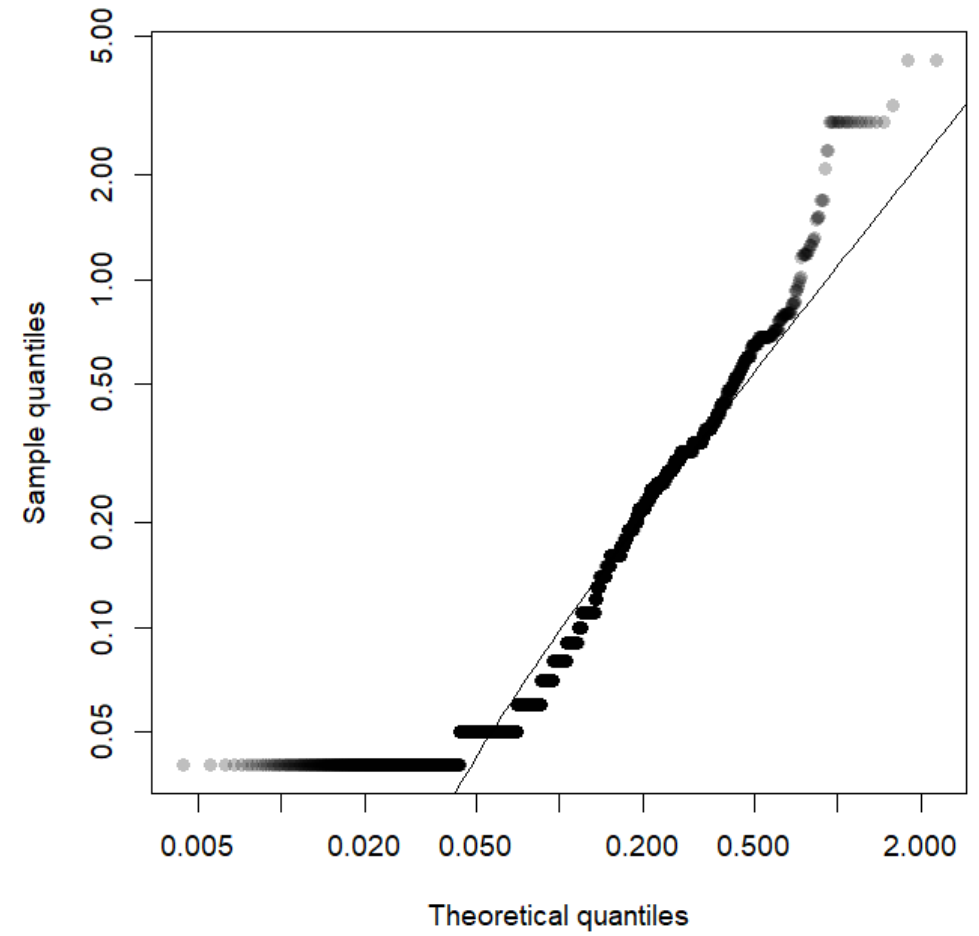


Figure B-47. Lombok fish quantile-quantile (Q-Q) plots with (A) bounded power law and (B) log-normal distributions. The axes of the Q-Q plots are in log scale.

Table B-5. Log-likelihoods for each distribution on fish biomass data. BPL: bounded power law; LN: log-normal. A larger log-likelihood indicates a better model fit. Green-shaded boxes indicate the better model.

Site	BPL log-likelihood	LN log-likelihood	BPL AIC	LN AIC
Raja Ampat	3695	2655	-7383	-5306
Wakatobi	2908	2914	-5810	-5825
Lombok	8287	6341	-16568	-12677

References

- Carvalho, P. G., Setiawan, F., Fahlevy, K., Subhan, B., Madduppa, H., Zhu, G., & Humphries, A. T. (2021). Fishing and habitat condition differentially affect size spectra slopes of coral reef fishes. *Ecological Applications*, 31(5), e02345. <https://doi.org/https://doi.org/10.1002/eap.2345>
- Chong, F., Sommer, B., Stant, G., Verano, N., Cant, J., Lachs, L., Johnson, M. L., Parsons, D. R., Pandolfi, J. M., Salguero-Gómez, R., Spencer, M., & Beger, M. (2023). High-latitude marginal reefs support fewer but bigger corals than their tropical counterparts. *Ecography*, 2023(12), e06835. <https://doi.org/https://doi.org/10.1111/ecog.06835>

Appendix C: Supporting information for Chapter 4

Table C-1. The 26 sampling site names, their geographic regions, their GPS coordinates in decimal degrees, the sampling date (yyyy/mm/dd) and the number of coral individuals sampled per site. Asterisks (*) indicate the sites that were sampled opportunistically.

Site name	Region	Latitude	Longitude	Sampling date (yyyy/mm/dd)	Coral individuals sampled
Nakano Beach	Iriomote	24.43152	123.7924	2023/06/09	15
Amitori	Iriomote	24.34577	123.69	2023/06/10	15

Sotopanari	Iriomote	24.38228	123.7196	2023/06/10	15
Nakano-Okii	Iriomote	24.43522	123.7993	2023/06/11	16
Ukibaru	Okinawa	26.34987	127.9936	2023/06/08	10
Sakiyama	Okinawa	26.70673	127.9662	2023/06/13	15
Kourijima	Okinawa	26.71213	128.0281	2023/06/13	16
Onna1	Okinawa	26.51351	127.8627	2023/06/15	16
Onna2	Okinawa	26.50093	127.8409	2023/06/15	15
Hentona plots*	Okinawa	26.75058	128.1848	2023/08/12	2
Tomori	Amami	28.46129	129.7186	2023/07/08	15
Saneku	Amami	28.19227	129.1905	2023/07/09	15
Ankyaba	Amami	28.11133	129.3473	2023/07/09	16
Sani	Amami	28.51297	129.667	2023/07/10	15
Shitoko	Yakushima	30.44893	130.5214	2023/07/11	16
Yudomari	Yakushima	30.23356	130.4736	2023/07/12	15
Owase	Sata	31.03699	130.6757	2023/07/14	2
Tajiri	Sata	31.00671	130.6765	2023/07/14	14
Amaji2	Kochi	32.80153	132.63	2023/07/18	15
Amaji1	Kochi	32.81577	132.6438	2023/07/18	15
Himeshima	Kochi	32.74289	132.4923	2023/07/19	12
Torinokubi	Kochi	32.75311	132.5493	2023/07/19	12
Kashiwajima plots*	Kochi	32.77418	132.6244	2023/08/24	1

Nishidomari plots*	Kochi	32.77917	132.7327	2023/08/22	11
Nahari	Kochi	33.41154	134.0309	2023/07/21	1
Kushimoto	Wakayama	33.47938	135.7461	2023/07/24	21

Table C-2. *Pocillopora* PCR reagents and volumes used per sample, and PCR conditions following (Flot et al., 2008).

Reagent	Volume (μ l)	Stages	Temperature ($^{\circ}$ C)	Time (minute: second)
HotStarTaq master mix	10	1	94	1:00
FATP6.1	1	2 (40 cycles)	94	0:30
RORF	1		53	0:30
CoralLoad	2		72	1:15
H ₂ O	5	3	72	5:00
Genomic DNA	1			
<i>Total volume</i>	<i>20</i>			

Table C-3. Symbiodiniaceae PCR reagents (* indicates items that are part of the TaKaRa Ex Taq® Hot Start kit) and volumes used per sample and PCR conditions used, adapted from Hume et al. (2018).

Reagent	Volume (μ l)	Stages	Temperature ($^{\circ}$ C)	Time (minute: second)

10x <i>ExTaq</i> buffer*	2	1	98	2:00
dNTP mixture*	1.6	2 (35 cycles)	98	0:10
SYM_VAR_5.8S2	1.2		56	0:30
SYM_VAR_REV	1.2		72	0:30
<i>ExTaq</i> HS*	0.2	3	72	7:00
H ₂ O	12.8			
Genomic DNA	1			
<i>Total volume</i>				<i>20</i>

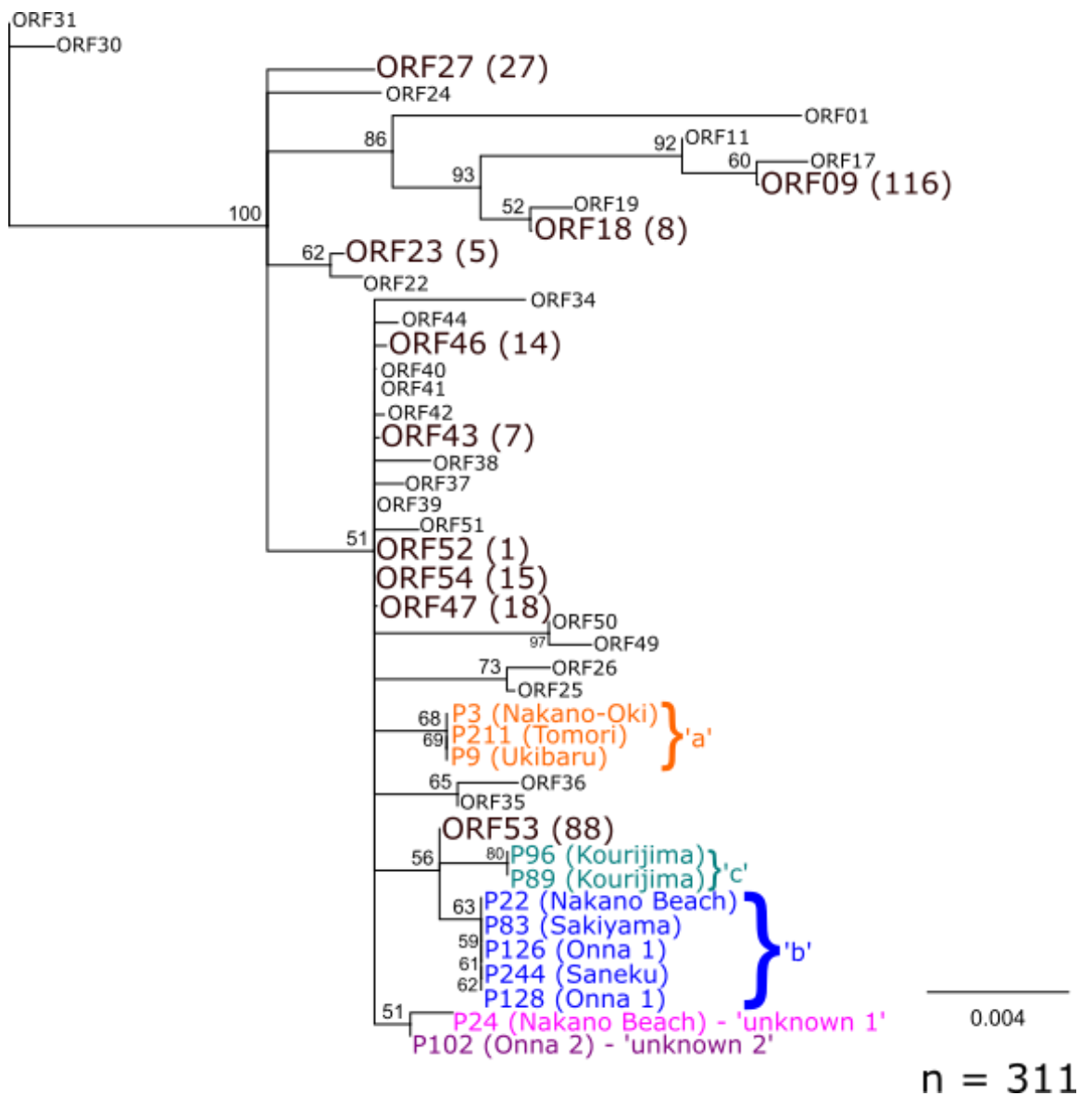


Figure C-1. Phylogenetic tree showing the relationship between selected known haplotypes (Gélin et al., 2017). Large, dark brown fonts indicate haplotypes that were found in this work, followed by the number of corals in brackets found to be in that haplotype. Coloured fonts mark previously unrecorded sequences/haplotypes found in this study, showing the sample number and the location. 'a' was found in three samples, 'b' in five, 'c' in two; while 'unknown 1' and 'unknown 2' are singletons

Table C-4. ORF haplotypes found in this study and the associated PSH, SSH and possible morphotypes according to Table 3 of Gélin et al. (2017).

ORF	PSH	SSH	Possible morphotypes according to SSH
-----	-----	-----	---------------------------------------

09	4	4	damicornis
18	5	5a-d	acuta, brevicornis, eydouxi, verrucosa
23	6	6	damicornis, verrucosa, elegans, meandrina
27	9	9a-c	eydouxi, meandrina, woodjonesi, verrucosa, molokensis, damicornis, zelli
43	13	13a	verrucosa, damicornis, meandrina, eydouxi, molokensis, kelleheri, zelli
46	13	13b	verrucosa, damicornis, eydouxi, meandrina, molokensis, kelleheri
47	13	13c	verrucosa, kelleheri, damicornis, meandrina
52	15	15	damicornis
53	16	16	verrucosa, damicornis, kelleheri, lingulata, meandrina
54			

Table C-5. Parameter estimates, p value and confidence interval of the ordinal logistical regression (model <- polr(rank ~ PC1+PC2)), where PC1 and PC2 scores are predictor variables, and 'rank' (the different number of haplotypes) is the response variable. All values are rounded to three significant figures.

	Value	Std. Error	t value	p value	CI (2.5%, 97.5%)
PC1	1.61	0.440	3.66	< 0.001	0.890, 2.65
PC2	0.409	0.288	1.42	0.156	-0.150, 0.997
1 2	-1.06	0.804	-1.32	0.188	

2 4	0.213	0.711	0.300	0.764
4 5	0.692	0.706	0.980	0.327
5 6	2.162	0.753	2.872	0.004
6 7	3.362	0.862	3.899	< 0.001
7 8	5.826	1.438	4.052	< 0.001

Table C-6. Defining Intragenomic Variants (DIVs) that make up symbiont ITS2 type profiles, ordered from high to low abundance. The total number of samples included are 325. Note that sample P26 fed into both type 88 and 92.

ITS2 type profile UID	85	89	94	86	96	88	90	95	91	84	87	92	93
Clade	C	C	C	C	C	C	C	C	C	C	C	C	D
ITS2 type profile	C1bi/ C1d- C1- C42.2- C3cg- C3cw- C1b	6597- 6601- 8157- 8156- C42.2 C42.2	6597- 6601- C42.2- 8157- C1- 8181	C42a- C42.2- C1- C1b- C1au	C1bi- C1- 10319 - C42.2- 10334	C1d/C 1- C42.2- C3cg- C1b	C42u/ C42a- C1- C42.2 C42.2	C42a- C1- C42.2- C42b- C1b- 8149	C1ag/ C42.2- C1- C3cg	25378 _C/C1 c- C42.2- C1- 4390_ C- 6682_ C	C42a- C1- C42.2- C1b- 8236	C1bb	D1
Majority ITS2 sequence	C1bi/ C1d	noName	noName	C42a	C1bi	C1d/C 1	C42u/ C42a	C42a	C1ag/ C42.2	noName/C1 c	C42a	C1bb	D1

Associated species	None	None	None	None	None	S. goreaui	None	None	None	None	None	None	S. glynnii
ITS2 profile abundance local	115	64	48	23	19	15	11	11	9	5	4	1	1

References

- Flot, J.-F., Magalon, H., Cruaud, C., Couloux, A., & Tillier, S. (2008). Patterns of genetic structure among Hawaiian corals of the genus *Pocillopora* yield clusters of individuals that are compatible with morphology. *Comptes Rendus. Biologies*, 331(3), 239-247. <https://doi.org/10.1016/j.crv.2007.12.003>
- Gélin, P., Postaire, B., Fauvelot, C., & Magalon, H. (2017). Reevaluating species number, distribution and endemism of the coral genus *Pocillopora* Lamarck, 1816 using species delimitation methods and microsatellites. *Mol Phylogenet Evol*, 109, 430-446. <https://doi.org/10.1016/j.ympev.2017.01.018>
- Hume, B., Ziegler, M., Poulain, J., Pochon, X., Romac, S., Boissin, E., de Vargas, C., Planes, S., Wincker, P., & Voolstra, C. (2018). An improved primer set and amplification protocol with increased specificity and sensitivity targeting the Symbiodinium ITS2 region. *PeerJ* 6, e4816. <https://doi.org/https://doi.org/10.7717/peerj.4816>